UNIVERSITÉ DE STRASBOURG

École Doctoral des Sciences de la Terre et de l'Environnement (ED 413)

THÈSE presenté par :

Pablo Alvarez-Zaldívar

soutenue le **25 Janvier 2019**

pour obtenir le grade de **Docteur de l'Université de Strasbourg**

Mention: Sciences de la Terre et de l'Univers

Spécialité: Géochimie

Pesticide degradation and transport at catchment scale

Compound-specific isotope analysis and numerical modelling

Thèse dirigée par:

Gwenaël Imfeld (Directeur de thèse, LHYGES)

Sylvain Payraudeau (Co-directeur de thèse, ENGEES)

Rapporteurs:

Boris van Breukelen, TU Delft, Pays-Bas

Mònica Rosell, Universidad de Barcelona, Espagne

Autres members du jury:

Jens Lange, Universität Freiburg, Allemagne

Paul van Dijk, Chambre d'Agriculture Grand Est, France

Ph.D. Thesis, University of Strasbourg

This research has been financially supported by an *Initiatives d'excellence (IDEX)* fellowship.

There are, it seems, two muses: the Muse of Inspiration, who gives us inarticulate visions and desires, and the Muse of Realization, who returns again and again to say "It is yet more difficult than you thought." This is the muse of form.

It may be then that form serves us best when it works as an obstruction, to baffle us and deflect our intended course. It may be that when we no longer know what to do, we have come to our real work and when we no longer know which way to go, we have begun our real journey.

The mind that is not baffled is not employed. The impeded stream is the one that sings.

— Wendell Berry, *Our Real Work*

Pablo ALVAREZ-ZALDÍVAR

Pesticide degradation & transport at catchment scale

Résumé :

Les herbicides sont une importante technologie de protection des cultures de l'agriculture moderne. Cependant, leur application sur de vastes étendues de terre génère des sources de pollution diffuses qui sont non seulement difficiles à surveiller et à contrôler, mais qui menacent également la qualité des ressources humaines en eau et des écosystèmes fluviaux dans le monde entier. Bien que des évaluations sur le terrain et des essais en laboratoire soient nécessaires avant l'introduction de matières actives sur le marché, le devenir et l'étendue de la dégradation des pesticides et de leurs métabolites dans l'environnement sont sujets à de grandes incertitudes. Ce travail de thèse établit une preuve de concept pour l'application de l'analyse isotopique des composés spécifiques (AICS) pour surveiller la dégradation et le transfert des pesticides à l'échelle du bassin versant. La thèse comprend à la fois la caractérisation sur le terrain et la modélisation numérique pour étudier la valeur de l'AICS comme outil de surveillance et comme technique de réduction de l'incertitude du modèle. Des expériences en laboratoire sont également utilisées pour appuyer l'interprétation des données sur le terrain et valider l'élaboration de structures de modèles numériques.

Mot clés :

AICS, pesticides, bassin versant, pollution diffuse, modèlisation

Summary :

Herbicides are an important crop protection technology of modern agriculture. However, their application over large extensions of land generates diffuse pollution sources that are not only difficult to monitor and control, but also that threaten the quality of human water resources and river ecosystems world-wide. Although field assessments and laboratory tests are required before active ingredients are introduced to market, the fate and degradation extent of pesticides and their metabolites in the environment is subject to significant uncertainty. This thesis work establishes a proof of concept for the application of compound specific isotope analysis (CSIA) to monitor pesticide degradation and transfer at catchment scale. The thesis includes both field characterization and numerical modelling to investigate the value of CSIA as a monitoring tool and as a model uncertainty reduction technique. Laboratory experiments are further employed to support interpretation of field data and validate numerical model structure development.

Key words :

CSIA, pesticides, catchment scale, diffuse pollution, modelling

Contents

List of Figures

List of Tables

Acknowledgements

This Ph.D. thesis was carried out at the Laboratory of Hydrology and Geochemistry of Strasbourg (LHyGeS), France, supported by an Initiatives d'excellence (IDEX) fellowship. I want to thank all persons and institutions who have directly or indirectly contributed to this work.

The path that I have taken towards the completion of this Ph.D has been anything but linear. I discovered the LHyGeS in a visit to Strasbourg, through a great project proposal to study and model Gwenaël Imfeld's constructed wetland experiment, introducing me not only to the field of reactive transport but also to insightful and brilliant teachers including, in addition to Gwenaël, Martin Thullner, Florian Centler and Uli Maier at the UFZ in Leipzig. The opportunity to work with you made the end of my Masters degree a hugely rewarding academic experience that would set the basis for this Ph.D., and one for which I will always be thankful.

My academic life would take a long detour into the private sector, only to find a path 3 yrs. later back to the place where I had started. A collaborative project under the title of this thesis with Sylvain Payraudeau and Gwenaël became an exciting opportunity to come back to the LHyGeS. Over the last three years I have learned enormously, both academically and personally, under your guidance, through our discussions, your perspectives and in your persistence. Thank you both for unending feedback working as a constant mirror and your relentless energy to push forward. Your flexibility and support with my split personality between Germany and France should also not go unrecognized. I thank you immensely for your trust.

Where I am today is also in huge part due to Kathy Baylis. The legacy of your trust and support at UBC lives in me to this day, and for that I will be always in debt. Thank you!

I would like to thank Benoît Guyot, Fatima Meite, Charline Wiegert, Jeremy Masbou, Eric Pernin, Sarah Wisselmann and Marceau Levasseur for all your support in making the first article possible though sampling, analysis and development. Sarah and Marceau, special thanks to you both for your organization and transparency in your lab work and positive attitude in the field, even on cold rainy days, helping to make our weekly field visits a true field-trip! Also special and extended thanks to Fatima and Benoît, for always being there to support me with academic, admin., endless bureaucracy or personal matters. Wednesdays were always my favorite! Benoît, hold on to that cup champion!

Eric Lascar, Marianna Marinoni, Jean-Michel Brazier and Ivan Toloni, without your humor, life experiences and good company my time outside of the lab would not have been nearly as much fun. I will miss you and wish you the best in your future adventures and discoveries! Guillaume Drouin, Boris Droz and Paula Prez, although your arrival came at my end, I

am no less thankful also to you for your support through open discussions, feedback and computer power! The last sprint of this Ph.D. would have been a serious challenge without your trust and support.

My special thanks to the members of the reading committee, Dr. Boris van Breukelen, Dr. Mònica Rosell, Dr. Jens Lange, and Dr. Paul van Dijk for the detailed assessment of this thesis.

I am most thankful for the support of my German-French family, my mother, my sisters and friends in the Netherlands and Germany. Thank you all for your unconditional support. Sylvie, Wolfgang, Céline und Robert, dank euch hatten wir immer einen Ort, an dem wir fliehen konnten, um zu atmen und unsere Energie zu erneuern. Sophie, meine Liebe, ohne dich würde diese These nicht existieren. Darum widme ich dich diese Doktorarbeit.

Summary

Herbicides are an important crop protection technology of modern agriculture. However, their application over large extensions of land generates diffuse pollution sources that are not only difficult to monitor and control, but also that threaten the quality of human water resources and river ecosystems world-wide [1, 2]. Although field assessments and laboratory tests are required before active ingredients are introduced to market, the fate and degradation extent of pesticides and their metabolites in the environment is subject to significant uncertainty [3]. Not only are most transformation products (TPs) not known, preventing any mass balance accounts of pesticide fate across space and time, but also their inherent toxicity on non-target organisms is disregarded in registration and approval dossiers [4]. Limitations in the ability to bridge information obtained under laboratory to field conditions and the uncertainty associated to pesticide characterization in realistic environmental contexts warrants the development of novel management strategies (e.g., [2]) that enable monitored natural or engineered attenuation.

Numerous environmental sinks can contribute to pesticide attenuation, including sorption, volatilization, degradation, leaching, plant uptake and offsite export through runoff and erosion. Relative to dilution processes, degradation is the only sink contributing to sustainable removal. Therefore the ability to quantify and distinguish its relative importance is of primary interest to the environmental manager. In this respect, compound specific isotope analysis (CSIA) represents an advantage over concentration based assessments, which cannot determine the extent of degradation that a contaminant undergoes between sources and receptors. In contrast, isotope fractionation can evidence degradation extent and pathways, even if no TPs are detected, as transformation leaves a biochemical imprint in the form of characteristic changes in isotope ratios of the reacting contaminant [5].

Although the use of CSIA to evidence degradation is well established for legacy compounds in contaminated sites [6, 7], the occurrence of very low ($ng\ L^{-1}$ to $\mu g\ L^{-1}$) concentrations of pesticides and their polarity lead to analytical challenges precluding CSIA applications at environmental scales [8]. Despite these analytical challenges, pesticide CSIA applications have begun to emerge from small scale lab scales to larger quasi(stationary) aquifer contexts [9–13]. However, its application to highly dynamic hydrological contexts at catchment scale are still lacking.

To address this gap, a proof of concept is presented in **Chapter 2**, establishing the applicability of carbon-based CSIA to monitor pesticide degradation and fate at catchment scale. Due to its environmental relevance (e.g., persistence and detection frequency [2]) and wide-spread use, S-metolachlor (SM) is used as a model compound. Comparison of three information sources (i.e., CSIA, mass balances (MB) and reported half-life ($t_{1/2}$) ranges) of SM demonstrated the validity of CSIA as a complementary line of evidence for quantifying degradation under dynamic hydrological and rainfall-runoff conditions. The CSIA

approach improved our understanding of pesticides fate by delineating the primary catchment areas regulating degradation (88%) and export losses (8%). Comparison of MB and CSIA approaches showed that degradation extent evolution was consistent between outlet and catchment-wide top soils, demonstrating the monitoring applicability of CSIA methods despite shifting hydrological regimes. Based on its ability to quantify degradation independently of TPs, CSIA may thus be considered as a valuable complementary tool to identify and monitor chemical risk at catchment scale.

Although **Chapter 2** demonstrated the value of CSIA as a complementary tool to evidence degradation and to estimate catchment losses, interpretation of field data provides only punctual estimates of observed catchment processes that, due to changes in environmental conditions, are inherently dynamic. For example, while total export losses where identified, characterization data was not able to provide information on how specific rainfall-runoff events (or their frequency) regulate pesticide export. Similarly, although interpretations of degradation extent can be used to derive mean pesticide degradation half-life, reaction rates are likely dependent on hydro-climatic conditions regulating bacterial activity. These conditions may not only change throughout the growing season but may vary throughout the catchment at any one time, generating spatial and temporal changes in degradation intensity and/or soil physical properties regulating pesticide transfer pathways (i.e., *hot/cold moments and periods*).

Predicting mobilization and export of pollutants from top soils (*hot/cold moments*) is essential to evaluate transfer risk and toxicological exposure [14, 15]. To do so, understanding of the relative importance of extrinsic (e.g., rainfall characteristics) and intrinsic factors (e.g., soil and pesticide properties), regulating pesticide mobilization and export is important. Evaluation of both extrinsic and intrinsic factors controlling pesticide transfer in agricultural soils was addressed in **Chapter 3** by combining a parsimonious model with a small scale soil column experiment designed to reproduce leaching and ponding processes typically observed in the field. This study revealed the primary influence that extrinsic factors, including rainfall frequency, duration and volume, have on the export by ponding and leaching of organic and inorganic pollutants from topsoils. Rainfall volumes were the primary determinant of pollutant export during the first rainfall after product application. Rainfall volumes and frequency also controlled pesticide transfer pathways (i.e., relative distribution of leaching and ponding) through their impact on soil compaction. Further, irrespective of aging time, all rainfall patterns significantly impacted the leaching of metalaxyl and SM during the first rainfall. However, only extreme rainfall patterns may generate significant metal leaching, as shown by observed concentrations below quantification levels for the long-lasting events with low and intermediate rainfall intensities. Therefore, one significant implication is that the first rainfall following field application of pre-emergence pesticides is of critical importance for pesticide export. In contrast, soil composition and aging had only a secondary influence on pollutant export from soils.

Hydrological functioning of the experimental design was confirmed by the parsimonious model, reproducing observed ponding and percolated waters across all rainfall patterns. The model could also generally reproduce the mass balance for both metalaxyl and SM leaching in soil. Although preferential flow in macropores may additionally increase pesticide transport, this model showed that chromatographic transfer may also be a significant export process, particularly with soils of good permeability ($K_{sat} > 13$ cm h^{-1}). As a result, leaching from topsoil of pre-emergence pesticides applied shortly after tillage on bare soils may represent a specific transfer risk. By refining the expected exports of pesticides and metals in different conditions, we anticipate this study to be a preliminary step to more systematically evaluate

the impact of rainfall patterns and frequency on pollutant export in benchmark soil tests.

Application of insights from small-scale experiments to large-scale environmental contexts is subject to uncertainty, as spatial heterogeneity and temporal hydro-climatic variability imply a departure from idealized laboratory controlled conditions. Transition to evaluate pesticide fate at catchment scale requires therefore numerical approaches that are able to account for non-linear processes and interaction between state variables across space and time. A review of current numerical approaches [16–20] used to represent pesticide fate at catchment scale indicates two primary challenges. On the one hand, to provide detail accounts of pesticide transport during periods of hydrological forcing at the event scale, models need to explicitly account for the spatial heterogeneity of agricultural landscapes [19], hydrological connectivity [21] and farm management practices [22]. However, the values of state variables (e.g., soil physical properties, moisture conditions and pesticide pools), which evolve across space and time, are key in representing the hydrological and chemical response during major hydrological events [22]. Therefore, models that are also able to seamlessly couple processes that are relevant at different time-scales (i.e., event-based *vs.* continuous) and yet remain computationally efficient are needed. On the other hand, there is a lack of available pesticide fate and transfer data, that is required to validate such models at catchment scale. In particular, current efforts to represent pesticide fate at catchment scale rely on concentration-based approaches, which as outlined above, are limited in their ability to distinguish between degradation and competing sinks.

Based on insights from the parsimonious model developed during **Chapter 3** and the unique soil concentration and CSIA data set collected for SM during catchment characterization of **Chapter 2**, a spatially distributed hydrological model capable of simulating moisture evolution [23] was further developed in **Chapter 4** to account for pesticide reactive and transport processes. This chapter evaluated the ability of PiBEACH, the developed model, to improve pesticide fate representation at catchment scale by incorporating hydro-climatic factors (moisture and temperature optimums for bacterial activity) regulating SM degradation. We show that, relative to constant degradation reference values (DT_{50}) retained in many physically based models, the use of hydro-climatic factors can significantly improve degradation rate representation in 2D spatially distributed models. By incorporating pesticide CSIA data, in addition to concentrations, we were not only able to reduced the equifinality of degradation parameters of the evaluated models, but also allowed to objectively determine the improvement associated to the inclusion of hydro-climatic processes in describing degradation within the catchment. Finally, uncertainty estimations for key management metrics including degradation, persistence and leaching extent *via* matrix flow were compared between models with (WC) and without (NC) CSIA constrains. Results showed that although both models provide approximately equivalent mean degradation extents towards the end of the study period for SM, the larger degradation uncertainty of NC models propagates across non-destructive pesticides sinks, leading to overestimations of leaching extents by a factor of 2.

While the continuous model in **Chapter 4** was able to reduce the uncertainty of degradation parameters in catchment top soils, significant limitations were observed in its ability to reproduce concentrations and isotope signatures at the outlet during periods of high transfer risk. Indeed, assessment of cumulative simulated export by runoff and drainage combined saw an overestimation of about a factor of 4, relative to dissolved outlet measurements ($\approx 0.5\%$). To address this limitation, coupling of PiBEACH with the open source Limburg Soil Erosion Model (LISEM), an event-scale model, specialized in the detailed representation of fast transport through run-off and erosion during intense rainfall periods is presented in **Chapter**

5. Preliminary results of the coupled model, PiBEACH-oL, have shown improvements in the representation of hydrological components contributing to outlet discharge, allowing to identify likely false-positive runoff events predicted by the uncoupled model. Ongoing developments include the coupling of mass transfer to outlet through runoff and integration of depth dependence factors regulating degradation rates to improve predictions of rapid runoff and drainage components.

In conclusion, **Chapter 6** provides a general discussion of the overarching approaches (i.e., characterization and modelling) and physical scales (i.e., laboratory and catchment) investigated during this Ph.D work. This section discusses main findings, as well as some limitations of the work presented in each of the above mentioned chapters by addressing aspects of field characterization, lab scale experimentation and numerical modelling. Based on this discussion, **Chapter 7** reflects on the implications of CSIA-based approaches for pesticide fate assessments at catchment scales and provides a number of recommendations for the use of CSIA in future studies at both lab and larger scales. These include (i) combination of water sampling strategies, potentially also including water dating techniques, to characterize different sources in flow components, (ii) the design of benchmark soil degradation experiments and their modelling under aerobic and anaerobic conditions, (iii) CSIA sampling strategies for larger river catchment scales, and (iv) ESIA characterization of in stream biofilm biodegradation by making use of, for example, streamside flumes under different modalities.

Résumé

Les herbicides sont largement utilisés pour éviter le développement d'adventices dans les cultures. Cependant, leur application sur des surfaces importantes génère une pollution diffuse par volatilisation, infiltration et ruissellement qui est non seulement difficile à quantifier, contrôler et prédire, mais qui menace également la qualité des ressources en eau et des écosystèmes aquatiques dans le monde entier [1, 2]. Bien que des évaluations *in situ* et des tests en laboratoire soient nécessaires pour l'homologation et la mise sur le marché de nouvelles molécules actives, la prédiction de leur persistance et des risques de transport vers les milieux aquatiques reste entachée d'une très large incertitude [3]. De plus les produits de dégradation de ces molécules actives sont très largement méconnues et donc ne peuvent pas être quantifiés, limitant toute tentative de bilan de masse du devenir des pesticides au sein des paysages agricoles. Il est également à noter que la toxicité de ces produits de dégradation pour les organismes non ciblés dans les sols et les milieux aquatiques n'est pas prise en compte dans les dossiers d'homologation de mise sur le marché des molécules actives [4]. Enfin la transposabilité des cinétiques de dégradation ou de paramètres de transport obtenues en laboratoire aux conditions environnementales a montré ses limites et justifie le développement de nouvelles stratégies de quantification *in situ* (e.g., [2]) de la persistance réelle de ces molécules.

De nombreux processus peuvent contribuer à la dissipation des pesticides dans les sols ou les cultures sur lesquels ils ont été appliqués. Certains sont non destructifs comme la dilution la sorption, la volatilisation, la lixiviation, l'absorption par les plantes et l'exportation hors site par ruissellement et érosion. Par rapport à ces processus non-destructifs, les processus de dégradation qu'ils soient biotiques ou abiotiques sont les seuls à contribuer à l'élimination des pesticides. Par conséquent, la possibilité de quantifier et prédire l'importance de la dégradation présente un intérêt primordial pour le gestionnaire de l'environnement. À cet égard, l'analyse isotopique des composés spécifiques (AICS) représente un avantage majeur par rapport aux évaluations basées sur la concentration, qui ne peuvent pas discriminer la part respective des processus non-destructifs et destructifs. Ainsi en induisant un fractionnement isotopique des éléments composants la molécule active (e.g. $^{13}C/^{12}C$, $^{15}N/^{14}N$), les processus de dégradation peuvent être mise en évidence en accédant potentiellement aux voies de dégradation même si aucun produit de dégradation n'est détecté [5].

L'utilisation de l'AICS pour quantifier la dégradation de polluants historiques existants dans les sols et aquifères contaminés est bien établie [7]. La présence des pesticides en très faibles concentrations (ng L^{-1} au μg L^{-1}) et leur polarité constituent un défis analytique pour développer l'AICS des pesticides *in situ* dans les agrosystèmes. En dépit de ces défis analytiques, les applications de l'AICS aux pesticides ont commencé à émerger à l'échelle de mésocosmes ou dans les aquifères [9–13]. Cependant, son application aux eaux de surface très dynamiques à l'échelle du bassin versant fait encore défaut.

Pour combler cette lacune, une preuve de concept est présentée au **chapitre 2**, établissant l'applicabilité de l'AICS basée sur le carbone ($^{13}C/^{12}C$) pour quantifier la dégradation du S-métachlore et son devenir à l'échelle du bassin versant. Le S-métolachlore a été retenu comme composé modèle en raison de sa persistance,de safréquence de détection [2]) et de son utilisation répandue. Cette preuve par concept s'appuie sur une comparaison de 3 méthodes : l'AICS, un bilan de masse (MB) et l'utilisation des durée de demi-vie (DT_{50}) fournies dans les bases de données physico-chimiques des pesticides.

La comparaison de trois méthodes (AICS, MB et DT_{50}) sur le S-métolachlore a démontré la validité de l'AICS comme outil de quantification de sa dégradation à l'échelle du petit bassin versant (47 ha) dans des conditions hydrologiques dynamiques. L'approche AICS a permis d'améliorer notre compréhension du devenir des pesticides en délimitant les principales zones au sein du bassin versant contribuant à la dégradation qui atteint 88%, et aux pertes par ruissellement à l'exutoire qui représente 8%. La comparaison des approches MB et AICS a démontré que la quantification de la dégradation était cohérente à la fois avec les concentrations et les signatures isotopiques dans la couche supérieure de sols et les eaux à l'exutoire. Ceci démontre ainsi l'applicabilité de la méthode AICS malgré la forte dynamique hydrologique qui caractérise les têtes de bassins versants. En offrant la capacité de quantifier la dégradation indépendamment de la quantification des produits de dégradation, l'AICS peut donc être considérée comme un outil complémentaire précieux pour quantifier et prédire la persistance des pesticides à l'échelle du bassin versant.

Bien que le **chapitre 2** ait démontré la valeur ajoutée de l'AICS comme outil complémentaire pour mettre en évidence la dégradation et estimer le transport *via* le ruissellement au niveau du bassin versant, l'interprétation des données de terrain ne fournit que des estimations ponctuelles des processus observés qui, en raison de changements des conditions environnementales, sont intrinsèquement dynamiques. Par exemple, alors que les pertes totales à l'exportation ont été identifiées, les données de caractérisation n'ont pas été en mesure de fournir des informations sur la manière dont les événements de pluie-débit spécifiques (ou leur fréquence) régulent l'exportation de pesticides. De même, bien que les interprétations de l'étendue de la dégradation puissent être utilisées pour obtenir des durées de demi-vies de dégradation biochimique moyenne des pesticides, les taux de réaction dépendent probablement des conditions hydro-climatiques qui régissent l'activité bactérienne. Ces conditions peuvent non seulement changer tout au long de la saison de croissance, mais peuvent varier à tout moment dans le bassin versant, générant des changements spatiaux et temporels de l'intensité de la dégradation et / ou des propriétés physiques du sol régulant les voies de transfert des pesticides (i.e., *hot/cold moments and periods*).

La couche de surface des sols agricoles joue un rôle majeur dans la mobilisation et l'export des polluants et conditionne donc fortement 'leur impact écotoxicologique sur les milieux aquatiques [14, 15]. Afin de hiérarchiser les facteurs qui modulent ce risque de mobilisation et de transport, il est important de distinguer les facteurs extrinsèques (caractéristiques des précipitations, par exemple) et intrinsèques (propriétés du sol et des pesticides, par exemple). L'évaluation des facteurs intrinsèques et extrinsèques contrôlant le transfert de pesticides dans les sols agricoles a été traitée au **chapitre 3** en combinant un modèle simple avec une expérience à petite échelle (21 cm^3 de sol) conçue pour reproduire les processus de lixiviation et de formation de flaque observée à la genèse de ruissellement. Cette étude a révélé que les facteurs extrinsèques, notamment la fréquence, la durée et le volume des précipitations, avaient une influence majeure sur l'exportation des polluants organiques et inorganiques (cuivre et zinc également étudiés). Les volumes de pluie ont été le principal déterminant de l'exportation de polluants lors de la première pluie après l'application du

produit. Les volumes de pluie et l'intensité ont contrôlé le poids relatif du transport vertical par la lixiviation ou horizontal vers les flaques en formation en raison de leur impact sur la compaction du sol. De plus, indépendamment du temps de contact entre le sol et les polluants précédant l'épisode de pluie, tous les régimes de précipitations ont eu un impact significatif sur le lessivage du métalaxyl et le S-Métolachlore lors de la première pluie. Pour les métaux, seuls les régimes de précipitations extrêmes ont généré un lessivage important en raison de la forte sorption de ceux-ci aux constituants du sol. Par conséquent, les propriétés des premières pluies après l'application de pesticides *in situ* ont un rôle majeur sur les voies de transport soit vers la nappe soit vers les eaux de surface.

Le fonctionnement hydrologique du dispositif expérimental a été confirmé par le modèle simple, en reproduisant l'eau surnageante à la surface du sol et l'eau percolées dans tous les régimes de précipitations. Le modèle a également permis de reproduire le bilan massique du lessivage du métalaxyl et du SM dans le sol. Bien que les flux préférentiels dans les macropores puissent augmenter le transport des pesticides, ce modèle a montré que le transfert par flux matriciels peut également constituer un processus d'exportation important, en particulier avec des sols de bonne perméabilité ($K_{sat} > 13$ cm h^{-1}). Par conséquent, le lessivage des pesticides, peu de temps après le labour, sur des sols nus peut représenter un risque spécifique. En affinant les exportations prévues de pesticides et de métaux dans différentes conditions, nous prévoyons que cette étude constituera une étape préliminaire permettant d'évaluer plus systématiquement l'impact des régimes pluviométriques et la fréquence des exportations de polluants dans des sols de référence.

L'application de connaissances issues d'expériences à petite échelle à des contextes environnementaux à grande échelle est sujette à des incertitudes, car l'hétérogénéité spatiale et la variabilité hydro-climatique temporelle limitent la transposition directe des résultats en conditions contrôlées au laboratoire. La transition pour évaluer le devenir des pesticides à l'échelle du bassin versant nécessite donc des approches numériques capables de prendre en compte les processus non linéaires et l'interaction entre les variables d'état dans l'espace et dans le temps. Une analyse des approches numériques actuelles [16–20] utilisées pour représenter le devenir des pesticides à l'échelle du bassin versant indique deux principaux défis. D'une part, pour fournir des informations détaillées sur le transport des pesticides pendant les périodes de forçage hydrologique à l'échelle de l'événement, les modèles doivent explicitement tenir compte de l'hétérogénéité spatiale des paysages agricoles, de la connectivité hydrologique et des pratiques culturales et itinéraires techniques. Cependant, les valeurs des variables d'état (propriétés physiques du sol, teneur en eau et concentrations en pesticides dans le sol, par exemple), qui évoluent dans l'espace et le temps, sont essentielles pour représenter la réponse hydrologique et chimique lors d'événements hydrologiques majeurs [22]. Par conséquent, des modèles capables de coupler des processus pertinents à différentes échelles de temps tout en restant opérationnels en termes de temps de calcul sont nécessaires. En revanche, les données disponibles sur le devenir et le transfert des pesticides sont insuffisantes pour valider ces modèles à l'échelle du bassin versant. En particulier, les efforts actuels pour représenter le devenir des pesticides à l'échelle du bassin versant reposent sur des approches basées sur la concentration, qui, comme indiqué ci-dessus, a une capacité limitée à faire la distinction entre les processus destructifs et non-destructifs.

Sur la base des données du modèle "mixing model" élaboré au **chapitre 3** et du set de données collectés sur le bassin versant d'Alteckendorf (chapitre 2), un modèle hydrologique spatialisé capable de simuler l'évolution de l'humidité et de la température des différentes couches du sol [23] a été développé (PiBEACH) pour améliorer la prédiction de la dégradation et du transport des pesticides. Nous montrons dans ce chapitre que, par rapport à l'utilisation

d'une valeurs fixe de dégradation (DT_{50}) retenue dans de nombreux modèles physiques, la modulation de la DT_{50} en utilisant des facteurs hydro-climatiques (teneur en eau et température du sol) améliore de manière significative la prédiction du taux de dégradation du S-métolachlore. En incorporant les données AICS sur les pesticides, en plus des concentrations lors du processus de calage des paramètres, nous avons (i) significativement réduit l'équifinalité entre paramètres de dégradation et de transport, (ii) démontré l'amélioration de la prédiction de la dégradation en conditionnant son intensité à l'humidité et à la température du sol - et (iii) réduit d'un facteur 2 l'incertitude des prédictions associées aux pertes par lessivage contribuant à la contamination des nappes.

Bien que le modèle continu présenté au **chapitre 4** ait permis de réduire l'incertitude des paramètres de dégradation dans les sols, des limitations importantes ont été observées quant à sa capacité à reproduire les concentrations et les signatures isotopiques à la sortie du bassin versant pendant les périodes de risque de transfert élevé. En effet, l'évaluation des exportations cumulées simulées par le ruissellement et le drainage combinés a abouti à une surestimation d'un facteur 4 environ, par rapport aux mesures à l'exutoire en phase dissoute ($\approx 0.5\%$). Pour répondre à cette limite, le couplage du modèle continu, PiBEACH, avec le modèle événementiel hydrologique LISEM, spécialisé dans la représentation détaillée du transport rapide par ruissellement et érosion pendant les périodes de pluie intense, est présenté au **chapitre 5**.

Les résultats préliminaires du modèle couplé, PiBEACH-oL, ont montré des améliora- tions dans la représentation des composants hydrologiques contribuant à l'écoulement en sortie. Ainsi, ce couplage a mis en évidence une surreprésentation des épisodes de ruissellement lorsque PiBEACH est utilisé seul. Les développements en cours visent à intégrer dans PiBEACH un taux de dégradation décroissant en fonction de la profondeur et de finaliser le codage du transport des pesticides via le ruissellement et l'érosion dans OPENLisem.

En conclusion, **Chapitre 6** propose une discussion générale sur les approches globales (i.e., caractérisation et modélisation numérique) et les échelles physiques (i.e., laboratoire et bassin) étudiées durant cette thèse. Cette section présente les principales conclusions, ainsi que certaines limites du travail présenté dans chacun des chapitres mentionnés ci-dessus, en abordant les aspects de la caractérisation de terrain, des expériences en laboratoire et de la modélisation numérique. Sur la base de cette discussion, le **Chapitre 7** pose les implications des approches fondées sur l'AICS pour l'évaluation du devenir des pesticides à l'échelle des bassins et fournit des recommandations sur l'utilisation de l'AICS dans des études futures, à la fois en laboratoire et à grande échelle.

References

1. Vörösmarty, C. J. *et al.* Global threats to human water security and river biodiversity. *Nature* **468,** 555–561. ISSN: 0028-0836 (2010).
2. Fenner, K., Canonica, S., Wackett, L. P. & Elsner, M. Evaluating Pesticide Degradation in the Environment: Blind Spots and Emerging Opportunities. *Science* **341,** 752–758. ISSN: 0036-8075 (2013).
3. Storck, V., Karpouzas, D. G. & Martin-Laurent, F. Towards a better pesticide policy for the European Union. *Science of the Total Environment* **575,** 1027–1033. ISSN: 18791026 (2017).
4. EC No. 283, E.-R. *EU-Regulation 283/2013/EC of 1 March 2013 setting out the data requirements for active substances, in accordance with Regulation (EC No 1107/2009 of the European Parliament and of the Council concerning the placing of plant protection products on the mark* 2013. `https://eur-lex.europa.eu/LexUriServ/LexUriServ.do?uri=OJ:L:2013:093:0001:0084:EN:PDF`.
5. Elsner, M. Stable isotope fractionation to investigate natural transformation mechanisms of organic contaminants: principles, prospects and limitations. *Journal of environmental monitoring : JEM* **12,** 2005–31. ISSN: 1464-0333 (2010).
6. Meckenstock, R. U., Morasch, B., Griebler, C. & Richnow, H. H. Stable isotope fractionation analysis as a tool to monitor biodegradation in contaminated acquifers. *Journal of Contaminant Hydrology* **75,** 215–255. ISSN: 01697722 (2004).
7. Thullner, M., Richnow, H.-h. & Fischer, A. in *Environmental and Regional Air Pollution* (eds Gallo, D. & Mancini, R.) chap. 2 (Nova Science Publishers, Inc., 2009).
8. Elsner, M. & Imfeld, G. Compound-specific isotope analysis (CSIA) of micropollutants in the environment - current developments and future challenges. *Current Opinion in Biotechnology* **41,** 60–72. ISSN: 18790429 (2016).
9. Elsayed, O. F. *et al.* Using compound-specific isotope analysis to assess the degradation of chloroacetanilide herbicides in lab-scale wetlands. *Chemosphere* **99,** 89–95. ISSN: 00456535 (2014).
10. Schürner, H. K. *et al.* Compound-Specific Stable Isotope Fractionation of Pesticides and Pharmaceuticals in a Mesoscale Aquifer Model. *Environmental Science and Technology* **50,** 5729–5739. ISSN: 15205851 (2016).
11. Milosevic, N. *et al.* Combined isotope and enantiomer analysis to assess the fate of phenoxy acids in a heterogeneous geologic setting at an old landfill. *Water Research* **47,** 637–649. ISSN: 00431354 (2013).
12. Schreglmann, K., Hoeche, M., Steinbeiss, S., Reinnicke, S. & Elsner, M. Carbon and nitrogen isotope analysis of atrazine and desethylatrazine at sub-microgram per liter concentrations in groundwater. *Analytical and bioanalytical chemistry* **405,** 2857–2867. ISSN: 16182650 (2013).
13. Bashir, S., Hitzfeld, K. L., Gehre, M., Richnow, H. H. & Fischer, A. Evaluating degradation of hexachlorcyclohexane (HCH) isomers within a contaminated aquifer using compound-specific stable carbon isotope analysis (CSIA). *Water Research* **71,** 187–196. ISSN: 18792448 (2015).
14. Arias-Estévez, M. *et al.* The mobility and degradation of pesticides in soils and the pollution of groundwater resources. *Agriculture, Ecosystems and Environment* **123,** 247–260. ISSN: 01678809 (2008).

15. Schafer, R. B. *et al.* Effects of pesticide toxicity, salinity and other environmental variables on selected ecosystem functions in streams and the relevance for ecosystem services. eng. *The Science of the total environment* **415,** 69–78. ISSN: 1879-1026 (Electronic) (Jan. 2012).

16. Borah, D. K. & Bera, M. Watershed-Scale Hydrologic and Nonpoint-Source Pollution Models: Review of Mathematical Bases. *Transactions of the ASAE* **46,** 1553–1566. ISSN: 2151-0059 (2003).

17. Merritt, W. S., Letcher, R. A. & Jakeman, A. J. A review of erosion and sediment transport models. *Environmental Modelling and Software* **18,** 761–799. ISSN: 13648152 (2003).

18. Quilbé, R., Rousseau, A. N., Lafrance, P., Leclerc, J. & Amrani, M. Selecting a pesticide fate model at the watershed scale using a multi-criteria analysis. *Water Quality Research Journal of Canada* **41,** 283–295. ISSN: 12013080 (2006).

19. Payraudeau, S. & Gregoire, C. Modelling pesticides transfer to surface water at the catchment scale: A multi-criteria analysis. *Agronomy for Sustainable Development* **32,** 479–500. ISSN: 17740746 (2012).

20. Pandey, A., Himanshu, S. K., Mishra, S. K. & Singh, V. P. Physically based soil erosion and sediment yield models revisited. *Catena* **147,** 595–620. ISSN: 03418162 (2016).

21. Frey, M. P., Schneider, M. K., Dietzel, A., Reichert, P. & Stamm, C. Predicting critical source areas for diffuse herbicide losses to surface waters: Role of connectivity and boundary conditions. *Journal of Hydrology* **365,** 23–36. ISSN: 00221694 (2009).

22. Lefrancq, M., Dijk, P. V., Jetten, V., Schwob, M. & Payraudeau, S. Improving runoff prediction using agronomical information in a cropped, loess covered catchment. *Hydrological Processes* **31,** 1408–1423 (2017).

23. Sheikh, V., Visser, S. & Stroosnijder, L. A simple model to predict soil moisture: Bridging Event and Continuous Hydrological (BEACH) modelling. *Environmental Modelling and Software* **24,** 542–556. ISSN: 13648152 (2009).

Chapter 1

General introduction

1.1 State of the art

1.1.1 Pesticide use and regulation

Agricultural pesticide use. Pesticide use represents a significant farm expenditure worldwide, ranging from 4 to 11% of total production costs [1] with herbicides making up to 65% of total pesticide expenditures [2]. Choloroacetanilides are an important family of pre-emergent herbicide used extensively for the control of annual grasses and broad leave weeds on a variety of crops including corn, sugar beet and sunflower. Of the acetanilide herbicides, S-metolachlor (SM) is one of the most persistent [3] with high sorptive properties [4] despite its relatively high water solubility (530 mg L^{-1} at 20 °C) and low organic carbon-water partition coefficient K_{oc} (62-372 ml g^{-1}). Although herbicides have diverse modes of action and target organisms, like most pesticides, they have in common that they are applied over large extensions of land. This represents an important source of diffuse pollution that is not only difficult to monitor and control but also leads to their frequent detection in ground and surface waters worldwide [5]. Their almost ubiquitous presence has led to important recent policy changes in the developed world [6]. However, despite both environmental policy plans and market promises of genetic engineering to reduce herbicide inputs [7], use extent has not seen significant improvements in the EU [8], and has worsen in the US for some of the most common crops over the last 25 yrs. [2, 7].

Development, approval and regulation. Pesticide legislation varies widely worldwide, with more stringent regulations typically found in developed countries [6]. Significant changes in legislation in recent years have been observed, allowing for example, implementation of new standards in the US and cross-country harmonization in the EU (Fig. 11). Developed countries in general require active substance manufacturers to submit an extensive application and environmental, health and safety dossier. In the EU for example, each member state then produces an initial draft assessment, which includes the active substance, its biological efficacy, toxicology and metabolism in mammals, its main metabolic pathway(s), residues, environmental fate and behavior in soil, water and air and ecotoxicological impact [9].

Although extensive registration and approval assessments are conducted for each new active ingredient, significant environmental behavior uncertainty remains for each new product for decades after its approval [9]. For example, environmental risk assessments only consider transformation products (TPs) that represent at least 10% of the initial active ingredient applied [10], irrespective of other TPs potential mobility characteristics or their inherent toxicity on non-target organisms [9]. Once in the environment active ingredients may be

reacted by a wide range of abiotic and biotic processes leading to a large number of unknown TPs whose ecotoxicological relevance may become apparent only 20-30 yrs. after market introduction [5]. Furthermore, many pesticides are chiral compounds (i.e., mirror images or non-superimposable structures) whose effect and environmental fate needs to be investigated separately as their impact and biodegradation may also be enantio-selective [11].

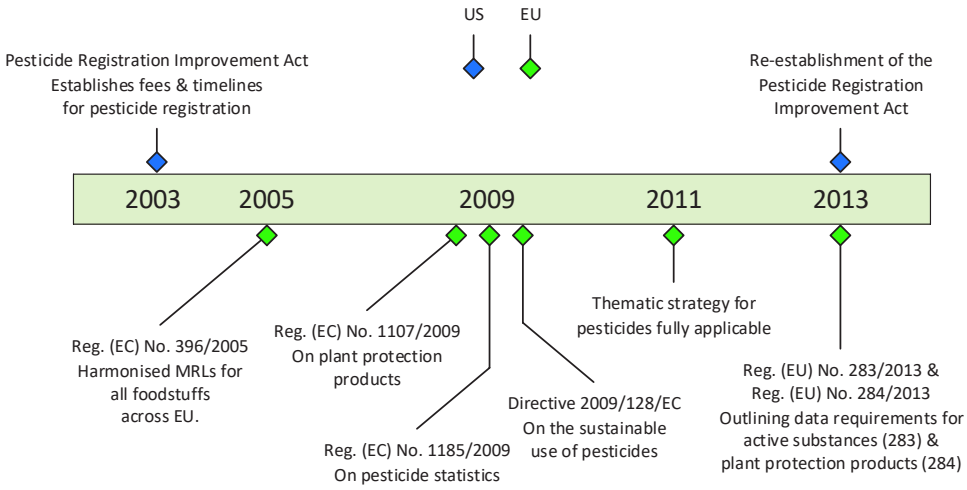

Figure 11: EU and US legislation changes since 2000, adapted from ref. [6].

1.1.2 Pesticide transformation and transport

Pesticide transformation in agricultural soils. Pesticides are degraded by chemical (abiotic) processes (i.e., photolysis, hydrolysis, oxidation and reduction reactions), and by microbial (biotic) activity following multiple pathways that may be dependent on climatic factors, microorganisms, soil constituents and individual pesticide properties [12]. SM degradation is primarily driven by biodegradation [13], with at least 25 TPs derived through oxidation, hydroxylation, O-demythlation, and N-dealkylation [14]. For SM, the major breakdown pathways in soils are mediated by aerobic and anaerobic microorganisms [3]. The transformation of SM into its two primary degradates (Fig. 12), metolachlor ethane sulfonic acid (MESA) and metolachlor oxanilic acid (MOXA), have been proposed to occur through the displacement of the chlorine atom of the parent compound *via* glutathione conjugation (i.e., antioxidant reaction) followed by enzymatic transformations [15]. Others also report the ability of soil indigenous fungi (*Aspergillus flavus and A. terricola*) to use SM as a carbon and nitrogen source with 6-methyl 2-ethyl acetanilide and 6-methyl 2-ethyl aniline as TPs [16].

While soil texture, pH and cation exchange capacity (CEC) have shown little influence on the degradation rate for SM [17], significant increases in degradation rates were observed in soils with higher organic matter (OM) content [13], higher ambient temperatures and moisture conditions [17]. Chemical (abiotic) transformation of SM has been shown to occur at rates 2.7 to 3.3 times lower than biological transformation [13]. SM hydrolysis' half-life at 20 °C under a wide range of pH values is expected at $>$ 200 days [18, 19]. More recently hydrolysis degradation rates ($k = 0.006 \pm 0.001$ days^{-1}, $DT_{50} \approx 115$ days) were obtained for SM under alkaline conditions (pH=12) at 30 °C and were insignificant at 20

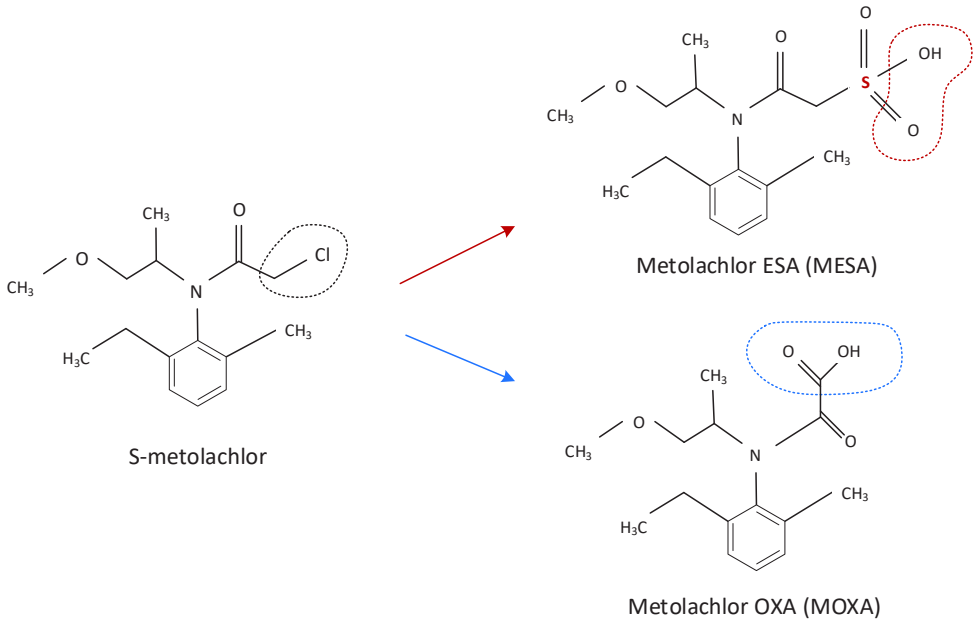

Figure 12: Principal S-metolachlor (SM) transformation products (TPs), MESA and MOXA.

°C [20]. Although photochemical breakdown in soils is expected to be low [21], in aquatic environments photolysis may yield several stable transformation products [22–24], some of which may in turn be further biodegraded into potentially more toxic stable compounds [25].

Degradation pathway studies can be expensive and time intensive with minor degradates being difficult to identify [26]. The use of quantitative structure activity relationship (QSAR) modelling software, constrained on biodegradability data from standardized OECD test guidelines [27], may thus be used as an alternative to experimental testing to predict degradation pathways and environmental persistence (e.g., BESS [28], CATABOL [29], PPS [30], PathPred [31], CATALOGIC [32], BNICE [33], and most recently, Eawag-PPS (former UM-PPS [34]). Statistical models include traditional regression as well as machine learning approaches and range from chemical class-specific to more broad approaches [27]. Although such approaches have experienced significant improvements in model sensitivity (i.e., accurate persistence classification and transformation products observed), model selectivity in contrast (i.e., prediction of irrelevant products) may need further development before they can be used as reliable tools for chemical risk assessments [26, 27]. In particular, the inclusion of biotransformation data (i.e. half-lives and pathway information) obtained from realistic scenarios (e.g. mixed soil microbial communities) and with well-defined environmental conditions is needed to improve validation across a wider range of environmental contexts [27].

The use of high-resolution mass spectrometry (HRMS) is also a novel analytical approach, with substantial harmonization across the scientific community [35], that is used to screen for target, suspect and non-target compounds in environmental samples. This approach now allows for the screening of a large number of pesticide metabolites (e.g., >150, [36–38]). Screening efforts however, are subject to greater uncertainty when analytical standards are not available, which is common place for pesticide transformation products. In this respect, the combination of HRMS and QSAR approaches (e.g., ref. [39]) supported by improvements

in software analytical features and the development of publicly available databases (e.g., ref. [27]) demonstrates the recent potential to improve screening through these efforts.

Although the combined use of HRMS and QSAR approaches provide an opportunity to improve mechanistic understanding of pesticide fate and evidence degradation in the environment, their use is limited in terms of providing quantitative accounts of degradation extent. Indeed, for management purposes, pesticide exposure predictive approaches at regional scales are needed [40], requiring the use of models to perform mass balance accounts that integrate landscape information [41] and that are able to reduce input and spatial uncertainty required to assess risk exposure [42]. Although HRMS and QSAR may be used for selecting priority substances to monitor [38], closing of mass balances by focusing on parent and TP concentrations alone is challenging to nearly impossible within large environmental contexts. Therefore, following organic contaminant research experience for legacy contaminants, a multiple lines of evidence approach that includes both detected TP concentrations and compound isotope signatures should be regarded as complementary and essential approaches for pesticide fate understanding and prediction in environmental systems.

Pesticide sinks and dynamics in agro-systems. The main pesticide sinks in agricultural soils include degradation, sorption, volatilization, leaching, plant uptake and offsite export *via* runoff and erosion. Although pesticide pools available for transport are primarily regulated by degradation, literature reported pesticide half-lives may typically range several orders of magnitude. This reflects the importance of both soil intrinsic conditions such as application histories, soil texture and soil biomass [43] and extrinsic factors such as meteorological conditions [17]. Similarly, although offsite transport is generally associated to the specific pesticide physico-chemical properties (e.g., pesticide-specific henry coefficient, solubility constant and the organic carbon-water partition coefficient (K_{oc} [44, 45]), phase transfer however, may be highly regulated also by both soil intrinsic factors (e.g., structure, organic matter content, clay content, iron oxides, etc.) and extrinsic factors such as hydrological conditions and agro-system context [46, 47].

Sorption may be an important process having impact on multiple scales. For example, although bioavailability to degrading microorganisms may decrease with ageing [48], pesticides may nevertheless accumulate in agricultural soils [49] and become available to larger organisms by soil ingestion (e.g., earthworms, cattle) and/or be transported to aquatic environments *via* erosion [50] with the potential to bioaccumulate on larger spatial scales [13, 51, 52]. Volatilization extent may not only be associated to the pesticide's henry constant, but may also be influenced by the application method (e.g. generating drift) [53] as well as climatic conditions (e.g., rainfall, temperature, wind and soil moisture) [54]. Pesticide uptake and persistence in plants can also be a significant process from a consumer perspective [55]. However, although metolachlor uptake has been observed to be negligible relative to other removal processes in some cases (e.g. [56]) in-plant metabolism and exudation back into soil have been found to be relevant, depending on plant type, amount applied and method of application [57, 58].

Principal hydrologically driven transport pathways may include artificial drainage and percolation to groundwaters through soil matrix- and preferential flows [59–61] as well as overland flows and erosion to surface waters [62]. Leaching risk has been positively correlated to the timing before rainfall after application, increasing also with pesticide persistence and clay content (i.e. due to earlier and more frequent generation of macropore flow) [47]. First rainfall events after application and major events in terms of total rainfall volumes may be however, the primary extrinsic factors regulating organic pesticide loss through leaching

[63]. The risk associated to pesticides being mobilized onto surface waters can be further associated to the landscape itself, where catchment connectivity [64, 65] and agricultural management practices (e.g., application periods, cropping systems, etc.) may be significant features in regulating transfer [66]. Rainfall-runoff mass export at the event-scale is regulated by multiple simultaneous processes [67] and includes diffusion through concentration gradients in top soils [68], ejection from the soil surface by rainfall impact and erosion [69–71], contact time of overland flow with top soil [72] and overland flow depth [73].

Understanding the relevance of the various simultaneous processes regulating pesticide attenuation is necessary to determine the sustainability of agricultural practices so as to minimize environmental risk and externalities incurred as costs by society at large. Quantification of the relative importance of each of these competing processes however, is a challenging task for the environmental manager. Although all processes contribute to reduce pesticide concentrations in the environment, degradation is the only process, beyond dilution, that contributes to sustainable pesticide removal, preventing long-term accumulation in environmental compartments with potential detrimental effects on ecosystems and water resources [49, 74]. In this respect, compound specific isotope analysis (CSIA) represents an advantage over concentration based assessments, which cannot determine the extent of degradation that a contaminant has undergone between sources and receptors in the field. In contrast, isotope fractionation can evidence degradation extent and pathways, even if no TPs are detected, as transformation leaves a biochemical imprint in the form of characteristic changes in isotope ratios of the reacting contaminant [75].

1.1.3 Pesticide compound specific isotope analysis (CSIA)

Definitions and basic concepts. Measuring isotope fractionation of stable elements (e.g., carbon, nitrogen) in organic compounds is a relatively new approach in contaminant hydrology to measure pollutant degradation [76]. Taking carbon as an example, with ^{13}C and ^{12}C referring to the heavy and light isotope respectively, the relative average abundance ($R = {}^{13}C/{}^{12}C$) in a compound such as SM is obtained by gas chromatography-isotope ratio mass spectrometry (GC-IRMS). The isotope ratio is reported in delta notation ($\delta^{13}C‰$) with respect to an international standard [77],

$$\delta^{13}C_{sample}[‰] = \frac{R_{sample} - R_{standard}}{R_{standard}} \cdot 1000 \tag{1.1}$$

where R_{sample} and $R_{standard}$ are the ratios ${}^{13}C/{}^{12}C$ of the sample and standard, respectively.

During chemical transformation, lighter isotopes (e.g., ^{12}C) exhibit lower activation energy, generally resulting in faster reaction times, relative to their heavier counterparts (e.g., ^{13}C). This difference in activation energies (Fig. 13) leads to a kinetic isotope effect (KIE) given by the ratio of the reaction constants (k) associated to each isotopologue (molecules containing light or heavy isotopes). For carbon, the KIE can be expressed as,

$$KIE_C = \frac{{}^{13}k}{{}^{12}k} \tag{1.2}$$

Normal isotope effects (KIE > 1) result in an enrichment of the heavier isotopologues in the non-degraded pesticide fraction remaining in environmental samples [75]. A fundamental

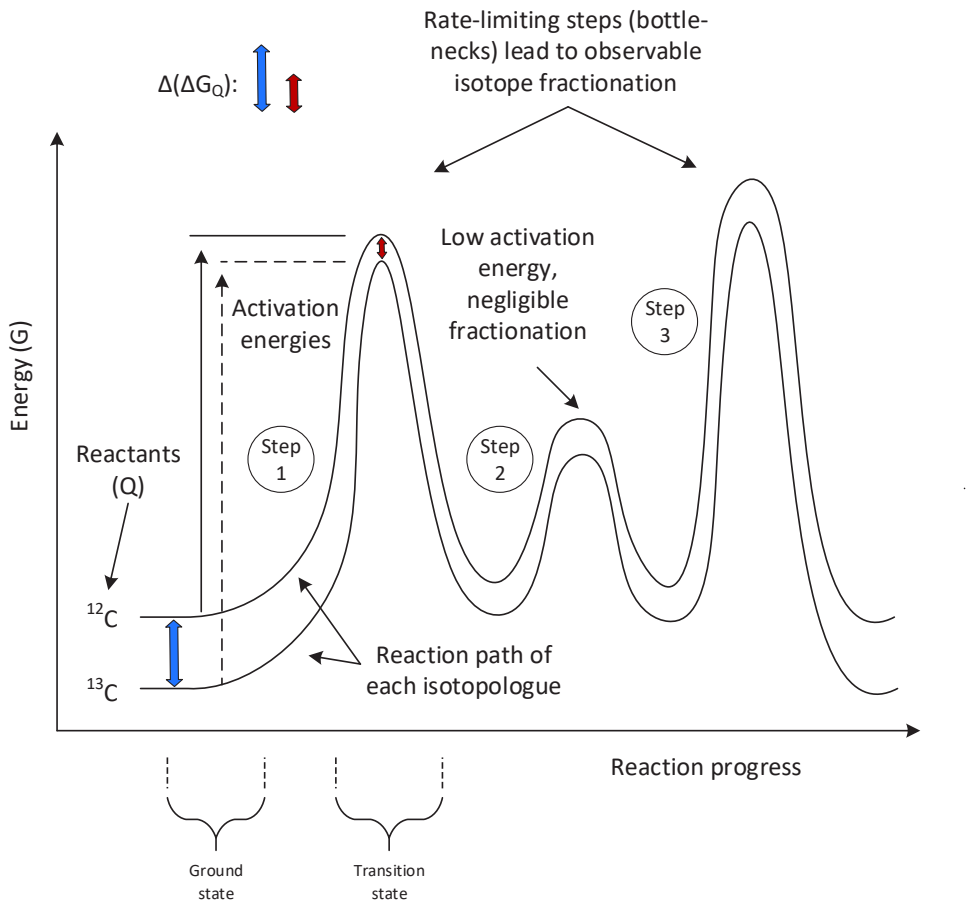

Figure 13: Energy differences between isotopologues during contaminant fractionation. Adapted from ref. [75].

assumption is that the bulk fractionation observed during degradation follows the Rayleigh distillation equation [78], allowing to relate changes in isotope ratios to changes in concentration [76],

$$\frac{R_t}{R_0} = \left(\frac{c_t}{c_0}\right)^{\alpha-1} \tag{1.3}$$

where c_t and c_0 are concentrations measured at any given time (subscript t) and at the start of the biochemical reaction (subscript 0). Changes in concentration due to degradation ($f_{deg} = c_t/c_0$) are then related to changes in isotope ratios through the fractionation factor α (-), typically expressed as characteristic enrichment ϵ (‰) $= \alpha - 1$ and obtained *via* the logarithmic form of eq. 1.3.

Isotope enrichment factors are obtained from laboratory experiments (microcosms or pure cultures) under closed system conditions and where changes in concentrations and isotope ratios are only affected by microbial biodegradation [79]. The obtained ϵ is usually only valid for a specific compound and specific degradation conditions [76]. Extrapolating these values

to field situations, where closed mass balances are not possible, can then be used to assess the extent of *in situ* biodegradation.

Bulk ϵ values typically reported may however, not be interpretable in terms of bond-specific rate constants, as the isotope of interest may be present on several positions, not all of which may be reactive [76]. To be able to compare the observed enrichment with values reported in the literature for well-defined reactions (i.e., reactions where KIE's are not "diluted" by multiple non-reactive positions), a correction is required to reflect the underlying apparent kinetic isotope effect (AKIE) such that [76],

$$AKIE = \frac{1}{1 + z \cdot \frac{n}{x} \cdot \epsilon_{bulk}/1000} \tag{1.4}$$

where n is the number of atoms of the given element, x is the number of indistinguishable reactive positions, and z is the number of positions in intramolecular competition. Using SM as an example, assuming a C-Cl reaction position, n = 15, x = 1 and z = 1.

Once an appropriate enrichment (ϵ_{lab}) has been obtained, its use during field application assessments as mentioned above, may be possible. Equation 1.3 can be rewritten based on the isotope signatures, once again for carbon, to obtain the degradation extent ($DE\%$) as,

$$f_{deg} = \Big(\frac{\delta^{13}C_t + 1}{\delta^{13}C_0 + 1}\Big)^{1/\epsilon_{lab}} \tag{1.5}$$

$$DE[\%] = (1 - f_{deg}) \cdot 100 \tag{1.6}$$

Application of the Rayleigh equation in the field however, requires an account of dilution processes as the measured remaining fraction in environmental samples is affected not only by degradation [80]. If a dilution factor F, reflecting the number of times the environmental sample has become diluted, could be determined, the total fraction observed in the field (f_{obs}) would equal [80],

$$f_{obs} = f_{deg} \cdot f_{dil} = \frac{f_{deg}}{F} \tag{1.7}$$

Incorporating F into the Rayleigh equation (i.e., eq. 1.5) in logarithmic form and simplifying the term on the right as $\frac{\delta^{13}C_t+1}{\delta^{13}C_0+1} = \Delta$,

$$\frac{1}{\epsilon_{lab}} \cdot ln\Big(\Delta\Big) = ln\Big(F \cdot f_{obs}\Big) \tag{1.8}$$

$$ln\ \Delta/\epsilon_{lab} = ln\ F + ln\ f_{obs} \tag{1.9}$$

$$F = e^{((ln\ \Delta/\epsilon_{lab}) - ln\ f_{obs})} \tag{1.10}$$

To obtain the relative contribution of degradation and dilution (e.g., off-site export, sorption), the open-system Rayleigh equation [80] can be applied to tops soils. The relative contribution of dilution and degradation to concentration decrease is represented by the factor ratio D*/B*, where dilution (D*) and breakdown (B*) factors are given by:

$$D^* = \frac{ln\ f_{dil}}{ln\ f_{obs}} \tag{1.11}$$

$$B^* = \frac{ln\ f_{deg}}{ln\ f_{obs}} = 1 - D^* \tag{1.12}$$

where $D^* \geq 0$ and $0 \leq B^* \leq 1$. For example, if $D^*/B^* = 0$ ($D^* = 0$; $B^* = 1$), the concentration decline is solely due to degradation, while if $D^*/B^* = 1$ ($D^* = B^* = 0.5$), the contribution of each processes to the logarithmic concentration decrease is equal [80].

Opportunity and challenges for pesticide CSIA. Research on legacy contaminants [81, 82] and nitrate pollution [83, 84], have shown CSIA to be a valuable complementary line of evidence to demonstrate degradation, persistence and source identification at various temporal and spatial scales. In contrast to degradation, non-destructive sinks (e.g., sorption, volatilization, dispersion) generally do not induce significant [85–87] or only minor isotope fractionation effects [88, 89]. Significant non-degrading fractionation has been observed to be relevant only under certain environmental conditions, such as plume fringes [90] under non-stationary states [91, 92], or when advective-diffusive processes do not control transport (i.e., dissolution of non-aqueous phase liquids) [93]. Therefore, provided that significant fractionation is not correlated with non-destructive sinks, CSIA generally allows to distinguish and quantify degradation extent [75, 94].

Although the use of CSIA to evidence degradation is well established for legacy compounds in contaminated sites [95], the occurrence of very low ($ng\ L^{-1}$ to $\mu g\ L^{-1}$) concentrations of pesticides and their polarity are two challenges precluding CSIA applications at environmental scales [96]. Even though environmental quantification limits for concentration based analysis are feasible within this range [36, 39], pre-concentration of sufficient amount of analyte (10-100 ng per injection) for CSIA requires sampling of large soil masses and/or water volumes. Extraction of target compounds from environmental samples however, is associated to concomitant enrichment of matrix components requiring purification or clean-up procedures [97, 98]. Extraction procedures may nevertheless lead to poor chromatographic resolution with insufficient baseline separation as well as method-specific isotope fractionation that can hardly be controlled or corrected [96].

Despite these analytical challenges, environmental applications in (quasi)stationary conditions are starting to emerge, as demonstrated from CSIA studies conducted in lab-scale wetlands [99], mesoscale aquifers [100], contaminated sites [101] and aquifers [97, 102]. A further level of complexity however, is the application of pesticide CSIA under nonstationary conditions, such as during event-based studies or over large spatial scales where multiple sources and events may lead to sudden pesticide pulses over an agricultural growing season. First efforts to track SM and acetochlor degradation *via* carbon isotope fractionation in water samples have been conducted for the Alteckendorf catchment (France) by combining conceptual modelling with plot runoff, drain and outlet observations during an agricultural season [103]. The study identified the value of using CSIA data to identify likely differences in degradation rates across catchment compartments. However, the limitations of this study

indicated one of the principal challenges of pesticide export monitoring at this scale, which is the requirement that sampling periods coincide with sudden pesticide load increases to be able to achieve minimum CSIA quantification limits. Indeed, this illustrates an important tradeoff for catchment studies seeking to either obtain detailed characterization of rainfall-runoff events or focus on long-term pesticide export from slow transport processes associated to flow components with typically low environmental concentrations. These challenges are thus further compounded when (i) continuous monitoring is required over a full growing season; (ii) where application dates may be unknown [104]; and/or (iii) where catchment response times evolve due to changes in soil hydraulic properties and agricultural practices [105].

1.1.4 Pesticide fate modelling: potential and existing limitations

Interest of modelling. To assess the sustainability of agricultural practices, interest in the development of modelling tools, whether indicators, conceptual, or physically based approaches, has grown significantly since the early 90's [65]. Physically based models, although often criticized as over-parameterized, have proven however to be the best approaches whenever process understanding, evolution of distributed state variables, or preservation of physical constraints is important [106]. In contrast to pesticide fate models (conceptual or process-based), environmental indicators (EIs) are intended to quickly and easily identify the risks associated to the use of pesticides at the farm or landscape level within a crop protection context [107]. They typically rely on empirical relationships to estimate risk transfer such as the GUS index [45] and the attenuation-retardation factor approach [108] and may include more complex information such as environmental conditions (e.g. distance to groundwater, soil properties) and pesticide use practices (e.g., quantities, application methods) [109]. Although EI's are generally more user-friendly and require only data that is readily available (e.g., [110]), their integration with process based approaches is necessary to account for (bio)chemical processes as well as spatial variability of physical properties (e.g. soil permeability) and agricultural landscape characteristics (e.g., connectivity) [65, 111]. Given the lack of validation approaches available for environmental indicators in the scientific literature, caution should be taken when these are employed as predictor tools [107]. The strong emphasis on pesticide properties in EIs (i.e., relative to process-based environmental interactions) may lead to a lack of applicability in contexts outside of their development scope [112]. In worst cases, policy programs, when considering EIs determined based on pesticide use quantity alone, may result in environmental perverse effects, such as for example by encouraging the use of higher risk products when such programs generate price dis-incentives of less risky products with higher standard dosages [113].

Parsimonious or conceptual models, in contrast to EI's, account for an increased level of environmental complexity. These types of models may divide the catchment into a series of interconnected reservoirs based on their hydrological functioning [65]. For example, approaches based on travel time distributions (TTDs), have provided insight into how reservoir mixing processes and flow component velocities can regulate stream solute concentrations for inorganic fertilizers [114] and herbicides [115]. More recently, this approach integrated CSIA to track herbicide fate, indicating distinct reactive reservoirs contributing to stream discharge concentrations and isotope signatures [103]. Although these types of models are valuable to characterize transport properties and conceptualize potentially distinct reactive reservoirs, they are limited in their ability to describe detailed interactions between spatially heterogeneous state variables and contaminant fate [106].

Physically-based distributed models integrate spatial variability of interdependent state vari-

ables (e.g., moisture, permeability, concentrations) and processes (e.g., rainfall, evapotranspiration) linked through mass conservation relationships (e.g., water and solute balances). The large number of detailed processes often requires also a large number of parameters, many of which can be constrained with a given uncertainty from measurements or expert knowledge [106]. Although the transferability of small scale physics (e.g., soil capillary potential, field capacity), validated in controlled environments, to the large-scale spatial grid (lumping-up) of distributed models has been questioned [116], all numerical models suffer from the need to simplify reality to greater or lesser degree. Therefore, choosing an appropriate model is dependent on the level of homogeneity to which a system (e.g., catchment) may be subject to while being able to provide the information sought [117]. As more detailed knowledge is required by environmental resource managers, physically based distributed models provide a specialized opportunity to improve pesticide fate understanding. In particular, to support risk assessments, numerical models can facilitate the evaluation of pesticide persistence and identify the primary transfer pathways for new or existing pesticides [65, 107, 117]. Models may also be used to evaluate agricultural practices, for example, by delineating areas of high transfer risk (and where application should be mitigated) [118] or to identify the potential impacts of climate change on pesticide fate [119].

Current gaps in pesticide fate modelling include the need to integrate detailed, spatially variable (bio)chemical and physical hydrological processes regulating degradation and transport at catchment scales. As discussed above, physically-based distributed models are ideal candidates for this task. However, significant improvements in numerical constraints are necessary given the large number of calibration parameters of such models. Parameters that control degradation rates are of particular importance given their relevance in controlling pesticide pools available for transfer [43] and the potential off-setting effect that persistence and mobility parameters may have with each other (i.e., due to parameter correlation) [104, 118]. In addition, accounting for temporal variability is of importance, as different pesticide processes may be of relevance at given temporal scales. Indeed, time-scale in distributed models may be used to define the level of detail to which hydrological processes (e.g., rainfall, ETP, etc.) interact with landscape features and land management practices. For example, while moisture and temperature may be of relevance for pesticide degradation over longer time scales (e.g., daily or seasonal) [117, 120], rapid transfer during hydrological forcing may be of most relevance at the event scale (e.g., minutes or hours). Therefore a further challenge is the integration of the relevant time scales in numerical approaches. On the one hand, these should provide an improved account of how daily fluctuations of hydro-climatic processes regulate pesticide degradation, and on the other hand, be capable of detailed representation of offsite export though runoff and erosion processes during significant hydrological events [60].

Existing models. A literature survey of 98 near-surface hydrological models developed over the last 20 yrs. [65, 117, 120–122] was conducted to identify existing model capabilities and limitations to simulate pesticide transport and degradation at catchment scale. From the identified models, 49% were spatially distributed, from which 25% included flexible time-step adjustment, allowing them to simulate both continuous and event-based scales. From the flexible and distributed models, 5 accounted for pesticide fate processes (AGNS, HSPF, MIKE SHE, NELUP and SHETRAN), including degradation, sorption, leaching, and mass export *via* runoff and erosion (Fig. 14), each of which is described below.

The Agricultural Non-Point Source model (AGNPS) was developed and is in current use by the US Department of Agriculture, Agricultural Research Service (USDA-ARS), the Minnesota Pollution Control Agency and the US Soil Conservation Service (SCS) [117, 123].

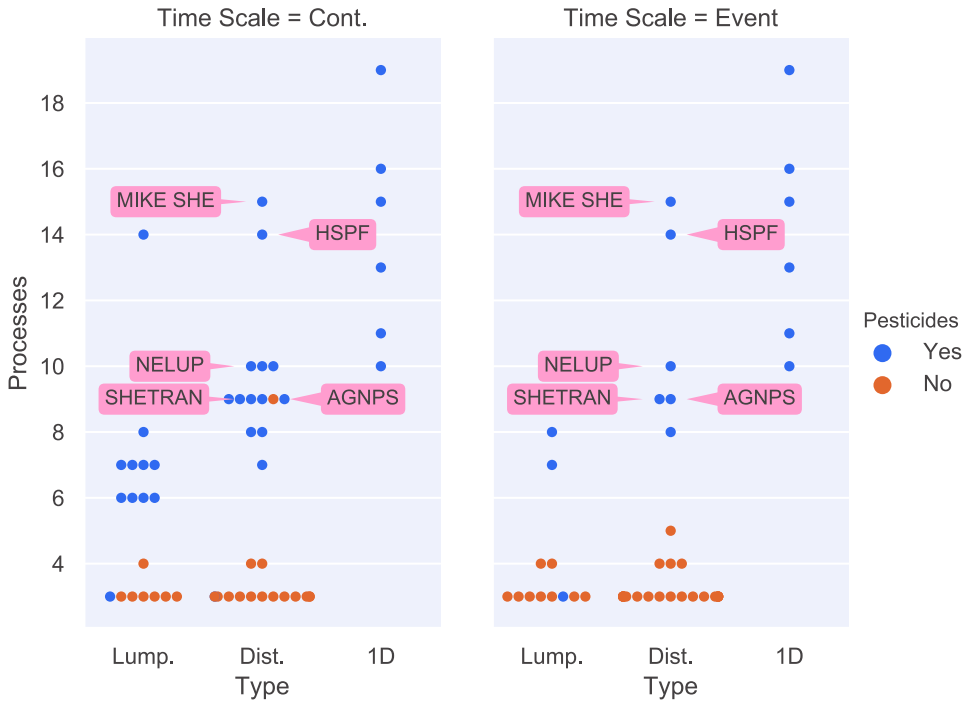

Figure 14: Survey of model types, including number of hydrological and pesticide processes considered. Models are categorized as lumped (Lump.), spatially distributed (Dist.) and those specialized for vertical transport (1D) across continuous (Cont.) and event-based (Event) time-scales. Orange dots depict models that account for only hydrological processes, while blue dots depict models that account for pesticides, in addition to hydrological processes.

AGNPS has a minimum spatial resolution of 0.4 ha, allowing it to simulate large watersheds up to 200 km^2 (max cell size: 16 ha) [117]. Although detailed hydrology and transport are considered, the minimum grid cell size requires a large degree of processes aggregation, resulting in a loss of spatial variability information that may be relevant for degradation processes [124] and catchment connectivity [64].

The Hydrological Simulation Program - Fortran (HSPF) was developed through contract with the U.S. Environmental Protection Agency (USEPA) to simulate watershed contaminant runoff processes including in-stream hydraulic and sediment-chemical interactions [121, 125, 126]. HSPF conceptualizes sub-basins as leveled detention storage areas and uses mass conservation-based continuity equations (simple storage-based non-linear reservoir) for flow routing. Due to its conceptualization of sub basins and spatially uniform continuity equations, HSPF is not adequate for simulating intense single-event storms [121]. Although HSPF has been incorporated as a non-point-source model into the USEPA's Better Assessment Science Integrating Point and Nonpoint Sources (BASINS) software [126], HSPF source code is a proprietary product and not available for public use or development.

The European Hydrological System model (MIKE SHE), developed by the Danish Hydraulic Institute [127] is perhaps one of the most complete simulation tools available in the market and accounting for the highest number of hydrological and pesticide-relevant fate processes from the reviewed tools. Multi-dimensional diffusive wave equations however, make SHE computationally intensive and subject to numerical instabilities when solving solution

schemes [121]. Although MIKE SHE would be suitable for small study catchments under either single rainfall events or continuous scales, computationally intensive numerical schemes may make it prohibitive for larger watersheds. Due to its proprietary nature, opportunity for open source code development remains limited.

The NERC-ESRC Land-Use Programme (NELUP) is a decision support system for predicting agricultural land use change impacts at river-basin scale [128]. The system is coupled with SHETRAN, a detailed physically based distributed model based on SHE [129] and therefore suffers from the same computational demands and limitations as MIKE SHE for large scale basins [130].

A class of 1D models accounting for the most number of both hydrological and pesticide-relevant processes are CRACK-NP, HYDRUS, MACRO and RZWQM (Fig 14). These models where initially developed to protect groundwater resources and therefore their focus has been on the detailed representation of macro pore flows along the soil column [59–61]. Different approaches have been taken to apply this type of models to the catchment scale where, for example, lateral flow processes where considered to be of marginal importance [131], or requiring coupling with GIS or 3D groundwater models [132–134]. Although models at this scale face a significant lack of data for validation, most applications consider simplified approaches to modelling runoff. Namely, only RZWQM accounts for pesticide solutes in runoff and none consider pesticide export *via* erosion [60]. Furthermore, although some of these models implement degradation dependence on temperature and moisture conditions, degradation rates are treated as calibration parameters with concentrations as sole data constraint.

Based on models reviewed, two principal challenges for modelling pesticide fate and transfer at catchment scale were identified. On the one hand, there is a need for models that account for both hydrological and chemical process with explicit integration of spatial heterogeneity and that are capable of integrating event-based and continuous temporal scales. Namely, integration of the spatial heterogeneity of agricultural landscapes [65], hydrological connectivity [64] and farm management practices [105] is required for the detail account of pesticide transport during periods of hydrological forcing at the event scale. However, the values of state variables (e.g., soil physical properties, moisture conditions and pesticide pools) at the onset of an event are not only key in representing the event response [105] but also evolve across space and time-scales beyond the event itself, requiring models that couple both time-scales seamlessly but that remain computationally efficient. On the other hand, there is a lack of available pesticide fate and transfer data, particularly with respect to better pesticide degradation constraints, that is required to validate such models at catchment scale. Therefore, models are needed that are capable of accounting for both the long-term evolution of state variables including how degradation regulates pesticide pools, while also being able to provide detailed account of pesticide transport processes, in particular during periods of high transfer risk.

Distributed, physically based models may be the most suitable candidates for this task, as they can simulate the impact of agricultural changes while integrating feedbacks between hydrological and chemical processes at various time-scales [65]. Although two physically-based distributed models capable of integrating this information were identified (MIKE SHE and HSPF), their application to large catchments is limited due to the long computation times required to solve their numerical schemes. Therefore, an appropriate alternative for the representation of processes beyond the event-scale would be the development of physically-based approaches capable of distributed water and chemical balance modelling that do not

make use of complex numerical schemes required to solve mass continuity equations. GIS and cartographic modelling systems such as PCRaster [135] allow for representation of state variables across space by discretization of the landscape into individual cells, each with its own set of attributes or properties, and with the ability to receive and transmit information to and from neighboring cells [135]. By using CSIA as data constraint, these models may thus be appropriate for representing the spatial evolution of state variables, such as degradation rates regulating pesticide pools available at the onset of major hydrological events. The output of these models may then be used as initial condition states, produced as input maps, for specialized event-based distributed models capable of representing rainfall-runoff and erosion driven pesticide export at catchment scale.

1.2 Summary of gaps of knowledge and implications

Herbicides are an important crop protection technology for conventional agriculture, taking a significant share of farmer's cost investments [2]. While herbicides have diverse modes of action and target organisms, they are generally applied over large extensions of land, being important sources of diffuse pollution that is not only difficult to monitor and control, but also results in their frequent detection in ground and surface waters worldwide [5]. S-metolachlor (SM), one of the most persistent members of the chloroacetanilide family [3], is a pre-emergent herbicide used world-wide for the control of annual grasses and broad leave weeds on major crops. Although field assessments and laboratory tests are required before active ingredients are introduced to market, the fate and degradation extent of pesticides and their metabolites in the environment is subject to significant uncertainty [9]. Not only are most transformation products (TPs) not known, preventing any detailed mass balance accounts of pesticide fate, but also their inherent toxicity on non-target organisms is disregarded in registration and approval dossiers [10]. Although the use of high-resolution mass spectrometry has increased the ability to screen for many analytes [39], the large number of TPs and the uncertainty of their degradation pathways [26] still prevents a reliable account of the extent of degradation that a given pesticide undergoes across space and time.

Disentangling pesticide degradation from dilution during field studies. Pesticide may be attenuated through various sinks in the environment, including sorption, volatilization, degradation, leaching, plant uptake and offsite export through runoff and erosion. The relative importance of each of these processes is dependent on the interaction of the pesticide physico-chemical properties with the local environment (e.g., soil properties) and the meteorological, hydrological and agro-system context [12, 44, 45, 64]. The numerous and simultaneous processes regulating pesticide attenuation present a challenging task for the environmental manager. Although all processes contribute to the reduction of pesticide concentrations in the environment, degradation is the only sink contributing to sustainable removal, preventing long-term accumulation in environmental compartments with potential detrimental effects on ecosystems and water resources [49, 74]. In this respect, compound specific isotope analysis (CSIA) represents an advantage over concentration based assessments, which cannot determine the extent of degradation that a contaminant undergoes between sources and receptors. In contrast, isotope fractionation can evidence degradation extent and pathways, even if no TPs are detected, as transformation leaves a biochemical imprint in the form of characteristic changes in isotope ratios of the reacting contaminant [75]. However, the potential of pesticide CSIA to identify pesticide sources, transport extent and reactive processes in soil and at agricultural catchment scale has yet to be evaluated.

Although the use of CSIA to evidence degradation is well established for legacy compounds

in contaminated sites [95, 136], the occurrence of very low ($ng\ L^{-1}$ to $\mu g\ L^{-1}$) concentrations of pesticides and their polarity lead to analytical challenges (i.e., detection sensitivity and matrix effects) precluding CSIA applications at environmental scales [96]. Despite these analytical challenges however, quasi(stationary) applications of pesticide CSIA ranging from small scale lab-based systems to contaminated site evaluations have begun to emerge [97, 99–102]. First efforts to track SM and acetochlor degradation in non-stationary environments [103] have demonstrated both the principal challenges of CSIA pesticide export monitoring and the potential value of CSIA to identify likely differences in degradation rates across catchment compartments. Indeed, characterization of pesticide degradation in source soils and representation of their fate and transport through physically-based distributed models for predicting export is still lacking.

Improving pesticide degradation constraints in field modelling. Interest in the development of modelling tools to evaluate pesticide fate has grown significantly since the early 90's [65]. From the various tools available to date, physically based models have proven to be the best approaches in cases where process understanding, evolution of distributed state variables (e.g., moisture, permeability, concentrations), or preservation of physical constraints are important [106]. A key drawback of these model types however is that, due to the large number of processes accounted for, also a large number of parameters is often required. Although many of these parameters may be constrained from measurements and expert knowledge [106], the interaction of physical and chemical processes with environmental conditions at different scales can lead to an important source of uncertainty when parameters controlling pesticide dissipation (e.g., phase transfer, transport and degradation) compensate one another [104, 137]. Therefore, as more detailed knowledge required by environmental resource managers has encouraged the development of more complex physically based models [65, 107, 117], a concomitant effort should be required to integrate improvements in data constraints. In this respect, having mechanistic information associated to degradation processes at different times and at different spatial locations would prove crucial in eliminating compensating effects from correlated parameters, which to date are associated to significant model equifinality and uncertainty.

Integrating CSIA into distributed models with variable time-scales. Despite the large number of models developed over the last two decades, only a few can integrate spatially distributed processes relevant for pesticide degradation and transport at multiple time-scales. Although highly detailed models exist (e.g., HSPF and MIKE SHE), their propriety rights often limit their open source development necessary to integrate novel approaches such as CSIA, which is critical for the constraint of models within realistic environmental contexts. Furthermore, the computationally intensive numerical schemes required to solve continuity equations of such models limits their application with large catchments over continuous time-scales. Therefore, to bridge this gap a combination of a computationally efficient, but physically realistic, distributed model capable of simulating continuous processes, and integrating CSIA, over a full growing season is required. The seamless coupling of such a model with a distributed event-based model capable of detailed representation of rapid pesticide export *via* runoff and erosion would then be required to account for relevant time-scales for predicting pesticide fate at catchment scale. Precluding the effective development and implementation of catchment scale models however, is the lack of available data sets able to improve pesticide degradation constraints. To do so, both concentration and CSIA data at various spatial and temporal scales is first required to characterize pesticide degradation in catchment source soils and their transport during hydrological pulses.

1.3 Thesis goal and objectives

The main goal of this thesis is to advance the use of pesticide CSIA to evaluate and predict pesticide degradation and fate in real environmental contexts. Although recent analytical advances have demonstrated the feasibility of CSIA to evaluate pesticides in lab-scale applications and groundwater contexts, their application under highly dynamic near-surface hydrological environments is yet to be validated. Based on the identified knowledge gaps, the specific objectives of this thesis are to:

i Design and implement a near-surface hydrological headwater catchment scale characterisation data collection campaign for monitoring S-metolachlor (SM) degradation and fate in source soils and discharged waters. The data set should be based on a multiple lines of evidence approach that includes SM and major metabolite concentrations, as well as carbon-based CSIA.

ii Based on the collected data set, establish a proof of concept for the use of CSIA to monitor pesticide fate and degradation in unsteady near-surface hydrological environments, outlining challenges, trade-offs and opportunities for larger scale applications. Interpretation of laboratory-based soil degradation mesocosm experiments should under specific moistures and temperatures should be used to support field data interpretation.

iii Investigate hydrological and transport formalisms at the laboratory and event scales to support their implementation in larger scale models.

iv Develop a continuous, physically-based distributed model capable of simulating evolution of soil hydraulic properties and pesticide pools by integrating CSIA data as degradation constraint. The model should be able to address the added value of incorporating pesticide CSIA towards the reduction of degradation parameter uncertainty during field scale applications

v Couple the continuous model developed during this work with an event-based model capable of detailed simulation of pesticide export, including CSIA, during intense hydrological events that generate runoff and erosion to aquatic ecosystems.

1.4 Thesis outline

The thesis is structured into an introductory section (**Chapter 1**) highlighting the main gaps of knowledge in the field and justifying the thesis objectives; a results section (**Chapters 2 - 5**) presenting published and working scientific contributions; and a general discussion and implications section (**Chapters 6 - 7**) that provides concluding remarks from the three approaches (lab experiments, field characterization and modelling at both scales) that guided this Ph.D. thesis work (Fig. 15). Namely, work approaches included two dimensions including system characterization (x-axis) and system modelling (y-axis) moving from controlled and well-defined lab experiments to larger scales with increasing complexity (z-axis).

Chapter 2 establishes a proof of concept for the use of carbon-based CSIA, in addition to SM and major transformation product (TP) concentrations, to monitor pesticide degradation and transport at the catchment scale. The study collected weekly soil samples along three transects representative of different locations of the Alteckendorf (France) catchment (47 ha). Continuous flow proportional water sampling at the outlet allowed for detailed hydrograph

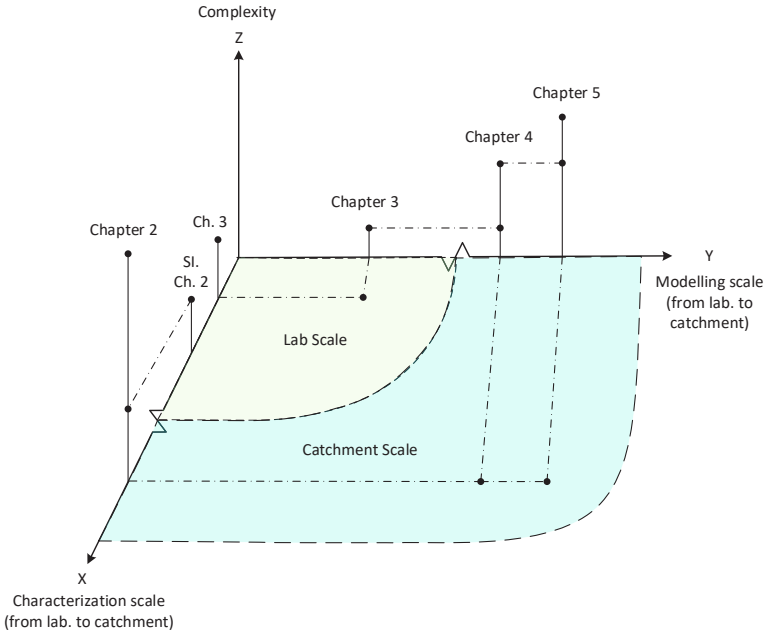

Figure 15: Ph.D. thesis work approaches, including system characterization (x-axis) and system modelling (y-axis), with increasing complexity (z-axis) from well-defined lab experiments to catchment scales. Intersection points indicate synergies between research conducted at different scales and/or levels of complexity.

characterization of SM $\delta^{13}C$ and concentration export in dissolved and particulate phases throughout one growing season. Comparisons of source soil isotope signatures across the catchment showed similar trends in outlet water samples ($\Delta\delta^{13}C \approx 3‰$, Deg. $\approx 87\%$), demonstrating the ability to continuously monitor catchment-wide degradation extent *via* through discharge sampling at the outlet.

Chapter 3 evaluates the impact of rainfall intensity and frequency on the export of heavy-metal and organic pesticides, including SM, from agricultural top soils. Twelve experimental modalities combining soil types (crop and vineyard), pollutant ageing (0 and 10 days) and rainfall patterns (intensity, duration and volume) were evaluated. A parsimonious numerical model was developed to simulate leaching and transfer to ponding waters, validate the experimental set-up and explore mobility parameter values regulating export across modalities. The study demonstrated the primary role that extrinsic factors (i.e., rainfall frequency and patterns) have on pesticide export relative to intrinsic factors (i.e., soil types). In particular, the first rainfall event and total rainfall volumes (rather than intensity) were the dominant factors controlling export.

Chapter 4 develops an existing distributed hydrological model (BEACH) by including transport and reactive processes and capable of accounting for pesticide CSIA, denoting the new model as Pesticide-isotopes BEACH (PiBEACH). In addition to the model's ability to simulate moisture evolution, capabilities to simulate temperature, soil hydraulic and crop property evolution over continuous (i.e., seasonal) scales are further integrated. In contrast to constant degradation reference values (DT_{50}) retained in many physically based models, the model capabilities are used to evaluate the impact of hydro-climatic factors (moisture and temperature optimums for bacterial activity) regulating degradation in top soils leading to

an improved representation of degradation rates and fluctuations across time. The inclusion of CSIA data however, was key as a numerical constraint, reducing both model equifinality and reference DT_{50} standard deviations by at least a factor of 2. The ability to constrain models considering hydro-climatic dependence on degradation rates also reduced 95% confidence interval ranges for offsite export through top soil leaching by a factor of 2. Results show that integrating CSIA data to constrain degradation in catchment source soils can significantly reduce uncertainty in pesticide field assessments where the pesticide half-life is a sensitive parameter to calibrate models describing and predicting pesticide fate. The use of long-term continuous models constrained by CSIA may thus be a significant contribution to the determination of pesticide pools available for transfer at the onset of major hydrological events.

Chapter 5 couples PiBEACH with the existing open source Limburg Soil Erosion Model (LISEM), denoting the coupled model as PiBEACH-oL. In addition to introducing the coupling logic, the chapter provides results from the coupling exercise, indicating improvement in the representation of hydrological components contributing to outlet discharge. Preliminary Monte Carlo simulation results of outlet SM concentrations and $\delta^{13}C$ from the coupled *vs.* the uncoupled model are provided and a discussion of model limitations and recommendations for its further development are provided.

Chapter 6 presents concluding remarks with respect to the approaches used to evaluate pesticide degradation and transport during this thesis including transversal discussion of (i) pesticide CSIA at the catchment scale in unsteady hydrological conditions; (ii) lab-scale experiments to support catchment-scale pesticide CSIA and modelling; and (iii) modelling pesticide fate at the catchment scale using CSIA data.

Chapter 7 summarizes implications of the Ph.D. thesis with respect to the use of CSIA for monitoring pesticide fate at catchment scale, improving numerical model constraints and reducing fate uncertainty. Finally, the chapter opens perspectives for larger-scale (e.g., river-catchment scale) pesticide fate studies.

1.5 Publication summary and author contribution

1.5.1 Published articles

Alvarez-Zaldívar, P., Payraudeau, S., Meite, F., Masbou, J., and Imfeld, G. (2018). Pesticide degradation and export losses at the catchment scale: Insights from compound-specific isotope analysis (CSIA). *Water Research*, 139:198-207.

Meite, F., **Alvarez-Zaldívar, P.**, Crochet, A., Wiegert, C., Payraudeau, S., and Imfeld, G. (2018). Impact of rainfall patterns and frequency on the export of pesticides and heavy metals from agricultural soils. *Science of the Total Environment*, 616-617 (Dec.): 500-509.

Lange, J., Olsson, O., Sweeney, B., Herbstritt, B., Reich, M., **Alvarez-Zaldívar, P.**, Payraudeau, S. & Imfeld, G. (2017) Fluorescent tracers to evaluate pesticide dissipation and transformation in agricultural soils. *Science of The Total Environment*, 619-620 (Oct.).

Alvarez-Zaldívar, P., Centler, F., Maier, U., Thullner, M. & Imfled, G. (2016) Biogeochemical modelling of *in situ* biodegradation and stable isotope fractionation of intermediate chloroethenes in a horizontal subsurface flow wetland. *Ecological Engineering*, Vol. 90 (May)

1.5.2 Articles in preparation

Alvarez-Zaldívar, P., Imfeld, G., Van Dijk, P. and Payraudeau, S. (Expected 2019). Constraining pesticide degradation in distributed catchment models with compound-specific isotope analysis (CSIA). *Submitted to ES&T, under review.*

Alvarez-Zaldívar, P., Imfeld, G., Lefrancq, M., Ackerer, P., Jetten, V., and Payraudeau, S. (Expected 2019). Coupling spatially distributed event-based and continuous models to improve long-term simulation of pesticide degradation and rapid export at catchment scales. *In preparation.*

References

1. Popp, J., Peto, K. & Nagy, J. Pesticide productivity and food security. A review. *Agronomy for Sustainable Development* **33,** 243–255. ISSN: 17740746 (2013).
2. Kniss, A. R. Long-term trends in the intensity and relative toxicity of herbicide use. *Nature Communications* **8,** 14865 (Apr. 2017).
3. Rivard, L. *Environmental Fate of Metolachlor* tech. rep. (Environmental Monitoring Branch, Sacramento, California, 2003). `http://www.cdpr.ca.gov/docs/emon/pubs/fatememo/metolachlor.pdf`.
4. Liu, W., Gan, J., Papiernik, S. & Yates, S. Structural influences in relative sorptivity of chloroacetanilide herbicides on soil. *Journal of Agricultural and Food Chemistry.* **48,** 4320–4325 (2000).
5. Fenner, K., Canonica, S., Wackett, L. P. & Elsner, M. Evaluating Pesticide Degradation in the Environment: Blind Spots and Emerging Opportunities. *Science* **341,** 752–758. ISSN: 0036-8075 (2013).
6. Handford, C. E., Elliott, C. T. & Campbell, K. A review of the global pesticide legislation and the scale of challenge in reaching the global harmonization of food safety standards. *Integrated Environmental Assessment and Management* **11,** 525–536. ISSN: 15513793 (2015).

7. Russell, K. & Hakim, D. *Broken Promises of Genetically Modified Crops* Oct. 2016. https://nyti.ms/2jRm1lS.
8. Hossard, L., Guichard, L., Pelosi, C. & Makowski, D. Lack of evidence for a decrease in synthetic pesticide use on the main arable crops in France. *Science of the Total Environment* **575,** 152–161. ISSN: 18791026 (2017).
9. Storck, V., Karpouzas, D. G. & Martin-Laurent, F. Towards a better pesticide policy for the European Union. *Science of the Total Environment* **575,** 1027–1033. ISSN: 18791026 (2017).
10. EC No. 283, E.-R. *EU-Regulation 283/2013/EC of 1 March 2013 setting out the data requirements for active substances, in accordance with Regulation (EC No 1107/2009 of the European Parliament and of the Council concerning the placing of plant protection products on the mark* 2013. https://eur-lex.europa.eu/LexUriServ/LexUriServ.do?uri=OJ:L:2013:093:0001:0084:EN:PDF.
11. Müller, T. A. & Kohler, H. P. Chirality of pollutants - Effects on metabolism and fate. *Applied Microbiology and Biotechnology* **64,** 300–316. ISSN: 01757598 (2004).
12. Arias-Estévez, M. *et al.* The mobility and degradation of pesticides in soils and the pollution of groundwater resources. *Agriculture, Ecosystems and Environment* **123,** 247–260. ISSN: 01678809 (2008).
13. Wu, X., Li, M., Long, Y. & Liu, R. Effects of adsorption on degradation and bioavailability of metolachlor in soil. *Soil Science and Plant Nutrition* **11,** 83–97. ISSN: 07189516 (2011).
14. Roberts, T. R., Roberts, T. R. & Hutson, D. H. *Metabolic Pathways of Agrochemicals, Part 1: Herbicides and Plant Growth Regulators* 849 (Royal Society of Chemistry, Great Britain, Cambridge, 1998).
15. Field, J. A. & Thurman, E. M. Glutathione conjugation and contaminant transformation. *Environmental Science and Technology* **30,** 1413–1418. ISSN: 0013936X (1996).
16. Sanyal, D. & Kulshrestha, G. Metabolism of metolachlor by fungal cultures. eng. *Journal of agricultural and food chemistry* **50,** 499–505. ISSN: 0021-8561 (Print) (Jan. 2002).
17. Long, Y. H., Li, R. Y. & Wu, X. M. Degradation of S -metolachlor in soil as affected by environmental factors. *Journal of Soil Science and Plant Nutrition* **14,** 189–198 (2014).
18. Kollman, W. & Segawa, R. *Interim Report of the Pesticide Chemistry Database* tech. rep. (Environmental Protection Agency, US, California, 1995), 1–20. https://www.cdpr.ca.gov/docs/emon/pubs/ehapreps/eh9504.pdf.
19. EXTOXNET. *EXTOXNET. Extension Toxicology Network. Pesticide Information Profiles.* 1996. http://extoxnet.orst.edu/pips/metolach.htm.
20. Masbou, J., Drouin, G., Payraudeau, S. & Imfeld, G. Carbon and nitrogen stable isotope fractionation during abiotic hydrolysis of pesticides. *Chemosphere* **213,** 368–376. ISSN: 00456535 (2018).
21. PPDB. *The Pesticide Properties Database* Developed by the Agriculture & Environment Research Unit (AERU), University of Hertfordshire, funded by UK national sources and the EU-funded FOOTPRINT project (FP6-SSP-022704). 2009.
22. Kochany, J. & Maguire, R. J. Sunlight Photodegradation of Metolachlor in Water. *Journal of Agricultural and Food Chemistry* **42,** 406–412. ISSN: 15205118 (1994).

23. Wilson, R. I. & Mabury, S. a. Photodegradation of metolachlor: Isolation, identification, and quantification of monochloroacetic acid. *Journal of Agricultural and Food Chemistry* **48,** 944–950. ISSN: 00218561 (2000).

24. Dimou, A. D., Sakkas, V. a. & Albanis, T. a. Metolachlor photodegradation study in aqueous media under natural and simulated solar irradiation. *Journal of Agricultural and Food Chemistry* **53,** 694–701. ISSN: 00218561 (2005).

25. Gutowski, L., Olsson, O., Leder, C. & Kümmerer, K. A comparative assessment of the transformation products of S-metolachlor and its commercial product Mercantor Gold(®) and their fate in the aquatic environment by employing a combination of experimental and in silico methods. *The Science of the total environment* **506-507,** 369–379. ISSN: 1879-1026 (Feb. 2015).

26. Boxall, A. B. A., Sinclair, C. J., Fenner, K., Kolpin, D. & Maund, S. J. Peer Reviewed: When Synthetic Chemicals Degrade in the Environment. *Environmental Science & Technology* **38,** 368A–375A. ISSN: 0013-936X (2004).

27. Latino, D. A. *et al.* Eawag-Soil in enviPath: a new resource for exploring regulatory pesticide soil biodegradation pathways and half-life data. *Environmental science. Processes & impacts* **19,** 449–464. ISSN: 20507895 (2017).

28. Punch, B., Patton, A., Miagkikh, V., Larson, B. & Forney, L. *A Biodegradability Evaluation and Simulation System (BESS), Applying and Discovering Knowledge of Biodegradation Pathways*

29. Jaworska, J., Dimitrov, S., Nikolova, N. & Mekenyan, O. Probabilistic assessment of biodegradability based on metabolic pathways: catabol system. eng. *SAR and QSAR in environmental research* **13,** 307–323. ISSN: 1062-936X (Print) (Mar. 2002).

30. Hou, B. K., Ellis, L. B. M. & Wackett, L. P. Encoding microbial metabolic logic: predicting biodegradation. eng. *Journal of industrial microbiology & biotechnology* **31,** 261–272. ISSN: 1367-5435 (Print) (July 2004).

31. Moriya, Y. *et al.* PathPred: an enzyme-catalyzed metabolic pathway prediction server. *Nucleic Acids Research* **38,** W138–W143. ISSN: 0305-1048 (July 2010).

32. Dimitrov, S. *et al.* Simulation of chemical metabolism for fate and hazard assessment. II CATALOGIC simulation of abiotic and microbial degradation. eng. *SAR and QSAR in environmental research* **22,** 719–755. ISSN: 1029-046X (Electronic) (Oct. 2011).

33. Finley, S. D., Broadbelt, L. J. & Hatzimanikatis, V. Computational framework for predictive biodegradation. eng. *Biotechnology and bioengineering* **104,** 1086–1097. ISSN: 1097-0290 (Electronic) (Dec. 2009).

34. Ellis, L. B. M., Gao, J., Fenner, K. & Wackett, L. P. The University of Minnesota pathway prediction system: predicting metabolic logic. *Nucleic Acids Research* **36,** W427–W432. ISSN: 0305-1048 (July 2008).

35. Schymanski, E. L. *et al.* Non-target screening with high-resolution mass spectrometry: Critical review using a collaborative trial on water analysis. *Analytical and Bioanalytical Chemistry* **407,** 6237–6255. ISSN: 16182650 (2015).

36. Reemtsma, T., Alder, L. & Banasiak, U. A multimethod for the determination of 150 pesticide metabolites in surface water and groundwater using direct injection liquid chromatography-mass spectrometry. *Journal of Chromatography A* **1271,** 95–104. ISSN: 00219673 (2013).

37. Moschet, C., Götz, C., Longrée, P., Hollender, J. & Singer, H. Multi-level approach for the integrated assessment of polar organic micropollutants in an international lake catchment: The example of lake constance. *Environmental Science and Technology* **47,** 7028–7036. ISSN: 0013936X (2013).

38. Rousis, N. I. *et al.* Monitoring a large number of pesticides and transformation products in water samples from Spain and Italy. *Environmental Research* **156,** 31–38. ISSN: 10960953 (2017).

39. Kern, S., Fenner, K., Singer, H. P., Schwarzenbach, R. P. & Hollender, J. Identification of transformation products of organic contaminants in natural waters by computer-aided prediction and high-resolution mass spectrometry. *Environmental Science and Technology* **43,** 7039–7046. ISSN: 0013936X (2009).

40. Finizio, A. & Villa, S. Environmental risk assessment for pesticides. *Environmental Impact Assessment Review* **22,** 235–248. ISSN: 01959255 (2002).

41. Verro, R. *et al.* GIS-based system for surface water risk assessment of agricultural chemicals. 1. Methodological approach. *Environmental science & technology* **36,** 1532–8. ISSN: 0013-936X (2002).

42. Verro, R., Finizio, A., Otto, S. & Vighi, M. Predicting Pesticide Environmental Risk in Intensive Agricultural Areas . II : Screening Level Risk Assessment of Complex Mixtures in Surface Waters Predicting Pesticide Environmental Risk in Intensive Agricultural Areas . II : Screening Level Risk Assess. **43,** 530–537. ISSN: 0013936X (2009).

43. Wang, Y., Lai, A., Latino, D., Fenner, K. & Helbling, D. E. Evaluating the environmental parameters that determine aerobic biodegradation half-lives of pesticides in soil with a multivariable approach. *Chemosphere* **209,** 430–438. ISSN: 18791298 (2018).

44. Whelan, G., Strenge, D. L., Droppo, J. J. G., Steelman, B. L. & Buck, J. W. *The Remedial Action Priority System (RAPS): Mathematical Formulations. PNL-6200* tech. rep. (Pacific Northwest Laboratory, Richland, Washington, 1987).

45. Gustafson, D. I. Groundwater ubiquity score: A simple method for assessing pesticide leachability. *Environmental Toxicology and Chemistry* **8,** 339–357 (1989).

46. Huang, B. *et al.* Aging effect on the leaching behavior of heavy metals (Cu, Zn, and Cd) in red paddy soil. *Environmental Science and Pollution Research* **22,** 11467–11477. ISSN: 0944-1344 (2015).

47. Nolan, B. T. *et al.* Identification of key climatic factors regulating the transport of pesticides in leaching and to tile drains. *Pest Management Science* **64,** 933–944. ISSN: 1526-4998 (2008).

48. Alexander, M. Aging, bioavaiability, and overestimation of risk from environmental pollutants. *Environmental Science & Technology* **34,** 4259–4265 (2000).

49. Sabatier, P. *et al.* Long-term relationships among pesticide applications, mobility, and soil erosion in a vineyard watershed. *Proceedings of the National Academy of Sciences of the United States of America* **111,** 15647–52. ISSN: 1091-6490 (2014).

50. Lefrancq, M., Payraudeau, S., Guyot, B., Millet, M. & Imfeld, G. Correction to Degradation and Transport of the Chiral Herbicide S-Metolachlor at the Catchment Scale: Combining Observation Scales and Analytical Approaches. *Environmental Science & Technology* **52,** 5517. ISSN: 0013-936X (May 2018).

51. Sadler, R. *et al.* Bioaccumulation of organochlorine pesticides from contaminated soil by cattle. *Toxicological & Environmental Chemistry* **87,** 575–582 (2005).

52. Katagi, T. & Ose, K. Toxicity, bioaccumulation and metabolism of pesticides in the earthworm. *Journal of Pesticide Science* **40,** 69–81 (2015).

53. Lefrancq, M. *et al.* Fungicides transport in runoff from vineyard plot and catchment: Contribution of non-target areas. *Environmental Science and Pollution Research* **21,** 4871–4882. ISSN: 16147499 (2014).

54. Prueger, J. H. *et al.* Solar radiation, relative humidity, and soil water effects on metolachlor volatilization. *Environmental Science and Technology* **39,** 5219–5226. ISSN: 0013936X (2005).

55. Juraske, R., Castells, F., Vijay, A., Muñoz, P. & Antón, A. Uptake and persistence of pesticides in plants: Measurements and model estimates for imidacloprid after foliar and soil application. *Journal of Hazardous Materials* **165,** 683–689 (June 2009).

56. Chen, Z., Chen, Y., Vymazal, J., Kule, L. & Koželuh, M. Dynamics of chloroacetanilide herbicides in various types of mesocosm wetlands. *Science of the Total Environment* **577,** 386–394. ISSN: 18791026 (2017).

57. Al-Khatib, K., Baumgartner Unland, J., Olson, B. L. S. & Graham, D. W. Alachlor and metolachlor transformation pattern in corn and soil. *Weed Science* **50,** 581–586. ISSN: 0043-1745 (Sept. 2002).

58. Henderson, K. L., Belden, J. B. & Coats, J. R. Mass balance of metolachlor in a grassed phytoremediation system. *Environmental Science and Technology* **41,** 4084–4089. ISSN: 0013936X (2007).

59. Kördel, W., Egli, H. & Klein, M. Transport of pesticides via macropores (IUPAC Technical Report). *Pure and Applied Chemistry* **80,** 105–160. ISSN: 1365-3075 (2008).

60. Köhne, J. M., Köhne, S. & Simunek, J. A review of model applications for structured soils: b) Pesticide transport. *Journal of Contaminant Hydrology* **104,** 36–60. ISSN: 01697722 (2009).

61. Klaus, J. *et al.* Controls of event-based pesticide leaching in natural soils: A systematic study based on replicated field scale irrigation experiments. en. *Journal of Hydrology* **512,** 528–539. ISSN: 00221694 (May 2014).

62. Oliver, D. P. *et al.* Off-site transport of pesticides in dissolved and particulate forms from two land uses in the Mt. Lofty Ranges, South Australia. *Agricultural Water Management* **106,** 78–85. ISSN: 03783774 (2012).

63. Meite, F. *et al.* Impact of rainfall patterns and frequency on the export of pesticides and heavy-metals from agricultural soils. *Science of the Total Environment* **616-617,** 500–509. ISSN: 18791026 (2018).

64. Frey, M. P., Schneider, M. K., Dietzel, A., Reichert, P. & Stamm, C. Predicting critical source areas for diffuse herbicide losses to surface waters: Role of connectivity and boundary conditions. *Journal of Hydrology* **365,** 23–36. ISSN: 00221694 (2009).

65. Payraudeau, S. & Gregoire, C. Modelling pesticides transfer to surface water at the catchment scale: A multi-criteria analysis. *Agronomy for Sustainable Development* **32,** 479–500. ISSN: 17740746 (2012).

66. Cassigneul, A. *et al.* Nature and decomposition degree of cover crops influence pesticide sorption: Quantification and modelling. *Chemosphere* **119,** 1007–1014. ISSN: 18791298 (2015).

67. Shi, X. N., Wu, L. S., Chen, W. P. & Wang, Q. J. Solute Transfer from the Soil Surface to Overland Flow: A Review. *Soil Science Society of America Journal* **75,** 1214–1225. ISSN: 0361-5995 (2011).

68. Wallach, R., Jury, W. A. & Spencer, W. F. Transfer of Chemicals from Soil Solution to Surface Runoff: A Diffusion-based Soil Model. *Soil Science Society of America Journal* **52,** 612–618 (1988).

69. Gao, B., Todd, Steenhuis, T., Hogarth, W. & Parlange, Y. Rainfall induced chemical transport from soil to runoff: theory and experiments. *Journal of Hydrology* **295,** 291–304. ISSN: 00221694 (2004).

70. Gao, B. *et al.* Investigating raindrop effects on transport of sediment and non-sorbed chemicals from soil to surface runoff. *Journal of Hydrology* **308,** 313–320. ISSN: 00221694 (2005).

71. Dong, W., Wang, Q., Zhou, B. & Shan, Y. A simple model for the transport of soil-dissolved chemicals in runoff by raindrops. *Catena* **101,** 129–135. ISSN: 03418162 (2013).

72. Wallach, R., Grigorin, G. & Rivlin, J. A comprehensive mathematical model for transport of soil-dissolved chemicals by overland flow. *Journal of Hydrology* **247,** 85–99. ISSN: 00221694 (2001).

73. Wallach, R., Grigorin, G. & Rivlin, J. The errors in surface runoff prediction by neglecting the relationship between infiltration rate and overland flow depth. *Journal of Hydrology* **200,** 243–259. ISSN: 00221694 (1997).

74. Vörösmarty, C. J. *et al.* Global threats to human water security and river biodiversity. *Nature* **468,** 555–561. ISSN: 0028-0836 (2010).

75. Elsner, M. Stable isotope fractionation to investigate natural transformation mechanisms of organic contaminants: principles, prospects and limitations. *Journal of environmental monitoring : JEM* **12,** 2005–31. ISSN: 1464-0333 (2010).

76. Elsner, M., Zwank, L., Hunkeler, D. & Schwarzenbach, R. P. A new concept linking observable stable isotope fractionation to transformation pathways of organic pollutants. *Environmental Science and Technology* **39,** 6896–6916. ISSN: 0013936X (2005).

77. Clark, I. & Fritz, P. *Environmental isotopes in hydrogeology* 328 (Lewis Publishers, New York, 1997).

78. Rayleigh, L. S. Theoretical considerations respecting the separation of gases by diffusion and similar processes. *Philosophical Magazine* **42,** 493–498 (1896).

79. Thullner, M., Kampara, M., Richnow, H. H., Harms, H. & Wick, L. Y. Impact of bioavailability restrictions on microbially induced stable isotope fractionation. 1. Theoretical calculation. *Environmental Science and Technology* **42,** 6544–6551. ISSN: 0013936X (2008).

80. Van Breukelen, B. M. Quantifying the degradation and dilution contribution to natural attenuation of contaminants by means of an open system Rayleigh equation. *Environ. Sci. Technol.* **41,** 4980–4985 (2007).

81. Sherwood Lollar, B. *et al.* Stable carbon isotope evidence for intrinsic bioremediation of tetrachloroethene and trichloroethene at Area 6, Dover Air Force Base. *Environmental Science and Technology* **35,** 261–269. ISSN: 0013936X (2001).

82. Hunkeler, D., Meckenstock, R. U., Lollar, B. S., Schmidt, T. C. & Wilson, J. T. A Guide for Assessing Biodegradation and Source Identification of Organic Ground Water Contaminants using Compound Specific Isotope Analysis (CSIA). *USEPA Publication* **EPA 600/R-,** 1–82. ISSN: ¡null¿ (2008).

83. Nestler, A. *et al.* Isotopes for improved management of nitrate pollution in aqueous resources: Review of surface water field studies. *Environmental Science and Pollution Research* **18,** 519–533. ISSN: 09441344 (2011).

84. Fenech, C., Rock, L., Nolan, K., Tobin, J. & Morrissey, A. The potential for a suite of isotope and chemical markers to differentiate sources of nitrate contamination: A review. *Water Research* **46,** 2023–2041. ISSN: 00431354 (2012).

85. Slater, G. F., Ahad, J. M., Sherwood Lollar, B., Allen-King, R. & Sleep, B. Carbon isotope effects resulting from equilibrium sorption of dissolved VOCs. *Analytical Chemistry* **72,** 5669–5672. ISSN: 00032700 (2000).

86. Schüth, C., Taubald, H., Bolaño, N. & Maciejczyk, K. Carbon and hydrogen isotope effects during sorption of organic contaminants on carbonaceous materials. *Journal of Contaminant Hydrology* **64,** 269–281. ISSN: 01697722 (2003).

87. Ratti, M., Canonica, S., McNeill, K., Bolotin, J. & Hofstetter, T. B. Isotope Fractionation Associated with the Indirect Photolysis of Substituted Anilines in Aqueous Solution. *Environmental Science and Technology* **49,** 12766–12773. ISSN: 15205851 (2015).

88. Ratti, M., Canonica, S., McNeill, K., Bolotin, J. & Hofstetter, T. B. Isotope Fractionation Associated with the Photochemical Dechlorination of Chloroanilines. *Environmental Science and Technology* **49,** 9797–9806. ISSN: 15205851 (2015).

89. Kopinke, F. D., Georgi, A., Imfeld, G. & Richnow, H. H. Isotope fractionation of benzene during partitioning - Revisited. *Chemosphere* **168,** 508–513. ISSN: 00456535 (2017).

90. Van Breukelen, B. M. & Rolle, M. Transverse hydrodynamic dispersion effects on isotope signals in groundwater chlorinated solvents plumes. *Environmental Science and Technology* **46,** 7700–7708. ISSN: 0013936X (2012).

91. Kopinke, F. D., Georgi, A., Voskamp, M. & Richnow, H. H. Carbon isotope fractionation of organic contaminants due to retardation on humic substances: Implications for natural attenuation studies in aquifers. *Environmental Science and Technology* **39,** 6052–6062. ISSN: 0013936X (2005).

92. Van Breukelen, B. M. & Prommer, H. Beyond the rayleigh equation: Reactive transport modeling of isotope fractionation effects to improve quantification of biodegradation. *Environmental Science and Technology* **42,** 2457–2463. ISSN: 0013936X (2008).

93. Aeppli, C. *et al.* Influence of mass-transfer limitations on carbon isotope fractionation during microbial dechlorination of trichloroethene. *Environmental Science and Technology* **43,** 8813–8820. ISSN: 0013936X (2009).

94. Thullner, M., Centler, F., Richnow, H.-H. & Fischer, A. Quantification of organic pollutant degradation in contaminated aquifers using compound specific stable isotope analysis – Review of recent developments. *Organic Geochemistry* **42,** 1440–1460. ISSN: 0146-6380 (Jan. 2012).

95. Thullner, M., Richnow, H.-h. & Fischer, A. in *Environmental and Regional Air Pollution* (eds Gallo, D. & Mancini, R.) chap. 2 (Nova Science Publishers, Inc., 2009).

96. Elsner, M. & Imfeld, G. Compound-specific isotope analysis (CSIA) of micropollutants in the environment - current developments and future challenges. *Current Opinion in Biotechnology* **41,** 60–72. ISSN: 18790429 (2016).

97. Schreglmann, K., Hoeche, M., Steinbeiss, S., Reinnicke, S. & Elsner, M. Carbon and nitrogen isotope analysis of atrazine and desethylatrazine at sub-microgram per liter concentrations in groundwater. *Analytical and bioanalytical chemistry* **405,** 2857–2867. ISSN: 16182650 (2013).

98. Masbou, J., Meite, F., Guyot, B. & Imfeld, G. Enantiomer-specific stable carbon isotope analysis (ESIA) to evaluate degradation of the chiral fungicide Metalaxyl in soils. *Journal of Hazardous Materials* **353,** 99–107. ISSN: 18733336 (2018).

99. Elsayed, O. F. *et al.* Using compound-specific isotope analysis to assess the degradation of chloroacetanilide herbicides in lab-scale wetlands. *Chemosphere* **99,** 89–95. ISSN: 00456535 (2014).

100. Schürner, H. K. *et al.* Compound-Specific Stable Isotope Fractionation of Pesticides and Pharmaceuticals in a Mesoscale Aquifer Model. *Environmental Science and Technology* **50,** 5729–5739. ISSN: 15205851 (2016).

101. Milosevic, N. *et al.* Combined isotope and enantiomer analysis to assess the fate of phenoxy acids in a heterogeneous geologic setting at an old landfill. *Water Research* **47,** 637–649. ISSN: 00431354 (2013).

102. Bashir, S., Hitzfeld, K. L., Gehre, M., Richnow, H. H. & Fischer, A. Evaluating degradation of hexachlorcyclohexane (HCH) isomers within a contaminated aquifer using compound-specific stable carbon isotope analysis (CSIA). *Water Research* **71,** 187–196. ISSN: 18792448 (2015).

103. Lutz, S. R. *et al.* Pesticide fate at catchment scale: conceptual modelling of stream CSIA data. *Hydrology and Earth System Sciences Discussions* **21,** 5243–5261. ISSN: 1812-2116 (2017).

104. Gassmann, M., Khodorkovsky, M., Friedler, E., Dubowski, Y. & Olsson, O. Uncertainty in the river export modelling of pesticides and transformation products. *Environmental Modelling and Software* **51,** 35–44. ISSN: 13648152 (2014).

105. Lefrancq, M., Dijk, P. V., Jetten, V., Schwob, M. & Payraudeau, S. Improving runoff prediction using agronomical information in a cropped, loess covered catchment. *Hydrological Processes* **31,** 1408–1423 (2017).

106. Fatichi, S. *et al.* An overview of current applications , challenges , and future trends in distributed process-based models in hydrology. *Journal of Hydrology* **537,** 45–60. ISSN: 0022-1694 (2016).

107. Dubus, I. & Surdyk, N. *State of the art on pesticide fate models and environmental indicators. Report DL#4 of the FP6 EU-funded FOOTPRINT project.* tech. rep. (EU-Footprint, 2006), 39. `www.eu-footprint.org`.

108. Rao, P. S., Hornsby, A. G. & Jessup, R. E. *INDICES FOR RANKING THE POTENTIAL FOR PESTICIDE CONTAMINATION OF GROUNDWATER* eng. Tech. rep. 0 (1985), 23–25.

109. Padovani, L., Trevisan, M. & Capri, E. A calculation procedure to assess potential environmental risk of pesticides at the farm level. *Ecological Indicators* **4,** 111–123. ISSN: 1470160X (2004).

110. Kudsk, P., Jørgensen, L. N. & Ørum, J. E. Pesticide Load—A new Danish pesticide risk indicator with multiple applications. *Land Use Policy* **70,** 384–393. ISSN: 0264-8377 (2018).

111. Brown, C., Hart, A., Lewis, K. & Dubus, I. p-EMA (I): simulating the environmental fate of pesticides for a farm-level risk assessment system. *Agronomie* **23,** 67–74. ISSN: 11254718 (2003).

112. Holmes, G. Australia's pesticide environmental risk assessment failure: The case of diuron and sugarcane. *Marine Pollution Bulletin* **88,** 7–13. ISSN: 18793363 (2014).

113. Möhring, N., Gaba, S. & Finger, R. Quantity based indicators fail to identify extreme pesticide risks. *Science of the Total Environment* **646,** 503–523. ISSN: 18791026 (2019).

114. Benettin, P., Van Der Velde, Y., Van Der Zee, S. E., Rinaldo, A. & Botter, G. Chloride circulation in a lowland catchment and the formulation of transport by travel time distributions. *Water Resources Research* **49,** 4619–4632. ISSN: 00431397 (2013).

115. Bertuzzo, E., Thomet, M., Botter, G. & Rinaldo, A. Catchment-scale herbicides transport: Theory and application. *Advances in Water Resources* **52,** 232–242. ISSN: 03091708 (2013).

116. Beven, K. Changing ideas in hydrology - The case of physically-based models. *Journal of Hydrology* **105,** 157–172. ISSN: 00221694 (1989).

117. Merritt, W. S., Letcher, R. A. & Jakeman, A. J. A review of erosion and sediment transport models. *Environmental Modelling and Software* **18,** 761–799. ISSN: 13648152 (2003).

118. Lindahl, A. M. L., Söderström, M. & Jarvis, N. Influence of input uncertainty on prediction of within-field pesticide leaching risks. *Journal of Contaminant Hydrology* **98,** 106–114. ISSN: 01697722 (2008).

119. Steffens, K. *et al.* Direct and indirect effects of climate change on herbicide leaching - A regional scale assessment in Sweden. *Science of the Total Environment* **514,** 239–249. ISSN: 18791026 (2015).

120. Quilbé, R., Rousseau, A. N., Lafrance, P., Leclerc, J. & Amrani, M. Selecting a pesticide fate model at the watershed scale using a multi-criteria analysis. *Water Quality Research Journal of Canada* **41,** 283–295. ISSN: 12013080 (2006).

121. Borah, D. K. & Bera, M. Watershed-Scale Hydrologic and Nonpoint-Source Pollution Models: Review of Mathematical Bases. *Transactions of the ASAE* **46,** 1553–1566. ISSN: 2151-0059 (2003).

122. Pandey, A., Himanshu, S. K., Mishra, S. K. & Singh, V. P. Physically based soil erosion and sediment yield models revisited. *Catena* **147,** 595–620. ISSN: 03418162 (2016).

123. Young, R. A., Onstad, C. A., Bosch, D. D. & Anderson, W. P. AGNPS: A nonpoint-source pollution model for evaluating agricultural watersheds. *Journal of Soil and Water Conservation* **44,** 168–173. ISSN: 1941-3300 (1989).

124. Ghafoor, A., Jarvis, N. J., Thierfelder, T. & Stenström, J. Measurements and modeling of pesticide persistence in soil at the catchment scale. *The Science of the total environment* **409,** 1900–8. ISSN: 1879-1026 (2011).

125. Donigian, A. S. J., Bicknell, B. R. & Kittle, J. L. J. *Conversion of the Chesapeake Bay basin model to HSPF operation. Prepared by AQUA TERRA Consultants for the Computer Sciences Corporation and U.S. EPA Chesapeake Bay Program* tech. rep. (AQUA TERRA Consultants, Annapolis, Md., 1986).

126. BASINS. *BASINS 4.1 (Better Assessment Science Integrating point & Non-point Sources) Modeling Framework.* North Carolina, 2015. `https://www.epa.gov/ceam/better-assessment-science-integrating-point-and-non-point-sources-basins` (2018).

127. Danish Hydraulic Institute. *MIKE SHE water movement – user guide and technical reference manual, Edition 1.1.* tech. rep. (DHI, 1998).

128. O'Callaghan, R. J. NELUP: an introduction. *Journal of Environmental Planning and Management* **38,** 5–20 (1995).

129. Ewen, J., Parkin, G. & O'Conell, P. E. SHETRAN : Distributed River Basin Flow Modeling System. *Journal of Hydrologic Engineering* **5,** 250–258. ISSN: 1084-0699 (2000).

130. Dunn, S. M., Mackay, R., Adams, R. & Oglethorpe, D. R. The hydrological component of the NELUP decision-support system: An appraisal. *Journal of Hydrology* **177,** 213–235. ISSN: 00221694 (1996).

131. Lindahl, A. M. L. *et al.* Stochastic modeling of diffuse pesticide losses from a small agricultural catchment. *Journal of environmental quality* **34,** 1174–85. ISSN: 0047-2425 (2005).

132. Herbst, M., Hardelauf, H., Harms, R., Vanderborght, J. & Vereecken, H. Pesticide fate at regional scale: Development of an integrated model approach and application. *Physics and Chemistry of the Earth, Parts A/B/C* **30,** 542–549. ISSN: 1474-7065 (2005).

133. Esposito, A. *et al.* A spatialising tool to simulate pesticide fate in the unsaturated zone on a catchment scale. *Agronomy for Sustainable Development* **25,** 279–283 (2005).

134. Sinkevich Jr., G. *et al.* A GIS-Based Ground Water Contamination Risk Assessment Tool for Pesticides. *Ground Water Monitoring & Remediation Water* **25,** 82–91 (2005).

135. Karssenberg, D., Schmitz, O., Salamon, P., de Jong, K. & Bierkens, M. F. P. A software framework for construction of process-based stochastic spatio-temporal models and data assimilation. *Environmental Modelling & Software* **25,** 489–502 (2010).

136. Meckenstock, R. U., Morasch, B., Griebler, C. & Richnow, H. H. Stable isotope fractionation analysis as a tool to monitor biodegradation in contaminated acquifers. *Journal of Contaminant Hydrology* **75,** 215–255. ISSN: 01697722 (2004).

137. Honti, M. & Fenner, K. Deriving persistence indicators from regulatory water-sediment studies - Opportunities and limitations in OECD 308 data. *Environmental Science and Technology* **49,** 5879–5886. ISSN: 15205851 (2015).

Preface to Chapter 2

Addressing the first and second goals of this thesis, the following chapter establishes a proof of concept for the use of carbon-based CSIA, to monitor pesticide degradation and transport at the catchment scale. The chapter describes in detail the characterization of catchment top soils and outlet waters, which in addition to CSIA, targeted SM and major transformation product (TP) concentrations following a multiple line of evidence approach.

Interpretation of field samples is supported by data obtained from previously validated soil and water extraction methods as well as closed system soil microcosm degradation experiments. The latter were used to determine reference isotope enrichment values, *via* the Rayleigh equation, allowing to derive field estimations of degradation and dilution extents.

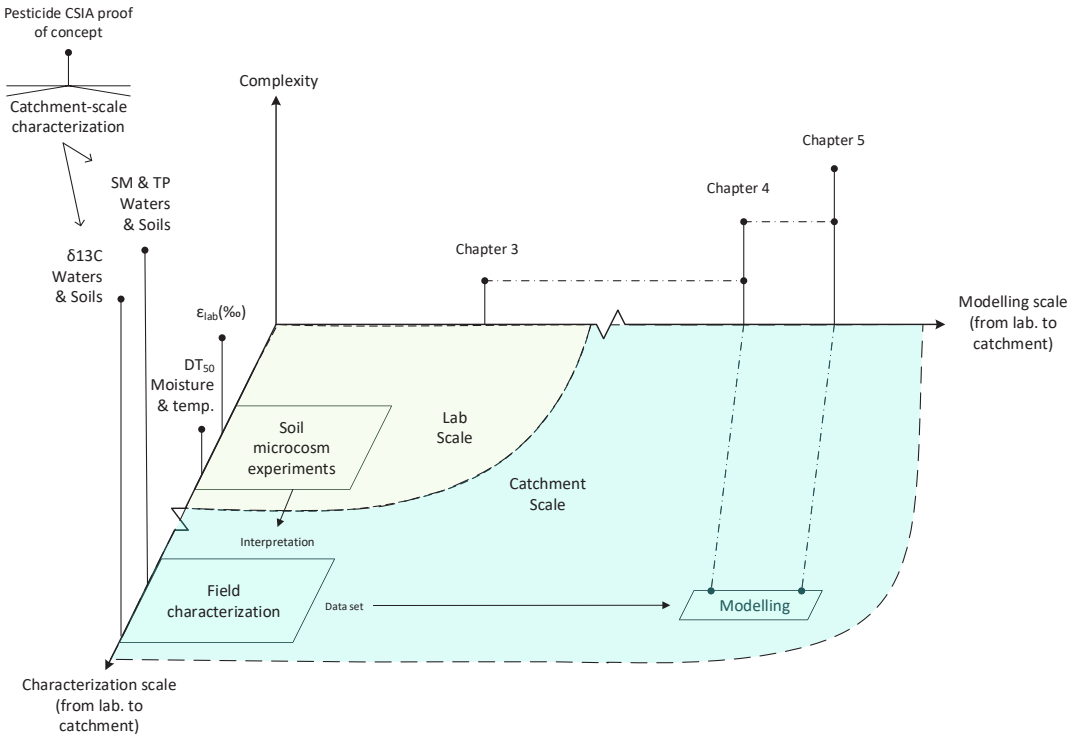

Chapter 2

Pesticide degradation and export losses at catchment scale: insights from compound-specific isotope analysis (CSIA)*

Abstract. Although pesticides undergo degradation tests prior to use, determining their export, degradation and persistence under field conditions remains a challenge for water resource management. Compound specific isotope analysis (CSIA) can provide evidence of contaminant degradation extent, as it is generally independent of non-destructive dissipation (e.g., dilution, sorption, volatilization) regulating environmental concentrations. While this approach has been successfully implemented in subsurface environments, its application to pesticides in near-surface hydrological contexts at catchment scale is lacking. This study demonstrates the applicability of CSIA to track pesticide degradation and export at catchment scale and identify pesticide source areas contributing to changes in stable isotope signature in stream discharge under dynamic hydrological contexts. Based on maximum shifts in carbon stable isotope signatures ($\Delta\delta^{13}C = 4.6 \pm 0.5‰$) of S-metolachlor (SM), a widely used herbicide, we estimate maximum degradation to have reached 96 ± 3% two months after first application. Maximum shifts in nitrogen isotope signatures were small and inverse ($\Delta\delta^{15}N = -1.3 \pm 0.6‰$) indicating potential secondary isotope effects during degradation. In combination with a mass balance approach including SM main degradation products, total catchment non-destructive dissipation was estimated to have reached 8 ± 7% of the applied product. Our results show that CSIA can be applied to evaluate natural attenuation of pesticides at catchment scale. By providing a more detailed account of pesticide dissipation and persistence under field conditions we anticipate the contribution of pesticide CSIA to the improvement of regulatory and monitoring strategies.

2.1 Introduction

The widespread occurrence of micro-pollutants in surface and groundwater poses a threat to human water security and river biodiversity on a global scale [1]. Among organic micro-pollutants, pesticides are one of the principal contributors to chemical risk [2] with the potential to accumulate over decades in various environmental compartments [3, 4]. Despite comprehensive exposure assessments and research evaluating toxicity, degradability

* This chapter is the edited version of: Alvarez-Zaldívar, P., Payraudeau, S., Meite, F., Masbou, J., and Imfeld, G. (2018). Pesticide degradation and export losses at the catchment scale: Insights from compound-specific isotope analysis (CSIA). *Water Research*, 139:198-207

and transformation products, current approaches often fail to determine where, when and how pesticide degradation occurs. This highlights the difficulties to bridge information obtained under laboratory and field conditions. Beyond regulatory testing, complementary novel management strategies (e.g., [5]) that enable monitored natural or engineered attenuation are thus warranted.

In contrast with current monitoring approaches, which are unable to distinguish among competing environmental sinks, compound specific isotope analysis (CSIA) allows for the direct quantification of pesticide degradation extent [6]. During chemical transformation, lighter isotopes (e.g., ^{12}C) exhibit lower activation energy, generally resulting in faster reaction times relative to their heavier counterparts (e.g., ^{13}C). This leads to an enrichment of the heavier isotopologues in the non-degraded pesticide fraction remaining in environmental samples [6]. The resulting average isotope value (e.g., $\delta^{13}C$) of the non-degraded fraction can then be used to quantify degradation by following the Rayleigh distillation equation [7]. Research on legacy contaminants [8, 9] and nitrate pollution [10, 11], have shown CSIA to be a valuable complementary line of evidence to demonstrate degradation, persistence and source identification at various temporal and spatial scales. Akin to these approaches, application of CSIA to pesticides relies on the ability to monitor changes in stable isotope composition between source(s) and outlet to quantify the extent of (bio)chemical conversion at the catchment scale.

This study evaluated the feasibility of carbon-based CSIA as a first characterization approach for monitoring pesticide fate at catchment scale under dynamic hydrological and rainfall-runoff conditions. The use of carbon-based CSIA to evidence natural attenuation is well established for legacy compounds in contaminated sites [12] and thus may be considered as a relevant approach to monitor pesticide degradation and export across distinct hydrological events. However, principal limitations to the applicability of pesticide CSIA at catchment scale are the occurrence of low (sub-μg L^{-1}) environmental concentrations, which lead to challenges in analyte extraction and quantification under field contexts [13, 14]. While changes in $\delta^{13}C$ tend to be smaller in larger molecules [6], the higher contribution of carbon atoms to the total molecular mass may allow for the collection of more environmental samples at or above quantification limits. This is of particular interest when seeking detailed characterization of rainfall-runoff events requiring high-resolution data made possible by flow-proportional sampling strategies. An important trade-off however, is the limitations in sample volumes that may be achieved due to automatic sampler unit capacities, therefore challenging catchment-scale CSIA studies during discharge periods where environmental concentrations are low. In this respect, although multi-element CSIA may also be desirable to further improve characterization [14], its feasibility will be challenged by the sampling window where quantification limits can be achieved.

Based on a carbon-based CSIA high resolution monitoring strategy, the objectives of this study were then to (i) demonstrate the validity of pesticide CSIA as a complementary line of evidence for quantifying degradation extent under field conditions; (ii) infer off-site losses due to non-destructive dissipation (e.g., dilution, volatilization, sorption) and; (iii) demonstrate applicability of pesticide CSIA under shifting hydrological regimes. To address these objectives, the study tracked S-metolachlor (SM) in an agricultural headwater catchment (47 ha) during one growing season, a period where degradation and off-site transfer risk is most relevant. As a well characterized and widely used herbicide (i.e., 4.2% of global pesticide use) that is frequently detected in groundwaters [5], SM is a relevant model compound for establishing a first effort of catchment-wide pesticide CSIA characterization.

Each component guiding the development of this chapter is illustrated in Fig. 21. Colored boxes in the schema outline information obtained from the catchment, farmer survey, laboratory and consulted databases. Numbered items represent subsections described in detail in appendix A.

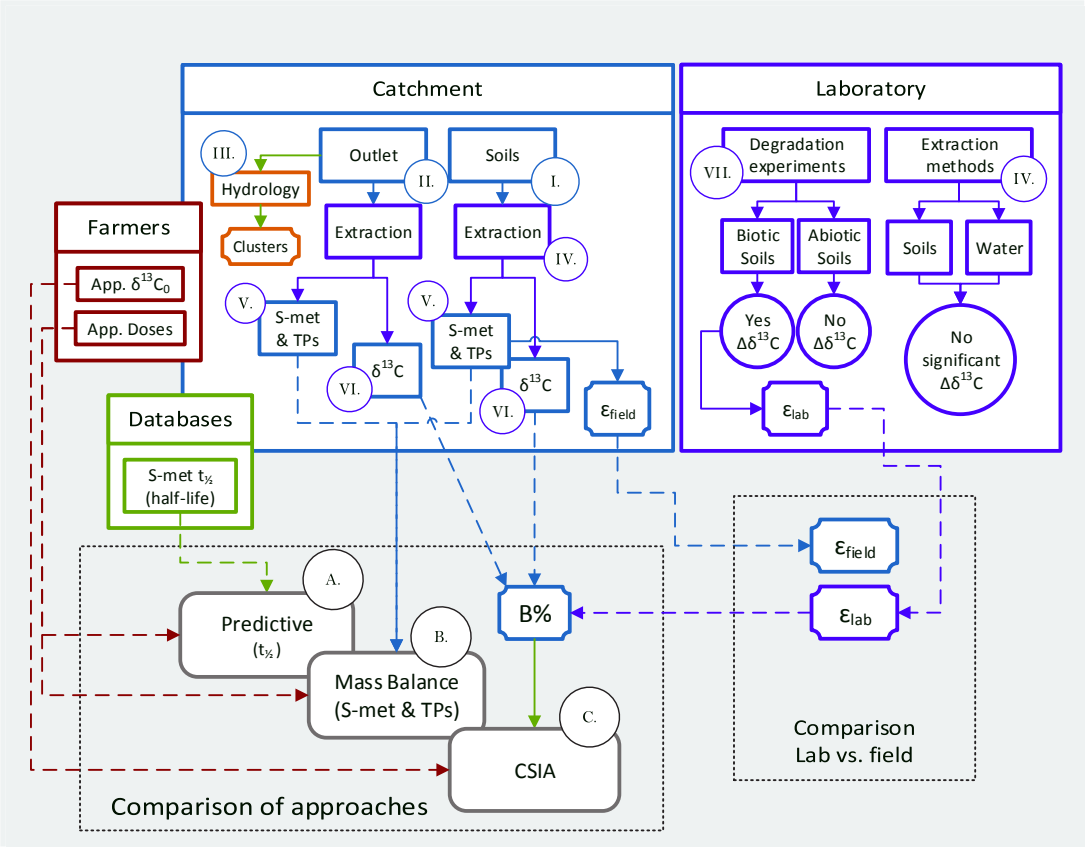

Figure 21: Study schema illustrating key steps of the study design (roman numerals) and informing the comparison of three approaches: predictive (A), mass balance (B) and CSIA (C).

2.2 Materials and methods

2.2.1 Catchment description

The 47 ha catchment is located 30 km north-east of Strasbourg (Bas-Rhin, France; 48 47 19,56 N; 7 35 2,27 E) and has been previously described by Lefrancq *et al.* 2018. The mean catchment slope is 6.7 ± 4.7% with altitude ranging between 190 and 230 m. Catchment water flows in ditches to a 50 cm diameter pipe at a single outlet. Roads represent 3.5% of the catchment surface and in 2016, 88% was arable land, from which sugar beet (70%) and corn (18%) were the principal crops sown between mid-March and late April (Fig. 5.2.1.A).

Overall, the soil characteristics indicate little variability. Surface soil samples (0 - 20 cm, n = 30) and soil profiles (2 m, n = 6) have a grain size distribution of clay 30.8 ± 3.9%, silt 61.0 ± 4.5%, and sand 8.5 ± 4.2%. The main soil type is Haplic Cambisol Calcaric Siltic and Cambisol Eutric Siltic on hillsides (north and south) and Cambisol Colluvic Eutric Siltic in the central valley. Soil characteristics were $CaCO_3$ = 1.1 ± 1.6%; organic matter = 2.2 ± 0.3%; pH = 6.7 ± 0.8; total soluble phosphorus = 0.11 ± 0.04 g Kg^{-1}, and CEC = 15.5 ±

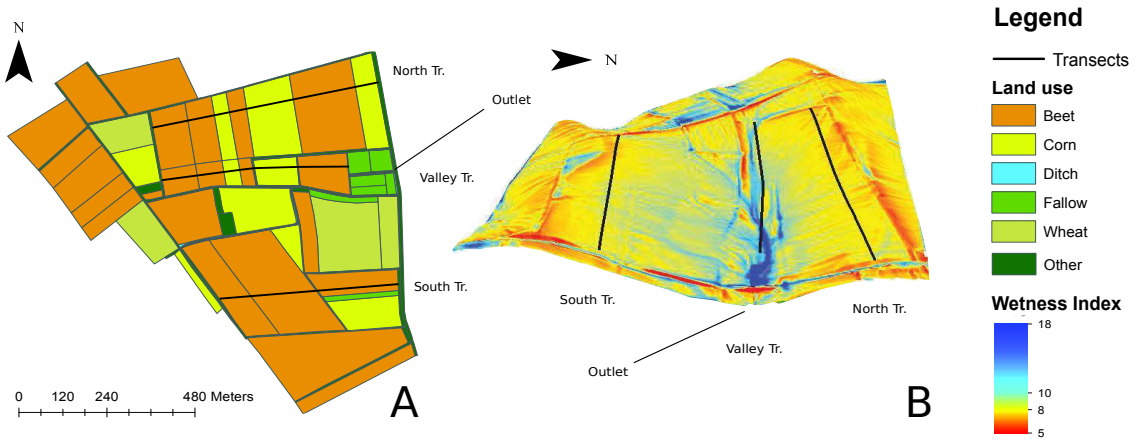

Figure 22: Catchment land-use (A) and topographical wetness index (B) [16]. The wetness index is computed with SAGA in QGIS 2.18 using the Topographical Wetness Index (TWI) tool with option "local upstream area" and the slope map in radian according to equation (eq.) 2.1.

1.3 cmol Kg^{-1}. A compacted layer (plough pan) was observed at a depth between 20 and 30 cm.

2.2.2 Hydrological conditions

A summary of the catchment hydrological conditions during the study period, between April 1^{st} and June 28^{th} 2016, is presented in Table 21. The summary data provided includes mean daily rainfall (P), mean rainfall intensity (P_{int}), total rainfall (P_{tot}), mean daily reference evapotranspiration (ETP), mean daily temperature (T), mean daily discharge normalized by the total catchment area (Q), the time of concentration (T_C) and the percent of days in a month were rainfall occurred (% Wet Days). The time of concentration (T_C) is defined as the time between the start of rainfall minus evapotranspiration and the resulting peak discharge [17]. Although subsurface travel times for this catchment range from 6 to 12 months [18], T_C values decreased from 2.2 to 0.5 h (Table 21). Soil crust development was generally observed across the catchment after around 100 mm of cumulative rainfall. A reduction in the soil infiltration capacity due to observed crusting and the progressive increase in mean daily and total monthly rainfall likely contributed to the observed decrease in the catchment's T_C.

Table 21: Catchment Hydrological Conditions (mean ± 1σ, total or %) between April 1^{st} and June 28^{th}, 2016

	P (mm d^{-1})	P_{int} (mm h^{-1})	P_{tot} (mm)	ETP (mm d^{-1})	T (°C)	Q (mm d^{-1})	T_C (h)	Wet Days
April	2.7±4.6	1.1±0.9	82.2	2.2±0.8	9.1±2.9	0.6±0.6	2.2±1.8, n=9	67%
May	4.6±7.1	1.7±2.8	136.8	3.1±1.2	14±3.2	0.9±1.3	0.9±0.6, n=13	63%
June	4.8±7.0	1.8±3.1	145.6	3.7±1.2	17.6±2.9	1.2±1.2	0.5±0.2, n=14	80%

Note: Abbreviations pertain to mean daily rainfall (P), mean rainfall intensity (P_{int}), total rainfall (P_{tot}), mean daily reference evapotranspiration (ETP), mean daily temperature (T), mean daily discharge normalized by the total catchment area (Q), the time of concentration (T_C) and the percent of days in a month were rainfall occurred (% Wet Days).

2.2.3 Top soil and water collection

Top soil (1 cm) concentrations and $\delta^{13}C$ were determined by weekly sampling on three transects across the catchment. Transects where selected to account for variability of moisture

conditions, drainage characteristics and to maximize the number of plots where SM was applied (Fig. 5.2.1). A digital Elevation Model (DEM), at 2 m resolution, was used to obtain local slopes and to estimate the topographical wetness index (TWI) [-] (Fig. 5.2.1.B), which quantifies the influence of topography on soil moisture such that [16]:

$$TWI = ln\Big(\frac{a}{tan(b)}\Big) \tag{2.1}$$

where a is the upslope area draining through a certain point per unit contour length and $tan(b)$, the local slope in radians.

Discharge at the catchment outlet was continuously measured by a Doppler flow-meter (2150 Isco, Lincoln, Nebraska, USA) with discharge precision of 3%. Water was collected by flow proportional sampling using a refrigerated automatic sampler with a total capacity of 3.96 L divided into 12 glass vials each of 330 mL (Isco Avalanche, Lincoln, Nebraska, USA). A predefined discharged volume based on the seasonal rainfall intensity expected for April (50 m^3), May (100 m^3) and June (150 m^3) was chosen allowing for 36 aliquots of 110 mL each per week. Water samples were then combined into composite samples according to hydrograph characteristics (base-flow, rising and/or falling limb), yielding one to four samples weekly of volumes $\geq$ 990 mL.

2.2.4 Farmer surveys

S-metolachlor was applied on three different dates, on March 25 (plots: 5, area: 14.9 ha), April 14 (plots: 8, area: 8.2 ha) and on May 25 (plots: 5, area: 5.9 ha) (Table 22 and Fig. 26.C). Farmers used one of two Syngenta product formulations, Mercantor Gold (area applied: 97%) or Dual Gold (area applied: 3%). Technical dosage specifications were 0.6 and 1.2 L ha^{-1}, with pure product SM concentrations of 960 g L^{-1} and 915 g L^{-1}, respectively. Signatures were obtained *via* dilution in Milli-Q water and followed the same solid-phase extraction (SPE) procedure described below for environmental waters. Initial $\delta^{13}C$ (-32.2 $\pm$ 0.5‰, n = 17) and $\delta^{15}N$ (1.9 $\pm$ 0.5‰, n = 17) were obtained from pure product and tractor tank dilutions. Pure product and tractor tank dilutions were not significantly different (Table 23).

Table 22: Applied mass (Kg) of active SM per transect by date

Date	North	Valley	South
March 20 - 25th, 2016	5.1	1.6	11.1
April 13 - 14th, 2016	8.0	1.8	2.9
May 25 - 31st, 2016	7.2	2.4	0.0
Total	20.2	5.9	14.0

Table 23: Pure & tractor tank dilutions for Syngenta's S-metolachlor (Mercantor Gold)

Source	Carbon $\delta^{13}C$ (‰)	Nitrogen $\delta^{15}N$ (‰)
Pure	-32.6±0.5, n=12	1.9 ±0.3, n=7
Tractor Dilution	-32.1±0.4, n=5	1.9 ±0.6, n=10

2.2.5 Pesticide extraction and quantification

SM and its degradation products metolachlor ethane sulfonic acid (MESA) and metolachlor oxanilic acid (MOXA) were extracted from soil and outlet water samples (Appendix section A.4, *IV. Pesticide extraction*). Water samples were extracted by solid-phase extraction

(SPE) using SolEx C18 cartridges (Dionex ®, Sunnyvale, CA, USA) and an AutoTrace 280 SPE system (Dionex ®) and quantified by GC-MS/MS (SM) and by LC-MS/MS (MESA and MOXA), as described previously [19]. Pesticide extraction and purification for soils were adapted from Ivdra *et al.* 2014 and Anastassiades *et al.* 2003. Environmental quantification limits for the soil samples were 0.001, 0.1, 0.1 μg g^{-1} dry weight (d.wt.) for SM, MOXA, and MESA with an analytical uncertainty of 16%, 40%, 8% respectively.

2.2.6 Isotope analysis

The carbon and nitrogen isotope composition of SM was analysed by adapting a previously described protocol [19] and further detailed in the SI. The GC-C-IRMS system consisted of a TRACE^{TM} Ultra Gas Chromatograph (ThermoFisher Scientific) coupled via a GC IsoLink/Conflow IV interface to an isotope ratio mass spectrometer (DeltaV Plus, ThermoFisher Scientific). The reproducibility of triplicate measurements was $\leq 0.2‰(1\sigma)$ for $\delta^{13}C$ and $\leq 0.5‰(1\sigma)$ for $\delta^{15}N$. The carbon and nitrogen isotope ratios are reported in δ notation in parts per thousand [‰] relative to the V-PDB standard for carbon and Air standard for nitrogen, according to:

$$\delta^{13}C_{sample} \text{ or } \delta^{15}N_{sample} = \frac{R_{sample} - R_{standard}}{R_{standard}} \tag{2.2}$$

where R_{sample} and $R_{standard}$ are the ratios $^{13}C/^{12}C$ or $^{15}N/^{14}N$ of sample and standard, respectively. Based on GC-IRMS linearity tests, the minimum peak amplitudes needed for accurate $\delta^{13}C$ and $\delta^{15}N$ measurements were established as about 300 mV and 200 mV, respectively (Fig. A4). These signals correspond to 10 ng of carbon and 20 ng of nitrogen injected on column.

2.2.7 Soil degradation experiments

To derive a carbon isotope enrichment factor (ε_{lab}) for SM, signatures and remaining concentrations were obtained from soil microcosm experiments and conducted over a period of 200 days over a set of temperatures (20 and 30 °C) and moisture conditions (20 and 40% volumetric water content). Derivation of ε_{lab} with eq. A.4 was then used to infer field degradation extent based on isotope signatures measured in field samples and eq. 2.15. Microcosms consisted of 20 g air-dried soil obtained from the catchment and were spiked to environmental concentrations (5.0 μg g^{-1} soil) in 20 mL crimp glass vials, with silicone/natural PTFE caps (Interchim ®, France). To maintain aerobic conditions while limiting water loss and avoiding contamination, a 0.2 μm syringe filter (Rotilabo ®, Carl Roth ®, France) was mounted on a syringe tip and installed through a vial cap (Fig. A5). To distinguish sorption from microbial degradation, and to determine whether isotope fractionation could arise due to non-destructive dissipation (i.e., sorption) or abiotic degradation (i.e., hydrolysis), half of the soil samples were three-times autoclaved in glass bottles and stored in the dark at room temperature for 12 hours between each autoclave run. Sacrificial sampling was conducted in triplicate at days 1, 10, 50, 100 and 200. Fractionation extent and dissipation kinetics are provided in Table A4.

Abiotic controls showed no significant isotope fractionation, confirming insignificant fractionation associated to sorption and hydrolysis (Fig. A6, appendix section A.7 *VII Degradation experiments*). A carbon SM enrichment (ε_{lab}) was derived from living microcosm experiments by following the classical Rayleigh equation [7]:

$$\frac{\delta^{13}C_t + 1}{\delta^{13}C_0 + 1} = f^{(\varepsilon)} \tag{2.3}$$

where $f = [\mathrm{SM}]_t/[\mathrm{SM}]_0$, is the remaining fraction of SM at time t.

2.2.8 Databases and predictive calculations

Predictive approaches required computing remaining masses based on farmer surveys and estimating degradation extent according to median (21 d), minimum (7.6 d) and maximum (37.6 d) half-lives ($t_{1/2}$) reported for SM [22]. Calculation in soils where computed according to:

$$M_{tot,t} = M_{tot,t_0}(\frac{1}{2})^{\frac{t}{t_{1/2}}} \tag{2.4}$$

where M_{tot} is the total catchment mass at time t.

2.2.9 Mass balance calculations

Soils. Pesticide mass along a catchment's transect area $M_{Tr,t}$ $[\mu g]$ is given by:

$$M_{Tr,t} = C_{Tr,t} \cdot \rho_{b_0} \cdot A_{Tr} \cdot D \tag{2.5}$$

were C_{Tr} is the dry weight SM soil concentration [μg g^{-1} soil d. wt.] on transect Tr at time t and A_{Tr} is the associated transect area $[m^2]$ and D is sampling depth (1 cm). A homogeneous bulk density ($\rho_{b_0} = 0.99\ g/cm^3$) was assumed based on sample measurements obtained across the catchment.

Transect signature and pesticide mass was then used to compute bulk signatures across the catchment ($\delta^{13}C_{bulk}$) and given by:

$$\delta^{13}C_{bulk,t} = \sum_{Tr=1}^{TR=3} \frac{M_{Tr,t}}{M_{tot,t}} \delta^{13}C_{Tr,t} \tag{2.6}$$

were $\delta^{13}C_{Tr}$ is the SM isotope signature in transect Tr and M_{tot} $[\mu g]$ the total catchment mass at time t.

Outlet. Outlet loadings (OL) $[\mu g]$ where calculated based on flow proportional samples given by:

$$OL_{ws} = C_{ws} \int_t^{\Delta t} V(t)dt \tag{2.7}$$

where C the concentration [μg L^{-1}] of water sample ws and V $[L]$ is discharge over the sample time interval Δt $[h]$. Transformation product (TP) loadings were expressed in SM mass equivalence (MEQ_{SM}) $[\mu g]$ such that:

$$MEQ_{SM} = MOXA \cdot (\frac{mw_{SM}}{mw_{MOXA}}) + MESA \cdot (\frac{mw_{SM}}{mw_{MESA}}) \tag{2.8}$$

where mw is the molar mass of each species measured at the outlet. MB errors associated to missed sampling intervals were corrected by linear interpolation between measured sample concentrations.

2.2.10 CSIA and open-system Rayleigh calculations

The Rayleigh equation assumes that $f = C_t/C_0$ reflects solely reduction in concentrations due to degradation and should thus be expressed as $f_{degradation}$. Accounting for dilution processes, the remaining fraction that is measured in the field sample becomes then f_{total} [23]:

$$f_{total} = f_{degradation} \cdot f_{dilution} \tag{2.9}$$

$$f_{dilution} = \frac{1}{F} \tag{2.10}$$

where F is the number of times the sampled volume has become diluted. F can be calculated if ϵ_{lab} is known such that:

$$F = e^{(\Delta*/\epsilon_{lab} - ln f_{total})} \tag{2.11}$$

$$\Delta* = 1000 \cdot ln\Big(\frac{10^{-3}\delta^{13}C_t + 1}{10^{-3}\delta^{13}C_0 + 1}\Big) \tag{2.12}$$

where $\Delta*$ is the isotopic shift of the measured sample at time t.

The total fraction remaining (f_{total}) was estimated based on the concentration measured along a transect (Tr) at any given time (C_t) relative to the cumulative initial concentration (C_{Tr_0}) [μg g^{-1} soil] after a timely application (a_t) and given by:

$$C_{Tr,t_0} = \frac{\sum_{a=1}^{A} M_{Tr,a_t}}{A_{Tr} \cdot D \cdot \rho_{b_0}} \tag{2.13}$$

where, M_{Tr,a_t} [μg SM] is the total mass applied on transect Tr due to application a at time t (Table 22), the total plot area [m^2] associated to the transect (A_{Tr}), which is proportional to sampling points along a transect, the sampling depth [m] and the initial soil bulk density (ρ_{b_0}) [g/m^3]. Measured concentrations ($C_{Tr,t}$) and remaining fractions ($f_{total} = C_{Tr,t}/C_{Tr,t_0}$) across time per transect are detailed in appendix tables A5, A6 and A7.

The carbon isotope enrichment factor (ε_{lab}), derived from closed microcosm degradation experiments under mixed aerobic and anaerobic conditions (section 2.2.7), was used to quantify field degradation ($B\%$). Degradation was then determined from the remaining fraction associated to degradation ($f_{degradation}$) such that [9]:

$$f_{degradation} = \left(\frac{\delta^{13}C_t + 1}{\delta^{13}C_0 + 1}\right)^{1/\varepsilon_{lab}} \tag{2.14}$$

$$B\% = (1 - f_{degradation}) \cdot 100 \tag{2.15}$$

To obtain the relative contribution of degradation and dilution (e.g., off-site export, sorption), the open-system Rayleigh equation [23] was adapted for tops soils. The relative contribution of dilution and degradation to concentration decrease is represented by the factor ratio D*/B*, where dilution (D*) and breakdown (B*) factors are given by:

$$D^* = \frac{lnf_{dilution}}{lnf_{total}} \tag{2.16}$$

$$B^* = \frac{lnf_{degradation}}{lnf_{total}} = 1 - D^* \tag{2.17}$$

and where D* $\geq$ 0 and 0 $\leq$ B* $\leq$ 1. For example, if D*/B* = 0 (D* = 0; B* = 1), the concentration decline is solely due to degradation, while if D*/B* = 1 (D* = B* = 0.5), the contribution of each processes to the logarithmic concentration decrease is equal [23].

2.3 Results and discussion

2.3.1 SM degradation and carbon isotope fractionation in top soils

SM $\delta^{13}C$ signatures and concentrations were obtained on a weekly basis on catchment top soils (1 cm) from April to June, 2016. Soil concentrations negatively correlated with changes in isotope shift ($\Delta\delta^{13}C$) across time ($r = -0.7, P < 0.001$) (Fig. 23.A). To allow quantification of field degradation extent, microcosm degradation experiments were conducted (section 2.2.7) to derive a carbon isotope enrichment factor ($\varepsilon_{lab} = -1.5 \pm 0.5‰$, $R^2 = 0.87$, $P < 0.001$). Assuming a reactive position at the C-Cl bond, this corresponds to an apparent kinetic isotope effect ($AKIE_C$) ranging from 1.02 to 1.03 (eq. A.5) compatible with S_N2 ($AKIE_C$ = 1.03-1.07) type substitution reactions and reductive cleavage of C-Cl bonds ($AKIE_C$=1.02-1.03) [24]. Although $\delta^{15}N$ values were also measured, derivation of a nitrogen isotope enrichment was not possible due to high matrix interference effects in soils leading to significant uncertainty in measured signals ($\geq 1‰$).

To estimate the error extent that could arise from derivation of enrichment values in the field, a carbon isotope field enrichment (ε_{field}) was also derived based on top soil samples and compared against ε_{lab} (Fig. 23.B). Due to open system conditions, the field derived enrichment is expected to underestimate ε_{lab} (i.e., be less negative) and consequently lead to an overestimation of degradation extent. As expected, a catchment-wide ε_{field} underestimated ε_{lab} (Fig. 23.B). However, this underestimation was small, likely reflecting SM high sorptive properties and indicating good transferability of ε values between laboratory and field conditions for this compound.

Abiotic controls for SM degradation experiments showed no significant isotope shift, which indicated no fractionation associated to sorption and agreement with previous results [25, 26] (section 2.2.7, appendix section A.7, Fig. A6 and Table A4). Field measurements of top soil and outlet signatures also support this observation, as fractionation extent in water samples taken both near application periods and towards the end of the season generally remains equivalent or slightly lower relative to top soil samples (Fig. 25). Based on a multiple lines of evidence approach derived from the combined CSIA, mass balance (MB) and predictive calculations in the following section, attribution of degradation extent to photochemical degradation is likely to be small (< 5%), if not negligible. Indeed, carbon isotope effects associated to photochemical degradation in aqueous solutions of aniline substructures have been reported to be negligible under indirect photolysis [27] and nearly insensitive to inverse fractionation at environmental pH [28]. If inverse fractionation where to be of relevance for this case, CSIA biodegradation estimations would therefore be regarded as conservative. Nevertheless, photochemical degradation is not expected [22] or may be low when incorporated into the top soil [29–32], which is supported by similar lab and field enrichment values

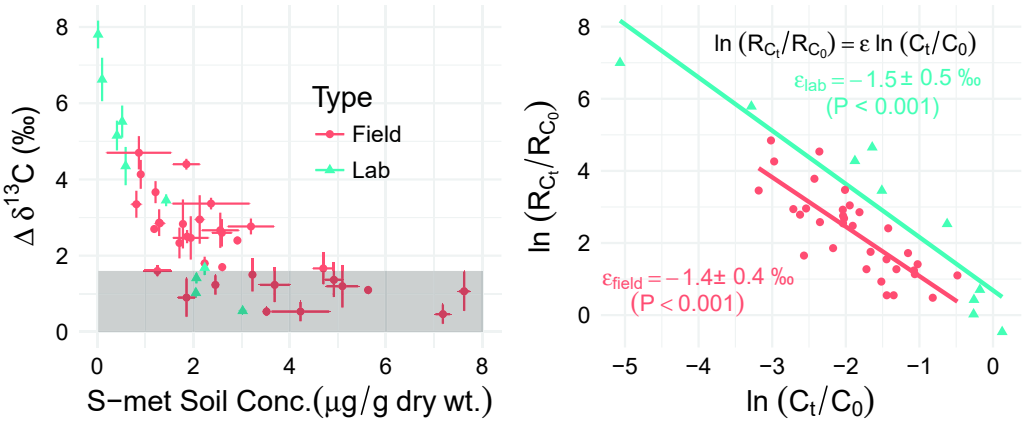

Figure 23: SM carbon isotope shift ($\Delta\delta^{13}C = \delta^{13}C_t - \delta^{13}C_0$) *vs.* concentration in transect soils, where $\delta^{13}C_0 = -32.2 \pm 0.5‰$. Error bars account for error propagation (e.p.) across $\pm 1\sigma$ (standard deviation) of initial product and $\pm 1\sigma$ from sample signatures (eq. A.3). Analytical uncertainty ($1\sigma \leq \pm 0.5‰$) incorporates both accuracy and reproducibility of $n \geq 3$ measurements. The shaded area represents the minimum shift below which degradation should not be concluded (i.e., uncertainty limit) due to maximum analytical uncertainties, sample error uncertainties, and minor shifts in the soil extraction method (eq. A.1)

as well as by comparisons of non-degraded fractions *vs.* remaining mass measured in top soils (see following section, Fig. 24. B *vs.* C).

2.3.2 Validation of the CSIA approach

The value of CSIA as a complementary monitoring tool was assessed by comparing information derived from both MB accounts and reported half-life ranges for SM (7.6 - 49.5 days) [22, 33, 34]. Results indicate good agreement between CSIA, MB and predictive calculations, which emphasizes the validity of the CSIA approach (Fig. 24). Based on CSIA estimations in soils (Fig. 24.B), SM was degraded by 50% and 88% by the end of April (32 days after 1^{st} application) and June (82 days after 1^{st} application), respectively. Propagation errors in catchment degradation extent associated to statistical variation of CSIA input parameters was estimated to be $|\Delta B| = 19\%$ in April and 9% in June [35]. Relative to the CSIA approach, single first-order degradation predictions (Fig. 24.A, eq. 2.4) based on a field half-life of 21 days [22], slightly overestimated degradation in April ($|\Delta B| = 10\%$) and were nearly equivalent in June ($|\Delta B| = 4\%$). Overestimation in April was likely due to low spring temperatures and largest degradation rates inherent to the single first-order rate model with higher concentrations. Comparison of a half-life of 34 days obtained during the degradation experiment (i.e., based on catchment soils) further indicates that field degradation rates may also be attributed to soil characteristics. Nevertheless, although both methods provide approximately equivalent estimations, CSIA was able to reduce the uncertainty margins relative to the reported half-life ranges (i.e., see error bars across methods in Fig. 24.A *vs.* Fig. 24.B).

Soil MB accounts during April and June (Fig. 24.C) indicated remaining fractions of 46% and 4%, with only 0.1% and 0.2% of SM reaching the outlet, respectively. Comparing information from CSIA (Fig. 24.B) and MB approaches (Fig. 24.C), inferred top soil non-destructive losses (e.g., sorption, infiltration, run-off and volatilization) were estimated to have reached 8% of the applied product. Plant uptake was considered to be negligible, as no

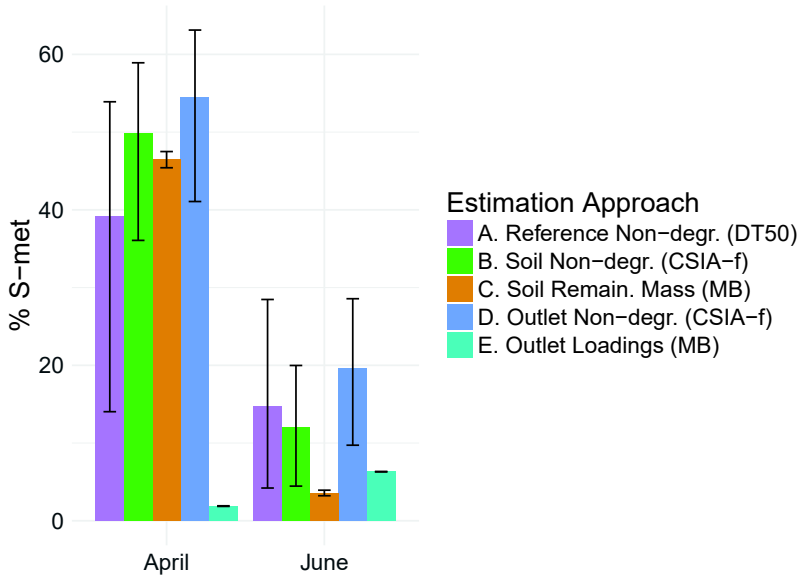

Figure 24: Estimation of remaining SM relative to the cumulative applied mass (%). Estimation of remaining fractions were based on the referenced typical field half-life, with error bars representing referenced half-life ranges (A); the non-degraded fraction ($CSIA - f$) calculated from isotope signatures in soils (B) and outlet waters (D), with error bars corresponding to 95% confidence intervals ($\pm 0.4‰$) of SM ε_{lab}; the remaining mass based on measured soil sample concentrations and standard deviations (C); and the total fraction of discharged mass in SM molar equivalents for MESA and MOXA (outlet loadings), with error bars representing the cumulative standard deviation (E).

correlation was found between remaining mass and crop growth (from 0 to 40 cm) or surface cover (from 0 to 100%) [15]. Although SM is considered to be a non-volatile compound (VP = 1.73 mPa) [36], based on environmental conditions [e.g., 37] and model based calculations [15] we estimate volatilization to have accounted for $\leq 5\%$ of the applied product.

Comparison of the type of information that can be derived from CSIA and MB approaches at the outlet illustrates a further advantage of tracking pesticide fate using CSIA. By tracking parent and major TPs, direct information regarding source zone degradation extent cannot be appreciated, as mass balances cannot be closed due to long subsurface travel times within the catchment, the potential for further TP degradation and difficulties in determining sorption extent without numerical modelling. On the other hand, the use of CSIA generally provided a good approximation of the degradation extent observed in source top soils (Fig. 24.B *vs.* 24.D), as tracking SM, carries information of its degradation extent independently of the total loads exported. In this respect, CSIA presents an opportunity as a complementary line of evidence to the rapidly developing capabilities of high-resolution mass spectrometry for target and non-target analyses of pesticide TPs [e.g., 38]. By providing information on the maximum degradation achieved by parent compounds, CSIA may thus contribute to monitoring programs seeking to develop chemical risk assessments requiring more accurate MB accounts.

2.3.3 CSIA-based monitoring under dynamic hydrological regimes

To determine whether CSIA could be implemented at reduced effort and be of relevance, for example, in larger catchments contexts, we evaluated whether a catchment-wide assessment

could be conducted by monitoring discharge water at the catchment outlet. To do so, we compared linear trends of isotope fractionation in bulk top soils against stream discharge at the catchment outlet across time (Fig. 25). Bulk top soils are computed by eq. 2.6 and provide a more accurate representation of the catchment wide signature evolution by taking mass balances into account. An approximately equivalent and general increase in $\Delta\delta^{13}C$ above uncertainty ranges (i.e., shaded area) was observed across time for bulk soils and waters. However, linear trends indicate that without top soil information, outlet trends would have underestimated catchment-wide degradation by $\Delta B \approx 8\%$ towards the end of the season (mid-June). This underestimation was however, likely related to an increase in variability of isotope signatures in source soils following a late season application on May 25^{th} (Fig. 25) and observed at the outlet due to significant changes in hydrological conditions taking place in late May and June (see appendix section A.3 for detailed analysis of hydrological variability).

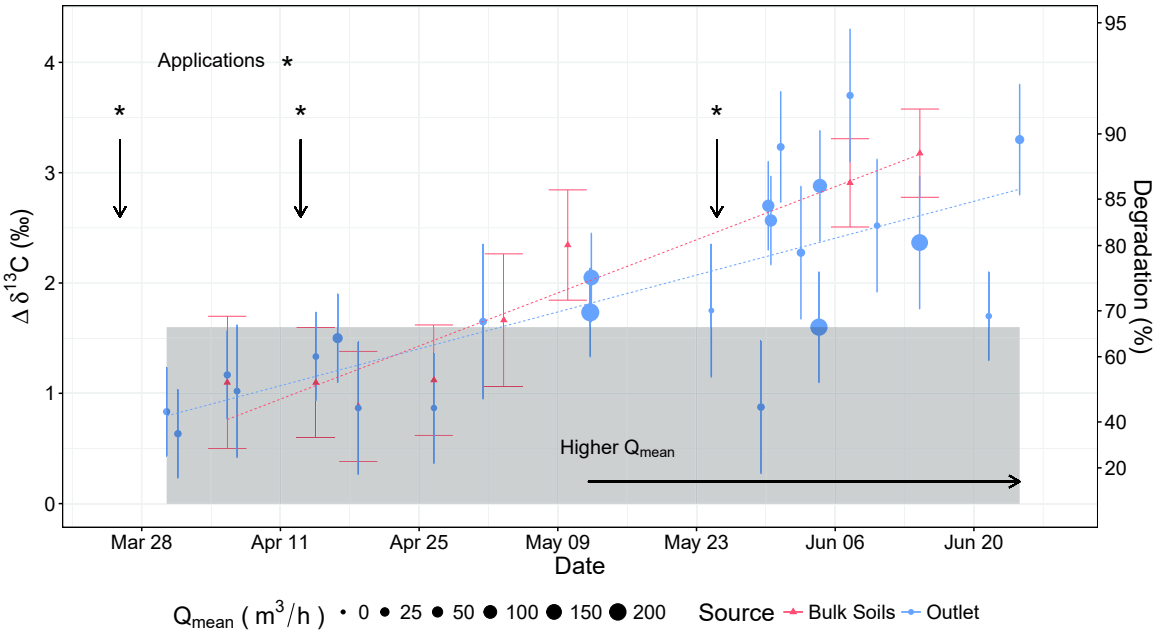

Figure 25: SM carbon isotope shift ($\Delta\delta^{13}C$) across time in bulk soils and outlet waters with vertical arrows indicating application dates ($\delta^{13}C_0 = -32.2 \pm 0.5‰$). Fitted linear models ($\Delta\delta(t) = mt$) for outlet signatures ($R^2_{out} = 0.5$) and bulk soils ($R^2_{soil} = 0.9$) *vs.* days (t) after first application illustrate similar trends in time, despite an increase in variability for outlet signatures during May and June. Error bars account for error propagation (e.p.) across $\pm 1\sigma$ (standard deviation) of initial product and $\pm 1\sigma$ from sample signatures (eq. A.3). Analytical uncertainty ($1\sigma \leq \pm 0.5‰$) incorporates both accuracy and reproducibility of $n \geq 3$ measurements. The shaded area represents the minimum shift below which degradation should not be concluded (i.e. uncertainty limit) due to maximum analytical uncertainties, sample error uncertainties, and minor shifts in the soil extraction method (eq. A.1). Degradation extent (%) shown on secondary y-axis is obtained from $\Delta\delta^{13}C$ transformations based on ε_{lab} (eq. 2.14 & 2.15).

To identify potential source contribution leading to isotope variability, the relative contribution of degradation and dilution to concentration decrease, given by the factor ratio D*/B*, in transect soils was estimated across time [23, section 2.2.10]. Although mass flux contributions from each area would be necessary for a quantitative source apportionment (i.e., *via* end-member analysis), D*/B* ratios in top soils may be used as qualitative source indicators

for outlet $\delta^{13}C$ and SM concentration variability. Weekly D*/B* calculations (Tables A5, A6 and A7) considered two enrichment scenarios based on the derived $\varepsilon_{lab} = -1.5‰$ and on $\varepsilon_{max} = -1.9‰$. The latter considers a conservative maximum kinetic isotope effect of KIE = 1.03 (C-Cl bond) expected for S_N2 reactions [24], and approximates degradation conditions observed during the microcosm experiment for saturated moisture levels (Table A4, $\theta = 40\%$).

A comparison between rainfall, discharge, SM concentrations in outlet and soils, and D*/B* ratios across time in Fig. 26 shows how D*/B* ratios were highest (Fig. 26.D) shortly after rainfall events, when outlet concentrations exceeded the seasonal trends (Fig. 26.B). Median D*/B* ratios for the north, valley and south transects (Table 24) indicate that dilution was more significant shortly after applications, with each transect showing dilution to be as important as degradation (D*/B* ≥ 1) at least once early in the season (April to mid-May). Further inference of D*/B* ratios indicates that dilution along the steeper slopes and better drained soils of the north transect continued to be of more importance during the late season relative to other transects, where drainage was poor. Low D*/B* ratios along the south during the late season indicate potential contributions to outlet concentrations of lesser importance. This is supported by significant differences ($P < 0.05$, Kruskal-Wallis) in $\delta^{13}C$ observed between outlet and the south transect during the late season (Fig. 27), indicating that the south transect was unlikely responsible for outlet isotope variability within this period. Finally, two major rainfall-runoff events, with outlet SM concentrations exceeding late-season trends, can be appreciated on May 29^{th} and June 25^{th}. With respect to the former event, no appreciable influence can be observed on the north and south transects. However, D*/B* ratios along the valley, which received a late season application on May 25^{th}, were significantly higher (D*/B* = 0.8-1.2) relative to its overall median values (D*/B* = 0.1-0.5), likely indicating this transect as the main source leading to drops in outlet $\delta^{13}C$ (and SM concentration increase) during this event. A comparable observation can also be made for the latter (June 25^{th}) event. However, this time the source of outlet variability shortly after the rainfall event may be most likely attributed to the north transect, where increases in outlet concentrations (Fig. 26.B) and a drop in outlet $\delta^{13}C$ (Fig. 25) coincide with an increase in D*/B* ratios (D*/B* = 1.1-1.7) measured on June 28^{th} (Fig. 26.D) for this transect relative to median values (D*/B* = 0.6-1.0).

Table 24: Degradation (B%), breakdown factors (B*) & D*/B* ratios for $\varepsilon_{lab} = -1.5‰$ and $\varepsilon_{max} = -1.9‰$ along the North, Valley and South transects

Transect	B_{lab} (%)	B_{max} (%)	B^*_{lab} (-)	B^*_{max} (-)	D*/B*$_{lab}$ (-)	D*/B*$_{max}$ (-)
North						
Early Season	53.1	45.0	0.6	0.5	0.7	1.1
Late Season	85.4	78.1	0.7	0.6	0.4	0.8
Overall	74.4	66.2	0.6	0.5	0.6	1.0
Valley						
Early Season	56.2	59.6	0.9	0.8	0.1	0.3
Late Season	82.1	75.6	0.9	0.7	0.2	0.5
Overall	80.8	73.3	0.9	0.7	0.1	0.5
South						
Early Season	61.0	52.4	0.6	0.4	0.8	1.3
Late Season	93.1	87.9	0.9	0.7	0.1	0.3
Overall	64.4	60.3	0.6	0.6	0.6	0.6

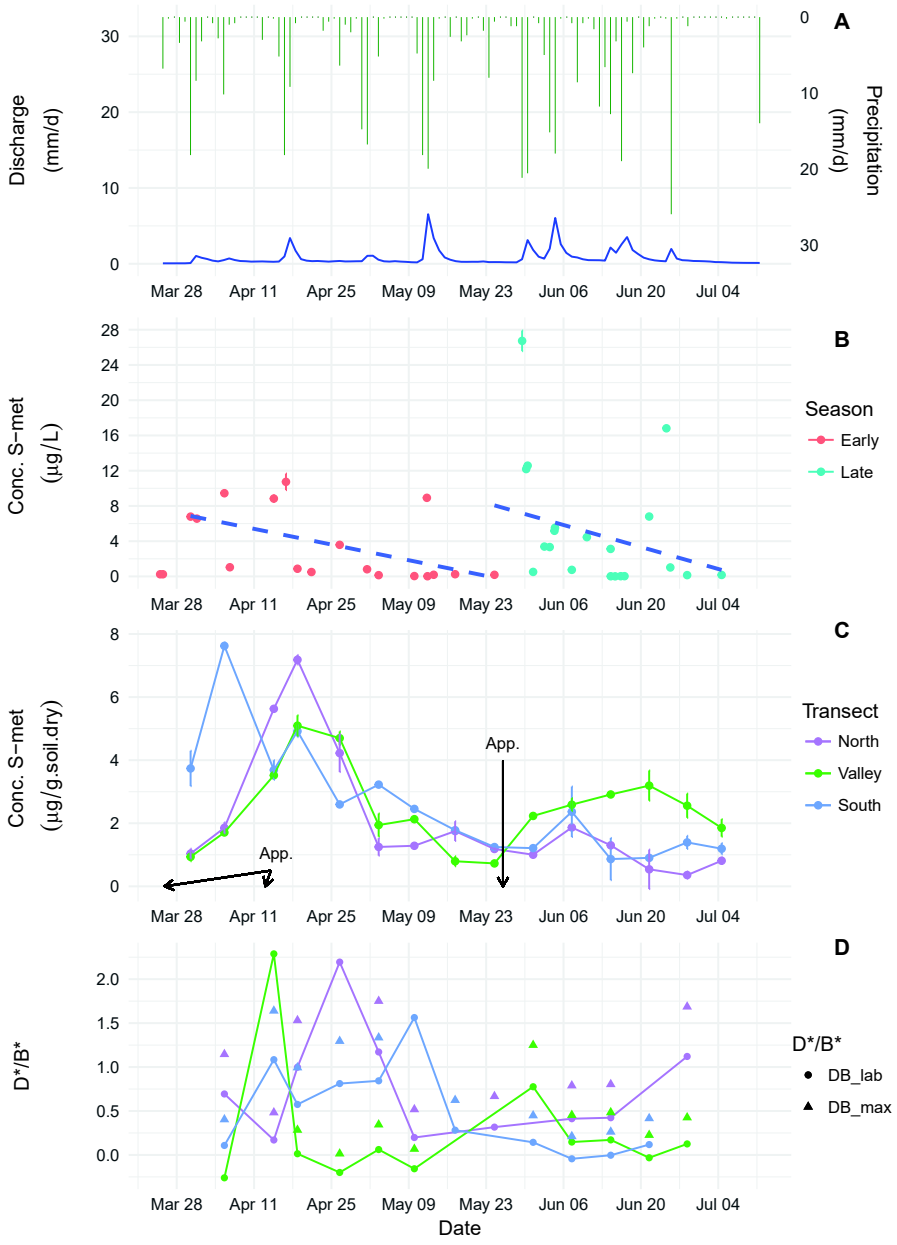

Figure 26: Hydrological forcing and catchment response to pesticide applications across the growing season. Error bars represent $\pm 1\sigma$. (A) Rainfall and discharge at the outlet (mm d^{-1}), (B) Outlet concentrations before (early season) and after (late season) second pesticide application (μg L^{-1}); (C) Composite transect soil concentrations (μg g^{-1} dry weight) and pesticide application (App.) dates; (D) D*/B* ratios based on $\varepsilon_{lab} = 1.5‰$and $\varepsilon_{max} = -1.9‰$.

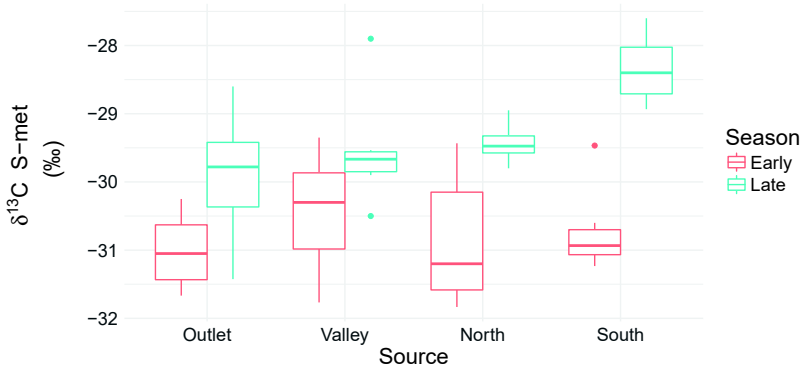

Figure 27: Distribution of carbon isotope signatures in outlet and soil transects across early and late season groups. Initial pesticide product isotope signature, $\delta^{13}C = -32.2 \pm 0.4‰$, n = 11.

Although these results alone cannot provide quantitative insights of the contribution of pesticide from each area to outlet, comparison of degradation extents to remaining masses can be used to estimate export losses from top soils. However, values of B* > 1 along the valley and in the late season along the south, indicate an overestimation of degradation extent based on the overall ε_{lab}. During these periods (e.g., where moisture levels were likely high in these areas), estimation based on the more conservative ε_{max} may thus be more appropriate, as observed during the microcosm experiment (Table A4, $\theta = 40\%$). A comparison of end of season (June 21^{st} - 28^{th}) remaining mass ($RM_{north} = 2\%$; $RM_{valley} = 13\%$; $RM_{south} = 4\%$) against degradation extents ($B_{north} = 85\%$; $B_{valley} = 84\%$; $B_{south} = 94\%$), yielded non-destructive losses of ≈ 16% along the north and valley transects *vs.* only 2% in the south. While the low relative losses observed in the south also support a minor role for volatilization [39] and photodegradation, the valley and north transect accounted for 91% of total export losses (2.8 kg of SM or 7% of the total applied product), despite representing only 50% of the catchment area. This highlights the potential value of CSIA approaches to identify critical areas of degradation and off-site export, even where complete MB accounts may not be available.

2.3.4 Perspectives for pesticide CSIA applications at catchment scale

Detailed soil and sub-event CSIA data allowed us to determine the evolution of pesticide degradation extent and export losses across the catchment. Additional insights on mechanisms of bond cleavage however, could have been obtained using multi-element CSIA of nitrogen, hydrogen or chlorine [40]. Unfortunately, the ability to implement multi-element isotope analysis was reduced by current limitations in CSIA quantification from environmental samples. Indeed, seeking sub-event information to better understand the catchment's primary pesticide transport processes limited our ability to collect sufficient volumes during each forcing event and also derive a nitrogen based high-resolution data set. Namely, given the small contribution of nitrogen (≈ 5%), hydrogen (≈ 8%), and chlorine (≈ 12%) to the molar mass of a SM molecule and the amount required of each element for analysis (about 20 ng on column for nitrogen and hydrogen and 10 ng for chlorine) significantly larger environmental concentrations would have been required to achieve the study objectives (i.e., a combined mass balance and carbon-based CSIA account under a high-resolution monitoring strategy). For example, at minimum environmental concentrations of ≈ 1 μg L^{-1} the extraction from about 56, 40 and 8 L, respectively for either nitrogen, hydrogen or chlorine, would have been required (Fig. 62).

Despite these challenges, additional concentration steps allowed quantification of nitrogen isotope fractionation ($\delta^{15}N$) for sub-event samples with highest concentrations (n = 7). These samples are associated to periods near application dates and during one major event. Maximum nitrogen isotope shifts were inverse but small ($\Delta\delta^{15}N = -1.3 \pm 0.6‰$, Fig. A3), indicating potential secondary isotope effects during biodegradation [14]. Attempts to construct laboratory and field nitrogen enrichment values from soils however, were not possible due to high matrix interference effects leading to significant uncertainty in measured $\delta^{15}N$ values (>1 ‰). In this respect, enrichment cultures isolated from relevant soils should prove crucial in the interpretation of field studies implementing multi-element pesticide CSIA.

Based on the observed limitations associated to the high-resolution approach followed in this study, catchment scale characterization campaigns implementing micropollutant CSIA should therefore account for a trade-off in information objectives inherent to pesticide CSIA analytical limitations and near-surface hydrological contexts. Namely, (i) improving understanding of pesticide fate during periods of high transfer risk, and (ii) seeking an evaluation of competing degradation processes across catchment compartments. Under the former objective (i), a high-resolution sampling scheme involving carbon-based CSIA should enable quantification of pesticide degradation across multiple events and catchment areas, as it was achieved in this study. However, when attempting to achieve the latter objective (ii), low-flow conditions may preclude obtaining information associated to base-flow components and therefore an understanding of long travel time degradation characteristics within the catchment. Evidently, similar challenges are to be expected under multi-element CSIA approaches. Therefore, monitoring strategies seeking subsurface compartment characterization, may be advised to target narrower sampling time-frames, particularly if MB accounts are of lesser priority relative to multi-element CSIA information.

2.4 Conclusion

This study evaluated the feasibility of carbon-based CSIA approaches as a tool to monitor pesticide fate at catchment scale. Comparison of three information sources (i.e., CSIA, MB and reported half-life ($t_{1/2}$) ranges) demonstrated the validity of pesticide CSIA as a complementary line of evidence for quantifying degradation under dynamic hydrological and rainfall-runoff conditions. The CSIA approach improved our understanding of pesticides fate by delineating the primary catchment areas regulating degradation (88%) and export losses (8%). Comparison of MB and CSIA approaches showed that degradation extent evolution was consistent between outlet and catchment-wide top soils, demonstrating the monitoring applicability of CSIA methods despite shifting hydrological regimes. It should be noted however, that due to potential artifacts in soil extraction methods, a minimum shift of $\Delta\delta^{13}C > 2‰$ ($\approx 75\%$ degradation) was considered before any conservative conclusion on degradation extent could be established. Based on its ability to quantify degradation independently of TPs and to delineate critical source areas, CSIA may thus be considered as a valuable complementary tool to identify and monitor chemical risk at catchment scale. Further efforts seeking to implement high-resolution CSIA approaches at greater scales should be supported by adequate characterization of dominant transport pathways regulating critical source areas. During periods of relatively low flow however, and where MB information is of lower priority, non-proportional (e.g., manual) sampling efforts may nevertheless be of interest to successfully characterize long-term discharge. In this respect, modelling of slow catchment response behavior may facilitate the selection of minimum sampling volumes and the design of extraction protocols required to achieve higher resolution of multi-dimensional CSIA.

References

1. Vörösmarty, C. J. *et al.* Global threats to human water security and river biodiversity. *Nature* **468,** 555–561. ISSN: 0028-0836 (2010).
2. Malaj, E. *et al.* Organic chemicals jeopardize the health of freshwater ecosystems on the continental scale. *Proceedings of the National Academy of Sciences of the United States of America* **111,** 9549–9554. ISSN: 1091-6490 (2014).
3. Sabatier, P. *et al.* Long-term relationships among pesticide applications, mobility, and soil erosion in a vineyard watershed. *Proceedings of the National Academy of Sciences of the United States of America* **111,** 15647–52. ISSN: 1091-6490 (2014).
4. Rasmussen, J. J. *et al.* The legacy of pesticide pollution: An overlooked factor in current risk assessments of freshwater systems. *Water Research* **84,** 25–32. ISSN: 18792448 (2015).
5. Fenner, K., Canonica, S., Wackett, L. P. & Elsner, M. Evaluating Pesticide Degradation in the Environment: Blind Spots and Emerging Opportunities. *Science* **341,** 752–758. ISSN: 0036-8075 (2013).
6. Elsner, M. Stable isotope fractionation to investigate natural transformation mechanisms of organic contaminants: principles, prospects and limitations. *Journal of environmental monitoring : JEM* **12,** 2005–31. ISSN: 1464-0333 (2010).
7. Rayleigh, L. S. Theoretical considerations respecting the separation of gases by diffusion and similar processes. *Philosophical Magazine* **42,** 493–498 (1896).
8. Sherwood Lollar, B. *et al.* Stable carbon isotope evidence for intrinsic bioremediation of tetrachloroethene and trichloroethene at Area 6, Dover Air Force Base. *Environmental Science and Technology* **35,** 261–269. ISSN: 0013936X (2001).
9. Hunkeler, D., Meckenstock, R. U., Lollar, B. S., Schmidt, T. C. & Wilson, J. T. A Guide for Assessing Biodegradation and Source Identification of Organic Ground Water Contaminants using Compound Specific Isotope Analysis (CSIA). *USEPA Publication* **EPA 600/R-,** 1–82. ISSN: ¡null¿ (2008).
10. Nestler, A. *et al.* Isotopes for improved management of nitrate pollution in aqueous resources: Review of surface water field studies. *Environmental Science and Pollution Research* **18,** 519–533. ISSN: 09441344 (2011).
11. Fenech, C., Rock, L., Nolan, K., Tobin, J. & Morrissey, A. The potential for a suite of isotope and chemical markers to differentiate sources of nitrate contamination: A review. *Water Research* **46,** 2023–2041. ISSN: 00431354 (2012).
12. Thullner, M., Richnow, H.-h. & Fischer, A. in *Environmental and Regional Air Pollution* (eds Gallo, D. & Mancini, R.) chap. 2 (Nova Science Publishers, Inc., 2009).
13. Schreglmann, K., Hoeche, M., Steinbeiss, S., Reinnicke, S. & Elsner, M. Carbon and nitrogen isotope analysis of atrazine and desethylatrazine at sub-microgram per liter concentrations in groundwater. *Analytical and bioanalytical chemistry* **405,** 2857–2867. ISSN: 16182650 (2013).
14. Elsner, M. & Imfeld, G. Compound-specific isotope analysis (CSIA) of micropollutants in the environment - current developments and future challenges. *Current Opinion in Biotechnology* **41,** 60–72. ISSN: 18790429 (2016).
15. Lefrancq, M., Payraudeau, S., Guyot, B., Millet, M. & Imfeld, G. Correction to Degradation and Transport of the Chiral Herbicide S-Metolachlor at the Catchment Scale: Combining Observation Scales and Analytical Approaches. *Environmental Science & Technology* **52,** 5517. ISSN: 0013-936X (May 2018).

16. Beven, K. J. & Kirby, M. J. A physically based, variable contributing area model of basin hydrology. *Hydrological Sciences Bulletin* **24,** 43–69. ISSN: 0303-6936 (1979).

17. Gericke, O. J. & Smithers, J. C. Review of methods used to estimate catchment response time for the purpose of peak discharge estimation. *Hydrological Sciences Journal* **59,** 1935–1971. ISSN: 0262-6667 (2014).

18. Lutz, S. R. *et al.* Pesticide fate at catchment scale: conceptual modelling of stream CSIA data. *Hydrology and Earth System Sciences Discussions* **21,** 5243–5261. ISSN: 1812-2116 (2017).

19. Elsayed, O. F. *et al.* Using compound-specific isotope analysis to assess the degradation of chloroacetanilide herbicides in lab-scale wetlands. *Chemosphere* **99,** 89–95. ISSN: 00456535 (2014).

20. Ivdra, N., Herrero-Martín, S. & Fischer, A. Validation of user- and environmentally friendly extraction and clean-up methods for compound-specific stable carbon isotope analysis of organochlorine pesticides and their metabolites in soils. *Journal of Chromatography A* **1355,** 36–45. ISSN: 0021-9673 (Aug. 2014).

21. Anastassiades, M., Lehotay, S. J., Štajnbaher, D. & Schenck, F. J. Fast and easy multiresidue method employing acetonitrile extraction/partitioning and "dispersive solid-phase extraction" for the determination of pesticide residues in produce. *Journal of AOAC International* **86,** 412–431. ISSN: 10603271 (2003).

22. PPDB. *The Pesticide Properties Database* Developed by the Agriculture & Environment Research Unit (AERU), University of Hertfordshire, funded by UK national sources and the EU-funded FOOTPRINT project (FP6-SSP-022704). 2009.

23. Van Breukelen, B. M. Quantifying the degradation and dilution contribution to natural attenuation of contaminants by means of an open system Rayleigh equation. *Environ. Sci. Technol.* **41,** 4980–4985 (2007).

24. Elsner, M., Zwank, L., Hunkeler, D. & Schwarzenbach, R. P. A new concept linking observable stable isotope fractionation to transformation pathways of organic pollutants. *Environmental Science and Technology* **39,** 6896–6916. ISSN: 0013936X (2005).

25. Imfeld, G., Kopinke, F. D., Fischer, A. & Richnow, H. H. Carbon and hydrogen isotope fractionation of benzene and toluene during hydrophobic sorption in multistep batch experiments. *Chemosphere* **107,** 454–461. ISSN: 18791298 (2014).

26. Kopinke, F. D., Georgi, A., Imfeld, G. & Richnow, H. H. Isotope fractionation of benzene during partitioning - Revisited. *Chemosphere* **168,** 508–513. ISSN: 00456535 (2017).

27. Ratti, M., Canonica, S., McNeill, K., Bolotin, J. & Hofstetter, T. B. Isotope Fractionation Associated with the Indirect Photolysis of Substituted Anilines in Aqueous Solution. *Environmental Science and Technology* **49,** 12766–12773. ISSN: 15205851 (2015).

28. Ratti, M., Canonica, S., McNeill, K., Bolotin, J. & Hofstetter, T. B. Isotope Fractionation Associated with the Photochemical Dechlorination of Chloroanilines. *Environmental Science and Technology* **49,** 9797–9806. ISSN: 15205851 (2015).

29. Kochany, J. & Maguire, R. J. Sunlight Photodegradation of Metolachlor in Water. *Journal of Agricultural and Food Chemistry* **42,** 406–412. ISSN: 15205118 (1994).

30. EXTOXNET. *EXTOXNET. Extension Toxicology Network. Pesticide Information Profiles.* 1996. `http://extoxnet.orst.edu/pips/metolach.htm`.

31. Wilson, R. I. & Mabury, S. a. Photodegradation of metolachlor: Isolation, identification, and quantification of monochloroacetic acid. *Journal of Agricultural and Food Chemistry* **48,** 944–950. ISSN: 00218561 (2000).

32. Dimou, A. D., Sakkas, V. a. & Albanis, T. a. Metolachlor photodegradation study in aqueous media under natural and simulated solar irradiation. *Journal of Agricultural and Food Chemistry* **53,** 694–701. ISSN: 00218561 (2005).

33. European Commission. *Review report for the active substance S-Metolachlor* tech. rep. (EU Commission Health & Consumer Protection Directorate General, 2004). `http://ec.europa.eu/food/plant/pesticides/eu-pesticides-database/public/?event=activesubstance.ViewReview%7B%5C&%7Did=381`.

34. Wu, X., Li, M., Long, Y. & Liu, R. Effects of adsorption on degradation and bioavailability of metolachlor in soil. *Soil Science and Plant Nutrition* **11,** 83–97. ISSN: 07189516 (2011).

35. Thullner, M., Centler, F., Richnow, H.-H. & Fischer, A. Quantification of organic pollutant degradation in contaminated aquifers using compound specific stable isotope analysis – Review of recent developments. *Organic Geochemistry* **42,** 1440–1460. ISSN: 0146-6380 (Jan. 2012).

36. Corbin, M. *et al. NAFTA Guidance Document for Conducting Terrestrial Field Dissipation Studies* 2006. `https://www.epa.gov/pesticide-science-and-assessing-pesticide-risks/nafta-guidance-document-conducting-terrestrial-field%7B%5C#%7DIC` (2017).

37. Prueger, J. H. *et al.* Solar radiation, relative humidity, and soil water effects on metolachlor volatilization. *Environmental Science and Technology* **39,** 5219–5226. ISSN: 0013936X (2005).

38. Kern, S., Fenner, K., Singer, H. P., Schwarzenbach, R. P. & Hollender, J. Identification of transformation products of organic contaminants in natural waters by computer-aided prediction and high-resolution mass spectrometry. *Environmental Science and Technology* **43,** 7039–7046. ISSN: 0013936X (2009).

39. Lefrancq, M., Dijk, P. V., Jetten, V., Schwob, M. & Payraudeau, S. Improving runoff prediction using agronomical information in a cropped, loess covered catchment. *Hydrological Processes* **31,** 1408–1423 (2017).

40. Wu, L. *et al.* Characterizing chemical transformation of organophosphorus compounds by 13 C and 2 H stable isotope analysis. *Science of The Total Environment* **615,** 20–28. ISSN: 00489697 (2018).

Preface to Chapter 3

Chapter 3 addresses the third goal of this Ph.D. work, which is to investigate hydrological and transport formalisms as a preliminary step for conceptual development of the larger scale numerical model. The chapter is set within the framework of a soil column experiment led by F. Meite to explore the impact of rainfall patterns on heavy-metal and organic pesticide export from agricultural top-soils. Based on data obtained from experimental modalities combining soil types, pollutant ageing (10 days) and rainfall patterns (intensity, duration & volume), my contribution included the development of a parsimonious model to reproduce pesticide export *via* leaching and ponding. The model allowed to validate the experimental setup and determined mobility parameter values informing Monte Carlo sets during catchment scale modelling in chapter 4.

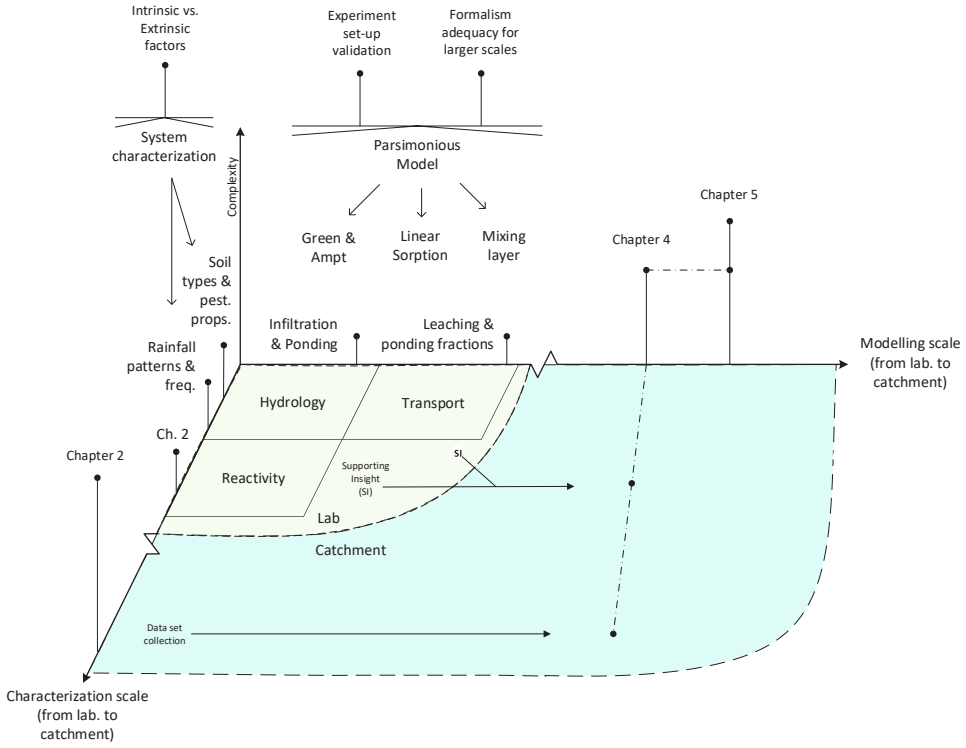

Chapter 3

Impact of rainfall patterns and frequency on the export of pesticides and heavy-metals from agricultural soils*

Abstract. The combined influence of soil characteristics, pollutant aging and rainfall patterns (i.e. intensity-duration-volume) on the export of pollutants from soils remains poorly understood. We used laboratory experiments and parsimonious modelling to examine the impact of rainfall patterns and successive rainfalls on the ponding and leaching of a pollutant mixture in crop and vineyard soils and with two pollutant aging stages (0 and 10 days). The pollutant mixture included the fungicide metalaxyl, the herbicide S-metolachlor (SM), and inorganic copper (Cu) and zinc (Zn). Four rainfall patterns, which differed in their durations and intensities, were applied twice successively with a 7 days interval on each soil type. The global export of pollutants was significantly controlled by the rainfall duration and frequency ($P < 0.01$). During the first rainfall event, the longest and most intense rainfall pattern yielded the largest export of metalaxyl (44.5 ± 21.5% of the initial mass spiked in the soils), SM (8.1 ± 3.1%) and Cu (3.1 ± 0.3%). Soil compaction observed after the first rainfall reduced in the second rainfall the leaching of remaining metalaxyl, SM, Cu and Zn by 2.4-, 2.9-, 30- and 50-fold, respectively. In contrast, soil characteristics and aging did not predominantly influence pollutant export (i.e., pollutant mass exported via leaching or in ponding water out of initial pollutant mass in soils). However, the leaching of Zn and Cu was significantly influenced by the soil type and aging, respectively. This underscores that extrinsic factors, such as rainfall characteristics, may prevail over soil-pollutants interactions to control pollutant export patterns when aging period is short. Overall, we anticipate our study to be a starting point for more systematic evaluation of the dissolved pollutant ponding/leaching partitioning and the export of pollutant mixtures from different soil types in relation to rainfall patterns.

3.1 Introduction

Pesticides are widely used to control pests while sludge from wastewater treatment plants (WWTP) containing heavy metals is often spread as fertilizers [1]. Pesticides and heavy-metals in sludge may thus accumulate in agricultural soils and, following rainfall-runoff

* This chapter is the edited version of: Meite, F., Alvarez-Zaldívar, P., Crochet, A., Wiegert, C., Payraudeau, S., and Imfeld, G. (2018). Impact of rainfall patterns and frequency on the export of pesticides and heavy metals from agricultural soils. *Science of the Total Environment*, 616-617(December):500-509.

events, eventually reach surface water and groundwater. Predicting the export of pollutants from soils into aquatic ecosystems is thus essential to limit transport risks and evaluate toxicological exposure [2, 3]. Pesticides and metals are exported from the soil to surface water by runoff, i.e., ponding and overland flow [4–6]. Ponding occurs when the rainfall intensity overcomes the top soil infiltration capacity. Depending of slope and upstream-downstream hydrological connectivity, ponded water will flow downstream generating runoff. Pollutants are also exported into sub-surface water by leaching when rainwater carries dissolved pollutants through the soil profile. However, the impact of rainfall characteristics on the export pathways of organic and inorganic pollutant mixtures from the soil remains largely unexplored.

Export of pollutants by ponding and runoff or leaching is controlled by intrinsic factors, such as the physico-chemical properties of the pollutant [7] as well as the soil hydrodynamics and characteristics [8, 9]. In particular, the availability and mobility of pollutants in soils tend to decrease over time due to pollutant diffusion and sorption into mineral and organic fractions, a process termed "aging" [10, 11]. Aging can control the fraction of pollutant mobilized and transported from the soil either in the freely-dissolved phase or associated with soil particles and colloids [7, 12–15]. Together with aging, pollutant transformation, including speciation of metals and degradation of organic pollutants, can influence the extent of pollutant export from soils. Pollutant aging and transformation are themselves controlled by soil-extrinsic factors, such as the time between an application and a rainfall event [12, 16]. Whereas pollutant aging in soils may decrease pollutant export, rainfall frequency may increase it [12, 17]. In addition, rainfall intensity and duration may primarily affect pollutant mobilization and export from the soil. Larger rainfall intensity have been shown to increase leaching of isoproturon from soil columns [18], while successive rainfall events doubled leaching of metolachlor from the soil at the second event [17]. In agricultural catchments prone to Hortonian runoff, ponding/leaching water partitioning is mainly controlled by top-soil (0-5 cm) hydraulic properties, i.e. bulk density and saturated hydraulic conductivity [19, 20]. This latter can decrease from 2 orders of magnitudes between crop sowing and harvest due to rainfall event frequencies modifying the ponding/leaching threshold [19, 21]. Landscape patchwork of top soil hydraulic properties also controls runoff connectivity [22] with associated pollutants both in dissolved and eroded phases. For pre-emergent herbicides such as SM, this top-soil layer (0-5 cm) plays a critical role to reduce or enhance water and pesticides fluxes the first weeks before development of a significant root compartment. Understanding and predicting the temporal evolution of top-soil hydraulic compartment along rainfalls frequency is then of utmost importance to better estimate water and pollutants fluxes reaching the deeper rhizosphere compartment and below, the groundwater table. If impacts of the deeper rhizosphere on pollutants leaching were identified [23, 24], lab-scale evidences on the boundary condition played by top-soil compartment on deeper water and solute leaching are still lacking. Besides, the contribution of intrinsic and extrinsic factors to the export of both organic and inorganic pollutants from soils has been, to date, rarely quantified [14, 16, 18]. In this context, laboratory experiments can help to constrain and hierarchize factors controlling pollutant export to drive modelling approaches potentially used in the field [25].

The purpose of this study was to evaluate how rainfall patterns (i.e., intensity-duration-volume) influence the export of synthetic pesticides and heavy metals from soils in relation to i) soil characteristics, ii) rainfall frequency, and iii) short-term pollutant aging (ten days). We used laboratory experiments with soils from experimental vineyard [26] or crop catchments [27], which cover relevant agricultural land uses receiving pesticides and heavy metals. Widely used anilide pesticides, i.e., the fungicide metalaxyl and the herbicide S-metolachlor (SM), as well as Cu and Zn were used as model pollutants in a mixture. To evaluate sensi-

tive parameters controlling pollutant ponding and leaching, a parsimonious physically-based model was developed to derive key parameters (i.e, the saturated hydraulic conductivity K_{sat} and the organic carbon partition coefficient K_{oc}) that regulate pollutant export.

3.2 Material and methods

3.2.1 Chemicals and artificial rainwater

Metalaxyl ($C_{15}H_{21}NO_4$), methyl N-(methoxyacetyl)-N-(2, 6-xylyl)-DL-alaninate and SM ($C_{15}H_{22}ClNO_2$), S-2-Chloro-N-(2-ethyl-6-methyl-phenyl)-N-(1-methoxypropan-2-yl) acetamide were purchased from Sigma-Aldrich (St. Louis, MO, USA), with purity of 99.8 and 98.2% respectively. Copper chloride ($CuCl_2$), zinc chloride ($ZnCl_2$) and salts used for the preparation of the artificial rainwater were purchased from Sigma-Aldrich (St. Louis, MO, USA) with purity $\geq$ 97%. Respectively, SM and Metalaxyl are moderately (480 mg L^{-1}) and highly (7100 mg L^{-1}) soluble, with high (3.05) and low (1.75) log octanol-water partition coefficients (log K_{ow}) and moderate (200 mL g^{-1}) to low (163 mL g^{-1}) organic carbon-water partition coefficients [28–30]. The logarithmic soil/water partition coefficient (log K_d) of Cu and Zn considered in this study were 2.7 and 3.1 L mg^{-1}, respectively [31].

The artificial rainwater was prepared according to the ERM-CA408 reference material (ERM certification report, 2010) with ultra-pure water (10 L) and NH_4Cl (19.6 mg), $Ca_2NO_3 \cdot 4H_2O$ (32 mg), $Mg_2NO_3 \cdot 6H_2O$ (28 mg), K_2HPO_4 (9 mg), $NaNO_3$ (4 mg), NaF (4.5 mg), Na_2SO_4 (22.2 mg) and $NH_4 \cdot H_2PO_4$ (11.2 mg). The targeted pH was 6.3 $\pm$ 0.6.

3.2.2 Soil collection

A calcareous clay-loamy surface soil (0 to 5 cm) (Rouffach, Haut-Rhin, Alsace, France) [26] and a silty-clay soil (0 to 5 cm) from a crop catchment (Alteckendorf, [4] were collected on August 6 and 7, 2015. About 50 kg of soil were collected in a conventional vineyard plot of 12.5x70 m with weeded rows every two rows (along seven naked rows). About 50 kg of soil from a 47 ha crop catchment (corn and wheat) were sampled systematically along three transects. Soils were thoroughly homogenized and sieved to 2 mm to increase reproducibility between experiments. As a result, this study focuses on soil matrix flow and excludes preferential flow through macropores [25]. Particle size distribution, saturated hydraulic conductivity and bulk density as well as pressure-soil water content were measured by laser granulometry using a Beckmann Coulter (LS230), head constant permeameter and direct measurement of soil cylinder, respectively (Table B2). The detailed physico-chemical characteristics of the soils are provided in Table B1. The vineyard soil contains more clays (68.5%) and carbonates (27.1%), while the crop soil contained more organic matter (5.52%), sand (10.3%) and silt (61.5%). The crop soil is neutral (pH 7.0) while the vineyard soil is more alkaline (pH 8.1).

3.2.3 Rainfall patterns

To retrieve the four rainfall patterns, the Alsatian foothills (France) has a temperate climate, where orographic effect (i.e., moist air cooling down as it moves from low to high elevation over rising terrain) intensifies extreme rainfalls (i.e., highest 1% of the daily rainfall amounts - 99^{th} percentile) [32]. The selected rainfall station (47° 57' 9" N, 07° 17' 3" E, Rouffach, Haut-Rhin, France) is located in the experimental vineyard catchment from which the vineyard soil was collected. The catchment is characterized by intense events generating both pesticide and Cu runoff [33, 34]. A Gumbel law [35, 36] was applied on the 6 min. MeteoFrance database

Table 31: Calibrated Ksat used to fit all rainfall modalities simultaneously with the model during the second pulse.

Parameter	Unit	Value				Rainfall No.
		Crop soil		Vineyard soil		
$K_{sat,pattern}$	[cm h^{-1}]	13.45		17.62		1 (measured)
		t = 0 day	t = 10 days	t = 0 day	t = 10 days	
$K_{sat,p1}$	[cm h^{-1}]	0.054	0.013	0.352	0.025	2 (calibrated)
$K_{sat,p2}$	[cm h^{-1}]	0.538	0.179	0.035	0.235	
$K_{sat,p3}$	[cm h^{-1}]	0.013	0.179	0.176	0.352	
$K_{sat,p4}$	[cm h^{-1}]	0.179	0.077	0.018	0.117	

Table 32: Rainfall patter characteristics

	Return pds. [years][a]	Duration [min][a]	Intensity [mm h^{-1}][b]	Rate [mL min^{-1}][c]	Volume [mL][c]	Description (pattern, intensity)
Pattern 1	2	30	30	1.1	31.5	Long-lasting, low
Pattern 2	2	12	55	1.9	23.1	Mid-lasting, intermediate
Pattern 3	20	30	55	1.9	57.8	Long-lasting, intermediate
Pattern 4	50	6	135	4.7	28.4	Short, high

[a]Selected return periods and rainfall durations; [b]Calculated intensities with Gumel law associated to return periods and durations; [c]Pump rate and associated rainfall volume using a soil column area of 7.07 cm^2.

(https://donneespubliques.meteofrance.fr/) from 1998 to 2016 to derive mean intensities for rainfall duration of 6, 12, and 30 minutes and return period of 2, 20 and 50 years. The four selected rainfall patterns differ in their intensities (from 30 to 135 mm h^{-1}), durations (from 6 to 30 min), volume (from 23 to 58 mL) and return period (from 2 to 50 years) (Table 32). The rationale behind this selection is to (i) cover the range of rainfall patterns observed on the regional scale, (ii) represent a wide panel of possible patterns in temperate climate, and (iii) generate a sufficient water volume for further pollutant quantification.

3.2.4 Experimental set-up and operations

Soil columns consisted of filtration units (Steriflip, MerckMillipore, Billerica, MA, USA) and 50 mL polyethylene centrifugation tubes (Fig. 31). The conical part of the centrifugation tubes were cut and tubes were screwed above the filtration units. Centrifugation tube caps (4 mm ⊘ digs) were drilled to insert a pipe connected to a multi-channel peristaltic pump (ICP-8, Ismatec, Wertheim, Germany). The pump delivered artificial rainwater on soil samples areas (7.07 cm^2) at rates corresponding to the four selected rainfall patterns, from 1.1 to 4.7 mL min^{-1} 32.

Soil samples were homogeneously spiked at 50 μg g^{-1} with an aqueous mixture of metalaxyl, SM, $CuCl_2$ and $ZnCl_2$ to reach a soil water content of 20% (weight/weight). Control soils consisted of non-spiked soil with water content of 20% (w/w). The upper part of each column was filled with 18 g of control or spiked soils to reach 3 cm height. The soil was retained in the column with a 20 μm mesh nylon membrane (Fig. 31). Half of the soil columns were exposed to rainfall immediately after spiking. To evaluate the effect of pollutants aging in the soils on the extent of pollutant export, the other half of the columns was incubated in the dark at 20 °C for 10 days before exposition to rainfall.

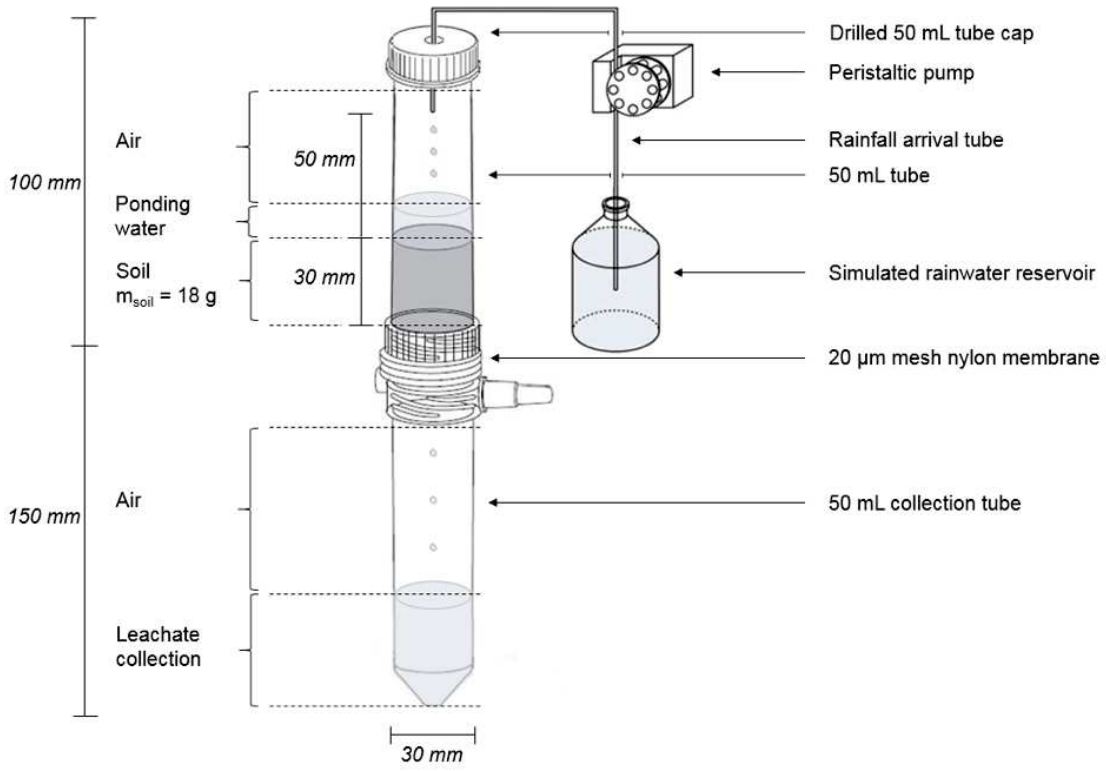

Figure 31: Experimental set-up for pesticide and heavy-metal hydrological forcing.

The four rainfall patterns were applied separately, yielding a total of 16 experiments, i.e., 4 rainfall patterns, applied on 2 soils (spiked vineyard and crop soils), with 2 aging times (0 and 10 days), each run in triplicate, requiring a total of 48 columns. In parallel, rainfall patterns generating the less and the most water volumes (i.e., patterns 1 and 4, respectively; Table 32) were applied on vineyard and crop control soils without pollutant spiking to evaluate the background export of pollutants. To evaluate the influence of rainfall frequency on pollutant export, each experiment received two successive and identical rainfalls separated by a seven days interval.

At the end of each rainfall, leached and ponded waters (the latter collected by a syringe immediately after the rainfall event) obtained from each triplicate experiments were collected and pooled to obtain a homogeneous sample for each conditions and sufficient amount of pesticides and metals for further quantification. The soil from each triplicate systems were collected and pooled at the end of the second rainfall. The water and soil samples were immediately frozen at -20 °C until further analyses. Soil samples were analyzed to quantify the remaining mass of pollutants after the second rainfall.

3.2.5 Elemental analysis

Dissolved organic carbon (DOC) in water samples was quantified using a carbon analyzer (Shimadzu TOC - VCPH). Acetate, major anions and cations (chloride, nitrate, sulfate, ammonium, sodium, potassium, magnesium and calcium ions) were quantified using ion chromatography (ICS 3000 Dionex, San Diego, CA, USA, ± 2%). For chemical composition analysis (including Cu and Zn), oven-dried (60 °C) soils were powdered using an agate disk mill (<100 μm) prior to alkaline fusion and total dissolution by acids. Measurements were carried out using ICP-AES (ICAP6500, Thermo Fisher Scientific) with the geological stan-

dards BCR-2 (US Geological Survey, Reston, VA, USA) and SCL-7003 (Analytika, Prague, Czech Republic) for quality control [34], with a total analytical uncertainty of ± 5%, that incorporates both accuracy and reproducibility, and a detection limit < 3 μg L^{-1}.

3.2.6 Metalaxyl and SM analysis

The volumes of leaching and ponding water were adjusted up to 25 mL with ultra-pure water prior to solid phase extraction (SPE). Metalaxyl and SM were extracted from leaching and ponding water samples using SolEx C18 cartridges (Dionex®, CA, USA) packed with 1 g bonded silica on an AutroTrace 280 SPE system (Dionex®, CA, USA), following a protocol adapted from US EPA method 525.2 and previously described [37].

Pesticides were extracted from the soil matrix using a solvent extraction procedure adapted from previous studies [38, 39] and detailed in the **SI**. Metalaxyl was extracted with recoveries of 68 ± 27% from the crop soil and 66 ± 29% from the vineyard soil. SM was extracted from 24 ± 8% and 23 ± 10% from the crop and vineyard soils, respectively. Metalaxyl and SM quantification was performed by gas chromatography (Trace 1300, Thermo Fisher Scientific) coupled to a mass spectrometer (ISQ, Thermo Fisher Scientific) (GC-MS) as previously described [37].

3.2.7 Data analysis

During the first rainfall, the relative loads ($RL1$) of pollutants were estimated according to

$$RL1_{x,j,p,s,a} = \frac{m_{x,j,p,s,a,r1}}{m_{init(x,s,a)}} \cdot 100 \tag{3.1}$$

where $m_{x,j,p,s,a,r1}$ (μg) is the mass of pollutant x - metalaxyl, SM, Cu or Zn - exported via process j ponding or leaching, with a rainfall pattern p -1, 2, 3 or 4, Table 32 - for the soil s - crop or vineyard - with aging process a - no aging or 10 days aging - after the first rainfall $r1$ and $m_{init(x,s,a)}$ (μg) the initial pollutant mass in soil for corresponding pollutant (x), soil (s) and aging process (a). For the experiments with 10 days of pollutant aging, $m_{init(x,s)}$ was measured for metalaxyl and SM before the first rainfall.

The relative loads during the second rainfall ($RL2$) expressed as a fraction (-) were calculated by mass balance adjustments and a first-order rate model (SFO) to account for pesticide degradation that occurred between the two successive rainfalls. Hence eq. 3.1 is updated to account for export losses during the first pulse and sinks associated to degradation in between the two pulses as

$$RL2_{x,j,p,s,a} = \frac{m_{x,j,p,s,a,r2}}{(m_{init(x,s,a)} - \sum_{j=1}^{J} m_{x,j,p,s,a,r1}) \cdot exp(-k_x \cdot t)} \cdot 100 \tag{3.2}$$

where, similar to eq. 3.1 $m_{x,j,p,s,a,r2}$ is the mass (μg) exported during the second rainfall ($r2$) due to process j (leaching and ponding). The dissipation rate constant k_x (d^{-1}) for pesticide x - metalaxyl or SM - was calculated by $k_x = ln(2)/DT50_x$ ($k_x = 0$ for metals), where DT50 (d) is the pesticide half-life obtained from ref. [30].

Table 33: Green-Ampt input parameters

Parameter	Unit	Crop soil	Vineyard soil	Source
ω, suction at the wetting front	[mm]	1100	1100	Ref. [46]
θ_{t_0}, initial moisture	[-]	0.2	0.2	Exp. measurement
θ_{sat}, saturation moisture	[-]	0.62	0.61	Exp. measurement

To evaluate differences in exported pollutants across rainfall patterns (i.e., intensity-duration-volume), rainfall frequency, soils or aging time, nonparametric Kruskal-Wallis and Wilcoxon tests were applied at a significance level of 0.05 using the R statistical software [40].

To visualize dissimilarities in patterns of pollutant export, two-dimensional non-metric multi-dimensional scaling (NMDS) [41] based on Bray-Curtis dissimilarities of Hellinger-transformed data (square-root transformation of relative masses of exported pollutants) was used. The relationship between the pollutant export patterns and the experimental variables (i.e. soil type, aging, rainfall frequency, intensity, volume and duration) was investigated by fitting vectors a posteriori onto the NMDS. The significance of the vector fitting was assessed using a Monte-Carlo permutation test (1000 permutation steps).

3.2.8 Modelling of pesticide ponding and leaching

Partitioning between infiltration and ponding was determined using the Green & Ampt formalism [9, 42], which simulates overland flow when rainfall intensity overcomes the soil infiltration capacity and given by

$$f = K_{sat}\left(\frac{\omega\Delta\theta}{F} + 1\right) \tag{3.3}$$

where f is infiltration (mm), K_{sat} is saturated hydraulic conductivity (mm h^{-1}), ω is suction at the wetting front (mm), $\Delta\theta$ is the moisture difference between initial and saturation conditions (-) and F is the cumulative infiltration (mm). Parameter values are presented in Table 31 and 33. The retention and release of pesticides in the top-soil was conceptualized with a mixing layer model [43, 44] (eq. 3.6) and a diffusion model across soil-ponded water interface [45] (eq. 3.7). The approach assumes linear equilibrium sorption where the initial pore water concentration (C_{aq}) is given by

$$C_{aq} = \frac{C_s}{K_d} \tag{3.4}$$

$$K_d = K_{oc} f_{oc} \tag{3.5}$$

Where C_s is the total concentration at the beginning of the experiment (t_0), K_d is the partition coefficient (ml g^{-1}). To fit pollutant export across rainfall patterns, K_{oc} values for metalaxyl, SM, Cu and Zn were calibrated within the range of values of ref. [30]. Organic carbon fractions (f_{oc}) (-) and soil bulk densities (ρ_b, g cm^{-3}) soils were measured (Table B1).

The total losses (μg) considered for a rainfall event include mass loss due to leaching (M_{lch}) and mass loss due to ponding (M_{pnd}). Masses due to leaching are computed by subtracting initial pore water mass from the remaining mass in pore water at the end of an event of time Δt,

$$M_{lch} = C_{aq,t_0}\left(1 - e^{\frac{-L_z \Delta t}{R D_z \theta_{sat}}}\right) \cdot D_z \theta_{sat} \tag{3.6}$$

where C_{aq,t_0} is initial concentration (μg L^{-1}) in pore water, L_z is leached depth (mm), D_z is the soil depth (mm), θ_{sat} the saturated moisture and R the retardation factor (-), which is given by

$$R = 1 + \frac{\rho_b + K_d}{\theta_{sat}} \tag{3.7}$$

Masses in ponding water were retrieved by calculating the mass flux across the top soil boundary based on the concentration gradient between soil pore and ponded water concentrations, such that

$$M_{pnd} = \int_{t_p}^{\Delta t} K_L\left(C_{aq,t} - C_{p,t}\right)\partial t \cdot A \tag{3.8}$$

where t_p is the time of ponding (min), K_L (mm min^{-1}) is the mass transfer coefficient that relates solute flux from the soil surface to the ponding water, C_p is the concentration in ponded water depth (μg L^{-1}) and A the soil-water boundary area (mm^2). The ability of the model to reproduce pollutant export by ponding or leaching was evaluated by comparing the observed and simulated ponded or leached volumes while maximizing the coefficient of determination (r^2).

3.3 Results and discussion

3.3.1 Partitioning of water ponding and leaching

Contrasted water flow paths were observed for the two successive rainfalls. The first rainfall generated only leaching without ponding, independently of the rainfall patterns, which indicates that the rainfall intensities never overcame the soil infiltration capacity. This is in agreement with relative high values of saturated hydraulic conductivity (K_{sat}), e.g., 135 and 176 mm h^{-1} measured for the crop and vineyard soils, respectively. High values of K_{sat} were a consequence of the soil sieving step and can be observed in the field just after tillage [47].

The observed volumes of ponded and leached water were compared to those simulated with the model to evaluate the ability of the experimental set-up to mimic water ponding and leaching. The Green-Ampt model predictions parametrized with the measured (before the first rainfall) and calibrated K_{sat} values (before the second rainfall) (Table 31 and 33) fitted well the observed leaching and ponded volumes (mean r^2 = 0.98) (Table 34). K_{sat} values before the second event were calibrated as they could not be measured without disturbing the soil in the columns. The calibrated K_{sat} values to fit the observed volumes for the second

Table 34: Observed and simulated ponding and leaching water volumes

		Crop				Vineyard			
Modality	Pattern	Observed		Modelled		Observed		Modelled	
		V_{lch} [mL]	V_{pnd} [mL]	V_{lch} [mL]	V_{pnd} [mL]	V_{lch} [mL]	V_{pnd} [mL]	V_{lch} [mL]	V_{pnd} [mL]
Fresh, (1st)	1	17.51	-	17.86	-	19.08	-	18.91	-
	2	5.9	-	9.66	-	11.11	-	11.6	-
	3	40.4	-	44.45	-	46.4	-	46.39	-
	4	12.96	-	14.18	-	13.61	-	14.18	-
Aged , (1st)	1	20.09	-	17.86	-	20.87	-	18.91	-
	2	10.6	-	9.66	-	11.29	-	11.6	-
	3	47.2	-	44.45	-	47.03	-	46.39	-
	4	14.29	-	14.18	-	17.71	-	14.18	-
Fresh, (2nd)	1	9.38	22.62	9.28	21.19	26.74	3.72	24.14	6.32
	2	19	3.91	19.24	3.95	3.67	17.73	3.8	18.03
	3	2.47	28.91	3.54	23.85	18.6	39.35	19.03	38.96
	4	8.25	20.94	8.4	19.96	0	26.63	1.1	25.79
Aged, (2nd)	1	3.39	27.31	3.57	26.39	6.2	22.83	5.94	24.56
	2	11.41	7.31	11.74	11.45	12.99	8.03	13.22	9.97
	3	20.29	33.48	19.42	38.56	29.23	23.69	27.24	30.74
	4	5.47	19.04	5.47	22.89	6.55	19.35	6.7	21.66

event were one to two orders of magnitude lower than those measured before the first rainfall event (Table 31). Such decrease of K_{sat} values was also observed in the field as a result of aggregate breakdown by rainfall and clogging of larger pores [19, 20]. Soil depth (i.e., 30 mm) also decreased by 4 to 11 mm after the first rainfall event, which further indicated changes of soil porosity, bulk density and hydraulic conductivity.

Overall, different ponding/leaching water partitioning between the first and the second rainfall events underlined that the threshold behaviour of ponding was controlled by top soil K_{sat} values, as observed in field conditions [46, 48]. The good fitting of simulated ponding and leaching water volumes by the Green-Ampt method underscored that soil matrix properties (i.e. , K_{sat}, ρ_b, θ) controlled the hydraulic properties of the columns without significant preferential flows along the boundary between the column surface and the soil. This validation step on column hydraulic functioning allowed inferring the impact of rainfall patterns on pollutant export from soil matrix by leaching and ponding.

3.3.2 Impact of rainfall patterns on pollutant export

No significant concentrations of metalaxyl, SM, Cu and Zn could be detected in leachates from the control soils (non-spiked soils). This confirmed that the experimental set-up enabled to evaluate the mass export of freshly spiked and short-term aged pollutants. While rainfall patterns did not significantly impact the ponding/leaching ratios (i.e., $RL2_{pond}/RL2_{leach}$) of pesticides (P>0.1), concentrations of heavy metals in ponding waters were too low to evaluate their ponding/leaching partitioning (<1 and <3 μg L^{-1} for Zn and Cu, respectively). Only up to $1.2 \pm 1.2\%$ and $0.2 \pm 0.1\%$ of metalaxyl and SM, respectively, was exported in ponding water (i.e., $RL2_{pond}$, crop, vineyard and aged systems taken together).

Several processes may control the transfer of dissolved pesticides into ponding water, in-

cluding i) diffusion (induced by concentration gradients), ii) ejection of solution from the soil surface by raindrops, iii) desorption of pesticides sorbed onto soil, and iv) desorption of pesticides bound to soil particles eroded by raindrops (and surface flow) [6]. Ejection of dissolved pesticides solution from the soil surface and bound pesticides desorption of soil particles eroded cannot explain dissolved pesticide loads in ponding waters because the impact of simulated raindrops on the transfer of dissolved pesticides to ponding water was likely limited in our case. Indeed, our experimental set-up, unlike in field conditions, did not allow for rain drops to approximate terminal velocities lowering the kinetic energy expected to drive solute entrainment [49, 50]. Desorption of pesticides sorbed onto soils and, to a minor extent, diffusion thus likely controlled pollutant transfer into ponding water in our experiment. The extent of pollutant transfer corresponded to pollutant physico-chemical properties. For example, ponding/leaching ratios (i.e. $RL2_{pond}/RL2_{leach}$) for SM, for example, were twice higher than those for metalaxyl (Fig. 32), which can be related to the higher solubility of metalaxyl (7100 mg L^{-1}) compared to SM (480 mg L^{-1}). In contrast, rainfall patterns significantly impacted leaching of metalaxyl ($P < 0.01$), SM ($P < 0.05$) and Cu ($P < 0.05$) during the first rainfall cycle.

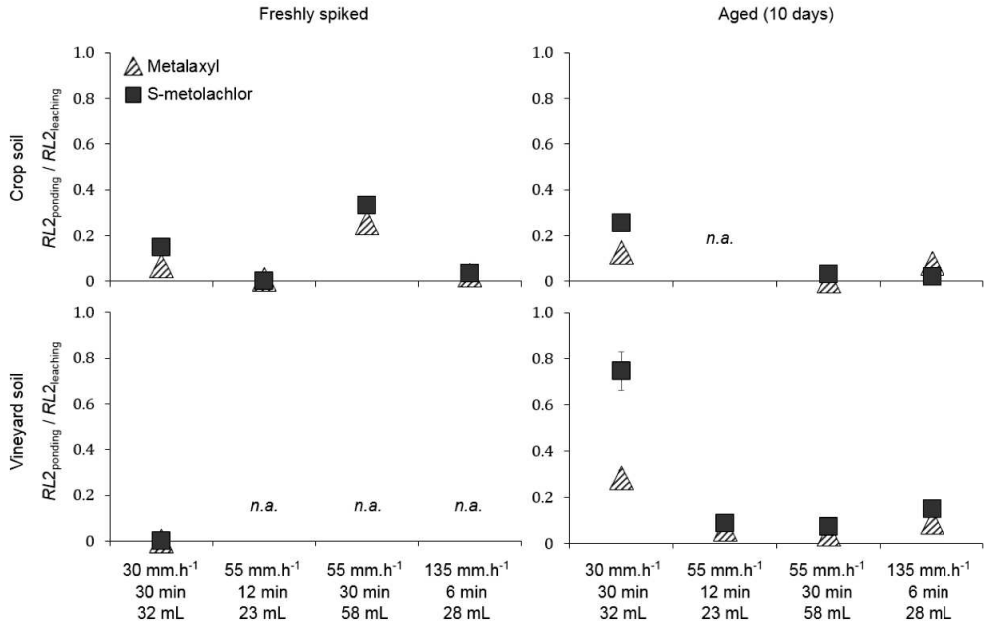

Figure 32: Ratios of ponding to leached metalaxyl and SM exports (second rainfall cycle only, $RL2_{pond}/RL2_{leach}$). Error bars denote 95% confidence intervals. "n.a." denotes the absence of value when no leaching or ponding water was produced.

Changes in pollutant leaching profiles were visualized by the NMDS ordination of metalaxyl, SM, Cu and Zn leached loads from the vineyard and the crop soils exposed to the four rainfall patterns in two successive events (Fig. 33). The ordination showed that leaching profiles produced by the third rainfall pattern (long-lasting pattern with intermediate intensity; Table 32) during the first rainfall significantly differed from the other profiles ($P < 0.001$) (Fig. 33). The third rainfall pattern induced the largest leached loads for both pesticides and metals. Amounts of metalaxyl, SM, Cu and Zn leached (i.e., $RL1_{leach}$ and $RL2_{leach}$) during the third rainfall pattern reached 44.5 ± 21.5%, 8.1 ± 3.1%, 3.1 ± 0.3% and 2.2 ± 0.2% of the spiked dose, respectively (all systems compounded) (Fig. 34 and 35).

To evaluate the relationship between the leaching profiles (i.e., $RL1_{leach}$ and $RL2_{leach}$), the

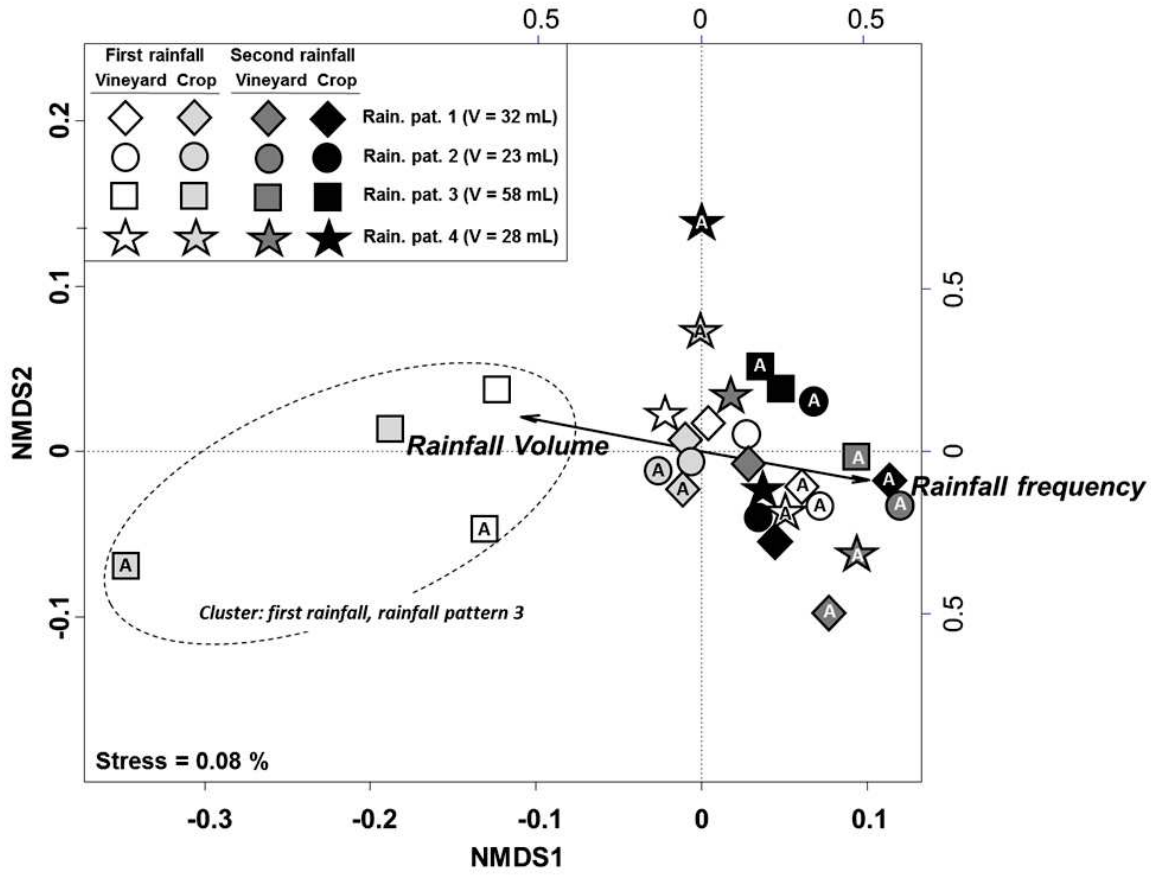

Figure 33: 2D-NMDS ordination of metalaxyl, SM, Cu and Zn export ($RL1_{leach}$ and $RL2_{leach}$) profiles from the vineyard and the crop soils exposed to the four rainfall patterns, following pollutant aging (A) or not, and after the first and the second rainfall. Vectors that correspond to experimental variables (rainfall frequency, aging, rainfall intensity, volume and duration) and significantly correlated with pollutant export profiles are shown (i.e., volume and cycles). The significance of fitted vectors was calculated by a posteriori permutation of variables at $P < 0.001$. Vector arrows were fitted to the NMDS ordination depicting the direction and magnitude of change of the variable.

rainfall patterns and the soil characteristics, the experimental variables (i.e., soil type, aging, rainfall frequency, intensity, volume and duration) were fitted onto the NMDS ordination of pollutant leaching profiles (Fig. 33). The analysis revealed that pollutant leaching profiles mainly correlated with changes in rainfall volumes and rainfall frequency ($P < 0.001$). This emphasizes the impact of rainfall volume on pollutant leaching from the soils. With the addition of water, the instantaneous sorption equilibria is shifted enabling higher leaching of pollutants to occur [2]. Overall, the leaching of metals and pesticides from the studied soils (Fig. 34 and 35) were in agreement with previous observations. For example, while cumulative leaching of metals from soils three years after their application were lower than 1% [1], up to 50% was exported from soil columns initially spiked with atrazine and metolachlor under various conditions to manage leaching losses [51].

On the field, the impact of rainfall patterns on pollutant export from soil matrix also depends on the rainfall event frequency impacting soil compaction and crusting. Assessing the impact of rainfall frequency on pollutant export is thus needed to quantify the temporal evolution

of export risk.

3.3.3 Impact of rainfall frequency on pollutant export

The same rainfall patterns were applied twice successively on the soil columns at seven days of interval to investigate the effect of successive rainfalls on pollutant leaching (i.e., $RL1_{leach}$ and $RL2_{leach}$ for all soils, freshly spiked and aged systems). The rainfall patterns had no significant impact during the second rainfall (p>0.1) when comparing the normalized leaching profiles (%) on the NMDS ordination (Fig. 33). Leaching profiles generated by the second rainfall (i.e., $RL2_{leach}$) event differed from those generated by the first rainfall event (i.e., $RL1_{leach}$). In particular, rainfall frequency had the highest impact on metalaxyl and SM leaching ($P < 0.0005$) compared to Cu and Zn ($P < 0.01$). Overall, the second rainfall leached 2.4-, 2.9-, 30- and 50-fold less metalaxyl, SM, Cu and Zn, respectively, compared to the first rainfall (Fig. 34 and 35). This supports the hypothesis that distinct pools of pollutants within soil aggregates were mobilized from the soils after a seven days interval following the first rainfall event.

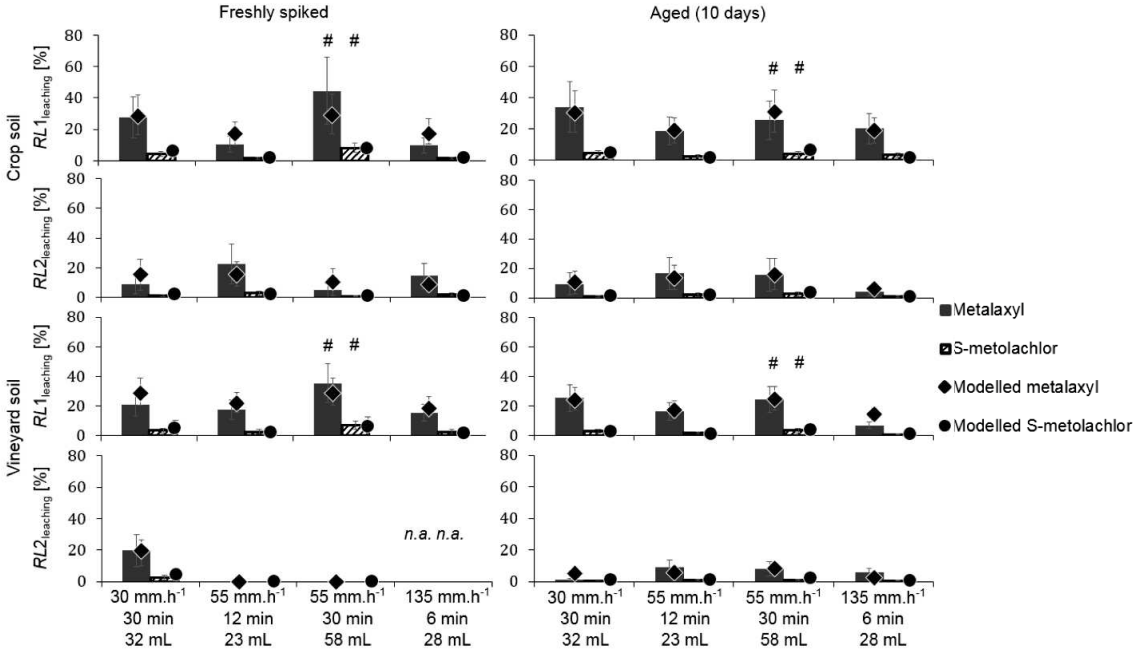

Figure 34: Experimental (bars) and modelled (points) percentages of metalaxyl and SM leached ($RL1_{leach}$ and $RL2_{leach}$) from the freshly spiked and aged (10 days) crop and vineyard soils after 1 rainfall (cycle 1) and 2 rainfalls (cycle 2) with 7 days of interval. Error bars denote 95% confidence intervals. "#" indicates the cluster "First rainfall - Rainfall pattern 3" of the NMDS ordination. "n.a." denotes the absence of value when no leaching water was produced.

Indeed, the sieved soils used for the experiment had initially no crust, lower bulk density and higher K_{sat} values, which likely facilitated water percolation within the soils during the first rainfall [52], and thus enhanced pollutant mobilization. Soil aggregation is expected to decrease with successive rainfalls, which can release pesticides trapped on aggregates [17]. In addition, wet-dry cycles have been observed to increased desorption of metolachlor from soils by up to a 2-fold factor [17]. However, an opposite trend was observed in our experiment. Soil compaction occurred after the first rainfall, which likely caused dissociation of soil aggregates during the first rainfall event by slaking and wetting processes [52]. Dissociation

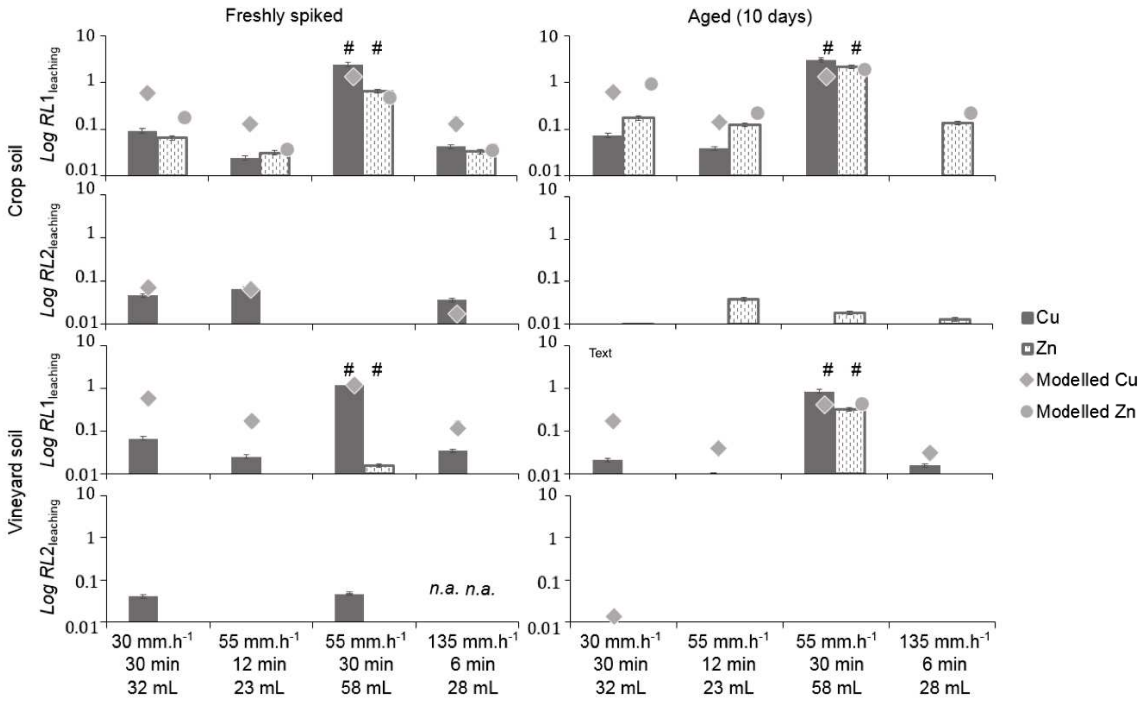

Figure 35: Experimental (bars) and modelled (points) logarithms of Cu and Zn leached ($RL1_{leach}$ and $RL2_{leach}$) from the freshly spiked and aged (10 days) crop and vineyard soils after 1 rainfall (cycle 1) and 2 rainfalls (cycle 2) with 7 days of interval. Error bars denote 95% confidence intervals. "#" indicates the cluster "First rainfall - Rainfall pattern 3" of the NMDS ordination. "n.a." denotes the absence of value when no leaching water was produced.

of soil aggregates likely then mobilized pollutants and enhanced pollutant leaching in a single rainfall. As a result, the occurrence of a pollutant pool available for leaching in a second rainfall, as previously reported [17], could not be observed in our case. In addition, soil compaction caused by the first rainfall clearly increased the ponding/leaching ratio in the second rainfall. This limited pollutants leaching during the second rainfalls and hid the impact of rainfall patterns on pollutant leaching during the second rainfall events. To some extent, our setup allowed exploring two extreme situations commonly observed in the field after 80 - 100 mm of rainfall over three weeks of an agricultural season. While the initial sieved soil mimicked the beginning of a crop season just after tillage (topsoil with low bulk density and high K_{sat}), soil compaction and crusting (especially for loamy soils) following the first rainfall was similar to that eventually observed in the field after a rainfall depth of 80 - 100 mm [19].

The model fitted well the observations of pollutant leaching without aging (average r^2 = 0.80 for the four pollutants, $RL1_{leach}$), although, for some experiments, it was necessary to use lower K_{oc} values than those retrieved from the literature (Table 35). This suggests that the time between pollutant spiking and the beginning of rainfall patterns (about 3 hours) was insufficient to reach complete sorption equilibrium, which is in agreement with previous observations [53]. The model could not accurately predict Cu and Zn loads in leaching waters for the first rainfall event and in ponding water for the second rainfall. This limitation may be due to the lack of representation in particle transport via erosion but also colloid-facilitated transport of metals. In addition, the low number of experiments generating Cu and Zn loads

Table 35: Calibrated K_{oc} used to fit model pesticide and metal exports

	K_{oc}, rainfall	Crop soil		Vineyard soil	
	[mL g^{-1}]	t = 0 day	t = 10 days	t = 0 day	t = 10 days
Metalaxyl	1st	15	14	25	30
	2nd	25	25	20	53
SM	1st	63	75	125	200
	2nd	125	125	98	196
Cu	1st	248	249	466	933
	2nd	784	39	7841	1568
Zn	1st	495	197	93041	933
	2nd	49	98951	49	99

limited the ability to evaluate the adequacy of alternative models. While extrinsic factors (i.e., rainfall patterns and frequencies) clearly controlled the risk of pollutant export from the soil matrix, intrinsic factors such as soil characteristic and aging process can also enhance or reduce pollutant mobilization.

3.3.4 Impact of soil characteristics and aging on pollutant export

Although soil type and aging were not predominant factors for pollutant leaching compared to rainfall patterns and frequency (Tables B1 and 31), Zn and Cu leaching were influenced by the soil type ($P < 0.005$) and aging ($P < 0.05$), respectively. Zn leaching ($RL1_{leach}$ and $RL2_{leach}$) from the vineyard soils was 9.4-fold smaller than that from crop soils (Fig. 34 and 35). In contrast, Cu, metalaxyl and SM leaching ($RL1_{leach}$ and $RL2_{leach}$) from the vineyard and crop soils were similar.

Larger Zn leaching from the crop soil may reflect both crop soil characteristics and different Zn speciation in the crop and the vineyard soils. Previous studies on the same vineyard soil showed that Zn was predominantly associated with the residual fraction (silicate matrix), secondly to carbonates, followed by organic matter and at last the oxide fraction, regardless of the soil type, depth or organic matter content [26]. Zn is known to diffuse into interlayers of silicates [54–56] and also to remain fixed in the soil matrix after its diffusion into carbonates [8, 57]. Clay and carbonate content of the crop soil were, respectively, 2 and 33 times lower compared to the vineyard soil (Table B1). Hence, Cu leaching was likely less impacted than Zn by differences in clays or calcite content among the studied soils.

Based on metalaxyl and SM physico-chemical characteristics and organic matter content of the crop and the vineyard soils, pesticides can also interact with soil minerals [58]. While uncharged pesticides, such as atrazine and isoproturon, can sorb onto pure kaolinite [58], pesticides generally have high affinity with organic matter. When TOC is larger than 0.1%, organic matter becomes the main sorbent of pesticides in soils [5, 58]. Because organic matter content was similar in both soils, the soil type likely was not the main factor that controlled leaching of metalaxyl and SM.

Over time, aging strengthens the association of a chemical with the soil components, thereby lowering pollutant export with increasing contact time [7]. In our case, the aging phase of ten days prior to rainfall applications only impacted Cu leaching. Indeed, Cu speciation may change for the 10-days of aging because the distribution of a freshly applied heavy metal in soils is expected to follow a multi-steps sorption. First, Cu, and to a lesser extent Zn, rapidly sorb onto mineral and organic surfaces, which is followed by a slower aging phase,

characterized by the diffusive penetration or chemisorption of surface-sorbed heavy metals into soil constituents, such as Fe-oxides, hydrous oxides of Al and Mn, clay minerals, as well as diffusion or precipitation into carbonates [13, 15]. During aging, Cu most probably underwent a diffusive penetration and interacted with oxides, clays and carbonates, which slightly decreased Cu export in the aged experiments compared to the freshly spiked experiments. The decrease of labile forms in soils over 10 days has been shown to be larger for Cu than for Zn, while the increase of the Cu reducible fraction mainly corresponded to the Cu associated with soil oxides [12]. As Zn was mainly associated to clays and carbonates [26], its mobility did not significantly change during the 10 days aging period. In comparison, a 65% decrease in Zn leaching was observed after a 63-days aging phase, as it might be remobilized from exchangeable sites to stronger ones [59].

Aging of metalaxyl and SM occurred differently. In addition to the degradation that pesticides undergo with time, increasing contact time with soils may create stronger bonds to soil particles [7, 10]. However, metalaxyl and SM had relatively weak affinity for the soils, as emphasized by K_d values lower than 2 L kg^{-1} in our soils (estimated based on the f_{oc} of the soils and the respective K_oc for each compound. Indeed, K_d values $\geq$ 100 L kg^{-1} indicate strongly sorbed pesticides [60]. The lower apparent K_d values calibrated in the model for the aged soils compared to those calculated from the K_{oc} values retrieved from databases [29] emphasizes the low impact of a ten day aging period on pesticides and Zn leaching in the soil experiments. To determine when rainfall characteristics predominate on soil type and aging to control pollutant export from topsoil, a longer aging period and a more systematic investigation of soil types to cover the diversity of agricultural lands may be needed.

3.4 Conclusion

This study revealed the primary influence of extrinsic factors, such as rainfall frequency, rainfall duration and volume, on the export by ponding and leaching of organic and inorganic pollutants from topsoil. The rainfall volumes particularly affected the export of pollutants during the first rainfall event after their application. The rainfall volumes and rainfall frequency, through their impact on soil compaction, were the main factors controlling pesticide leaching. Most importantly, the rainfall patterns significantly impacted the leaching of metalaxyl, S-metolachlor (SM) and Cu during the first rainfall, in both freshly spiked and aged soils. One significant implication is that the first rainfall following the field application of pre-emergence pesticides may be critical for pesticide export. In contrast, soil composition and aging had a secondary influence on pollutant export from soils. For instance, Cu and Zn leaching was also controlled by the aging period and the soil type, respectively.

The adequate hydrological functioning of the experimental design was confirmed by simulation of ponding and percolated waters using a parsimonious numerical model. The model could generally reproduce the mass balance for both metalaxyl and SM leaching in soil. In field conditions, preferential flow in macropores may additionally increase pesticide transport. As a result, leaching from topsoil of pre-emergence pesticides applied shortly after tillage on bare soils may represent a specific risk. In contrast, provided that pH and redox conditions do not dramatically vary, only extreme rainfall patterns may generate significant metal leaching, as showed here for the long-lasting events with low and intermediate rainfall intensities. Such rainfall patterns may particularly result in metal leaching at the beginning of the agricultural season, before soil compaction over the season reduces metal leaching. By refining the expected exports of pesticides and metals in different conditions, we anticipate this study to be a preliminary step to more systematically evaluate the impact of rainfall

patterns and frequency on pollutant export in benchmark soil tests.

References

1. McLaren, R. G., Clucas, L. M., Taylor, M. D. & Hendry, T. Leaching of macronutrients and metals from undisturbed soils treated with metal-spiked sewage sludge. 2. Leaching of metals. *Soil Research* **42,** 459–471 (June 2004).
2. Arias-Estévez, M. *et al.* The mobility and degradation of pesticides in soils and the pollution of groundwater resources. *Agriculture, Ecosystems and Environment* **123,** 247–260. ISSN: 01678809 (2008).
3. Schafer, R. B. *et al.* Effects of pesticide toxicity, salinity and other environmental variables on selected ecosystem functions in streams and the relevance for ecosystem services. eng. *The Science of the total environment* **415,** 69–78. ISSN: 1879-1026 (Electronic) (Jan. 2012).
4. Lefrancq, M. *Transport and attenuation of pesticides in runoff from agricultural headwater catchments: from field characterisation to modelling* PhD thesis (Université de Strasbourg, 2014).
5. Schwarzenbach, R. P. & Westall, J. Transport of nonpolar organic compounds from surface water to groundwater. Laboratory sorption studies. *Environmental Science & Technology* **15,** 1360–1367. ISSN: 0013-936X (Nov. 1981).
6. Shi, X. N., Wu, L. S., Chen, W. P. & Wang, Q. J. Solute Transfer from the Soil Surface to Overland Flow: A Review. *Soil Science Society of America Journal* **75,** 1214–1225. ISSN: 0361-5995 (2011).
7. Gevao, B., Semple, K. T. & Jones, K. C. Bound pesticide residues in soils: a review. *Environmental Pollution* **108,** 3–14. ISSN: 0269-7491 (2000).
8. Buekers, J. *Fixation of cadmium, copper, nickel and zinc in soil: kinetics, mechanisms and its effect on metal bioavailability. PhD thesis.* PhD thesis (Katholieke Universiteit Leuven, 2007). `https://lirias.kuleuven.be/handle/1979/940`.
9. Green, H. & Ampt, G. . Studies on Soil Phyics. *The Journal of Agricultural Science* **4,** 1–24. ISSN: 0021-8596 (1911).
10. Komárek, M., Čadková, E., Chrastný, V., Bordas, F. & Bollinger, J.-C. Contamination of vineyard soils with fungicides: A review of environmental and toxicological aspects. *Environment International* **36,** 138–151. ISSN: 0160-4120 (2010).
11. Ma, Y. B., Lombi, E., Nolan, A. L. & McLaughlin, M. J. Determination of labile Cu in soils and isotopic exchangeability of colloidal Cu complexes. *European Journal of Soil Science* **57,** 147–153. ISSN: 1351-0754 (2006).
12. Huang, B. *et al.* Aging effect on the leaching behavior of heavy metals (Cu, Zn, and Cd) in red paddy soil. *Environmental Science and Pollution Research* **22,** 11467–11477. ISSN: 0944-1344 (2015).
13. Jalali, M. & Khanlari, Z. V. Effect of aging process on the fractionation of heavy metals in some calcareous soils of Iran. *Geoderma* **143,** 26–40. ISSN: 0016-7061 (2008).
14. Sauvé, S., Hendershot, W. & Allen, H. E. Solid-Solution Partitioning of Metals in Contaminated Soils: Dependence on pH, Total Metal Burden, and Organic Matter. *Environmental Science & Technology* **34,** 1125–1131. ISSN: 0013-936X (2000).

15. Tang, X., Zhu, Y., Cui, Y., Duan, J. & Tang, L. The effect of ageing on the bioaccessibility and fractionation of cadmium in some typical soils of China. *Environment International* **32,** 682–689. ISSN: 0160-4120 (2006).

16. Nolan, B. T. *et al.* Identification of key climatic factors regulating the transport of pesticides in leaching and to tile drains. *Pest Management Science* **64,** 933–944. ISSN: 1526-4998 (2008).

17. Goldreich, O., Goldwasser, Y. & Mishael, Y. G. Effect of soil wetting and drying cycles on metolachlor fate in soil applied as a commercial or controlled-release formulation. *Journal of Agricultural and Food Chemistry* **59,** 645–653. ISSN: 00218561 (2011).

18. Beulke, S., Brown, C. D., Fryer, C. J. & Walker, A. Lysimeter study to investigate the effect of rainfall patterns on leaching of isoproturon. *Pest Management Science* **58,** 45–53. ISSN: 1526-498X (2001).

19. Armand, R., Bockstaller, C., Auzet, A. & Van Dijk, P. Runoff generation related to intra-field soil surface characteristics variability. Application to conservation tillage context. *Soil and Tillage Research* **102,** 27–37. ISSN: 0167-1987 (2009).

20. Chahinian, N., Voltz, M., Moussa, R. & Trotoux, G. Assessing the impact of the hydraulic properties of a crusted soil on overland flow modelling at the field scale. *Hydrological Processes* **20,** 1701–1722. ISSN: 0885-6087 (2006).

21. Lefrancq, M., Jadas-Hécart, A., La Jeunesse, I., Landry, D. & Payraudeau, S. High frequency monitoring of pesticides in runoff water to improve understanding of their transport and environmental impacts. *Science of the Total Environment* **587-588,** 75–86. ISSN: 18791026 (2017).

22. Harel, M.-A. & Mouche, E. Is the connectivity function a good indicator of soil infiltrability distribution and runoff flow dimension? *Earth Surface Processes and Landforms,* n/a–n/a. ISSN: 0197-9337 (2014).

23. Crowley, D. E., Luepromechai, E. & Singer, A. *Metabolism of Xenobiotics in the Rhizosphere* 2000. doi:10.1021/bk-2001-0777.ch018. http://dx.doi.org/10.1021/bk-2001-0777.ch018.

24. Diez, M. C. *et al.* Rhizosphere effect on pesticide degradation in biobeds under different hydraulic loads. *Journal of soil science and plant nutrition,* 0. ISSN: 0718-9516 (2015).

25. Banzhaf, S. & Hebig, K. H. Use of column experiments to investigate the fate of organic micropollutants – a review. *Hydrology and Earth System Sciences* **20,** 3719–3737. ISSN: 1607-7938 (2016).

26. Duplay, J. *et al.* Copper, zinc, lead and cadmium bioavailability and retention in vineyard soils (Rouffach, France): The impact of cultural practices. *Geoderma* **230-231,** 318–328. ISSN: 0016-7061 (2014).

27. Lefrancq, M., Payraudeau, S., Guyot, B., Millet, M. & Imfeld, G. Correction to Degradation and Transport of the Chiral Herbicide S-Metolachlor at the Catchment Scale: Combining Observation Scales and Analytical Approaches. *Environmental Science & Technology* **52,** 5517. ISSN: 0013-936X (May 2018).

28. Hansch, C., Leo, A. & Hoekman, D. *Exploring QSAR - Hydrophobic, Electronic, and Steric Constants.* 134 (American Chemical Society, Washington, DC, 1995).

29. Kegley, S., Hill, B., Orme, S. & Choi, A. *PAN Pesticide Database* 2014. http://www.pesticideinfo.org.

30. PPDB. *The Pesticide Properties Database* Developed by the Agriculture & Environment Research Unit (AERU), University of Hertfordshire, funded by UK national sources and the EU-funded FOOTPRINT project (FP6-SSP-022704). 2009.

31. Allison, J. & Allison, T. *Partition coefficients for metals in surface water, soil, and waste (EPA report 600/R-05/074)* tech. rep. (U.S. Environmental Protection Agency, Washington, DC, 2005), 93.

32. Dankers, R. & Hiederer, R. Extreme Temperatures and Precipitation in Europe: Analysis of a High-Resolution Climate Change Scenario. *JRC Scientific and Technical Reports,* 82. ISSN: 1018-5593 (2008).

33. Lefrancq, M. *et al.* Fungicides transport in runoff from vineyard plot and catchment: contribution of non-target areas. *Environmental Science and Pollution Research* **21,** 4871–4882. ISSN: 0944-1344 (2013).

34. Babcsányi, I., Imfeld, G., Granet, M. & Chabaux, F. Copper stable isotopes to trace copper behavior in wetland systems. *Environmental Science and Technology* **48,** 5520–5529. ISSN: 15205851 (2014).

35. Gumbel, E. *Statistics of Extremes* 400 (Columbia University Press, New York, 1958).

36. Papalexiou, S. M. & Koutsoyiannis, D. Battle of extreme value distributions: A global survey on extreme daily rainfall. *Water Resources Research* **49,** 187–201. ISSN: 0043-1397 (2013).

37. Elsayed, O. F. *et al.* Using compound-specific isotope analysis to assess the degradation of chloroacetanilide herbicides in lab-scale wetlands. *Chemosphere* **99,** 89–95. ISSN: 00456535 (2014).

38. Anastassiades, M., Lehotay, S. J., Štajnbaher, D. & Schenck, F. J. Fast and easy multiresidue method employing acetonitrile extraction/partitioning and "dispersive solid-phase extraction" for the determination of pesticide residues in produce. *Journal of AOAC International* **86,** 412–431. ISSN: 10603271 (2003).

39. Ivdra, N., Herrero-Martín, S. & Fischer, A. Validation of user- and environmentally friendly extraction and clean-up methods for compound-specific stable carbon isotope analysis of organochlorine pesticides and their metabolites in soils. *Journal of Chromatography A* **1355,** 36–45. ISSN: 0021-9673 (2014).

40. R Core Team. *R: A Language and Environment for Statistical Computing* R Foundation for Statistical Computing (Vienna, Austria, 2017). `https://www.r-project.org/`.

41. Smith, J. M. & Mather, M. E. Using assemblage data in ecological indicators: A comparison and evaluation of commonly available statistical tools. *Ecological Indicators* **13,** 253–262. ISSN: 1470-160X (2012).

42. Mein, R. G. & Larson, C. L. Modeling infiltration during a steady rain. *Water Resources Research* **9,** 384–394. ISSN: 0043-1397 (1973).

43. Joyce, B. a., Wallender, W. W. & Mailapalli, D. R. Application of pesticide transport model for simulating diazinon runoff in California's central valley. *Journal of Hydrology* **395,** 79–90. ISSN: 00221694 (2010).

44. McGrath, G. S., Hinz, C. & Sivapalan, M. Modeling the effect of rainfall intermittency on the variability of solute persistence at the soil surface. *Water Resources Research* **44,** 1–10 (2008).

45. Havis, R. N., Smith, R. E. & Adrian, D. D. Partitioning solute transport between infiltration and overland flow under rainfall. *Water Resources Research* **28(10),** 2569–2580. ISSN: 0043-1397 (1992).

46. Lefrancq, M., Payraudeau, S., Benoit, G., Millet, M. & Imfeld, G. SI: Degradation and transport of the chiral herbicide S-metolachlor at the catchment scale: combining observation scales and analytical approaches. *Environ. Sci. Technol.* **51,** 13231–13240 (2017).

47. Zeng, C., Wang, Q., Zhang, F. & Zhang, J. Temporal changes in soil hydraulic conductivity with different soil types and irrigation methods. *Geoderma* **193-194,** 290–299. ISSN: 0016-7061 (2013).

48. Zehe, E., Becker, R., Bárdossy, A. & Plate, E. Uncertainty of simulated catchment runoff response in the presence of threshold processes: Role of initial soil moisture and precipitation. *Journal of Hydrology* **315,** 183–202. ISSN: 0022-1694 (2005).

49. Assouline, S. & Mualem, Y. Modeling the dynamics of seal formation and its effect on infiltration as related to soil and rainfall characteristics. *Water Resources Research* **33,** 1527. ISSN: 0043-1397 (1997).

50. Gao, B. *et al.* Investigating raindrop effects on transport of sediment and non-sorbed chemicals from soil to surface runoff. *Journal of Hydrology* **308,** 313–320. ISSN: 00221694 (2005).

51. Kumar Ghosh, R. & Singh, N. Managing metolachlor and atrazine leaching losses using lignite fly ash. *Ecotoxicology and Environmental Safety* **84,** 243–248. ISSN: 01476513 (2012).

52. Vaezi, A. R., Ahmadi, M. & Cerdà, A. Contribution of raindrop impact to the change of soil physical properties and water erosion under semi-arid rainfalls. *Science of The Total Environment* **583,** 382–392. ISSN: 0048-9697 (2017).

53. Gulkowska, A., Buerge, I. J., Poiger, T. & Kasteel, R. Time-dependent sorption of two novel fungicides in soils within a regulatory framework. *Pest Management Science* **72,** 2218–2230. ISSN: 15264998 (2016).

54. Al-Qunaibit, M. H., Mekhemer, W. K. & Zaghloul, A. A. The adsorption of Cu(II) ions on bentonite—a kinetic study. *Journal of Colloid and Interface Science* **283,** 316–321. ISSN: 0021-9797 (2005).

55. Ma, Y., Lombi, E., Oliver, I. W., Nolan, A. L. & McLaughlin, M. J. Long-Term Aging of Copper Added to Soils. *Environmental Science & Technology* **40,** 6310–6317. ISSN: 0013-936X (2006).

56. Ma, Y. B. Dehydration, Diffusion and Entrapment of Zinc in Bentonite. *Clays and Clay Minerals* **46,** 132–138. ISSN: 0009-8604 (1998).

57. Ma, Y., Liu, W. P. & Wen, Y. Z. Enantioselective degradation of rac-metolachlor and S-metolachlor in soil. *Pedosphere* **16,** 489–494. ISSN: 10020160 (2006).

58. Clausen, L., Fabricius, I. & Madsen, L. Adsorption of Pesticides onto Quartz, Calcite, Kaolinite, and α-Alumina. *Journal of Environment Quality* **30,** 846. ISSN: 1537-2537 (2001).

59. Sayen, S. & Guillon, E. Aging effect on Zn retention on a calcareous soil: Column experiments and synchrotron X-ray micro-spectroscopic investigation. en. *Science of The Total Environment* **487,** 545–556. ISSN: 00489697 (July 2014).

60. Wauchope, R. D. *et al.* Pesticide soil sorption parameters: Theory, measurement, uses, limitations and reliability. *Pest Management Science* **58,** 419–445. ISSN: 1526498X (2002).

Preface to Chapter 4

In chapter 4 an existing distributed hydrological model (BEACH) was adapted to account for temperature and water content control of pesticide degradation (hydro-climatic optimums for bacterial activity) and non-reactive transport of pesticide isotopologues, denoting the new model Pesticide-isotopes BEACH (PiBEACH). Based on soil data obtained during field characterization (chapter 2), PiBEACH evaluates the added value of both inclusion of hydro-climatic controls on degradation and the ability of CSIA to reduce model parameter and pesticide fate uncertainty. The chapter is a preliminary step towards coupling with an event-based model to improve pesticide transport predictions during hydrological forcing.

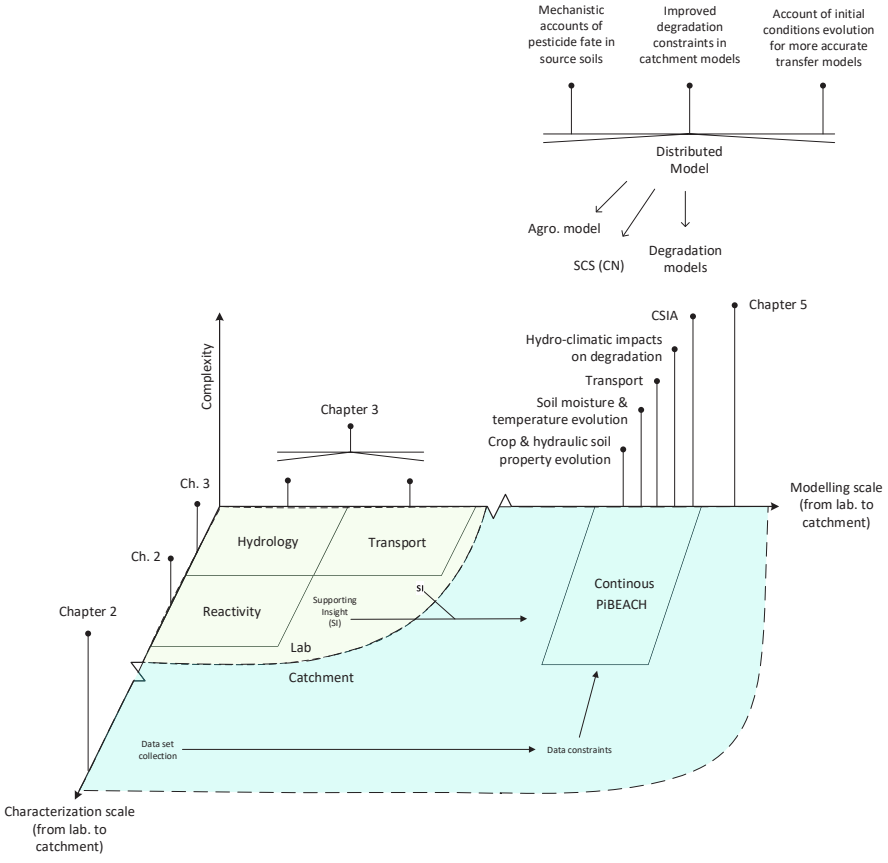

Chapter 4

Constraining pesticide degradation in distributed catchment models with compound-specific isotope analysis (CSIA)*

Abstract. Predicting pesticide dissipation in distributed physically based models at hydrological catchment scale remains challenging, as pesticide degradation kinetics are usually fixed across space and time. In addition, field data distinguishing degradative from non-degradative pesticide dissipation processes for model calibration are scarce. Here control of degradation half-life (DT_{50}) by topsoil water content and temperature was introduced in the pesticide degradation and transport component of a distributed model, and further tested in a 47-ha agricultural catchment. Controlled DT_{50} values improved predictions of S-metolachlor (SM) degradation across the catchment and the agricultural season, and decreased prediction uncertainties (i.e., 95% confidence intervals) of top soil pesticide leaching by a factor of 2. In contrast, constant DT_{50} values, independent of hydro-climatic conditions, increased prediction uncertainties. Compound-specific isotope analysis (CSIA) data constrained DT_{50} values and allowed to validate model predictions of SM degradation in soil and off-site export from the catchment. SM stable isotope data and concentrations reduced model equifinality by teasing apart degradative and non-degradative SM dissipation processes. The range of DT_{50} values was reduced by a factor 2 when including SM stable isotope data into the calibration process. Pesticide CSIA data from topsoil collected weekly across the catchment helped to constrain SM degradation in the PiBEACH model. We anticipate our results as a preliminary step to develop daily long-term continuous models that include hydro-climatic control of pesticide degradation. More reliable predictions of pesticide degradation dynamics at catchment scale may eventually guide pesticide risk assessment and management practices.

4.1 Introduction

The widespread occurrence of pesticides in surface and groundwater threatens aquatic ecosystems and drinking water supply [1–3]. This situation requires accurate predictions of pesticide dissipation and off-site transport at the agricultural catchment scale. Prediction of

* This chapter is the edited version of: Alvarez-Zaldívar, Imfeld, G., Van Dijk, P. and Payraudeau, S. (Expected 2019). Constraining pesticide degradation in distributed catchment models with compound-specific isotope analysis (CSIA) *Submitted to Env. Sci. & Tech.*

pesticide fate at the catchment scale has improved over the last decades, moving from approaches relying on pesticide-properties (e.g., refs. 4, 5) to more complex models integrating hydrological functioning or (bio)chemical dissipation [6–11]. However, discrepancy between complexity of reactive transport models and field datasets available to calibrate and validate such models has dramatically increased [12, 13].

Detailed conceptual and physically-based models account for many processes, including pesticide dissipation, each of which is typically described by several parameters [14]. However, linking pesticide fate parameters obtained under laboratory conditions with field processes is difficult as the relevance of a given parameter may differ under environmental conditions, thereby requiring parameter calibration to fit observed data [15, 16]. For instance, the range of DT_{50} values (i.e., the time required for 50% dissipation of the parent compound), which control pesticide concentration in soil and water, are typically derived under laboratory conditions. As a result, DT_{50} is generally considered as a lumped calibration parameter [17] grouping degradation across different phases and redox conditions [18], and thus typically spanning several orders of magnitude [19]. When extrapolated to field conditions other process-controlling parameters can also influence pesticide concentrations (e.g., K_{OC}, organic carbon and porosity distributions, etc.). Because of this, model prediction of pesticide dissipation and off-site transport towards, for e.g., aquatic ecosystems, suffers from field data limitations to constrain model parameters.

Pesticide concentration at catchment outlet is currently the most accessible information for modelling pesticide reactive transport at catchment scale. Model prediction has been improved by monitoring pesticide concentration and related transformation products in soils, runoff or aquifers [20, 21]. However, pesticide concentration data rarely help to disentangle degradative from non-degradative pesticide dissipation processes [2] in open and dynamic catchments [22]. This distinction is nevertheless important, as degradation is the only process, beyond dilution, that contributes to sustainable removal, preventing long-term pesticide accumulation in environmental compartments. Unlike calibration approaches in reactive transport models that rely solely on pesticide concentration data, pesticide compound specific isotope analysis (CSIA) can evidence degradation independently of transformation products or non-degradative processes [23]. During chemical and biological degradation of pesticides, molecules with lighter isotopes (e.g., ^{12}C) are degraded at slightly higher rates relative to their heavier counterparts (e.g., ^{13}C), which results in a kinetic isotope effect leaving a biochemical imprint in the form of characteristic changes in isotope ratios of reacting molecules [23]. In contrast, non-degradative dissipation processes generally do not result in significant isotope fractionation [24, 25]. Incorporation of pesticide CSIA data in catchment models bears the potential to reduce uncertainty of pesticide sinks, which result from compensating effects across competing dissipation processes, as previously shown for legacy contaminants in aquifers [26].

Pesticide CSIA may thus provide an independent evaluation of *in situ* degradation to examine the benefit of hydro-climatic control of pesticide degradation in catchment models. Incorporation of pesticide CSIA data in a parsimonious lumped model [27] based on transport formulation by travel-time distributions (e.g., refs. 28, 29) has showed recently that CSIA data can constrain pesticide reactive transport. However, lumped models only provide an overall hydrological behavior without spatial information, such as soil water content or temperature, across the catchment [14]. Physically-based distributed models, in contrast, explicitly represent spatial hydro-climatic dynamics regulating hydrological processes (e.g., runoff, infiltration). However, control of hydro-climatic dynamics on pesticide degradation [30–32] in catchment physically-based models and associated formalisms is currently missing.

In this context, the purpose of this study was to improve prediction and reduce uncertainty of parameter ranges controlling pesticide degradation and off-site transport in hydrological catchment models. Dependence of pesticide degradation on soil hydro-climatic conditions was integrated in a distributed catchment model using pesticide CSIA data collected in soil and water. The first objective was to compare a modelling approach including dynamic control of pesticide degradation by hydro-climatic conditions with a classical approach using constant DT_{50} values across the catchment and the growing season. The Bridge Event Continuous Hydrological (BEACH) model [33, 34], a spatially distributed model simulating variation of soil water content conditions, was modified to integrate (i) spatio-temporal evolution of soil temperature [35], (ii) temporal variation of soil hydraulic properties based on a land-use-specific agronomical model [36], (iii) reactive transport of pesticides, (iv) pesticide carbon isotopic fractionation and isotopologue (e.g. ^{13}C and ^{12}C) transport. To address limitations of degradation parameter constraints in catchment models [16, 37], we then examined the benefit of incorporating in the calibration phase both soil pesticide concentration and CSIA data collected at different spatial resolutions (i.e., weekly catchment transects, weekly composite soil samples and individual plot samples). A unique data set [25] of catchment soil characterization including concentrations and carbon isotope signatures ($\delta^{13}C$) of S-metolachlor (SM), a widely used and well characterized pre-emergent herbicide [38, 39], was used to interpret stable isotope fractionation and constrain pesticide degradation. The generalized likelihood uncertainty estimation (GLUE) technique using Monte-Carlo sampling was adopted to compare formalism benefits on prediction and parameter identification [40, 41].

4.2 Materials and methods

4.2.1 Field site characterisation

Field data was collected from the Alteckendorf (France) headwater catchment (47-ha) previously described [20, 25]. Climate and hydrological characteristics are provided in Table 21. Arable land dominates, with corn (18%), beet (70%) and wheat (3%) as the principal crops (2016). The catchment has a tile drainage system of unknown spatial extent at 0.8 m depth and water flows in ditches to a 50 cm diameter pipe at a single outlet (Fig. S1). Soil characteristics indicate low spatial variability [36] with a grain size distribution of clay 30.8±3.9%, silt 61.0±4.5%, and sand 8.5±4.2%. Soil composition was $CaCO_3$=1.1±1.6%; organic matter=2.2±0.3%; pH=6.7±0.8; total soluble phosphorus=0.11±0.04 g kg^{-1}, and CEC=15.5±1.3 cmol Kg^{-1}. A compacted plough layer was observed between 20 and 30 cm depth. Farmer surveys, including application date, dose and formulation (Table 41) indicated pre-emergent herbicide applications during mid-April and early-May 2016 containing S-metolachlor (SM) (active ingredient).

Table 41: Applied mass (Kg) of active ingredient (SM) per transect by date and days since 1^{st} application. Ranges indicates uncertainty of exact application date.

App. No.	Date	Days	North	Valley	South
A1	March 20 - 25^{th}	0 - 5	5.1	1.6	11.1
A2	April 13 - 14^{th}	25 - 26	8.0	1.8	2.9
A3	May 25 - 31^{st}	67 - 73	7.2	2.4	0.0
Total (Kg)			20.2	5.9	14.0

4.2.2 Plot and transect soil sampling design

Top-soils (0-1 cm) were sampled at different spatial resolutions (Fig. 4.2.2) and described previously in chapter 2. Briefly, north, valley and south transects (weekly) and 13 marked plots (before and at 1, 50 and 100 days after application) targeted SM δC^{13} in addition to SM concentrations to evaluate the benefit of SM isotope data to constrain model parameterization.

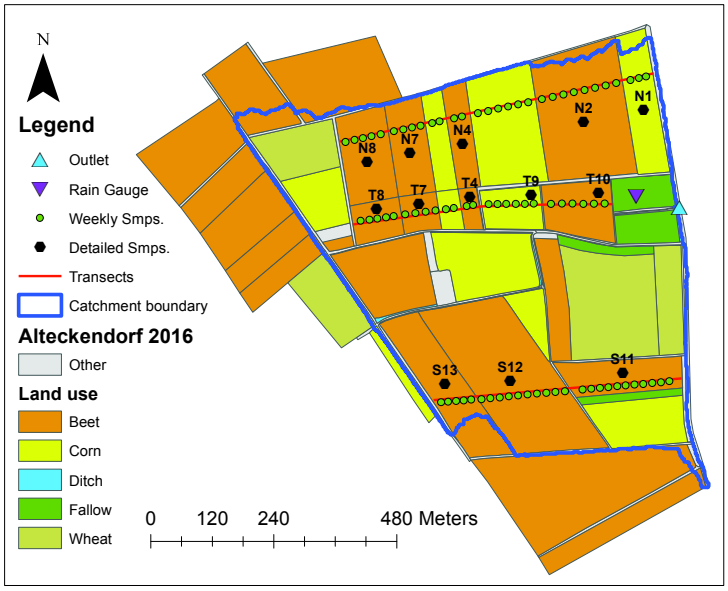

Figure 41: Transects (weekly) and plot (1, 50 and 100 days) catchment sampling.

4.2.3 Outlet Discharge

Outlet discharge was measured using a Doppler flowmeter (2150 Isco). Automatic, refrigerated continuous flow proportional sampling (Isco Avalanche) was conducted at fixed discharge volumes ranging from 50 to 150 m^3 in 2016 to capture increasing minimum baseflow discharges from April to June. To obtain water SM concentrations and carbon isotope signatures ($\delta^{13}C$), composite samples were combined according to hydrograph base-flow, rising and/or falling limb, yielding volumes $\geq$ 990 mL.

4.2.4 SM concentration and $\delta^{13}C$ analysis

Soil and water SM extraction was detailed in ref. 25. To separate dissolved and particulate phases, water samples were filtered through 0.7-μm glass fibre filters, then extracted by solid-phase extraction (SPE) using SolEx C18 cartridges (Dionex ®, Sunnyvale, CA, USA) and an AutoTrace 280 SPE system (Dionex ®), and quantified by GC-MS/MS (SM) (ThermoFisher Scientific) [42]. Pesticide extraction and purification for soils were adapted from ref. 43 and 44. Environmental quantification limits for SM were 0.01 μg L^{-1} water and 0.001 μg g^{-1} dry weight soils (d. wt.), with an analytical uncertainty of 16%. Carbon isotope composition of SM was analysed using GC-C-IRMS system by adapting ref. 42 and detailed in ref. 25. The reproducibility of triplicate measurements was $\leq 0.2‰(1\sigma)$ for $\delta^{13}C$. Minimum peak amplitudes needed for accurate $\delta^{13}C$ measurements was 300 mV [25] corresponding to about 10 ng of carbon injected on column.

4.2.5 Model description

The BEACH model generates spatially distributed soil water content conditions based on daily meteorological records, soil physical properties (e.g., permeability, bulk density, porosity) and crop-specific agronomical information. The Alteckendorf catchment was represented with a 2 × 2 m resolution and 5-layers (Fig. 42), including a pesticide mixing top-soil layer (z0=1 cm) [45], a plow layer (z1=30 cm) and a layer controlled by artificial drainage pipes (z2=50 cm). The water table layer is divided into upper (z3) and lower (z4) water table layers. Percolation through the vadose zone is routed to outlet as a global linear reservoir [46] via the bottom-most layer (z4). Depth distribution (z_f) between the two water table layers is considered as a calibration parameter ($z3+z4 = 23.2$ m; $z3 = 23.2 \cdot z_f$; $z4 = 23.2 \cdot (1-z_f)$).

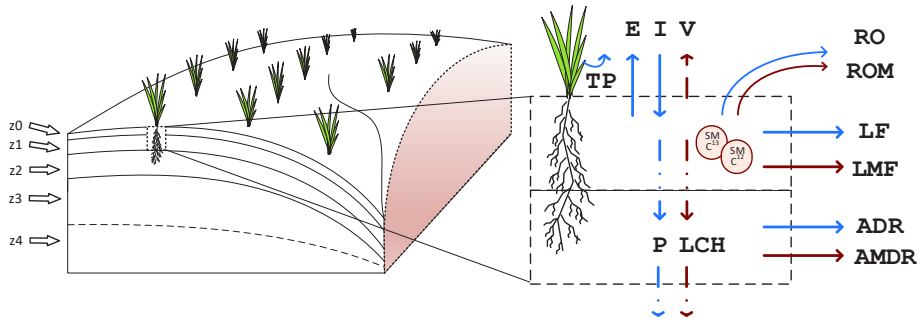

Figure 42: Conceptual 5-layer spatially distributed hydrological and reactive-transport model.

BEACH was adapted to account for temperature and water content control of pesticide degradation and nonreactive transport of pesticide isotopologues, denoting the new model as Pesticide-isotopes BEACH (PiBEACH). To constrain pesticide degradation, stable isotope fractionation was incorporated by treating compound isotopologues as individual species. The hydrological balance was previously described in ref. 33 and detailed implementation is provided in SI-4. Overall, change in soil water content (θ, $m^3\ m^{-3}$) at each cell i is given by:

$$Z\frac{d\theta_i}{dt} = R_i - RO_i + \Delta LF_i - Ea_i - Ta_i - P_i \tag{4.1}$$

where, for each component (mm $H_2O\ d^{-1}$) including the soil column (Z) water content, rainfall (R), runoff (RO), net cell lateral inflow-outflow (ΔLF), actual evaporation (Ea), actual transpiration (Ta) and percolation (P).

The pesticide mass balance is given by,

$$\frac{dM_i}{dt} = A_i - ROM_i + \Delta LMF_i - V_i - LCH_i - DEG_i \tag{4.2}$$

where, for each mass component (g SM d^{-1}) including the mass applied (A), loss to runoff (ROM), change due to lateral flux (ΔLMF), volatilization (V), leaching (LCH) and degradation (DEG).

Mass distribution into the dissolved, adsorbed and gaseous phases follows ref. 47 and detailed in appendix C.4.1. Partition into the dissolved and adsorbed phases is determined by linear sorption, considering the organic carbon-water partition coefficient K_{oc} (mL g^{-1}) normalized by the fraction of organic carbon f_{oc} (kg kg^{-1}) in soil, where the pesticide dissociation coefficient is given by $K_d = K_{oc} \cdot f_{oc}$. Partition into the gas phase is obtained from the dimensionless Henry constant, $K_H^{cc} = 9.55 \cdot 10^{-5}$ for SM [48]. Generalized pesticide mass flux J ($\mu g\ d^{-1}$) for each model layer is given by:

$$J = \mathbf{q_{x,z}} \cdot c_{aq} \tag{4.3}$$

where $\mathbf{q}$ is the water flux vector ($mm\ d^{-1}$) along the lateral ($\mathbf{x}$) and vertical ($\mathbf{z}$) direction. For the topsoil layer (z_0), runoff and volatilization are also considered such that:

$$J_{z_0} = J + c_{aq}(ROe^{-\beta_{RO} D_{z0}} + \frac{1}{r_a + r_s}) \tag{4.4}$$

where RO is run-off (mm) and β_{RO} is a calibration constant ($1 \geq \beta_{RO}$¿0) and D_{z0} (mm) is topsoil depth [49]. Volatilization is considered only during the first 5 days after application [50, 51], and follows ref. 47, where flux across topsoil is regulated by air transport resistance, r_a, ($d\ m^{-1}$) and diffusion resistance, r_s ($d\ m^{-1}$) [47] (derivation details are included in appendix C.4.2).

Biodegradation is assumed to occur only in bioavailable fractions of adsorbed (ads) and aqueous (aq) phases [52]. The bioavailable fraction is controlled kinetically by an ageing rate k_{age} on the adsorbed fraction [53, 54]. Representing SM mass (M) as separate light (l) and heavy (h) isotopologues, the change in aqueous and adsorbed phases is given by:

$$\frac{\partial M_{ads}}{\partial t} = -k_{age}(M_{ads}^l + M_{ads}^h) - k_{deg}(M_{ads}^l + \alpha M_{ads}^h) \tag{4.5}$$

$$\frac{\partial M_{aq}}{\partial t} = -k_{deg}(M_{aq}^l + \alpha M_{aq}^h) \tag{4.6}$$

where $k_{deg} = ln(2)/DT_{50}$ and DT_{50} (days) is the observed degradation half-life. Isotope fractionation is considered through the fractionation factor (α), also expressed as $\alpha = \epsilon/1000+1$, where ϵ (‰) is the characteristic SM enrichment. Although a decrease in degradation rates may be correlated to depth (e.g., due to microbial activity [27, 55]) or sorption [56], the lack of SM concentration and isotope data at deeper soil profiles did not allow to consider depth dependence, and was thus not included. Moreover, SM degradation rates did not decrease with increased sorption [57, 58], and thus it was considered to be equivalent to the dissolved phase.

In contrast, to consider the effect of a reduction in pesticide extraction efficiency on the aged fraction (e.g., due to increasing irreversible sorption over time [56, 59]), a rate k_{irs} (d^{-1}) on the aged SM mass was given by:

$$\frac{\partial M_{age}}{\partial t} = -k_{irs}(M^{l}_{age} + M^{h}_{age}) \tag{4.7}$$

Decrease in M_{age} due to abiotic degradation [60] was not included because SM did not show significant fractionation after 200 days of incubation under abiotic conditions [25].

To evaluate the benefit of introducing hydro-climatic control on SM degradation, a degradation half-life dynamically adjusted with soil temperature (F_T) and water content (F_θ), denoted as dynamic DT_{50}, was implemented as follows [31]:

$$k_{Dynamic} = k_{ref} \cdot F_T \cdot F_\theta \tag{4.8}$$

where k_{ref} is the degradation rate constant from biochemical degradation half-life (days) at reference conditions ($k_{ref} = ln(2)/DT_{50,ref}$). For the formalism considering constant dissipation rates, F_T and F_θ were equal to 1. For temperature dependence, this formalism is based on the modified Arrhenius equation for low temperatures [9, 31] such that:

$$F_T = \begin{cases} 0, & \text{if, } T_C \leq 0 \\ \frac{T_{K,obs}-273.15}{5} exp\Big(\frac{E_a}{R}(\frac{1}{T_{K,ref}} - \frac{1}{T_{K,obs}})\Big), & \text{if, } 0 < T_C \leq 5 \\ exp\Big(\frac{E_a}{R}(\frac{1}{T_{K,ref}} - \frac{1}{T_{K,obs}})\Big), & \text{if, } T_C > 5 \end{cases} \tag{4.9}$$

where T_K and T_C are soil temperatures in Kelvin and Celsius, respectively and $T_{K,ref}$ is the reference temperature at 293.15 K. E_a is the SM activation energy (23.91 KJ mol^{-1})[61] and R is the gas constant 8.314 (J mol^{-1} K^{-1}). Influence of water content follows [9, 30]:

$$F_\theta = \Big(\frac{\theta_t}{\theta_{ref}}\Big)^{\beta_\theta} \tag{4.10}$$

where β_θ is a calibration constant and θ_{ref} the water content at 0.2 (m^3 m^{-3}).

4.2.6 Model limitations

Plant SM uptake was not considered as no correlation was observed between remaining mass and crop growth (0 to 40 cm) or surface cover extent [20]. By using a daily time step, PiBEACH was not designed for accurate simulation of fast flow dynamics, i.e. runoff genesis and preferential flow [33]. In contrast, PiBEACH targets soil water content dynamics controlling vertical and horizontal water and pesticides fluxes with daily transit times.

4.2.7 Parameter sampling space

Formalism with DT_{50} dynamically controlled by hydro-climatic conditions *vs.* those with constant DT_{50} were compared with the generalized likelihood uncertainty estimation (GLUE) technique [40, 41]. Rather than seeking an optimal model solution, the GLUE approach recognizes that more than one model structure or parameter set may lead to acceptable model results, i.e. equifinality [40]). Equifinality is used here to explore the parameter space associated to acceptable model representations. Sampling and interpretation was conducted in 3

steps. First, parameter sets were identified (Table 42), assumed to be uniformly distributed, and likely boundaries defined based either on literature or field data collected in 2012 and 2016. Second, *a posteriori* parameter distributions were derived from acceptable simulations, i.e. providing SM concentration and $\delta^{13}C$ predictions closed to field observations. Third, acceptable model results, e.g. SM export, leaching or remaining mass in topsoil were reported as an ensemble, drawn from the 95% confidence interval obtained from acceptable simulations.

Due to large computation time (i.e., 2505 CPU sec./ hydrological year on an Intel(R) Core(TM) machine i7-8650U CPU@ 1.90GHz, 2.11 HGz), *via* Latin-Hypercube sampling [62] was used to reduce sample numbers. To reduce the number of parameters during GLUE analysis, a pre-sensitivity analysis based on the Morris method[62, 63] was conducted (data not shown). Although the Morris method yields a qualitative indication of relative parameter importance, it is efficient compared to other sensitivity approaches [64] screening for sensitive parameters [65]. Key parameter ranges retained are presented in Table 42. To further reduce computation times, the GLUE assessment was focused on the growing period (March 14^{th} to July 12^{th}, 2016), where pesticide degradation and export are of most significance. Initial hydrological state was estimated from a spin-up period of one full hydrological year (Oct. 1^{st}, 2015 - Sept. 30^{th}, 2016) and hydrological parameters calibrated against observed discharge (March 25^{th} and July 12^{th}, 2016) using particle swarm optimization [66].

4.2.8 Model predictability evaluation

To determine model predictability, the Kling-Gupta efficiency (KGE) [67] metric was adopted. Goodness of fit between simulations and observations are given relative to a maximum efficiency of 1 and given by:

$$KGE = 1 - \sqrt{(r-1)^2 + (\alpha_{KGE} - 1)^2 + (\beta_{KGE} - 1)^2} \tag{4.11}$$

where r is a linear correlation coefficient, $\alpha_{KGE} = \frac{\sigma_i}{\sigma_o}$, and $\beta_{KGE} = \frac{\mu_i}{\mu_o}$, where σ and μ represent the standard deviation and mean of simulated (i) and observed (o) values, respectively.

The KGE metric was selected to provide equal weight across correlation, bias and variability measures. KGE metric is also an improved measure of model performance relative to other metrics, such as the mean squared error or the Nash-Sutcliffe efficiency, which favor parameter values underestimating variance of model results [67]. KGE values where computed separately for SM concentration and $\delta^{13}C$. To quantify uncertainty reduction between formalisms, the PUCI (Percentage of observations bracketed by the Unit Confidence Interval)[68] index was used, which incorporates resolution and reliability measures given by the ARIL (Average Relative Interval Length)[69] and the PCI (Percentage of observations bracketed by the Confidence Interval)[70] indices, respectively, such that:

$$PUCI = (1.0 - Abs(PCI - 0.95))/ARIL \tag{4.12}$$

$$ARIL = \frac{1}{n} \sum \frac{CI_{upper} - CI_{lower}}{y_o} \tag{4.13}$$

$$PCI = \frac{Y_o}{n} \tag{4.14}$$

where n is the number of time steps, CI are the simulated upper and lower 95% confidence intervals, y_o is the observed measure, Y_o is the number of observations contained within the 95% CI.

4.3 Results and discussion

4.3.1 Benefit of DT_{50} hydro-climatic dependency

DDT_{50} dependence on hydro-climatic conditions (i.e. dynamic DT_{50}) yielded lower degradation rates early in the season, compared to the formalism with constant DT_{50} values. Based on dynamic DT_{50} values (Fig. 43 C), lower degradation rates during the first 10 days corresponded to an early cold and dry period (Fig. 43 D), followed by fluctuating dry and cold periods until $\approx$ 50 days after the first application. Comparison of formalisms with a constant and a dynamic DT_{50} showed that both formalisms could reproduce SM soil concentrations (Fig. 43 A) with equivalent reliability and resolution (PUCI = 0.1), although constant and dynamic DT_{50} values significantly differed (Fig. 43 C).A sampling strategy relying only on SM soil concentrations may thus not help to evaluate the benefit of a dynamic DT_{50}. Equivalent reliability of constant and dynamic formalisms of DT_{50} values to predict SM concentrations in soil therefore indicated that degradative and non-degradative processes compensated each other. In contrast, prediction of stable isotope fractionation of SM with a constant DT_{50} was less reliable (PCI_{Con} = 0.05) than with a dynamic DT_{50} (PCI_{Dyn} = 0.06), as shown also visually by mean isotope fractionation trends and higher PUCI index values for the dynamic formalism (ΔPUCI = 0.1, Fig. 43 C). Consequently, inclusion of CSIA data to tease apart degradative and non-degradative SM dissipation processes indicate that prediction of SM degradation with a constant DT_{50} formalism was overestimated, whereas prediction of SM off-site transport was underestimated (data not shown).

Altogether, risk assessments relying solely on a concentration-based calibration approach may yield key parameter ranges that do not reflect actual degradation conditions. In the presented case for 2016, this would have led to an underestimation of SM off-site transport immediately following the first SM application on the catchment. Integrating hydro-climatic control, and possibly other factors (e.g., microbial populations, redox conditions), can thus help improving prediction of degradation rates under field conditions in spatially distributed models. Therefore, numerical and conceptual efforts aimed to improve pesticide degradation representation should include physical and/or biological proxies in their formalisms, as was considered here for DT_{50} hydro-climatic dependence. However, such efforts should be paralleled by inclusion of data constraints that directly reflect *in situ* degradation extent, allowing to constrain parameters during calibration [15, 16], thereby reducing uncertainty of model predictions.

4.3.2 Uncertainty reduction through incorporation of CSIA data

The formalism of hydro-climatic DT_{50} dependence was considered with a calibration based on topsoil SM concentration data only (NIC: no isotope constraint), or with both topsoil SM concentration and SM CSIA data (WIC: with isotope constraint). The $DT_{50,ref}$ (Fig. 44) was calibrated to obtain a daily dynamic DT_{50} from hydro-climatic conditions (Eq. 4.8). For the composite soil (Fig. 44), mean $DT_{50,ref}$ (μ) values were equivalent for calibration

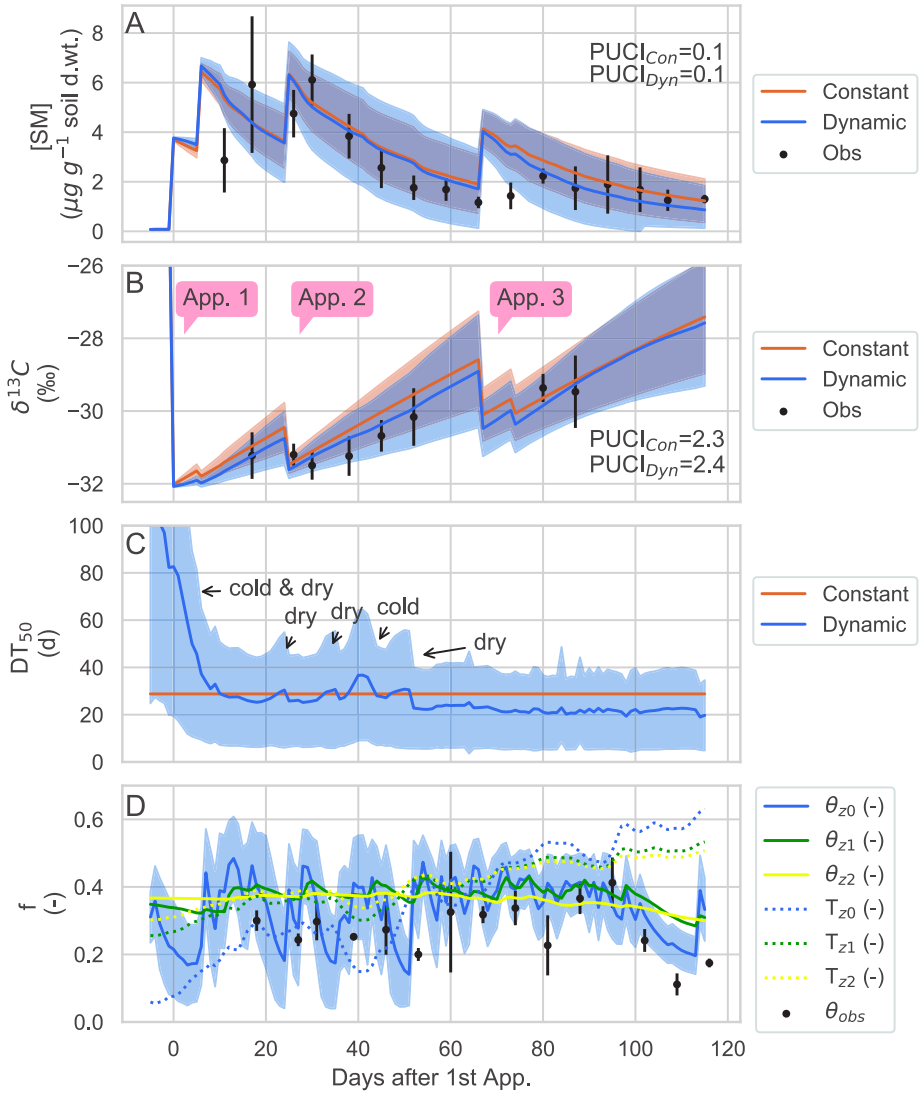

Figure 43: S-metolachlor (SM) concentrations (A) and $\delta^{13}C$ values (B) for observed composite topsoil soils (i.e., z0) and simulated model ensemble mean and CI's with dynamic DT_{50} (n=2,500) and constant DT_{50} (n=2,500) formalisms between March 14^{th} (day -5, before 1st application) and July 12^{th} (day 115). Error bars indicate standard deviations. Three application periods are indicated as App. 1 (days 0 & 6), App. 2 (day 25), and App. 3 (Days 67 & 74) in panel B. Mean degradation half-life (DT_{50}) for the dynamic and constant formalisms are shown for the top soil layer (z0) (C). Shaded area in panel C represents 95% confidence intervals (CI) for effective DT_{50} from the dynamic formalism. Catchment soil water content (m^3 m^{-3}) and temperatures controlling DT_{50} (D). Soil temperature is shown as a fraction relative to maximum seasonal air temperature ($T_z/T_{air,max}$), where $T_{air,max} = 27°C$. Observed topsoil layer water content (θ_{obs}) represents punctual measurements during weekly soil sample collection. Error bars represent 95% CI for soil bulk density estimations required for gravimetric to volumetric conversions.

with (WIC) and without CSIA data (NIC). However, $DT_{50,ref}$ standard deviations for NIC calibration were 2 times larger than for WIC calibration (Fig. 44), indicating that CSIA data significantly reduced pesticide degradation uncertainty.

Constraining degradation uncertainty is necessary because degradation half-lives typically range several orders of magnitude in the field [19], which may severely bias degradation estimates when predicting pesticide dissipation. In this respect, low standard deviations (SD $<$ 5 days) of $DT_{50,ref}$ for WIC calibration suggest that aerobic (14.5 - 21 days [39]) conditions dominated SM degradation in the topsoil layer, whereas anaerobic (23.4 - 62 days [58, 71]) degradation was less important.

Comparison of calibrated mean $DT_{50,ref}$ values between the composite soil, transects and plot resolutions showed small differences ($<$ 4 days) (Fig. 44). Similar uncertainty reduction (i.e., SD) was observed with WIC compared to NIC for the 3 spatial resolutions, indicating that more detailed spatial soil sampling (i.e., plots $>$ transects $>$ composite sample) did not contribute to constrain model parameterization for this catchment (47-ha). Hence, pooling transect samples into one composite soil sample for CSIA may constrain degradation parameters while reducing sampling and analytical efforts.

In addition, incorporation of CSIA allowed identifying isotopic enrichment and potential degradation mechanism of SM in top-soils. Modelling results yielded $\epsilon = -2.7 \pm 0.6‰$, suggesting S_N2-reactions ($AKIE_C = 1.04 \pm 0.01$) [72]. Although reaction mechanisms agree with previous inferences for this catchment (see ref. 25), ϵ values used in that study ($\epsilon = -1.5 \pm 0.5‰$) may have slightly overestimated degradation extent, albeit within uncertainty ranges obtained here from the model ensemble. Differences between lab-derived isotopic fractionation values and modelled values may be due to static water content and temperature conditions in the lab experiments, providing more stable and possibly better conditions for microbial development. In addition, oxygen gradients in soil may have resulted in a mix of aerobic and anaerobic conditions under laboratory conditions. In contrast, oxygen gradients were unlikely in the top 1 cm of soils, and maximum soil saturation, lower than 0.5 (Fig. 43D), suggesting that aerobic conditions in the field prevailed over time.

In contrast, CSIA data in soil did not reduce uncertainty of K_{OC} values across all soil sample resolutions. This may be due to pesticide extraction protocols from soil samples, that account for both the dissolved phase and the extractable sorbed phase [25], and because sorption generally does not result in significant isotope fractionation [24]. CSIA does not help evaluate sorption and thus constrain K_{OC} values because isotope signatures for pesticides in the dissolved and particulate phase of soil samples are generally similar.

4.3.3 Risk assessment metrics

Six metrics to evaluate SM persistence and transport risk from topsoil across the catchment were simulated with the PiBEACH model. The metrics (Fig. 45) included SM degradation, remaining bioavailable mass (BAM) in topsoil (i.e. dissolved and reversibly-sorbed SM), remaining mass of irreversibly sorbed SM (aged), SM off-site transport by leaching, volatilization, and export to outlet by runoff and drainage since the 1^{st} application day on March 19^{th} (day 0) to July 12^{th}, 2016 (day 115). For 3 metrics, i.e. degradation, export to outlet and remaining mass in topsoil, PiBEACH provided estimates close to available extrapolated observations. SM export to catchment outlet (2±6%) estimated with CSIA data constraints was within an order of magnitude of that observed from March 25^{th} to July 12^{th}, 2016 (0.5±0.1%). Model degradation extent (72±13%) in the last observed bulk isotope

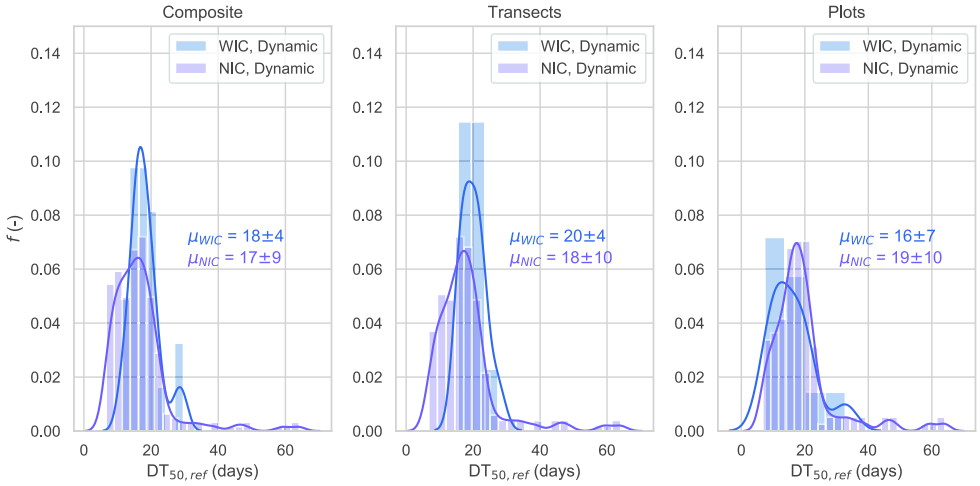

Figure 44: Distribution (n=2,500) of DT_{50} calibrated with no isotope constraint (NIC) and with isotope constraint (WIC) at three sampling resolutions (i.e., composite, transect and plot soils) for the dynamic formalism. NIC models considered $KGE_{SM} > 0.5$, while WIC considered in addition $KGE_{\delta} > 0.8$. Statistics for $DT_{50,ref}$ distributions are provided as mean and standard deviations ($\mu \pm SD$).

Table 42: Model parameter values retained

Parameter	Units	Bounds	95% CI	Description	Source
Layers	-	5	-	Number of model layers	Conceptual
$z0$	mm	10	-	Layer depth	Conceptual
$z1$	mm	300	-	*ibid.*	Conceptual
$z2$	mm	500	-	*ibid.*	Conceptual
$z3$	mm	zDat · (zf)	-	Depth to datum (zDat), upper water table	Conceptual
$z4$	mm	zDat · (1-zf)	-	Depth to datum (zDat), lower water table	Conceptual
z_f	-	0.75, 0.99	0.87, 0.99	z3 and z4 distribution fraction	Calibration
c_{z0z1}	d^{-1}	0, 1	0, 1	Lateral flow coefficient [46], z0, z1	Calibration
c_{z2z3z4}	d^{-1}	0, 1	0.2, 0.6	*ibid.*	Calibration
c_{adr}	d^{-1}	0, 1	0.03, 0.92	Drainage lateral flow coefficient	Calibration
K_G	d	1100, 3650	1522, 3650	Linear reservoir constant regulating baseflow discharge	Calibration
γ_{z0z1}	-	0, 1	0.32, 1	$log(K_{sat})$ adjustment factor for layer (z)	Calibration
γ_{z2z3}	-	0, 1	0, 0.81	*ibid.*	Calibration
$K_{sat,z0z1}$	mm d^{-1}	112.9, 781.8	-	Saturated hydraulic conductivity (adjusted by γ)	Agro. model
$K_{sat,z1z2z3}$		643.2	-	*ibid.*	Agro. model
θ_{WP}	-	0.19	-	Wilting point, all layers; 0.16 ± 0.03	Agro. model
$\theta_{FC,z0z1}$	-	0.37, 0.40	-	Field capacity, plow layer (0 - 300 mm); 0.37 ± 0.01	Agro. model
$\theta_{SAT,z0z1}$	-	0.49, 0.63	-	Saturation capacity, plow layer; 0.57 ± 0.04	Agro. model
$\theta_{FC,z2z3z4}$	-	0.37	-	Field capacity, z ¡ 310 mm depth; 0.37 ± 0.03	Field charac.
$\theta_{SAT,z2z3z4}$	-	0.57	-	Saturation capacity, z ¡ 310 mm depth; 0.57 ± 0.04	Field charac.
f_{transp}	-	0, 1	0.38, 1	Adjustment factor, transpiration	Calibration
f_{evap}	-	0, 1	0.1, 0.88	Adjustment factor, evaporation	Calibration
$p_{bAgr,z0z1}$	g cm^{-3}	0.98, 1.36	-	Soil bulk density ; 1.17 ± 0.11	Agro. model
$p_{b,z2,z3,z4}$	g cm^{-3}	1.5	-	Soil bulk density, below plough layer; 1.5 ± 0.09	Field charac.
f_{oc}	kg kg^{-1}	0.01, 0.05	0.01, 0.05	Fraction of organic carbon [20]	Calibration
K_{oc}	mlg^{-1}	0.3, 16180	0.3, 2000	Adsorption coefficient[20, 73–76]	Calibration
K_d	mlg^{-1}	0.003, 809	0.003, 76.9		Calibration
β_{runoff}	mm	0, 1	0, 0.4	Calibration constant for runoff mass transfer [49]	Calibration
K_{age}	d	0.0002, 0.07	0.0002, 0.005	Ageing rate; mass transfer to non-bioav. frac.	Calibration
K_{irs}	d	0.002, 0.01	0.002, 0.009	Rate of irreversible sorption / loss of recoverable fraction	Calibration
$DT_{50_{ref}}$	d	1, 50	9.2, 24.9	Ref. degradation half-life	Calibration
ϵ_{iso}	-	-4.0, -1.0	-3.47, -1.72	Enrichment factor	Calibration
β_{θ}	-	0, 1	0.03, 1.0	Constant exponent, degradation factor[30]	Calibration

measure (day 87) was approximately equivalent when compared to the Rayleigh equation and the model derived ϵ value (day 87, 68±1%). The remaining dissolved and reversibility sorbed or bioavailable SM mass (BAM), extrapolated from measured soil concentrations and delimited transect areas (Fig. C2) also fell within the uncertainty range of the model and was approximately equivalent on the last measurement day (day 115, at 18±3%). Finally, SM volatilization during the first 120 h (< 1%) was consistent with SM low vapor pressure (< 1.8 mPa) [77]. However, SM volatilization measured in the field has ranged from 5 to 63% of the applied mass, depending on meteorological conditions [50, 51].

Comparison of 95% confidence intervals for the 6 metrics of SM transport risk indicates that calibration with both topsoil SM concentration and isotope data reduced uncertainty at least two-fold at the end of the season (day 115) compared to calibration with topsoil SM concentration data only. Although mean degradation extent between both dynamic DT_{50} models was similar at the end of the season (i.e., $\Delta\mu = 1\%$), uncertainty of degradation extent calibrated without isotope data was 1.6 times larger. Larger uncertainty of degradation extent for model calibration without isotope data propagated across other dissipation processes. Namely, in the NIC model ensemble, this led to overestimations of both mean and uncertainty ranges of pesticide leaching by approximately a factor of 2. Altogether, the 6 metrics used for pesticide transport risk confirmed that CSIA data reduced uncertainty of pesticide degradation estimates and other pesticide dissipation processes in distributed catchment models.

4.3.4 Implications for prediction of pesticide dissipation at catchment scale

Our study highlighted that hydro-climatic control of DT_{50} values under an uncertainty framework bears potential for guiding pesticide management practices by providing more reliable assessment of pesticide degradation and transport at the headwater catchment scale. Firstly, potential users, including farmer advisors and water agencies, expect tools to accurately predict pesticide off-site transport to design preventive and curative actions, in a context of increasing pressure of agricultural activities on ecosystems. Secondly, considering hydro-climatic factors on pesticide degradation is particularly relevant in a context of climate change, subject to changing daily rainfall and temperature patterns [11]. Thirdly, determination of risk assessment metrics often requires the use of probability and confidence intervals (CI) [78, 79]. As such, to support management decision, modelling approaches should systematically integrate an uncertainty framework to analyze range of likely parameter value ranges that can be expected to describe pesticide transfer risk.

This study also addressed an important discrepancy between the potential complexity that reactive transport models can accommodate on the one hand and the available field datasets for their calibration and validation on the other. Namely, although representation of the relationship between hydro-climatic factors, biogeochemical conditions and degradation extent and pathways have progressed significantly over the last decades, they are nevertheless in some cases over-simplified in 2D catchment models [15], or not made explicit in others [80]. When more complex, physically- or biologically-based representations of degradation across the catchment are included, additional data to identify valid parameter value ranges while reducing model uncertainty is required. Our results suggest that pesticide concentration data alone may not be sufficient to support future developments to improve model representation of pesticide degradation, for example, by including dynamics of microbial diversity and biomass on biodegradation extent [81].

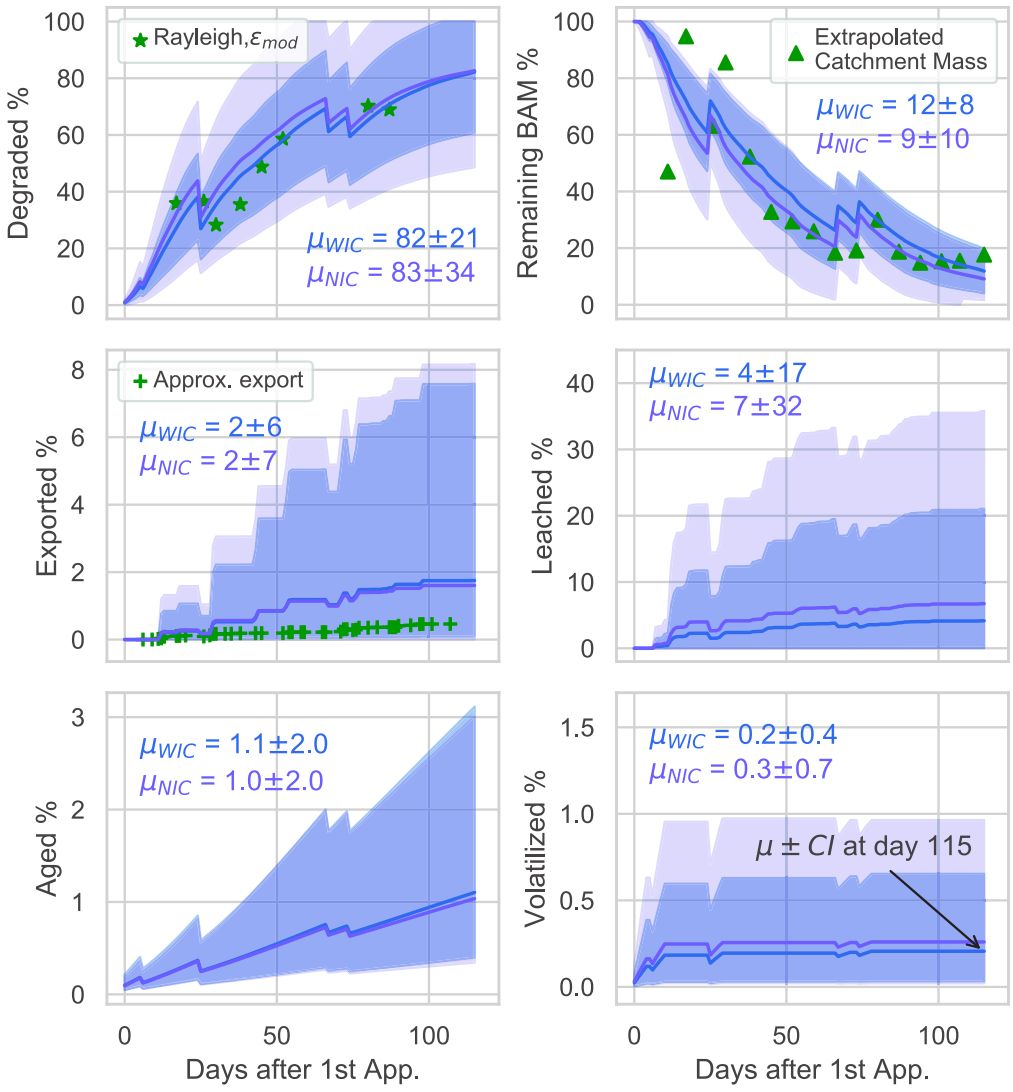

Figure 45: Pesticide dissipation processes and associated ensemble mean from 5,000 simulations. 95% confidence intervals (CI) with isotope constraints (WCI) without isotope constraints (NIC) are depicted in blue and purple, respectively. All metrics are reported as percent of applied cumulative masses for the entire catchment after the first day of application on March 19, 2016. Final values of dissipation processes (μ_{WCI} and $\mu_{NIC} \pm 95\%$ CI) are provided on day 115.

Consequently, complementary datasets, including pesticide CSIA data [2, 82], may help disentangling degradative *vs.* from non-degradative processes. By providing evidence of *in situ* degradation independent of transformation products, pesticides CSIA may open the door to novel field-based investigations and applications to close pesticide mass balances and validate models. Even a moderate sampling effort including CSIA data, i.e. weekly sampling of mixed topsoil samples across the catchment, may be sufficient to identify hot spots and hot moments of pesticide degradation at the catchment scale. As the field of pesticide CSIA continuous to develop, for example, though the development of multi-element CSIA, more reliable evaluation of pesticide degradation and constraining competing pathways [82] will allow for more detailed degradation accounts.

References

1. Vörösmarty, C. J. *et al.* Global threats to human water security and river biodiversity. *Nature* **468,** 555–561. ISSN: 0028-0836 (2010).
2. Fenner, K., Canonica, S., Wackett, L. P. & Elsner, M. Evaluating Pesticide Degradation in the Environment: Blind Spots and Emerging Opportunities. *Science* **341,** 752–758. ISSN: 0036-8075 (2013).
3. Stone, W. W., Gilliom, R. J. & Ryberg, K. R. Pesticides in U.S. streams and rivers: Occurrence and trends during 1992-2011. *Environmental Science and Technology* **48,** 11025–11030. ISSN: 15205851 (2014).
4. Gustafson, D. I. Groundwater ubiquity score: A simple method for assessing pesticide leachability. *Environmental Toxicology and Chemistry* **8,** 339–357 (1989).
5. Guardo, A. D., Williams, R. J., Matthiessen, P., Brooke, D. N. & Calamari, D. Simulation of pesticide runoff at Rosemaund Farm (UK) using the SoilFug model. eng. *Environmental science and pollution research international* **1,** 151–160. ISSN: 0944-1344 (Print) (Sept. 1994).
6. FOCUS. *FOCUS groundwater scenarios in the EU review of active substances.* tech. rep. 321 (FOCUS Groundwater Scenarios Workgroup, EC, 2000), 1–202.
7. Tiktak, A. *et al. Manual of FOCUS PEARL version 1.1.1* tech. rep. (Alterra Green World Research, Wageningen, Netherlands, 2000), 1–144.
8. Tiktak, A., van der Linden, A. & Boesten, J. *The GeoPEARL Model: Model Description, Applications and Manual* tech. rep. (Wageningen, Netherlands, 2003), 1–79.
9. Larsbo, M. & Jarvis, N. MACRO 5.0 A Model of water flow and solute transport in macroporous soil. *MACRO Technical description.* 1–43 (2003).
10. Larsbo, M., Roulier, S., Stenemo, F., Kasteel, R. & Jarvis, N. An Improved Dual-Permeability Model of Water Flow and Solute Transport in the Vadose Zone. *Vadose Zone Journal* **4,** 398. ISSN: 1539-1663 (2005).
11. Steffens, K. *et al.* Direct and indirect effects of climate change on herbicide leaching - A regional scale assessment in Sweden. *Science of the Total Environment* **514,** 239–249. ISSN: 18791026 (2015).
12. Medici, C., Wade, A. J. & Francés, F. Does increased hydrochemical model complexity decrease robustness? *Journal of Hydrology* **440-441,** 1–13. ISSN: 00221694 (2012).
13. Birkel, C. & Soulsby, C. Advancing tracer-aided rainfall-runoff modelling: A review of progress, problems and unrealised potential. *Hydrological Processes* **29,** 5227–5240. ISSN: 10991085 (2015).

14. Fatichi, S. *et al.* An overview of current applications , challenges , and future trends in distributed process-based models in hydrology. *Journal of Hydrology* **537,** 45–60. ISSN: 0022-1694 (2016).

15. Malone, R. W. *et al.* Application of the Root Zone Water Quality Model (RZWQM), to pesticide fate and transport: An overview. *Pest Management Science* **60,** 205–221. ISSN: 1526498X (2004).

16. Köhne, J. M., Köhne, S. & Simunek, J. A review of model applications for structured soils: b) Pesticide transport. *Journal of Contaminant Hydrology* **104,** 36–60. ISSN: 01697722 (2009).

17. Dubus, I. G., Beulke, S. & Brown, C. D. Calibration of pesticide leaching models: Critical review and guidance for reporting. *Pest Management Science* **58,** 745–758. ISSN: 1526498X (2002).

18. Honti, M. & Fenner, K. Deriving persistence indicators from regulatory water-sediment studies - Opportunities and limitations in OECD 308 data. *Environmental Science and Technology* **49,** 5879–5886. ISSN: 15205851 (2015).

19. Wang, Y., Lai, A., Latino, D., Fenner, K. & Helbling, D. E. Evaluating the environmental parameters that determine aerobic biodegradation half-lives of pesticides in soil with a multivariable approach. *Chemosphere* **209,** 430–438. ISSN: 18791298 (2018).

20. Lefrancq, M., Payraudeau, S., Guyot, B., Millet, M. & Imfeld, G. Correction to Degradation and Transport of the Chiral Herbicide S-Metolachlor at the Catchment Scale: Combining Observation Scales and Analytical Approaches. *Environmental Science & Technology* **52,** 5517. ISSN: 0013-936X (May 2018).

21. Sidoli, P., Lassabatere, L., Angulo-Jaramillo, R. & Baran, N. Experimental and modeling of the unsaturated transports of S-metolachlor and its metabolites in glaciofluvial vadose zone solids. *Journal of Contaminant Hydrology* **190,** 1–14. ISSN: 18736009 (2016).

22. Kirchner, J. W. Catchments as simple dynamical systems: Catchment characterization, rainfall-runoff modeling, and doing hydrology backward. *Water Resources Research* **45,** 1–34. ISSN: 00431397 (2009).

23. Elsner, M. Stable isotope fractionation to investigate natural transformation mechanisms of organic contaminants: principles, prospects and limitations. *Journal of environmental monitoring : JEM* **12,** 2005–31. ISSN: 1464-0333 (2010).

24. Schmidt, T. C. *et al.* Compound-specific stable isotope analysis of organic contaminants in natural environments: A critical review of the state of the art, prospects, and future challenges. *Analytical and Bioanalytical Chemistry* **378,** 283–300. ISSN: 16182642 (2004).

25. Alvarez-Zaldívar, P., Payraudeau, S., Meite, F., Masbou, J. & Imfeld, G. Pesticide degradation and export losses at the catchment scale: Insights from compound-specific isotope analysis (CSIA). *Water Research* **139,** 198–207 (2018).

26. Hunkeler, D., Meckenstock, R. U., Lollar, B. S., Schmidt, T. C. & Wilson, J. T. A Guide for Assessing Biodegradation and Source Identification of Organic Ground Water Contaminants using Compound Specific Isotope Analysis (CSIA). *USEPA Publication* **EPA 600/R-,** 1–82. ISSN: ¡null¿ (2008).

27. Lutz, S. R. *et al.* Pesticide fate at catchment scale: conceptual modelling of stream CSIA data. *Hydrology and Earth System Sciences Discussions* **21,** 5243–5261. ISSN: 1812-2116 (2017).

28. Benettin, P., Van Der Velde, Y., Van Der Zee, S. E., Rinaldo, A. & Botter, G. Chloride circulation in a lowland catchment and the formulation of transport by travel time distributions. *Water Resources Research* **49,** 4619–4632. ISSN: 00431397 (2013).

29. Bertuzzo, E., Thomet, M., Botter, G. & Rinaldo, A. Catchment-scale herbicides transport: Theory and application. *Advances in Water Resources* **52,** 232–242. ISSN: 03091708 (2013).

30. Walker, A. A Simulation Model for Prediction of Herbicide Persistence1. English. *Journal of Environmental Quality* **3.** doi:10.2134/jeq1974.00472425000300040021x. http://dx.doi.org/10.2134/jeq1974.00472425000300040021x (1974).

31. Boesten, J. J. T. I. & van der Linden, A. M. A. Modeling the Influence of Sorption and Transformation on Pesticide Leaching and Persistence. *Journal of Environment Quality* **20,** 425. ISSN: 0047-2425 (1991).

32. Schroll, R. *et al.* Quantifying the effect of soil moisture on the aerobic microbial mineralization of selected pesticides in different soils. *Environmental Science and Technology* **40,** 3305–3312. ISSN: 0013936X (2006).

33. Sheikh, V., Visser, S. & Stroosnijder, L. A simple model to predict soil moisture: Bridging Event and Continuous Hydrological (BEACH) modelling. *Environmental Modelling and Software* **24,** 542–556. ISSN: 13648152 (2009).

34. Karssenberg, D. Land surface process modelling with Python. http://karssenberg.geo.uu.nl/labsAnswers/ (2014).

35. Neitsch, S. L., Arnold, J. G., Kiniry, J. R. & Williams, J. R. Soil & Water Assessment Tool - Theoretical Documentation Version 2009. ISSN: 2151-0040 (2009).

36. Lefrancq, M., Dijk, P. V., Jetten, V., Schwob, M. & Payraudeau, S. Improving runoff prediction using agronomical information in a cropped, loess covered catchment. *Hydrological Processes* **31,** 1408–1423 (2017).

37. Gassmann, M., Khodorkovsky, M., Friedler, E., Dubowski, Y. & Olsson, O. Uncertainty in the river export modelling of pesticides and transformation products. *Environmental Modelling and Software* **51,** 35–44. ISSN: 13648152 (2014).

38. Rivard, L. *Environmental Fate of Metolachlor* tech. rep. (Environmental Monitoring Branch, Sacramento, California, 2003). http://www.cdpr.ca.gov/docs/emon/pubs/fatememo/metolachlor.pdf.

39. PPDB. *The Pesticide Properties Database* Developed by the Agriculture & Environment Research Unit (AERU), University of Hertfordshire, funded by UK national sources and the EU-funded FOOTPRINT project (FP6-SSP-022704). 2009.

40. Beven, K. & Binley, A. The future of distributed models: model calibration and uncertainty prediction. *Hydrological Processes* **6,** 279–298. ISSN: 1099-1085 (1992).

41. Beven, K. & Binley, A. GLUE: 20 years on. *Hydrological Processes* **28,** 5897–5918. ISSN: 10991085 (2014).

42. Elsayed, O. F. *et al.* Using compound-specific isotope analysis to assess the degradation of chloroacetanilide herbicides in lab-scale wetlands. *Chemosphere* **99,** 89–95. ISSN: 00456535 (2014).

43. Ivdra, N., Herrero-Martín, S. & Fischer, A. Validation of user- and environmentally friendly extraction and clean-up methods for compound-specific stable carbon isotope analysis of organochlorine pesticides and their metabolites in soils. *Journal of Chromatography A* **1355,** 36–45. ISSN: 0021-9673 (Aug. 2014).

44. Anastassiades, M., Lehotay, S. J., Štajnbaher, D. & Schenck, F. J. Fast and easy multiresidue method employing acetonitrile extraction/partitioning and "dispersive solid-phase extraction" for the determination of pesticide residues in produce. *Journal of AOAC International* **86,** 412–431. ISSN: 10603271 (2003).

45. McGrath, G. S., Hinz, C. & Sivapalan, M. Modeling the effect of rainfall intermittency on the variability of solute persistence at the soil surface. *Water Resources Research* **44,** 1–10 (2008).

46. Manfreda, S., Fiorentino, M. & Iacobellis, V. DREAM: a distributed model for runoff, evapotranspiration, and antecedent soil moisture simulation. *Advances in Geosciences* **2,** 31–39. ISSN: 1680-7359 (2005).

47. Leistra, M., van der Linden, A. M. A., Boesten, J. J. T. I., Tiktak, A. & van den Berg, F. *PEARL model for pesticide behaviour and emissions in soil-plant systems; Description of the processes in FOCUS PEARL v 1.1.1.* tech. rep. (2001).

48. Feigenbrugel, V., Le Calvé, S. & Mirabel, P. Temperature dependence of Henry's law constants of metolachlor and diazinon. *Chemosphere* **57,** 319–327. ISSN: 00456535 (2004).

49. Ahuja, L. R. & Lehman, O. R. The Extent and Nature of Rainfall-soil Interaction in the Release of Soluble Chemicals to Runoff. English. *Journal of Environmental Quality* **12,** 34–40 (1983).

50. Gish, T. J. *et al.* Comparison of Field-scale Herbicide Runoff and Volatilization Losses: An Eight-Year Field Investigation. *Journal of Environment Quality* **40,** 1432–1442. ISSN: 0047-2425 (2011).

51. Prueger, J. H. *et al.* Solar radiation, relative humidity, and soil water effects on metolachlor volatilization. *Environmental Science and Technology* **39,** 5219–5226. ISSN: 0013936X (2005).

52. Thullner, M., Kampara, M., Richnow, H. H., Harms, H. & Wick, L. Y. Impact of bioavailability restrictions on microbially induced stable isotope fractionation. 1. Theoretical calculation. *Environmental Science and Technology* **42,** 6544–6551. ISSN: 0013936X (2008).

53. Schwarzenbach, R. P., Gschwend, P. M. & Imboden, D. M. *Environmental Organic Chemistry* 2nd (Wiley, New York, 2003).

54. Thullner, M., Fischer, A., Richnow, H.-H. & Wick, L. Y. Influence of mass transfer on stable isotope fractionation. *Applied Microbiology and Biotechnology* **97,** 441–452. ISSN: 0175-7598 (2013).

55. Rodríguez Cruz, M. S., Jones, J. E. & Bending, G. D. Study of the spatial variation of the biodegradation rate of the herbicide bentazone with soil depth using contrasting incubation methods. *Chemosphere* **73,** 1211–1215. ISSN: 00456535 (2008).

56. Arias-Estévez, M. *et al.* The mobility and degradation of pesticides in soils and the pollution of groundwater resources. *Agriculture, Ecosystems and Environment* **123,** 247–260. ISSN: 01678809 (2008).

57. Wu, X., Li, M., Long, Y. & Liu, R. Effects of adsorption on degradation and bioavailability of metolachlor in soil. *Soil Science and Plant Nutrition* **11,** 83–97. ISSN: 07189516 (2011).

58. Long, Y. H., Li, R. Y. & Wu, X. M. Degradation of S -metolachlor in soil as affected by environmental factors. *Journal of Soil Science and Plant Nutrition* **14,** 189–198 (2014).

59. Sander, M., Lu, Y. & Pignatello, J. J. Conditioning-Annealing Studies of Natural Organic Matter Solids Linking Irreversible Sorption to Irreversible Structural Expansion. *Environmental Science & Technology* **40,** 170–178. ISSN: 0013-936X (Jan. 2006).

60. Xu, Z., Liu, W. & Yang, F. A new approach to estimate bioavailability of pyrethroids in soil by compound-specific stable isotope analysis. *Journal of Hazardous Materials* **349,** 1–9. ISSN: 18733336 (2018).

61. Jaikaew, P., Malhat, F., Boulange, J. & Watanabe, H. Aspect of the degradation and adsorption kinetics of atrazine and metolachlor in andisol soil. *Hellenic Plant Protection Journal* **10,** 1–14. ISSN: 17913691 (2017).

62. Herman, J. & Usher, W. SALib: An open-source Python library for Sensitivity Analysis. *The Journal of Open Source Software* **2,** 9–10. ISSN: 2475-9066 (2017).

63. Morris, M. D. Factorial plans for preliminary computational experiments. *Technometrics* **33,** 161–174 (1991).

64. Gan, Y. *et al.* A comprehensive evaluation of various sensitivity analysis methods: A case study with a hydrological model. *Environmental Modelling and Software* **51,** 269–285. ISSN: 13648152 (2014).

65. Herman, J. D., Kollat, J. B., Reed, P. M. & Wagener, T. Technical Note: Method of Morris effectively reduces the computational demands of global sensitivity analysis for distributed watershed models. *Hydrology and Earth System Sciences* **17,** 2893–2903. ISSN: 16077938 (2013).

66. Lee, A. *Particle swarm optimization (PSO) with constraint support* 2014. `https://pythonhosted.org/pyswarm/index.html%7B%5C#%7D`.

67. Gupta, H. V., Kling, H., Yilmaz, K. K. & Martinez, G. F. Decomposition of the mean squared error and NSE performance criteria: Implications for improving hydrological modelling. *Journal of Hydrology* **377,** 80–91. ISSN: 00221694 (2009).

68. Li, L., Xu, C. Y., Xia, J., Engeland, K. & Reggiani, P. Uncertainty estimates by Bayesian method with likelihood of AR (1) plus Normal model and AR (1) plus Multi-Normal model in different time-scales hydrological models. *Journal of Hydrology* **406,** 54–65. ISSN: 00221694 (2011).

69. Jin, X., Xu, C. Y., Zhang, Q. & Singh, V. P. Parameter and modeling uncertainty simulated by GLUE and a formal Bayesian method for a conceptual hydrological model. *Journal of Hydrology* **383,** 147–155. ISSN: 00221694 (2010).

70. Li, L., Xia, J., Xu, C.-y., Chu, J. & Wang, R. Analyse the sources of equifinality in hydrological model using GLUE methodology. *Symposium JS.4 at the Joint Convention of the International Association of Hydrological Sciences (IAHS) and the International Association of Hydrogeologists (IAH),* 130–138. ISSN: 01447815 (2009).

71. Seybold, C. A., Mersie, W. & McNamee, C. Anaerobic Degradation of Atrazine and Metolachlor and Metabolite Formation in Wetland Soil and Water Microcosms. English. *Journal of Environmental Quality* **30,** 1271–1277 (2001).

72. Elsner, M., Zwank, L., Hunkeler, D. & Schwarzenbach, R. P. A new concept linking observable stable isotope fractionation to transformation pathways of organic pollutants. *Environmental Science and Technology* **39,** 6896–6916. ISSN: 0013936X (2005).

73. Kollman, W. & Segawa, R. *Interim Report of the Pesticide Chemistry Database* tech. rep. (Environmental Protection Agency, US, California, 1995), 1–20. `https://www.cdpr.ca.gov/docs/emon/pubs/ehapreps/eh9504.pdf`.

74. *National Center for Biotechnology Information. PubChem Compound Database* (2017).

75. European Commission. *Review report for the active substance S-Metolachlor* tech. rep. (EU Commission Health & Consumer Protection Directorate General, 2004). http://ec.europa.eu/food/plant/pesticides/eu-pesticides-database/public/?event=activesubstance.ViewReview%7B%5C&%7Did=381.

76. Boithias, L. *et al.* New insight into pesticide partition coefficient Kd for modelling pesticide fluvial transport: Application to an agricultural catchment in south-western France. *Chemosphere* **99,** 134–142. ISSN: 00456535 (2014).

77. Maillard, E. *et al.* Dissipation of hydrological tracers and the herbicide S-metolachlor in batch and continuous-flow wetlands. *Chemosphere* **144,** 2489–2496. ISSN: 18791298 (2016).

78. Beven, K. J. & Prophecy. Reality and Uncertainty in Distributed Hydrological Modelling. *Adv. Water Resour.* **16,** 41–51 (1993).

79. Song, X. *et al.* Global sensitivity analysis in hydrological modeling: Review of concepts, methods, theoretical framework, and applications. *Journal of Hydrology* **523,** 739–757. ISSN: 00221694 (2015).

80. DeMars, C. *et al.* Integrating GLEAMS sedimentation into RZWQM for pesticide sorbed sediment runoff modeling. *Environmental Modelling and Software* **109,** 390–401. ISSN: 13648152 (2018).

81. König, S. *et al.* Functional resistance to recurrent spatially heterogeneous disturbances is facilitated by increased activity of surviving bacteria in a virtual ecosystem. *Frontiers in Microbiology* **9,** 1–14. ISSN: 1664302X (2018).

82. Elsner, M. & Imfeld, G. Compound-specific isotope analysis (CSIA) of micropollutants in the environment - current developments and future challenges. *Current Opinion in Biotechnology* **41,** 60–72. ISSN: 18790429 (2016).

Preface to Chapter 5

Addressing the last objective of this thesis, the following chapter introduces the first steps required in coupling of PiBEACH with the existing open source Limburg Soil Erosion Model (LISEM). Based on insights from chapter 2 (i.e., leaching soil column experiments), selection of longer duration events but with lower intensity are also included resulting in observed improvements in the representation of hydrological components. Preliminary results of the coupled model's ability to represent outlet SM concentrations and $\delta^{13}C$ are presented and a discussion of model limitations and potential improvements is provided.

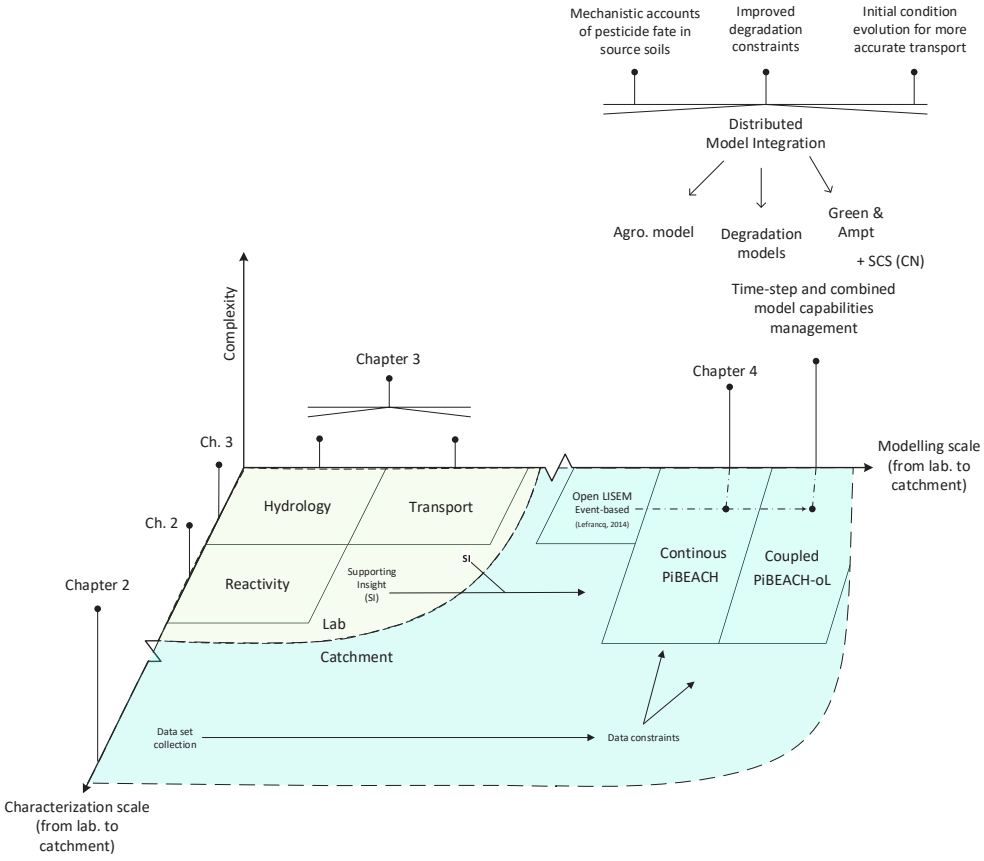

Chapter 5

Pesticide persistence and transport at the headwater catchment scale: coupling continuous and event-based models

5.1 Introduction

Headwater catchments are upland landscapes estimated to contribute to as much as 90% of a river's flow [1, 2], making them vital sources of water supply, biodiversity hotspots [3] and key regulators of downstream water quality [4]. Despite their value in providing ecosystem services [5], the remoteness of headwater catchments may explain that they are often overlooked in management and policy [3]. However, diffuse pesticide pollution originating from agricultural headwater catchments can affect larger river-basin scales [6]. Therefore, improvement of reactive transport models at this under-studied scale is a prerequisite to address and predict pesticide concentration dynamics and associated toxicity downstream in relation to hydrological conditions.

Headwaters are typically small (0 - 1 km^2) and ubiquitous [4], making them ideal open system laboratories for validation and application of new reactive transport models. Indeed, at this scale system inputs and outputs can be readily identified with low uncertainty, for example, through direct measurements and surveying. Relative to plot-level study scales, headwaters introduce an increased level of complexity, allowing to infer and integrate impacts of spatial heterogeneity, such as land-use and hydrological connectivity, on catchment hydrological functioning [7]. From a societal view point, headwater scales also provide an opportunity to evaluate predictive tools intended, for example, to aid farmer advisors in the design of preventive pesticide export management strategies [8]. Such tools may thus facilitate the design of preventive (e.g., reduce pesticide applications) [9] and curative (e.g., artificial buffer zones) strategies [10] to mitigate pesticide transfer from sources to vulnerable receptors.

A principal challenge for modelling pesticide fate and transfer at the headwater catchment scale is the need for models capable of accounting for hydrological and pesticide fate processes that are relevant at distinct temporal and spatial scales. On the one hand, there is a need to account for dynamic spatial state variables (e.g., soil hydraulic properties and pesticide pool availability) that depend on the long-term impacts of hydro-climatic or soil biological processes (e.g., rainfall patterns, temperature, microbial biomass and functions). On the

other hand, models that account for spatial heterogeneity of agricultural landscapes [7], hydrological connectivity [11] and farm management practices [12] are needed for a detail account of rapid flow and associated transport processes, in particular during periods of high transfer risk. Therefore, models capable of integrating both long-term, continuous and event-base hydrological scales should contribute to both the improvement of pesticide transfer risk science and the design of preventive and curative environmental land management strategies.

Distributed, physically based models can be suitable candidates for this task [13], as they can account for a large number of physical processes such as impacts of agricultural changes and feedbacks between hydrological and chemical processes at various time-scales [7]. However, such models are often criticized as over-parameterized and compensation effects between multiple parameters may lead to uncertain model solutions due to limited constraints of adopted formalisms with available data [14, 15]. Indeed, model validation at the catchment scale is still limited by the lack of available measurements in general [16], including data linking processes-based sinks. Indeed, although there has been a large number of models developed over the last two decades (e.g., refs. [7, 17–20], only a few can integrate spatially distributed processes relevant for pesticide degradation and transport at both continuous (e.g. seasonal) and event (e.g., minutes to hours) scales (e.g., HSPF and MIKE SHE) [17, 21–23]. Existing available models however, are limited in their potential for upscaling from headwater to larger watershed catchments over continuous time-scales due to the long computation times required to solve their numerical schemes. Furthermore, development of these codes to incorporate alternative formalisms is generally challenged due to their proprietary nature.

Recent developments in the ability to evaluate pesticide fate by compound specific isotope analysis (CSIA) [24, 25] provides an opportunity to reduce model uncertainty of remaining source pesticide pools and transport by linking isotope fractionation to degradation extent. During chemical transformation, lighter isotopes (e.g., ^{12}C) exhibit lower activation energy, generally resulting in faster reaction times relative to their heavier counterparts (e.g., ^{13}C). This leads to an enrichment of the heavier isotope in the non-degraded pesticide fraction remaining in environmental samples [26]. In contrast, concentration based assessments cannot determine the extent of degradation that a contaminant has undergone between sources and receptors in the field. This is the case because mass balance accounts can often not be closed, as pesticide transformation products can be numerous, are often not known/not quantifiable or can be further degraded.

In this context, this study addresses the need to integrate and link at different time-scales relevant pesticide fate processes in headwater catchments in a modelling framework. The specific objectives were to: (i) couple a computationally efficient distributed model capable of simulating continuous processes (PiBEACH) with a distributed event-based model, the Limburg Soil Erosion Model (LISEM) capable of detailed representation of rapid pesticide export *via* runoff and erosion [27] to evaluate improvements of pesticide transport prediction in headwater catchments by combining temporal scales (event and growing season), and; (ii) to evaluate the use of CSIA to constrain and validate dominant water pathways useful in identifying prevailing zones of pesticide mobilization affecting stream water quality. To bridge the need for improved degradation constraints in pesticide fate models at multiple time-scales, this study makes use of a unique data set of catchment soil and outlet samples including concentrations and carbon isotope signatures ($\delta^{13}C$) [25] of S-metolachlor (SM), a widely used and well characterized pre-emergent herbicide [28, 29]. Finally, to ensure propagation of model parameter uncertainty, and thereby allowing the use of such a tool to associate risk assessment metrics to confidence intervals (CI) for management decision-

making (Beven1993, Song2015), the generalized likelihood uncertainty estimation (GLUE) technique using Monte-Carlo sampling was adopted [30, 31].

5.2 Material and methods

5.2.1 Field site characterization

Field data was collected from the Alteckendorf (France) headwater catchment (47-ha) previously described in refs. 32 and 25. The catchment has a tile drainage system of unknown spatial extent at 0.8 m depth and water flows in ditches to a 50 cm diameter pipe at a single outlet (Fig.). A compacted plough layer was observed between 20 and 30 cm depth. Arable land dominates, with corn (18%), beet (70%) and wheat (3%) as the principal crops in 2016. Soil characteristics indicate low spatial variability [12] with a grain size distribution of clay 30.8±3.9%, silt 61.0±4.5%, and sand 8.5±4.2%. Soil composition was $CaCO_3$=1.1±1.6%; organic matter=2.2±0.3%; pH=6.7±0.8; total soluble phosphorus=0.11±0.04 g kg^{-1}, and CEC=15.5±1.3 cmol Kg^{-1}. Farmer surveys, including application date, dose and formulation (Table 22) indicated pre-emergent herbicide applications during mid-April and early-May 2016 containing S-metolachlor (SM) (active ingredient).

5.2.2 Plot and transect soil sampling design

Top-soils (0 - 1 cm) were sampled at different spatial resolutions, including transects and individual farm plots, and described previously in ref. 25. Briefly, north, valley and south transects (weekly) and 13 marked plots (before and at 1, 50 and 100 days after application) targeted SM $\delta^{13}C$ in addition to SM concentrations to evaluate the benefit of SM isotope data to constrain model parameterization.

5.2.3 Outlet Discharge

Outlet discharge was measured using a Doppler flowmeter (2150 Isco). Automatic, refrigerated continuous flow proportional sampling (Isco Avalanche) was conducted at fixed discharge volumes ranging from 50 to 150 m^3 in 2016 to capture increasing monthly baseflow discharges from April to June. Summary climate and hydrological conditions are provided in Table 21. Although subsurface travel times for this catchment have been estimated to range from 6 to 12 months [24], the time of concentration (T_C), defined as the time between the start of rainfall minus evapotranspiration and the resulting peak discharge [33], decreased from 2.2 to 0.5 h (Table 21). Soil crust development was generally observed across the catchment after around 100 mm of cumulative rainfall. A reduction in the soil infiltration capacity due to observed sealing and the progressive increase in mean daily and total monthly rainfall likely contributed to the observed decrease in the catchment's T_C.

5.2.4 SM concentration and $\delta^{13}C$ analysis

Soil and water SM extraction was detailed in ref. 25. To separate dissolved and particulate phases, water samples were filtered through 0.7-μm glass fibre filters, then extracted by solid-phase extraction (SPE) using SolEx C18 cartridges (Dionex ®, Sunnyvale, CA, USA) and an AutoTrace 280 SPE system (Dionex ®), and quantified by GC-MS/MS (SM) (ThermoFisher Scientific) [34]. Pesticide extraction and purification for soils were adapted from ref. 35 and 36. Environmental quantification limits for SM were 0.01 μg L^{-1} water and 0.001 μg g^{-1} dry weight soils (d. wt.), with an analytical uncertainty of 16%. Carbon isotope composition of SM was analysed using GC-C-IRMS system by adapting ref. 34 and detailed in ref. 25. The reproducibility of triplicate measurements was $\leq 0.2‰(1\sigma)$ for $\delta^{13}C$. Minimum peak

amplitudes needed for accurate $\delta^{13}C$ measurements was 300 mV [25] corresponding to about 10 ng of carbon injected on column.

5.2.5 Sub-daily sample treatment

To obtain water SM concentrations and carbon isotope signatures ($\delta^{13}C$), composite samples were combined according to hydrograph base-flow, rising and/or falling limb, yielding volumes $\geq$ 990 mL. Samples extending across multiple days were assumed to carry equal concentrations. Sub-daily samples were extrapolated based on proportional volume contribution to daily sample, such that:

$$\bar{C}_s = \frac{\sum_{s=1}^{S} Vol_s \cdot C_s}{\sum_{s=1}^{S} Vol_s} \tag{5.1}$$

Sub-daily cumulative samples with duration lower than 90% of the day were omitted from the daily observations.

5.2.6 Coupling event choice

Selection of events to couple with LISEM were made based on three criteria, including qualitative observations for daily discharge simulated by the uncoupled model PiBEACH, days with cumulative rainfall >10 mm and the ability to constrain the event-based model with concentration and/or isotope data. Event model duration was determined as <5 hrs to reduce simulation run times, resulting in simulation of 11 coupled events.

5.2.7 Continuous model description

Use of the Bridge Event Continuous Hydrological (BEACH) model [37] and its adaptation for pesticides persistence and transport prediction (PiBEACH) were described previously (See chapter 4.2.5 and Appendix C.2). Briefly, the continuous PiBEACH model generates spatially distributed soil water content conditions based on daily meteorological records, soil physical properties (e.g., permeability, bulk density, porosity) and crop-specific agronomical information. The Alteckendorf catchment was represented in PiBEACH with a 2 × 2 m resolution with 5-layers (Fig. 42), including a pesticide mixing top-soil layer (z0=1 cm) [38], a plow layer (z1=30 cm) and a layer controlled by artificial drainage pipes (z2=50 cm). The deeper layer with variable saturation depth was divided into upper (z3) and lower (z4) sublayers. Percolation through z3 is routed to outlet as a global linear reservoir [39] *via* the bottom-most sublayer (z4). In terms of hydrological processes, only information from the mixing layer (z0), plow layer (z1) and drainage layers (z2) were transferred to the LISEM event-based model as a two-layer hydrological model, where z0=31 cm and z1= 50cm. Therefore, only the upper layers (z0 to z2) where considered in the LISEM event-based model as its scope was the representation of runoff processes.

The PiBEACH model accounts for temperature and water content control on pesticide degradation and nonreactive transport, as previously described (See chapter 4). Biodegradation is assumed to occur only in bioavailable fractions of adsorbed (ads) and aqueous (aq) phases [40]. The bioavailable fraction is controlled kinetically by an ageing rate k_{age} on the adsorbed fraction [41, 42]. Representing SM mass (M) as separate light (l) and heavy (h) isotopologues, the change in aqueous and adsorbed phases is given by:

$$\frac{\partial M_{ads}}{\partial t} = -k_{age}(M^l_{ads} + M^h_{ads}) - k_{deg}(M^l_{ads} + \alpha M^h_{ads}) \tag{5.2}$$

$$\frac{\partial M_{aq}}{\partial t} = -k_{deg}(M^l_{aq} + \alpha M^h_{aq}) \tag{5.3}$$

where $k_{deg} = ln(2)/DT_{50}$ and DT_{50} (days) is the observed degradation half-life. Isotope fractionation is considered through the fractionation factor (α), also expressed as $\alpha = \epsilon/1000+1$, where ϵ (‰) is the characteristic SM enrichment. Although a decrease in degradation rates may be correlated to depth (e.g., due to microbial activity [24, 43]) or sorption [44], the lack of SM concentration and isotope data at deeper soil profiles did not allow to consider depth dependence, and was thus not included. SM degradation extent did not decrease for reversibility sorbed fraction [45, 46], and thus it was considered to be equivalent to the dissolved phase.

Degradation half-life was dynamically adjusted with soil temperature (F_T) and water content (F_θ), and give as [47]:

$$k_{Dynamic} = k_{ref} \cdot F_T \cdot F_\theta \tag{5.4}$$

Where the temperature dependence factor (F_T) is based on the modified Arrhenius equation for low temperatures [47, 48] such that:

$$F_T = \begin{cases} 0, & \text{if, } T_C \leq 0 \\ \frac{T_{K,obs}-273.15}{5} exp\Big(\frac{E_a}{R}(\frac{1}{T_{K,ref}} - \frac{1}{T_{K,obs}})\Big), & \text{if, } 0 < T_C \leq 5 \\ exp\Big(\frac{E_a}{R}(\frac{1}{T_{K,ref}} - \frac{1}{T_{K,obs}})\Big), & \text{if, } T_C > 5 \end{cases} \tag{5.5}$$

where T_K and T_C are soil temperatures in Kelvin and Celsius, respectively and $T_{K,ref}$ is the reference temperature at 293.15 K. E_a is the SM activation energy (23.91 KJ mol^{-1})[49] and R is the gas constant 8.314 (J mol^{-1} K^{-1}). Influence of water content (F_θ) follows [48, 50]:

$$F_\theta = \Big(\frac{\theta_t}{\theta_{ref}}\Big)^{\beta_\theta} \tag{5.6}$$

where β_θ is a calibration constant and θ_{ref} the water content at 0.2 ($m^3\ m^{-3}$).

5.2.8 Event-based model description

Hydrological model. The open source code version (4.96) of the Limburg Soil Erosion Model (openLISEM) [51], a physically based runoff and soil erosion model for event-based predictions in small agricultural catchments (<10,000 ha), was initially modified to include pesticide transfer in the dissolved phase [52]. In this Ph.D. thesis work, pesticide isotopologues were considered as individual species. Water partitioning between infiltration and surface runoff was calculated with the Green and Ampt equation solved explicitly [53] such that:

$$q_{inf} = -K_{sat}\Big(1 + \frac{(\psi + h)(\theta_{sat} - \theta_i)}{F}\Big) \tag{5.7}$$

where q_{inf} is the infiltration rate (m s^{-1}), K_{sat} is the saturated hydraulic conductivity (m s^{-1}), F is the cumulative infiltration from the beginning of the event (m), ψ is the average matrix suction at the wetting front (m), h is the overpressure depth of the water layer at the soil surface (m), θ_{sat} is the saturated water content (-), and θ_i is the initial water content (-). The maximum depression storage in the micro-relief was estimated based on an empirical equation from ref. 54. Once the maximum depression storage was exceeded, runoff was generated. Erosion detachment was generated by rainfall splash based on rainfall kinetic energy [55] and/or overland flow. Flow detachment was calculated with a stream-power based transport capacity based on the EUROSEM formalism [56]. Sediment traps were considered to represent vegetal barriers as, observed within the catchment. The flow velocity was calculated with the Manning equation, and surface runoff was routed over the landscape with the 1D kinetic wave equation [57]:

$$\frac{\partial A}{\partial t} + \frac{\partial Q}{\partial x} = q_{sur} \tag{5.8}$$

where Q is the discharge (m^3 s^{-1}), and A is the wetted cross-section (m^2), x and t are the spatial (m) and temporal (s) localizations and q_{sur} is the infiltration surplus (m^2 s^{-1}). The relationship between A and Q is given by:

$$\begin{cases} A = \alpha Q^{\beta} \\ \alpha\Big[\frac{n}{\sqrt{S}} P^{2/3}\Big]^{\beta} \end{cases} \tag{5.9}$$

where n is the Manning coefficient (-), S is the sine of the slope gradient (-), P is the wetted perimeter (m) and β is a constant (0.6). Equations 5.7 and 5.8 indicate that the compensation in rainfall-runoff model parameters may occur in one cell during the water partitioning between runoff and infiltration (eq. 5.7) or spatially between the cells during the transport step (eq. 5.8).

Differentiation and combination of eq. 5.8 and 5.9 gives the implicit numerical scheme (eq. 5.10) solved using a Newton backward-difference method [57]:

$$\begin{cases} \alpha\beta Q^{\beta-1}\frac{\partial Q}{\partial t} + \frac{\partial Q}{\partial x} = q_{sur} \\ \alpha\beta \bar{Q}^{\beta-1}\frac{Q_{i+1}^{n+1} - Q_{i+1}^{n}}{\Delta t} + \frac{Q_{i+1}^{n+1} - Q_{i}^{n+1}}{\Delta x} = q_{sur}, \quad with\ \bar{Q} = \frac{1}{2}\Big(Q_i^{n+1} + Q_{i+1}^{n}\Big) \end{cases} \tag{5.10}$$

where n is the current time-step, $n+1$ the end of the time step, i the upstream side of the grid cell, $i+1$ the downstream side of the gird cell, Q_{i+1}^{n+1} the new discharge (m^3 s^{-1}), Q_i^{n+1} the new discharge at the upstream end of the grid cell, equivalent to the sum of all incoming upstream water generated by the kinematic wave (m^3 s^{-1}), Q_{i+1}^{n} the discharge of the previous time-step outflowing the grid cell (m^3 s^{-1}) $\bar{Q}$ the diagonal average discharge in a space time diagram (m^3 s^{-1}), q the average infiltration surplus over the length of the

grid cell (m^2 s^{-1}). At each time step, the grid cells were re-arranged in order to start the flow calculation at the top of the branches of the drainage network and progress towards the outlet, using as input for the downstream grid cell the sum of the discharges of the upstream grid cells at the end of the time-step.

Transport equations (water and sediment) are solved in one dimension and routed from up- to down-stream over a predefined flow network that connects cells in 8 directions (quasi 2D). For each predicted runoff event, the initial surface soil characteristics, hydrodynamic parameters and initial water content (Table 51) were required for the hydrological predictions with LISEM and were provided by the continuous PiBEACH model.

Pesticide transfer model. As a future objective is to predict solid-bound pesticide transport, consistency with the numerical scheme used to solve the sediment and pesticide transport equations was targeted. Before computing the kinematic wave, splash, flow detachment and sediment deposition were solved separately based on rainfall intensity and updated velocity calculated with effective rainfall depth. Erosion procedures give an intermediate sediment concentration noted C* (calculations not detailed here) [52]. Suspended sediment in runoff is then routed using a similar equation as equation 5.11. The equations are analogous for each isotopologue. Taking the light carbon isotope (^{12}C) as example:

$$\frac{\partial Q_{12C,S}}{\partial x} + \frac{\partial C_{12C} A}{\partial t} = 0 \tag{5.11}$$

where $Q_{12C,S}$ is the sediment flux (kg s^{-1}) associated to the light isotope and C_{12C} the sorbed concentration (kg m^{-3}) of the light isotope.

Pesticide mobilization at the soil/surface runoff interface was predicted by assuming that a very thin layer (i.e., mixing layer) at the soil surface exists where water from infiltration, runoff and soil pore mix instantaneously [58]. Pesticide loss below the mixing zone was considered as a sink term and distributed further by the daily model. The governing equations describing heavy and light isotope transport in runoff are given as an example for ^{12}C by:

$$\begin{cases} \frac{1}{\Delta x}\left(\frac{\partial A C_{12C}}{\partial t} + \frac{\partial Q_{12C,p}}{\partial x}\right) = K_{film}(C_{12C,M} - C_{12C,ro}) - q_{inf} C_{12C,ro} \\ \theta_{sat} D_{z0,ML} \frac{\partial C_{12C,M}}{\partial t} = \\ \quad K_{film}(C_{12C,ro} - C_{12C,M}) + q_{inf}(C_{12C,ro} - C_{12C,M}) - D_{z0,ML} \cdot \rho_b k_r (K_d C_{12C,M} - C_{12C,ad}) \\ \frac{\partial C_{12C,ad}}{\partial t} = k_r (K_d C_{12C,M} - C_{12C,ad}) \end{cases} \tag{5.12}$$

where $Q_{^{12}C}$ is ^{12}C-specific flux (kg s^{-1}), A the wet cross section (m^2), q_{inf} the infiltration rate (m s^{-1}), K_{film} the film transport coefficient (m s^{-1}), k_r the rate of desorption (s^{-1}), K_d the soil water partition coefficient (m^3 kg^{-1}), $C_{^{12}C,ro}$ the pesticide concentration in runoff (kg m^3), $C_{aq,^{12}C,M}$ the pesticide concentration in the soil water of the mixing zone (kg m^3), $C_{^{12}C,ad}$ the adsorbed pesticide mass per dry unit weight of soil in the mixing zone (kg kg^{-1}), θ_{sat} the soil porosity (m^3 m^{-3}), $D_{z0,ML}$ the mixing layer depth (m) and ρ_b the soil bulk density (kg m^{-3}).

5.2.9 Coupling continuous and event-based models

Selection of coupled events resulted in three types of coupling routines (Fig. 51) required to account for events that fall within the boundaries of one simulated PiBEACH day (Type 1), events that fall between the boundaries of two simulated PiBEACH days (Type 2) and events that take place within two consecutive simulated PiBEACH days (Type 3). Two or more events taking place within the boundaries of one simulated PiBEACH day were not observed and thus not included within the coupling routines. Information exchange between PiBEACH and LISEM is depicted by input and output states depicted with circles denoted as 1, 2 and 3 (Fig. 51) across routines.

To prepare rainfall input files, rainfall allocated to event-based simulations with LISEM were subtracted from daily rainfall input files for the continuous model. At the end of each continuous PiBEACH model simulation period, initial conditions for the event-based simulation were produced Table 51.

Suction pressure (ψ) was determined from moisture and suction pressure from Alteckendorf data soil core samples (n = 6, 2 m depth) obtained during 2012 [12] and the re-arranged Van Genuchten 1980 equation, such that [60]:

$$\psi = \frac{1}{a}\Big[\big(\frac{\theta_{sat}}{\theta_i}\big)^{1/m} - 1\Big] \tag{5.13}$$

Parameters to solve eq. 5.13 were fitted using the Microsoft excel GRG Nonlinear solver.

Output files of the LISEM event-based model incorporated into the PiBEACH continuous model included cumulative infiltration and total discharge to outlet, pesticide mass losses from the mixing layer (z0) due to leaching and export *via* runoff and mass inputs to the mixing layer due to runoff re-infiltration (Table 51). The results provided in the next sections focus on improvement of PiBEACH prediction on discharge, SM concentration and $\delta^{13}C$ by integration of infiltration and discharge generated by LISEM. The full coupling with LISEM, i.e. dissolved heavy and light isotopologues leached and transported under dissolved and sorbed phases with runoff is under current progress.

Table 51: PiBEACH output maps required for LISEM initial conditions

Output map	**Units**	**Description**	**Notes**
$K_{sat,\ z0,z1}$	mm hr^{-1}	Saturated hydraulic conductivity	Adjusted by calibrated by $\gamma_{z0,z1}$
$K_{sat,\ z2}$	mm hr^{-1}	*ibid*	Adjusted by calibrated by γ_{z2}
$theta_{z0,z1}$	mm^3 mm^{-3}	Volumetric soil moisture	
$theta_{z2}$	mm^3 mm^{-3}	*ibid*	
$theta_{sat,\ z0,z1}$	mm^3 mm^{-3}	Soil moisture at saturation capacity	
$theta_{sat,\ z2}$	mm^3 mm^{-3}	*ibid*	
rr	cm	Random roughness	Only for the mixing layer (z0)
n	-	Manning's coefficient	*ibid.*
LAI	m^2 m^{-2}	Leaf area index	
$\psi_{z0,z1}$	cm	Suction pressure at the wetting front.	$a = 6.458$, $m = 0.007$, $n = 5.563$
ψ_{z2}	cm	*ibid*	$a = 3.452$, $m = 0.007$, $n = 5.890$
$M^l_{z0,z1}$	g SM	Mass of light isotope	Only for the mixing layer (z0)
$M^h_{z0,z1}$	g SM	Mass of heavy isotope	*ibid.*

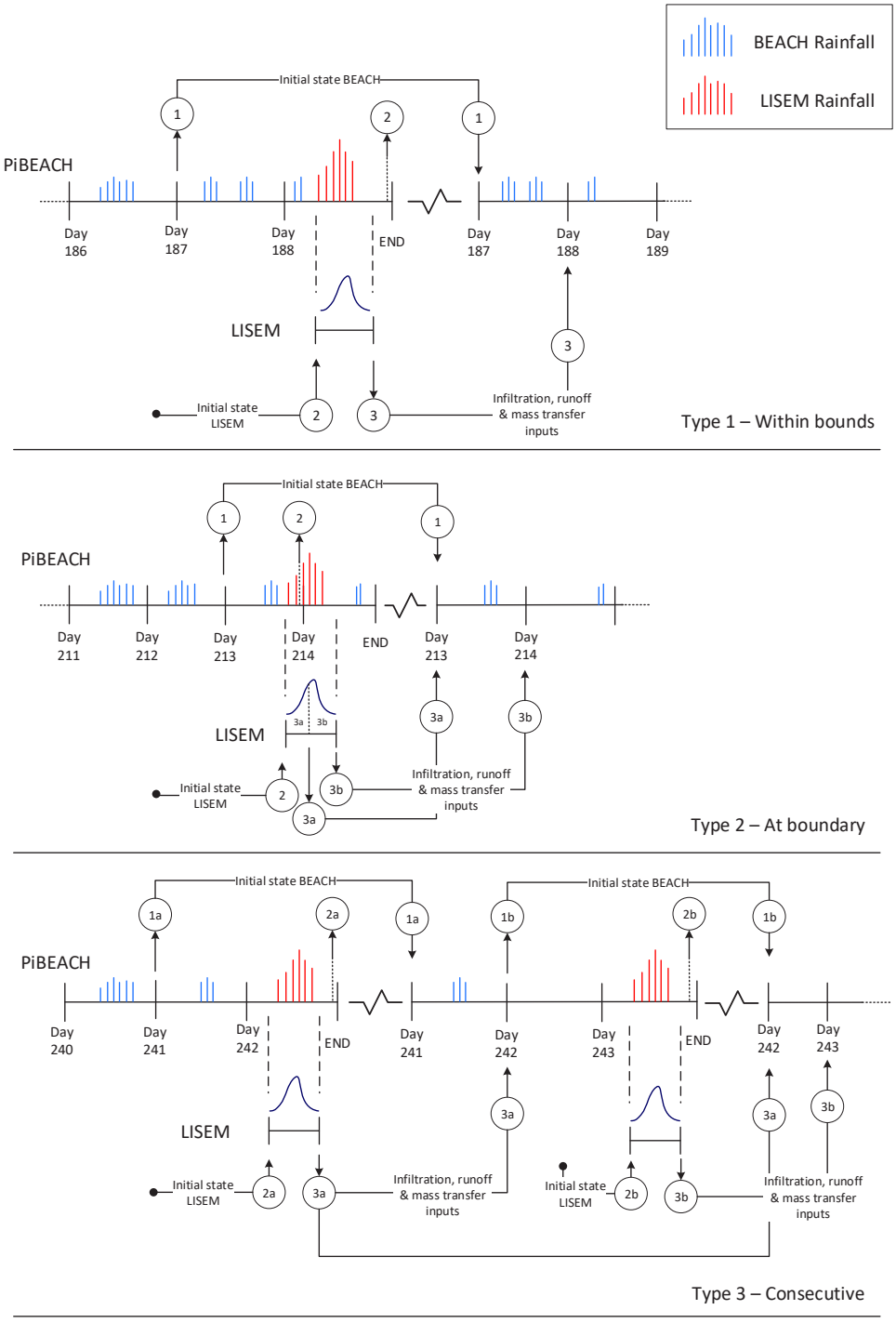

Figure 51: Coupling routines for events taking place within PiBEACH day boundaries (Type 1), at a BEACH boundary (Type 2) and over consecutive PiBEACH days within boundaries (Type 3). Output and input states exchanged between PiBEACH and LISEM are depicted as circles. These include PiBEACH output state files required to re-initialize PiBEACH after LISEM run (state 1), PiBEACH output state files required to initialize LISEM (state 2), and LISEM output states required as additional inputs to correct PiBEACH day on re-initialization (state 3).

5.2.10 Parameter sampling space

Hydrological and transport parameters were evaluated with the generalized likelihood uncertainty estimation (GLUE) technique [30, 31]. Rather than seeking an optimal model solution, the GLUE approach recognizes that more than one model structure or parameter set may lead to acceptable model results, i.e. equifinality [30]). Equifinality is used here to explore the parameter space associated to acceptable model representations. Sampling and interpretation was conducted in 3 steps. First, parameter sets were identified (Table 42), assumed to be uniformly distributed, and likely boundaries defined based either on literature or field data collected in 2012 [32] and 2016 [25]. Boundaries for $DT_{50_{ref}}$ (15 to 23 d) and ϵ (-1.7 to -3.2‰) where set based on retained model distributions from previous GLUE simulation experiments in chapter 4. Second, *a posteriori* parameter distributions were derived from acceptable simulations, i.e. providing SM concentration and $\delta^{13}C$ predictions closed to outlet observations. Third, acceptable model results, e.g. outlet discharge and SM concentrations $\delta^{13}C$ were reported as an ensemble, drawn from the 95% confidence interval obtained from 2500 and 171 simulations for the uncoupled and coupled models, respectively.

Due to large computation time (i.e., 7515 CPU sec./ hydrological year on an Intel(R) Core(TM) machine i7-8650U CPU@ 1.90GHz, 2.11 HGz), *via* Latin-Hypercube sampling [61] was used to reduce sample numbers. To reduce the number of parameters during GLUE analysis, a pre-sensitivity analysis based on the Morris method[61, 62] was conducted in chapter 4 (data not shown). To further reduce computation times, the GLUE assessment was focused on the growing period (March 14^{th} to July 12^{th}, 2016), where pesticide degradation and export are of most significance. Initial hydrological state was estimated from a spin-up period of one full hydrological year (Oct. 1^{st}, 2015 - Sept. 30^{th}, 2016) and hydrological parameters calibrated against observed discharge (March 25^{th} and July 12^{th}, 2016) using particle swarm optimization [63].

5.2.11 Model predictability evaluation

To determine model predictability, the Kling-Gupta efficiency (KGE) [64] metric was adopted. Goodness of fit between simulations and observations are given relative to a maximum efficiency of 1 and given by:

$$KGE = 1 - \sqrt{(r-1)^2 + (\alpha_{KGE} - 1)^2 + (\beta_{KGE} - 1)^2} \tag{5.14}$$

where r is a linear correlation coefficient, $\alpha_{KGE} = \frac{\sigma_i}{\sigma_o}$, and $\beta_{KGE} = \frac{\mu_i}{\mu_o}$, where σ and μ represent the standard deviation and mean of simulated (i) and observed (o) values, respectively.

The KGE metric was selected to provide equal weight across correlation, bias and variability measures. KGE metric is also an improved measure of model performance relative to other metrics, such as the mean squared error or the Nash-Sutcliffe efficiency, which favor parameter values underestimating variance of model results [64]. KGE values where computed separately for SM concentration and $\delta^{13}C$. To quantify uncertainty reduction between formalisms, the PUCI (Percentage of observations bracketed by the Unit Confidence Interval)[65] index was used, which incorporates resolution and reliability measures given by the ARIL (Average Relative Interval Length)[66] and the PCI (Percentage of observations bracketed by the Confidence Interval)[67] indices, respectively, such that:

$$PUCI = (1.0 - Abs(PCI - 0.95))/ARIL \tag{5.15}$$

$$ARIL = \frac{1}{n} \sum \frac{CI_{upper} - CI_{lower}}{y_o} \tag{5.16}$$

$$PCI = \frac{Y_o}{n} \tag{5.17}$$

where n is the number of time steps, CI are the simulated upper and lower 95% confidence intervals, y_o is the observed measure, Y_o is the number of observations contained within the 95% CI.

5.3 Results and discussion

5.3.1 Outlet discharge and hydrological components

Simulated outlet discharge (Fig. 52) showed generally good agreement with observed data for both models, with maximum KGE values for the uncoupled (PiBEACH) and coupled (PiBEACH-oL) models of 0.75 and 0.74, respectively. In terms of predictive resolution (i.e., with of CI) measured by the ARI index, approximately equivalent performance is obtained between the uncoupled (1.51) and coupled (1.52) models. The reliability of interval estimates (i.e., number of observations within the CI) measured by the PCI index on the other hand is greater for the coupled (0.89) relative to the uncoupled (0.83) model. Combination of both performance indices into the PUCI index, higher combined accuracy and reliability is obtained for the coupled (0.62) vs. the uncoupled (0.58) model.

Although both models generally do well in predicting daily discharges, the coupled model is better account for individual hydrological components. In particular, the PiBEACH-oL coupled model allocated a larger percentage of total discharge to artificial drainage (75%) relative to the uncoupled model (65%). The opposite was also true for runoff, where the uncoupled model allocated a higher percentage (15%) relative to the coupled model (5%). A tendency to overestimate runoff generation in the uncoupled model was due to simplifying assumptions of the SCS-CN approach. Namely, based on the SCS-CN approach, when total daily rainfall is able to saturate the first 31 cm of the soil profile, the remaining rainfall is routed to outlet through runoff (without re-infiltration). In this respect, the daily time-step misses important information about the distribution of rainfall intensity throughout the day, leading to overestimation of runoff due to an inability to account for actual soil infiltration rates. This is in agreement with field observations. Indeed, the development of shallow soil trenches associated to sediment transport during runoff was only observed after the 1st week of May ($\approx$ 55-60 days after 1st application). High infiltration rates may occur both during the early season, where recently tilled soils increase soil permeability, as well as during the late season, where drier initial conditions may increase infiltration rates. Accounting only for saturation capacities within the daily model, therefore leads to wrong predictions of runoff events (false-positive) both during the early (Fig. 53A) and late (Fig. 53B) season for these reasons. More accurate representation of runoff genesis by the PiBEACH-oL coupled model also leads to higher infiltration amounts, generating smoother catchment drainage rates that more closely approximate observed discharge (Fig. 52).

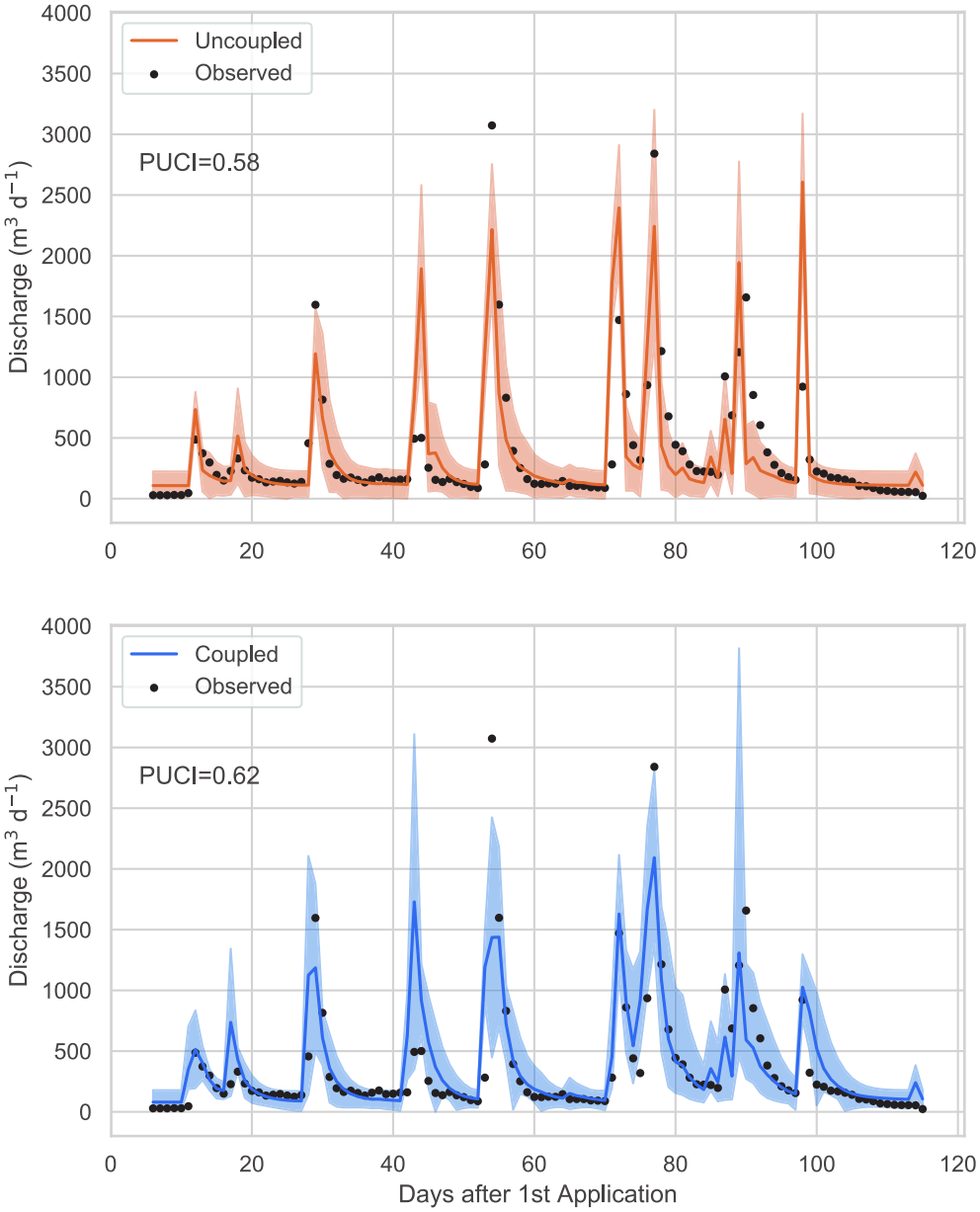

Figure 52: Simulated mean vs. observed daily outlet discharge for the uncoupled PiBEACH (top) and coupled PiBEACH-oL (bottom) model. Shaded area depicts 95% confidence intervals (CIs) for the model ensemble. 95% confidence intervals (CI) where computed based on 312 (out of 2500) and 5 (out of 171) retained number of simulations with KGE_Q >0.5 for the uncoupled and coupled models, respectively.

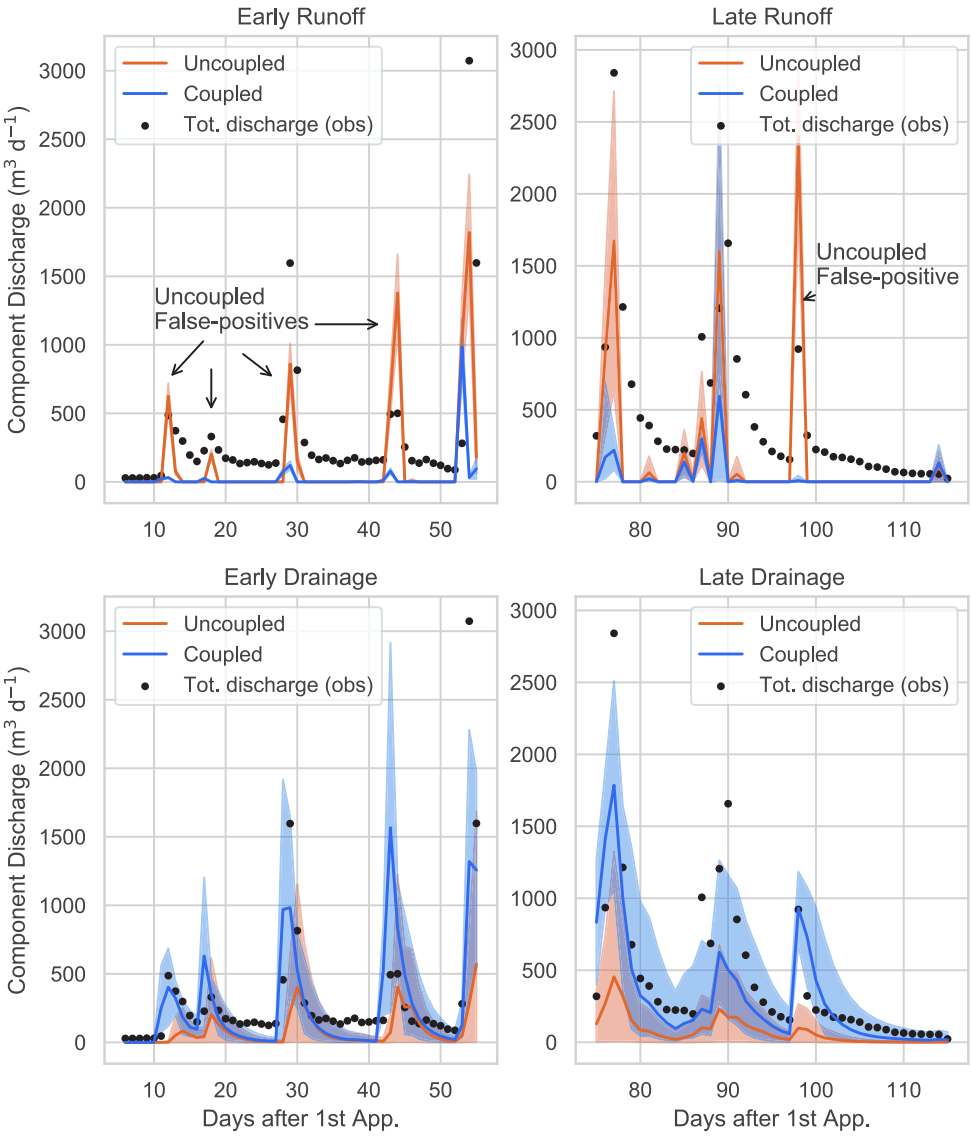

Figure 53: Runoff and drainage components contributing to total daily discharge (observed) during the early (A & C) and late (B & D) season periods. Shaded area depicts 95% confidence intervals (CIs) for the model ensemble and computed based on 312 (out of 2500) and 5 (out of 171) retained number of simulations with KGE_Q >0.5 for the uncoupled and coupled models, respectively.

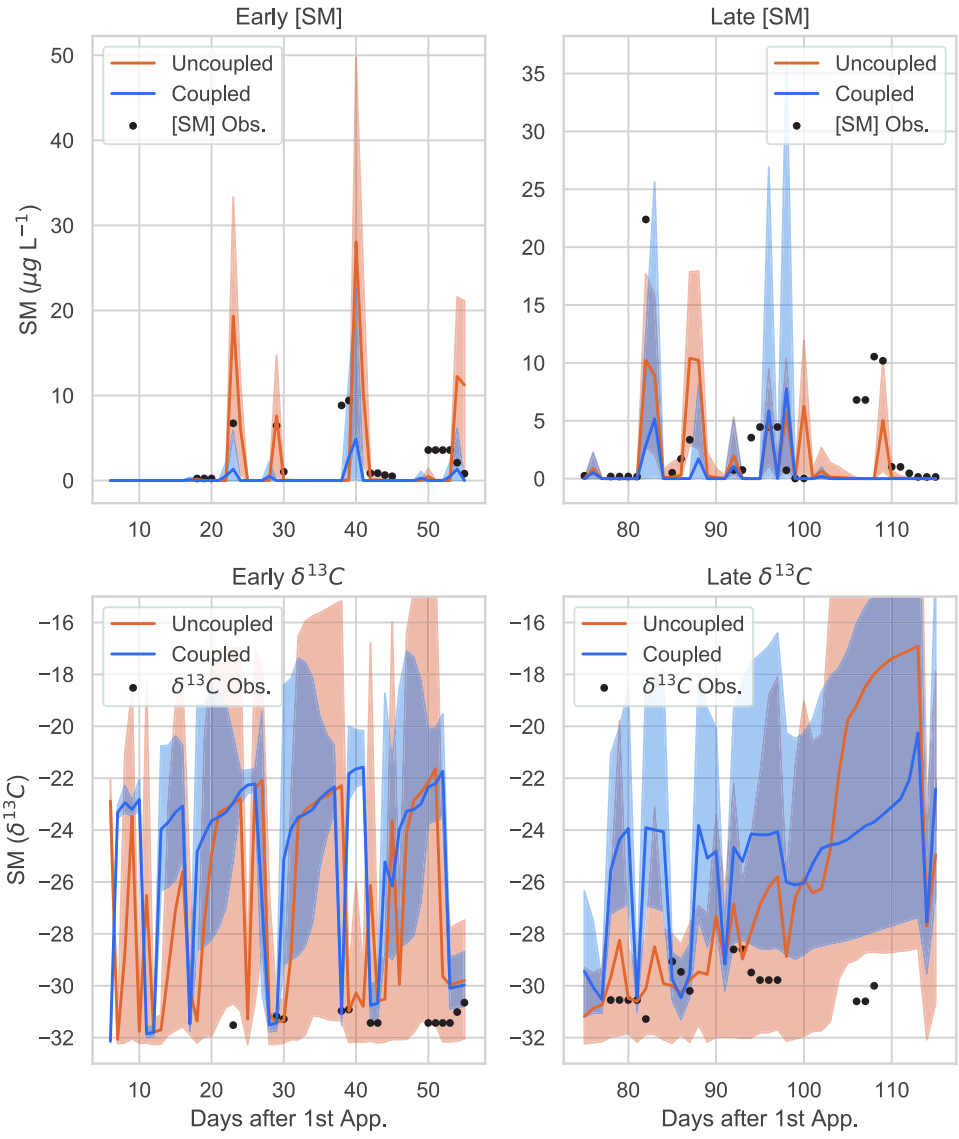

Figure 54: Simulated and observed outlet SM concentrations and carbon isotope signatures ($\delta^{13}C$) for early and late season periods. Shaded area depicts 95% confidence intervals (CIs) for the model ensemble and where computed based on 312 (out of 2500) and 5 (out of 171) retained number of simulations with KGE_Q >0.5 for the uncoupled and coupled models, respectively.

5.3.2 SM outlet concentrations and $\delta^{13}C$

Both models can generally reproduce outlet SM concentrations and isotope signatures during the early season (Fig. 54). However, predictability of both models markedly falls after 50 days following the first application. This is primarily associated to tail-end periods of catchment drainage, which are unable to reproduce the export of pesticide pools reflecting little degradation extent (i.e., see days: 50, 80 and 95). Note that this is not the case for the main run-off event around day 85 for the uncoupled model, which correctly accounted for likely fresh pesticide pools at high concentrations from top soils from a late season application on corn plots (late May to early June). Note that the current version of the coupled model, does account for run-off mass transfer to outlet.

The above observations indicate on the one hand, the need to account for mass transfer to outlet *via* run-off within LISEM. On the other hand, there is a potential need for conceptual improvement in the representation of degradation rates with increasing depth. Namely, reducing the effective degradation depths at lower depths could reflect lower bacterial activity or less degradation potential due to varying redox conditions. Such a representation may lead to an accumulation of non-degraded pesticides in lower soil profiles, which is mobilized only during extended periods of catchment drainage. Degradation rates may decrease with depth (e.g., due to microbial activity [43]) or sorption [44], due to the lack of SM concentration and isotope data at deeper soil profiles. However, depth dependence was not considered in current degradation formalisms, and was thus initially not accounted. Indeed, to better constrain additional model complexity, characterization of outlet samples during low-flow should be of significant interest, allowing to constrain background conditions of the studied catchment.

5.3.3 Implications for prediction of pesticide transport at catchment scale

Pesticide fate in the environment is affected by multiple processes, each with a relative importance depending on the intrinsic and extrinsic factors considered. Extrinsic factors, such as rainfall patterns and application periods [68, 69], may dominate export from soils within relatively short periods at the event-scale. In contrast, intrinsic factors, such as soil and pesticide properties regulating sorption or degradability, may be more relevant over extended periods at the continuous-scale. Accounting for the relative contribution of each factor towards total dissipation typically then requires the use of numerical methods to compute competing impacts and non-linear interactions between relevant variables [13].

Although pesticide fate models typically specialize on one of the above mentioned time scales, simultaneous scale representation is necessary to address the need to reduce initial model boundary uncertainty evolving daily (e.g., soil hydraulic properties, available pesticide pools) [12, 15], while maintaining detailed physical process representations relevant over seconds or minutes [17, 70]. Coupling approaches such as those developed here under PiBEACH-oL and applied at the headwater scale can thus become useful tools to investigate different scenarios of pesticide fate process with greater detail.

Firstly, by improving infiltration-runoff partition at the event-scale, leading to better account of hydrological components at the outlet, the coupled model showed that drainage is much more frequent than runoff especially early in the growing season. Therefore, drainage plays an essential role in connecting source soils with stream concentrations and isotope signatures. Secondly, based on isotope signatures observed at the outlet, the improved ability

of the coupled model to reproduce higher rates of delayed drainage highlight the need to identify additional formalisms to explain the sustained potential of headwaters to release non-degraded pesticide fractions. Both of these observations have implications for sampling design. Namely, flow-proportional sampling strategies may not be sufficient to characterize pesticide exports at these scales. As such, water sampler units could thus be programmed to automatically switch-on/off at pre-defined discharge thresholds, with continuous proportional flow only accounted for above such thresholds. Alternatively, with similar sampler capacities used in the study, a weekly servicing protocol may not be ideal, as capacities where often reached shortly after major events, thereby reducing the number of observations obtained during periods of delayed drainage.

The use of coupling approaches presents an opportunity to more quickly assess the effectiveness of pesticide management strategies, such as mitigation of transfer through artificial drainage [71]. Indeed, models such as MACRO have been previously employed for this specific task (e.g., [9, 72]). To address the uncertainty associated to transferring parameter values from laboratory to field conditions, such approaches typically employ a well justified stochastic analysis. While statistical descriptions of spatially distributed parameters allow to determine correlations between, for example, soil organic matter content and mobility or degradation constants [73, 74], they are limited in terms of describing causality and mechanistic linkage. In contrast, the added value here was the ability to relate degradation parameter values (i.e., during continuous modelling) to observed fractionation extent of the pesticide under study. The constraint of *in situ* degradation conditions can thus lead to a reduction of parameter uncertainty, as shown in chapter 4, and simultaneously be used to assess the validity of degradation formalisms or the relevance of distinct water pathways.

Combination of temporal scales (event and growing season) through the coupled model allowed for a stream-line assessment of pesticide degradation and export at the catchment scale, removing the need to calibrate initial conditions for each individual hydrological event. This has important implications for pesticide field assessments, as PiBEACH-oL provides a trade-off between parsimony and complexity that can be employed to improve prediction of pesticide degradation and transfer at various scales. Namely, stream-lining was achieved through the integration of agronomical knowledge linking temporal evolution of key topsoil hydraulic properties with climatic conditions, soil properties, vegetation, and crop management techniques [12]. This did not only improve initial event-based model constraints, but also allowed to constrain top soil degradation formalisms by making use of CSIA information. This implies that whenever pesticide degradation is assumed to be a primary sink over seasonal scales, PiBEACH (i.e., without -oL) can be used as a stand-alone model to constrain top soil degradation parameters based on hydro-climatic conditions and CSIA data. This allowed to reduce simulation run-times by a factor of 3, which is valuable for predictive assessments employing an uncertainty framework. As coupling nevertheless, increases simulation run-times, larger catchment scale studies could therefore benefit from a similar step-wise assessment, consisting first of a top-soil degradation assessment (PiBEACH), followed by a water pathway and subsurface degradation assessment (PiBEACH-oL).

5.3.4 Model limitations and perspectives

Preliminary results from coupling efforts demonstrated the ability of PiBEACH-oL to improve the description of water pathways and their evolution throughout the growing season, progressing from drainage- to runoff-driven export within the studied catchment. Although run-off contribution to total outlet pesticide loadings was small, current LISEM development does not account for pesticide mobilization through run-off or solid particulate transport,

which is currently ongoing development, and may be expected to not only contribute to outlet signatures but also affect re-distribution of pesticide mass across the catchment through runoff generation and re-infiltration, thereby also affecting drainage response.

Limitations of the coupled model were also noticeable during mid-season (i.e., after day 50), where discharge dominated by the tail-end components of catchment drainage is not able to reproduce isotope signatures that reflect fresh product fractions. Indeed, rapid transport connecting macropores to artificial drains is not accounted for in the model, although this phenomenon may be of particular importance in clayey soils [75]. Conceptualization of the late drainage component could also be improved, for example, by limiting the drainage network extent, helping to achieve a less pronounced discharge curve associated to lower drainage rates (i.e., both lower maximums and higher minimums). This could in turn increase soil water content, resulting in additional leaching fractions from top-soils and potentially improving outlet signatures associated to delayed transfer from top-soils *via* drainage components.

Alternatively, degradation conditions below top soils currently do not account for possibly lower degradation rates (e.g., [24, 47, 76]), which could be associated to a significant reduction in pesticide concentrations with depth and reducing redox conditions, both of which could potentially contribute to a shift in dominant degradation pathways (e.g., co-metabolic, anaerobic). Indeed, SM degradation rates have been observed to be positively correlated with organic matter content [46], the latter of which slightly decreased with depth. Therefore, further evaluation of degradation formalisms or process hypothesis could include further testing for different transformation rates on sorbed fractions [77], rate dependencies associated to increasing depths [24, 47, 76] or bioavailability limitations associated to the heterogenous distribution of degrading bacteria in subsurface transport paths [78]. Unfortunately, without additional mechanistic information evidencing a change in dominant degradation pathways, which may be obtained in the future using multi-element CSIA, such approaches may nevertheless suffer from similar drawbacks of existing models, therby limiting the ability to constrain additional parameters based on available data.

References

1. Kirby, M. J. *Hillslope hydrology* (Wiley, Chichester, 1978).
2. Saunders, D., Meeuwig, J. & Vincent, A. Freshwater protected areas: Strategies for conservation. *Conservation Biology* **16,** 1523–1739 (2002).
3. Springgay, E. in *Ecosystem Services of Headwater Catchments* (eds Křeček, J., Haigh, M., Hofer, T., Kubin, E. & Promper, C.) (Springer, Cham, 2017).
4. Dodds, W. & Oakes, R. Headwater influences on downstream water quality. *Environmental Management* **41,** 367–377 (2008).
5. Ariza, C., Maselli, D. & Kohler, T. *Mountains: Our life, our future. Progress and perspectives on Sustainable Mountain development from Rio 1992 to Rio 2012 and beyond.* tech. rep. (Swiss Agency for Development and Cooperation (SDC), Bern, 2013).
6. Szöcs, E., Brinke, M., Karaoglan, B. & Schäfer, R. B. Large Scale Risks from Agricultural Pesticides in Small Streams. *Environmental Science and Technology* **51,** 7378–7385. ISSN: 15205851 (2017).

7. Payraudeau, S. & Gregoire, C. Modelling pesticides transfer to surface water at the catchment scale: A multi-criteria analysis. *Agronomy for Sustainable Development* **32,** 479–500. ISSN: 17740746 (2012).
8. Trépos, R., Masson, V., Cordier, M. O., Gascuel-Odoux, C. & Salmon-Monviola, J. Mining simulation data by rule induction to determine critical source areas of stream water pollution by herbicides. *Computers and Electronics in Agriculture* **86,** 75–88. ISSN: 01681699 (2012).
9. Lindahl, A. M. L., Söderström, M. & Jarvis, N. Influence of input uncertainty on prediction of within-field pesticide leaching risks. *Journal of Contaminant Hydrology* **98,** 106–114. ISSN: 01697722 (2008).
10. Mander, Ü., Tournebize, J., Tonderski, K., Verhoeven, J. T. & Mitsch, W. J. Planning and establishment principles for constructed wetlands and riparian buffer zones in agricultural catchments. *Ecological Engineering* **103,** 296–300. ISSN: 09258574 (2017).
11. Frey, M. P., Schneider, M. K., Dietzel, A., Reichert, P. & Stamm, C. Predicting critical source areas for diffuse herbicide losses to surface waters: Role of connectivity and boundary conditions. *Journal of Hydrology* **365,** 23–36. ISSN: 00221694 (2009).
12. Lefrancq, M., Dijk, P. V., Jetten, V., Schwob, M. & Payraudeau, S. Improving runoff prediction using agronomical information in a cropped, loess covered catchment. *Hydrological Processes* **31,** 1408–1423 (2017).
13. Fatichi, S. *et al.* An overview of current applications , challenges , and future trends in distributed process-based models in hydrology. *Journal of Hydrology* **537,** 45–60. ISSN: 0022-1694 (2016).
14. Beven, K. A manifesto for the equifinality thesis. *Journal of Hydrology* **320,** 18–36. ISSN: 00221694 (2006).
15. Gassmann, M., Khodorkovsky, M., Friedler, E., Dubowski, Y. & Olsson, O. Uncertainty in the river export modelling of pesticides and transformation products. *Environmental Modelling and Software* **51,** 35–44. ISSN: 13648152 (2014).
16. Köhne, J. M., Köhne, S. & Simunek, J. A review of model applications for structured soils: b) Pesticide transport. *Journal of Contaminant Hydrology* **104,** 36–60. ISSN: 01697722 (2009).
17. Borah, D. K. & Bera, M. Watershed-Scale Hydrologic and Nonpoint-Source Pollution Models: Review of Mathematical Bases. *Transactions of the ASAE* **46,** 1553–1566. ISSN: 2151-0059 (2003).
18. Merritt, W. S., Letcher, R. A. & Jakeman, A. J. A review of erosion and sediment transport models. *Environmental Modelling and Software* **18,** 761–799. ISSN: 13648152 (2003).
19. Quilbé, R., Rousseau, A. N., Lafrance, P., Leclerc, J. & Amrani, M. Selecting a pesticide fate model at the watershed scale using a multi-criteria analysis. *Water Quality Research Journal of Canada* **41,** 283–295. ISSN: 12013080 (2006).
20. Pandey, A., Himanshu, S. K., Mishra, S. K. & Singh, V. P. Physically based soil erosion and sediment yield models revisited. *Catena* **147,** 595–620. ISSN: 03418162 (2016).
21. Donigian, A. S. J., Bicknell, B. R. & Kittle, J. L. J. *Conversion of the Chesapeake Bay basin model to HSPF operation. Prepared by AQUA TERRA Consultants for the Computer Sciences Corporation and U.S. EPA Chesapeake Bay Program* tech. rep. (AQUA TERRA Consultants, Annapolis, Md., 1986).

22. Danish Hydraulic Institute. *MIKE SHE water movement – user guide and technical reference manual, Edition 1.1.* tech. rep. (DHI, 1998).

23. BASINS. *BASINS 4.1 (Better Assessment Science Integrating point & Non-point Sources) Modeling Framework.* North Carolina, 2015. `https://www.epa.gov/ceam/better-assessment-science-integrating-point-and-non-point-sources-basins` (2018).

24. Lutz, S. R. *et al.* Pesticide fate at catchment scale: conceptual modelling of stream CSIA data. *Hydrology and Earth System Sciences Discussions* **21,** 5243–5261. ISSN: 1812-2116 (2017).

25. Alvarez-Zaldívar, P., Payraudeau, S., Meite, F., Masbou, J. & Imfeld, G. Pesticide degradation and export losses at the catchment scale: Insights from compound-specific isotope analysis (CSIA). *Water Research* **139,** 198–207 (2018).

26. Elsner, M. Stable isotope fractionation to investigate natural transformation mechanisms of organic contaminants: principles, prospects and limitations. *Journal of environmental monitoring : JEM* **12,** 2005–31. ISSN: 1464-0333 (2010).

27. Baartman, J. E., Jetten, V. G., Ritsema, C. J. & de Vente, J. Exploring effects of rainfall intensity and duration on soil erosion at the catchment scale using openLISEM: Prado catchment, SE Spain. *Hydrological Processes* **26,** 1034–1049. ISSN: 08856087 (2012).

28. Rivard, L. *Environmental Fate of Metolachlor* tech. rep. (Environmental Monitoring Branch, Sacramento, California, 2003). `http://www.cdpr.ca.gov/docs/emon/pubs/fatememo/metolachlor.pdf`.

29. PPDB. *The Pesticide Properties Database* Developed by the Agriculture & Environment Research Unit (AERU), University of Hertfordshire, funded by UK national sources and the EU-funded FOOTPRINT project (FP6-SSP-022704). 2009.

30. Beven, K. & Binley, A. The future of distributed models: model calibration and uncertainty prediction. *Hydrological Processes* **6,** 279–298. ISSN: 1099-1085 (1992).

31. Beven, K. & Binley, A. GLUE: 20 years on. *Hydrological Processes* **28,** 5897–5918. ISSN: 10991085 (2014).

32. Lefrancq, M., Payraudeau, S., Guyot, B., Millet, M. & Imfeld, G. Correction to Degradation and Transport of the Chiral Herbicide S-Metolachlor at the Catchment Scale: Combining Observation Scales and Analytical Approaches. *Environmental Science & Technology* **52,** 5517. ISSN: 0013-936X (May 2018).

33. Gericke, O. J. & Smithers, J. C. Review of methods used to estimate catchment response time for the purpose of peak discharge estimation. *Hydrological Sciences Journal* **59,** 1935–1971. ISSN: 0262-6667 (2014).

34. Elsayed, O. F. *et al.* Using compound-specific isotope analysis to assess the degradation of chloroacetanilide herbicides in lab-scale wetlands. *Chemosphere* **99,** 89–95. ISSN: 00456535 (2014).

35. Ivdra, N., Herrero-Martín, S. & Fischer, A. Validation of user- and environmentally friendly extraction and clean-up methods for compound-specific stable carbon isotope analysis of organochlorine pesticides and their metabolites in soils. *Journal of Chromatography A* **1355,** 36–45. ISSN: 0021-9673 (Aug. 2014).

36. Anastassiades, M., Lehotay, S. J., Štajnbaher, D. & Schenck, F. J. Fast and easy multiresidue method employing acetonitrile extraction/partitioning and "dispersive solid-phase extraction" for the determination of pesticide residues in produce. *Journal of AOAC International* **86,** 412–431. ISSN: 10603271 (2003).

37. Sheikh, V., Visser, S. & Stroosnijder, L. A simple model to predict soil moisture: Bridging Event and Continuous Hydrological (BEACH) modelling. *Environmental Modelling and Software* **24,** 542–556. ISSN: 13648152 (2009).

38. McGrath, G. S., Hinz, C. & Sivapalan, M. Modeling the effect of rainfall intermittency on the variability of solute persistence at the soil surface. *Water Resources Research* **44,** 1–10 (2008).

39. Manfreda, S., Fiorentino, M. & Iacobellis, V. DREAM: a distributed model for runoff, evapotranspiration, and antecedent soil moisture simulation. *Advances in Geosciences* **2,** 31–39. ISSN: 1680-7359 (2005).

40. Thullner, M., Kampara, M., Richnow, H. H., Harms, H. & Wick, L. Y. Impact of bioavailability restrictions on microbially induced stable isotope fractionation. 1. Theoretical calculation. *Environmental Science and Technology* **42,** 6544–6551. ISSN: 0013936X (2008).

41. Schwarzenbach, R. P., Gschwend, P. M. & Imboden, D. M. *Environmental Organic Chemistry* 2nd (Wiley, New York, 2003).

42. Thullner, M., Fischer, A., Richnow, H.-H. & Wick, L. Y. Influence of mass transfer on stable isotope fractionation. *Applied Microbiology and Biotechnology* **97,** 441–452. ISSN: 0175-7598 (2013).

43. Rodríguez Cruz, M. S., Jones, J. E. & Bending, G. D. Study of the spatial variation of the biodegradation rate of the herbicide bentazone with soil depth using contrasting incubation methods. *Chemosphere* **73,** 1211–1215. ISSN: 00456535 (2008).

44. Arias-Estévez, M. *et al.* The mobility and degradation of pesticides in soils and the pollution of groundwater resources. *Agriculture, Ecosystems and Environment* **123,** 247–260. ISSN: 01678809 (2008).

45. Wu, X., Li, M., Long, Y. & Liu, R. Effects of adsorption on degradation and bioavailability of metolachlor in soil. *Soil Science and Plant Nutrition* **11,** 83–97. ISSN: 07189516 (2011).

46. Long, Y. H., Li, R. Y. & Wu, X. M. Degradation of S -metolachlor in soil as affected by environmental factors. *Journal of Soil Science and Plant Nutrition* **14,** 189–198 (2014).

47. Boesten, J. J. T. I. & van der Linden, A. M. A. Modeling the Influence of Sorption and Transformation on Pesticide Leaching and Persistence. *Journal of Environment Quality* **20,** 425. ISSN: 0047-2425 (1991).

48. Larsbo, M. & Jarvis, N. MACRO 5.0 A Model of water flow and solute transport in macroporous soil. *MACRO Technical description.* 1–43 (2003).

49. Jaikaew, P., Malhat, F., Boulange, J. & Watanabe, H. Aspect of the degradation and adsorption kinetics of atrazine and metolachlor in andisol soil. *Hellenic Plant Protection Journal* **10,** 1–14. ISSN: 17913691 (2017).

50. Walker, A. A Simulation Model for Prediction of Herbicide Persistence1. English. *Journal of Environmental Quality* **3.** doi:10.2134/jeq1974.00472425000300040021x. http://dx.doi.org/10.2134/jeq1974.00472425000300040021x (1974).

51. De Roo, A. P. J., Wesseling, C. G. & Ritsema, C. J. LISEM: A single-event physically based hydrological and soil erosion model for drainage basins. I: Theory, Input and Output. *Hydrological Processes* **10,** 1107–1117. ISSN: 0885-6087 (Nov. 1996).

52. Lefrancq, M. *Transport and attenuation of pesticides in runoff from agricultural headwater catchments: from field characterisation to modelling* PhD thesis (Université de Strasbourg, 2014).

53. Kutílek, M. & Nielsen, D. R. *Soil Hydrology* (Catena Verlag, Cremlingen-Destedt, Germany, 1994).

54. Kamphorst, E. C. *et al.* Predicting Depressional Storage from Soil Surface Roughness 1 Trade names are included for the benefit of the reader and do not imply endorsement of the INRA or the UU. English. *Soil Science Society of America Journal* **64,** 1749–1758 (2000).

55. Sanchez-Moreno, J. F., Mannaerts, C. M., Jetten, V. & Löffler-Mang, M. Rainfall kinetic energy–intensity and rainfall momentum–intensity relationships for Cape Verde. *Journal of Hydrology* **454-455,** 131–140. ISSN: 0022-1694 (2012).

56. Morgan, R. P. C. *et al. The EUROSEM Model BT - Modelling Soil Erosion by Water* in (eds Boardman, J. & Favis-Mortlock, D.) (Springer Berlin Heidelberg, Berlin, Heidelberg, 1998), 389–398. ISBN: 978-3-642-58913-3.

57. Chow, V., Maidment, D. & Mays, L. *Applied Hydrology* 2nd (McGraw-Hill Companies, Inc., 2013).

58. Wallender, W., Joyce, B. & Ginn, T. Modeling the Transport of Spray-Applied Pesticides from Fields with Vegetative Cover. *Transactions of the Asabe* **51,** 1963–1976 (2008).

59. Van Genuchten, M. T. *A Closed-form Equation for Predicting the Hydraulic Conductivity of Unsaturated Soils* 1980. doi:10.2136/sssaj1980.03615995004400050002x.

60. Fredlund, D. G., Sheng, D. & Zhao, J. Estimation of soil suction from the soil-water characteristic curve. *Canadian Geotechnical Journal* **48,** 186–198. ISSN: 0008-3674 (2011).

61. Herman, J. & Usher, W. SALib: An open-source Python library for Sensitivity Analysis. *The Journal of Open Source Software* **2,** 9–10. ISSN: 2475-9066 (2017).

62. Morris, M. D. Factorial plans for preliminary computational experiments. *Technometrics* **33,** 161–174 (1991).

63. Lee, A. *Particle swarm optimization (PSO) with constraint support* 2014. https://pythonhosted.org/pyswarm/index.html%7B%5C#%7D.

64. Gupta, H. V., Kling, H., Yilmaz, K. K. & Martinez, G. F. Decomposition of the mean squared error and NSE performance criteria: Implications for improving hydrological modelling. *Journal of Hydrology* **377,** 80–91. ISSN: 00221694 (2009).

65. Li, L., Xu, C. Y., Xia, J., Engeland, K. & Reggiani, P. Uncertainty estimates by Bayesian method with likelihood of AR (1) plus Normal model and AR (1) plus Multi-Normal model in different time-scales hydrological models. *Journal of Hydrology* **406,** 54–65. ISSN: 00221694 (2011).

66. Jin, X., Xu, C. Y., Zhang, Q. & Singh, V. P. Parameter and modeling uncertainty simulated by GLUE and a formal Bayesian method for a conceptual hydrological model. *Journal of Hydrology* **383,** 147–155. ISSN: 00221694 (2010).

67. Li, L., Xia, J., Xu, C.-y., Chu, J. & Wang, R. Analyse the sources of equifinality in hydrological model using GLUE methodology. *Symposium JS.4 at the Joint Convention of the International Association of Hydrological Sciences (IAHS) and the International Association of Hydrogeologists (IAH),* 130–138. ISSN: 01447815 (2009).

68. Nolan, B. T. *et al.* Identification of key climatic factors regulating the transport of pesticides in leaching and to tile drains. *Pest Management Science* **64,** 933–944. ISSN: 1526-4998 (2008).

69. Meite, F. *et al.* Impact of rainfall patterns and frequency on the export of pesticides and heavy-metals from agricultural soils. *Science of the Total Environment* **616-617,** 500–509. ISSN: 18791026 (2018).

70. Borah, D. K. & Bera, M. WATERSHED-SCALE HYDROLOGIC AND NONPOINT-SOURCE POLLUTION MODELS: REVIEW OF APPLICATIONS. *Transactions of the ASAE* **47,** 789–804 (2004).

71. Tournebize, J., Chaumont, C. & Mander, Ü. Implications for constructed wetlands to mitigate nitrate and pesticide pollution in agricultural drained watersheds. *Ecological Engineering* **103,** 415–425. ISSN: 09258574 (2017).

72. Lindahl, A. M. L. *et al.* Stochastic modeling of diffuse pesticide losses from a small agricultural catchment. *Journal of environmental quality* **34,** 1174–85. ISSN: 0047-2425 (2005).

73. Charnay, M. P., Tuis, S., Coquet, Y. & Barriuso, E. Spatial variability in14C-herbicide degradation in surface and subsurface soils. *Pest Management Science* **61,** 845–855. ISSN: 1526498X (2005).

74. Rodríguez-Cruz, M. S., Jones, J. E. & Bending, G. D. Field-scale study of the variability in pesticide biodegradation with soil depth and its relationship with soil characteristics. *Soil Biology and Biochemistry* **38,** 2910–2918. ISSN: 00380717 (2006).

75. Tiktak, A., Hendriks, R. F. A., Boesten, J. J. T. I. & van der Linden, A. M. A. A spatially distributed model of pesticide movement in Dutch macroporous soils. *Journal of Hydrology* **470-471,** 316–327. ISSN: 00221694 (2012).

76. Leistra, M., van der Linden, A. M. A., Boesten, J. J. T. I., Tiktak, A. & van den Berg, F. *PEARL model for pesticide behaviour and emissions in soil-plant systems; Description of the processes in FOCUS PEARL v 1.1.1.* tech. rep. (2001).

77. Ren, X. *et al.* Sorption, transport and biodegradation – An insight into bioavailability of persistent organic pollutants in soil. *Science of the Total Environment* **610-611,** 1154–1163. ISSN: 18791026 (2018).

78. Schmidt, S. I., Kreft, J. U., Mackay, R., Picioreanu, C. & Thullner, M. Elucidating the impact of micro-scale heterogeneous bacterial distribution on biodegradation. *Advances in Water Resources* **116,** 67–76. ISSN: 03091708 (2018).

Chapter 6

General discussion

The overarching goal of this work was to investigate pesticide degradation and transport at different temporal and spatial scales, with the specific objective of improving representation and prediction of pesticide persistence and reactive transport at the catchment scale. Figure 61 provides a visual summary of the work conducted during this Ph.D. thesis based on two principal investigation axes: characterization and modelling. Each axis moves from small laboratory-based work towards larger catchment scales. Increasing scales correlate with increasing complexity and heterogeneity level, represented on a third, vertical axis.

Moving away from the origin of Fig. 61, laboratory experiments where conducted to investigate the impact of intrinsic and extrinsic factors on pesticide export (characterization axis). This was supported by a parsimonious model, helpful to validate the soil column experimental setup and the leaching formalism that can be adopted at the catchment scale (modelling axis). A second small-scale pesticide soil degradation experiment (characterization axis) provided supporting information to make interpretation of degradation extent at the more complex catchment scale possible. The data set obtained from this laboratory characterization study was then employed to develop the catchment models. The combination of both scales and investigation methods (i.e., experimental and numerical) finally allowed to demonstrate not only the value of pesticide CSIA as a monitoring technique at catchment scale, but also its ability to reduce uncertainty of degradation parameter range controlling pesticide pools available before the onset of major hydrological events. Altogether, this Ph.D. work has therefore contributed to advance current understanding of the potential value of and limitations from the application of pesticide CSIA as both a monitoring technique for headwater catchments and data constrain for predictive modelling.

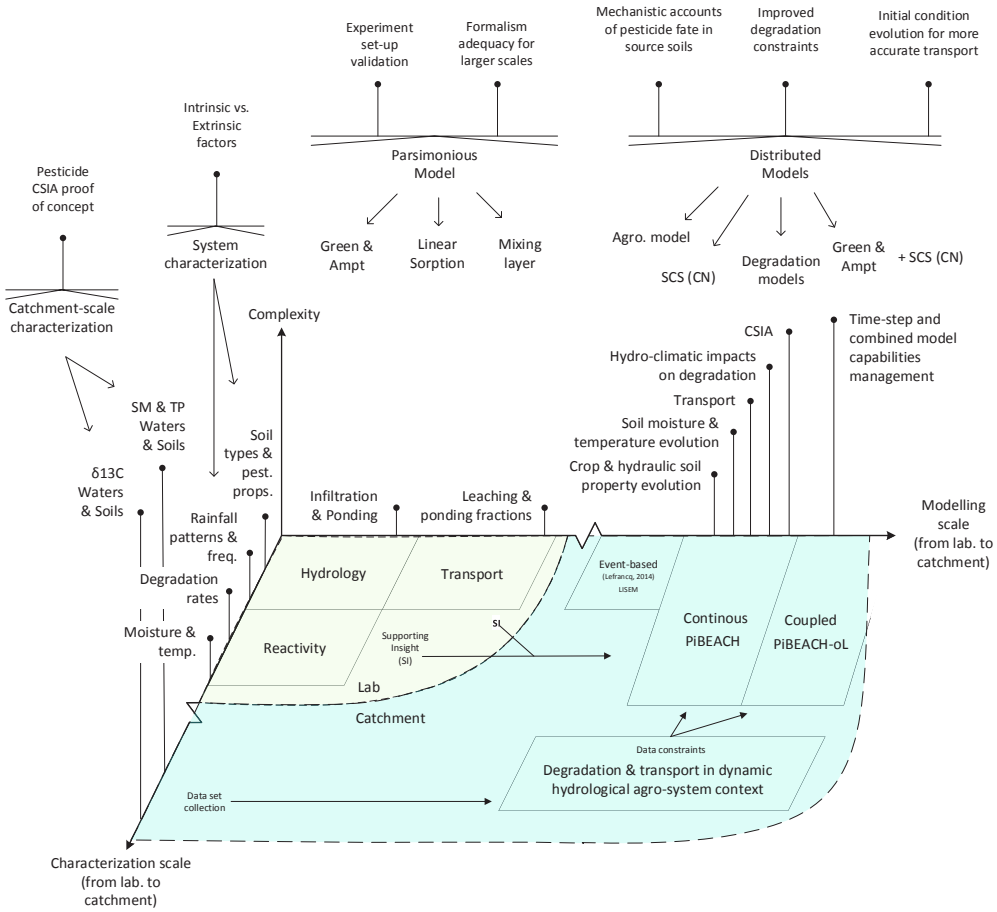

Figure 61: Approaches (characterization and modelling) employed and physical scales (lab and catchment) investigated during this Ph.D. work.

6.1 Characterizing pesticide fate under unsteady hydrological conditions

Determination of the relative contribution of pesticide export, degradation and persistence to total pesticide dissipation under field conditions remains a significant challenge for water resource management as *in situ* evidence of the extent of each of these processes is difficult to obtain under dynamic environmental and hydrological conditions. Typically, characterization approaches (i.e., methods used to describe likely processes controlling pesticide fate) involve the use of pesticide physico-chemical properties and persistence constants obtained from defined laboratory conditions under closed-systems. Extrapolation of this information to field conditions, thus requires adjustments that indirectly account for potential measurement errors [1, 2] and the relative importance that extrinsic factors, such as temperature and hydrological regime fluctuations, can have on each dissipation process. Quantification of parallel processes contributing to pesticide dissipation at a specific site (or even under well-defined systems [3]) will then typically require numerical modelling followed by parameter calibration or inverse techniques, which may nevertheless be subject to significant uncertainty [4, 5]. However, without the use of complementary techniques providing a multiple lines of evidence approach (e.g., [6]), current uncertainties associated with pesticide fate determination in hydrological systems will likely continue to challenge efforts to achieve the sustainable management of our water resources [7].

To improve on this limitation, **chapter 2** demonstrated the applicability of high resolution carbon-based CSIA to evidence degradation extent as a primary dissipation process in top soils, thereby improving descriptions of pesticide transfer within a realistic environmental monitoring context. While CSIA has been successfully implemented to evidence degradation in subsurface environments for legacy contaminants [8, 9] and nitrate source apportionment in surface waters [10, 11], its application to evidence pesticide degradation has been limited. Application of pesticide CSIA information to describe degradation in unsteady hydrological systems was first implemented by Lutz *et al.* [12], making use of plot runoff and catchment outlet water signatures to constrain a model based on travel time distributions. Despite limited CISA observations (i.e., due to observed low environmental sample concentrations), the study found that models considering constant degradation half-lives could lead to catchment-wide overestimations of degradation extent, and thus overly optimistic expectations of environmental protection. Missing information from different catchment areas however, limited the ability of this first study to corroborate whether observed outlet signatures could be used to determine catchment-wide degradation extent.

Validation of this hypothesis, and demonstrating the value of pesticide CSIA as a monitoring approach, was conducted in chapter 2 by comparing CSIA soil and outlet data with information derived from mass balance accounts and typically reported reference half-life ranges for SM. First, bulk soil and outlet $\delta^{13}C$ showed comparable trends across time, indicating that outlet signatures can be used as a proxy for catchment-wide degradation extent assessments [13], thereby reducing the need for more extensive sampling efforts. Reduction of sampling effort may be of value, for example, where monitoring resources are limited and where complementary lines to evidence degradation are sought to support pesticide persistence assessments. Second, estimation of degradation extent in top soils, based on a typical field half-life for SM, was found to over-estimate degradation (relative to CSIA-based interpretation) early in the season. This indicated that degradation extent errors from fixed degradation half-lives may be associated to depth-dependencies [12] as well as to variations in degradation rates across space and time. Third, the use of CSIA measurements in top soils allowed to not only reduce degradation uncertainty margins relative to literature-reported half-life ranges but also to derive estimations of top soil losses from remaining mass concentrations. This is of particular relevance for field studies involving numerical approaches, as it provides an opportunity to directly constrain not only parameters controlling pesticide persistence, but also parameters controlling export through leaching and runoff processes [14–16].

Some limitations for the use of pesticide CSIA at catchment scale however, are worth noting. Although outlet CSIA may be used as a proxy to monitor catchment-wide pesticide degradation, the variability of outlet signatures, and the fact that signal detection is more likely shortly after fresh applications (i.e., due to higher concentrations), may lead to underestimations of degradation extent. This tendency may be especially pronounced under lower hydrological sampling resolutions and/or where tardive applications are made in areas with high hydrological connectivity. Therefore, tracking catchment wide degradation *via* outlet monitoring may, to a certain extent, be restricted to headwater scales, where: (i) variability in degradation conditions across space, as regulated by soil characteristics, temperature fluctuations and local hydrological conditions, is low, and (ii) likely critical source areas (i.e., with high hydrological connectivity) can be identified. In most cases, estimations of degradation extent are expected to be conservative as an overestimation of pesticide degradation at the catchment scale is unlikely. This has important implications for applications of pesticide CSIA at river and larger catchment scales and is discussed further in the following chapter.

A second limitation of the current monitoring capabilities of pesticide CSIA under unsteady hydrological conditions is the focus on single element isotopes, as it was done for carbon during this work. Indeed, additional insights on mechanisms of bond cleavage, can be obtained by secondary elements such as nitrogen, hydrogen or chlorine [17]. Such insights may be used to identify main degradation pathways, which may have implications on the appropriate choice of enrichment values during field interpretation if different mechanisms are involved during contaminant transformation [18] and/or if bioavailability limitations are expected to reduce apparent enrichments [19].

However, the opportunity to obtain a multi-element data set was challenged by quantification limits from environmental samples. In fact, although analytical development for nitrogen isotopes was conducted [20] and environmental signatures targeted during the field characterization campaign, only 7 water samples at environmental concentrations $\geq 7\ \mu$ g L^{-1} with sample volumes of 0.8 - 2.5 L could be obtained. In terms of the chosen volumes for extraction, the objective during this work was to seek information relevant to the sub-event scale, so as to characterize the catchment's dominant pesticide transport routes. This required a continuous water sampling strategy involving aliquot breakdown according to hydrograph characteristics (base-flow, rising and/or falling limb). This strategy thus limited collection of sufficiently large water volumes during each forcing event to derive a high-resolution data set also including a secondary element (Fig. 62). While sensitivity at low concentrations was the primary limitation in waters, matrix effects precluded clear signal determination of nitrogen signatures in all soil samples, even in soils with highest concentrations ($\approx 8\ \mu$g g^{-1} soil dry wt. for sampled masses of 5 g of soil). This illustrates the need for improved extraction methods in complicated matrices like soils. In contrast to pure or laboratory enriched microbial cultures, such improvements may then be useful to understand the influence of environmental factors on degradation pathways and respective enrichments.

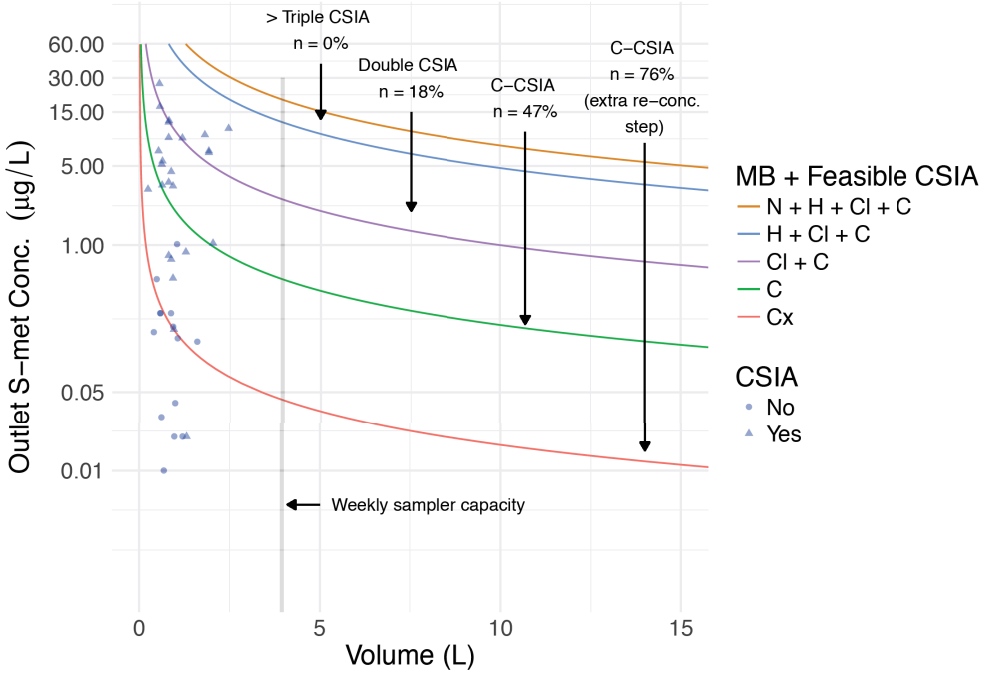

Figure 62: Sampled volumes with refrigerated automatic sampler unit. Isolines depict volumes and environemntal concentration requirements for combined mass balance (MB) and multi-/single-element CSIA.

The field of isotope fractionation investigations is however, continuously expanding and improvements in strategies for enrichment and clean-up from matrix-interfaces or instrument sensitivity can be expected from future achievements [21]. Such improvements allowing for multi-element CSIA, should lead to identification of dominant degradation pathways and better understanding of transformation bottlenecks. This is of relevance as, in some cases, bacterial strains with identical enzymatic reactions, may exhibit different rate-limiting steps during contaminant transformation. This may then lead to differences in isotope fractionation extents and potential estimation errors of degradation extent despite identical enzymatic reactions [22]. In this respect, combined understanding of both dominant pathways and strain-specific rate-limiting steps, may facilitate information transfer from laboratory to field conditions, thereby reducing uncertainty for interpretation of field CSIA data.

Better understanding of degradation processes may also assist during environmental monitoring design of chiral molecules, although effective enantiomer separation could not be achieved in this work for metolachlor. At least 25% of current pesticides worldwide are chiral molecules [23], whose degradation in soils may be enantioselective [24, 25], resulting in changes in enantiomer concentrations displaying different levels of toxicity [26]. The combination of CSIA and enantioselective analysis techniques, i.e., enantioselective stable isotope analysis (ESIA), may also provide evidence of pesticide transformations [27]. For example, in cases where only one enantiomer may be associated to isotope fractionation, enrichment may be masked if enantiomer isotopologues are not evaluated independently [28]. On the other hand, targeting enantiomer fractionation instead of or in addition to isotope fractionation may prove advantageous. For example, active transport through cell membranes during degradation of phenolic acid herbicides (i.e., the rate-limiting step in this case) has been observed to lead to significant enantiomer fractionation while masking instead isotope fractionation [29]. Understanding of rate limiting steps in this context is thus of importance to derive accurate interpretations of degradation extent under field contexts. Finally, understanding of dominant degradation pathways and its associated fractionation extent, whether enantiomeric or isotopic, may not only facilitate interpretation of observed field dissipation, but also help develop and validate quantitative structure activity relationship (QSAR) models useful for the prediction of previously unstudied compounds [30].

6.2 Lab-scale experiments to support pesticide CSIA characterization & modelling

Lab-scale experiments conducted during this Ph.D. work provided supporting information that enabled both field interpretation (chapter 2) and conceptual development of the catchment scale model (chapter 4). On the one hand, data from soil microcosm degradation experiments at various temperature and moisture conditions over a period of 200 days, allowed derivation of characteristic enrichments by relating carbon fractionation extent to concentration decrease *via* the Rayleigh equation. In contrast, analogous experiments conducted under abiotic conditions over the same period showed no significant isotope fractionation, indicating that observed SM dissipation was primarily driven by biodegradation. The derivation of enrichment factors therefore allowed to obtain first estimations of field SM degradation extents based on observed carbon isotope signatures and independently of transformation products.

Indeed, low pesticide concentrations typically observed under field conditions may challenge interpretations based on ϵ values derived under laboratory conditions under high concentrations, as bioavailability transfer limitations may lead to changes in observed ϵ values [19].

In addition, at low-concentrations pollutants in general, may degrade co-metabolically [31], involving different enzymes, and therefore reflecting distinct ϵ values. However, when multiple bacterial strains are involved in degradation, similar effects can be expected even at high concentrations for the same enzymatic reaction [22]. As one of the primary objectives of these microcosm experiments was the transferability to field conditions, spiked concentrations (2.5 μg SM g^{-1} soil dr. wt.) were designed to be comparable with those typically observed in the field ($\approx$ 5 μg SM g^{-1} soil dr. wt.) shortly after application. Although this does not exclude bioavailability restrictions or co-metabolic processes (e.g., towards the end of the observation period), the equivalent concentration ranges in both field and laboratory experiments, as a rule of thumb, were expected to lead to similar enrichment values. As noted previously, soil matrix effects precluded determination of isotope fractionation of a secondary element (nitrogen in this case), limiting our ability to confirm that the primary degradation pathway in soil microcosms was also responsible for degradation in field top-soils. Microcosm experiments where however, prepared from the same catchment tops soils. Assuming that the experimental set-up allowing for aerated conditions was sufficient to replicate field-conditions, it is then likely that similar bacterial communities where responsible for the observed enrichment. This latter aspect could be evaluated in future studies using laboratory-derived variables for interpretation of field data. Nevertheless, it remains plausible that, for example, due to fluctuations in temperatures, changes in organic carbon, and/or better oxygen diffusion in field top-soils through rainfall and microbial community evolution may have differed. Therefore, to further corroborate the validity of enrichment values from microcosm experiments, additional information such as that which could be obtained from microbial gene sequencing, may serve as supplementary line of evidence for such studies in the future [32, 33].

To assist conceptual development of the catchment scale model presented in chapter 4, **chapter 3** investigated the impact of extrinsic (i.e., rainfall frequency and intensity) and intrinsic (i.e., soil characteristics, pesticide properties) factors in controlling pesticide export during rainfall events. It was observed that pesticide mass transfer to ponding water during the experiment was low, representing, for example, 0.2 $\pm$ 0.1% of the initial mass for SM, while leaching dominated export across all modalities. The model generally fitted well observations of pollutant leaching, although, for some experiments, it was necessary to use lower K_{oc} values than those found in the literature, suggesting insufficient contact time (3 h) to reach sorption equilibrium [34]. Altogether, these results indicated on the one hand, that simulation of leaching by linear sorption, and considering only chromatographic flow could be sufficient to approximate pesticide losses from top soils in the continuous catchment scale model. On the other hand, the low K_d values found during the leaching experiment (e.g., SM: 63-200 L kg^{-1}) however, did not permit constraining likely upper bounds for K_{oc}, thereby encouraging exploration of a wide range of values through Monte Carlo sampling when implementing the catchment scale model.

Single flow domain (chromatographic flow) models have been previously regarded as a limitation when considered as a sole transport mechanism during field studies [35]. Indeed, although top soil observations were well represented by the continuous model, simulated concentrations and isotope signatures at the outlet were generally poorly fitted. Furthermore, although relative improvements were made by coupling PiBEACH with LISEM, the most evident weaknesses of the coupled model was still its ability to represent slow flow and mass export by drainage. Failure to observe such limitations during the soil column experiment were likely associated to the dimensions considered (i.e., 21 cm^3 of top soil), which could not accurately account for field scale heterogeneity [36, 37]. Therefore, potential improvements to the conceptual catchment model may be envisioned and are further discussed

in Chapter 7.

Despite the limitations of the soil column experiment, the need to calibrate K_{sat} values during the second rainfall demonstrated the importance of rainfall impacts on changes in top soil hydraulic properties (K_{sat}, ρ_b, θ). While the initial sieved soil mimicked soil characteristics at the beginning of a crop season just after tillage (topsoil with low bulk density and high K_{sat}), soil compaction and sealing (especially for loamy soils) following the first rainfall was similar to that which may eventually be observed in the field after an accumulated rainfall depth of 80 - 100 mm [38]. The change in hydraulic properties may be likely due to soil aggregate breakdown and clogging of larger pores [38, 39], but also to soil compaction by slaking and wetting [40]. Temporal change of these properties may be important factors to account for during modelling at catchment scale. These observations therefore motivated consideration of changes in characteristics CN numbers [41] within the PiBEACH continuous catchment model, from soils with general good permeability (type A) shortly after tillage, to poorly drained soils (type C) based on observed cumulative rainfall depths >80 mm. Although infiltration-runoff representation through the CN number would be replaced by the Green & Ampt method during coupling [42], considering of a dynamic CN significantly improved outlet discharge for the continuous model.

Finally, a key finding from the soil column experiments was the importance of extrinsic factors (i.e., rainfall frequency and intensity) controlling pesticide export. Rainfall patterns showed not only that the first rainfall is important, as generally observed in the field [43, 44], but also that long-lasting rainfalls, even if not of highest intensity, largely control pesticide leaching. In contrast, relative differences in pesticide export between vineyard and crop soils for synthetic pesticides were small, highlighting that soil composition and aging had only a secondary influence on pollutant export from soils compared to extrinsic factors. These observations contributed to the selection of candidate events to be coupled with LISEM. Although LISEM is specialized in reproducing runoff and erosion processes associated to intense rainfalls, the decision to couple also events with long-lasting rainfalls led to improvements in representation of leaching extent, which were otherwise under-estimated by the uncoupled model. Altogether, and despite its noted limitations, the lab-scale soil columns demonstrated an added value towards the design of larger scale conceptual approaches by evidencing changes in soil hydraulic properties and by highlighting the impact of rainfall volumes and frequencies on pesticide leaching.

6.3 Modelling pesticide fate at catchment scale using CSIA data

A review of current numerical models [45–49] indicated the need for explicit account of the evolution of distributed state variables (e.g., soil physical properties, moisture conditions and pesticide pools) to improve pesticide fate predictions at catchment scale. Defining parameter values that control the evolution of such state variables however, is subject to uncertainty. In the case of pesticide pools available across space and time, for example, observed hydro-climatic variability may imply a departure from idealized laboratory conditions under which reference parameter values, such as degradation and mobility constants, are obtained. Accounting for uncertainty in numerical representations of pesticide fate can capture potential sources of variability affecting the reliability of pesticide degradation and transfer predictions. Therefore, efforts to minimize it is of importance.

Predicting pesticide dissipation in distributed models at catchment scale however, remains

challenged, as degradation kinetics are usually artificially considered to be fixed across space and time. This challenge is further compounded by the scarcity of field data that is able to distinguish between degradative from non-degradative dissipation, limiting validation of more complex numerical formalisms. By making use of concentration and CSIA data for catchment top soils presented in chapter 2, **chapter 4** introduced the development of PiBEACH, a continuous distributed catchment scale model capable of accounting for hydro-climatic controls (i.e., soil water content and temperature) on pesticide degradation. By making use of top soil carbon CSIA data, improvements in the constraint of hydro-climatic conditions regulating degradation rates was possible. This led to a reduction of uncertainty (i.e., reduction of confidence intervals) not only in terms of reference DT_{50} values, which indicated dominance of aerobic degradation conditions, but also in terms of dilution processes such as topsoil leaching.

The value of CSIA as a complementary line of evidence is not only useful as a model validation and uncertainty reduction tool, but is also valuable for its ability to account for environmental *in situ* conditions. This should be of particular interest, as the ability to integrate *in situ* conditions into model predictions may facilitate evaluation of plausible fast and/or profound environmental disturbances associated to, for example, climate change scenarios (e.g., droughts and rainfall patterns) or changes in natural ecosystem services (e.g., altered soil microbial diversity) [50]. Within the context of this Ph.D. work, additional information regarding the validity of ϵ values derived from laboratory microcosm experiments could be obtained from field CSIA. Namely, although microcosm degradation allowed to make field degradation extent inferences during field characterization (chapter 2), ϵ values derived from such experiments (-1.4 to -1.8 ‰) were obtained under a specific set of environmental conditions. In contrast, evaluation of isotope fractionation through PiBEACH, indicated larger absolute ϵ values (-1.7 to -3.5) pointing to potential degradation over-estimations from field characterization assessment (chapter 2) based on data from microcosm experiments. In addition, the mean reference half-life obtained from PiBEACH results was almost half (16 - 20 d) of those observed in the microcosm experiments (28 - 41 d), the latter suggesting a range of aerobic-anaerobic to anaerobic conditions [51] and indicating potential aeration limitations during microcosm tests. *In situ* degradation modelled in field top soils on the other hand, was likely not affected by poor aeration due to enhanced oxygen input into the soil matrix from dissolved oxygen in rain-water. A second indication of the limitation of the microcosm experiment to characterize aerobic degradation rates was further observed during PiBEACH calibration. Indeed, when treating both top-soil and outlet isotope data simultaneously, mean reference half-lives increased to values comparable to those observed during the microcosm experiments ($\approx$ 30 d, simulations not shown), indicating a compensating effect between two distinct reactivity areas. These observations suggests, on the one hand, an important limitation in the continuous model to account for different reactivity zones simultaneously, as observed by Lutz *et al.* [12]. On the other hand, they also suggest an opportunity to improve field characterization interpretations by modelling microcosm experiments to better characterize and validate experimental set-up. For example, simulation of microcosm experiments accounting for oxygen diffusivity across the soil profile, could be used to more clearly delineate conditions under which derived enrichment factors remain valid. Potential design for such modelling and experimental set-up as well as inclusion of additional microcosm modalities to improve field interpretation are presented in the following chapter.

The improvement of degradation constraints controlling available pesticide pools in continuous catchment scale models is also a preliminary step in the development of more accurate event-based models. From a societal view point, the development of predictive event-based

tools, may aid farmer advisors and state agencies in the design of good agricultural management practices [52]. Through identification of field hot-spots, for example, such tools may facilitate the design of both preventive (e.g., reduced pesticides applications) [53] and curative (e.g., artificial buffer zones) strategies [54] to mitigate pesticide transfer from sources to vulnerable receptors. Within this context, tracking isotope signatures of available pools in top soils may then be of further use to improve representation of transport pathways contributing to stream pollution. As noted above however, limitations observed in the ability of the developed continuous model, PiBEACH, in chapter 4 to simulate outlet concentrations and isotope signatures, indicates a need to improve accounts of transport processes during hydrological forcing. To address this need, **chapter 5** coupled PiBEACH with an existing distributed open source model, the Limburg Soil Erosion model (LISEM) [55], capable of detailed representation of rapid pesticide export *via* runoff and erosion. Insights from the impact of rainfall patterns investigated in chapter 3, allowed to identify candidate rainfall events to include during evaluation of the coupled model, PiBEACH-oL. That is, although LISEM is specialized in reproducing runoff and erosion processes associated to intense rainfalls, soil column experiments showed that long-lasting rainfalls, even if not of highest intensity could be of primary importance for pesticide export through leaching. An appropriate trade-off however, needed to be found between improvement in transport representation and simulation run times, as each candidate event to be simulated by LISEM, required a reduction in model time-step size down to seconds (i.e., max 10 s) significantly increasing simulation run times.

Preliminary results of combining temporal scales (event and growing season) through the coupled model demonstrated the ability of PiBEACH-oL to improve the description of water pathways and their evolution throughout the growing season, progressing from drainage- to runoff-driven export within the studied catchment. Significant limitations of the coupled model are most notable during mid-season (i.e., after day 50), where discharge dominated by the tail-end components of catchment drainage is not able to reproduce isotope signatures that reflect fresh product applications. This limitation may be associated to the model's lack of account of rapid transport through macropores, which may be of particular importance in clayey soils [56]. Alternatively, degradation conditions below top soils currently do not account for possible reduction in degradation rates (e.g., [12, 57, 58]), which could be associated to a significant reduction in pesticide concentrations with depth and a shift in redox conditions, both of which could potentially contribute to a shift in dominant degradation pathways (e.g., co-metabolic, anaerobic). Furthermore, although run-off contribution to total outlet loadings is small, current LISEM development does not account for pesticide mobilization through run-off, which may be expected to not only contribute to outlet signatures but also to the re-distribution of pesticide mass across the catchment through runoff re-infiltration, thereby also affecting drainage response. Specific improvements to current model conceptualization are discussed further in Chapter 7.

References

1. Beven, K. & Binley, A. The future of distributed models: model calibration and uncertainty prediction. *Hydrological Processes* **6,** 279–298. ISSN: 1099-1085 (1992).
2. Beven, K. & Binley, A. GLUE: 20 years on. *Hydrological Processes* **28,** 5897–5918. ISSN: 10991085 (2014).
3. Honti, M. & Fenner, K. Deriving persistence indicators from regulatory water-sediment studies - Opportunities and limitations in OECD 308 data. *Environmental Science and Technology* **49,** 5879–5886. ISSN: 15205851 (2015).

4. Dubus, I. G., Beulke, S. & Brown, C. D. Calibration of pesticide leaching models: Critical review and guidance for reporting. *Pest Management Science* **58,** 745–758. ISSN: 1526498X (2002).
5. Beven, K. A manifesto for the equifinality thesis. *Journal of Hydrology* **320,** 18–36. ISSN: 00221694 (2006).
6. Fenner, K., Canonica, S., Wackett, L. P. & Elsner, M. Evaluating Pesticide Degradation in the Environment: Blind Spots and Emerging Opportunities. *Science* **341,** 752–758. ISSN: 0036-8075 (2013).
7. Storck, V., Karpouzas, D. G. & Martin-Laurent, F. Towards a better pesticide policy for the European Union. *Science of the Total Environment* **575,** 1027–1033. ISSN: 18791026 (2017).
8. Meckenstock, R. U., Morasch, B., Griebler, C. & Richnow, H. H. Stable isotope fractionation analysis as a tool to monitor biodegradation in contaminated acquifers. *Journal of Contaminant Hydrology* **75,** 215–255. ISSN: 01697722 (2004).
9. Hunkeler, D., Meckenstock, R. U., Lollar, B. S., Schmidt, T. C. & Wilson, J. T. A Guide for Assessing Biodegradation and Source Identification of Organic Ground Water Contaminants using Compound Specific Isotope Analysis (CSIA). *USEPA Publication* **EPA 600/R-,** 1–82. ISSN: ¡null¿ (2008).
10. Nestler, A. *et al.* Isotopes for improved management of nitrate pollution in aqueous resources: Review of surface water field studies. *Environmental Science and Pollution Research* **18,** 519–533. ISSN: 09441344 (2011).
11. Fenech, C., Rock, L., Nolan, K., Tobin, J. & Morrissey, A. The potential for a suite of isotope and chemical markers to differentiate sources of nitrate contamination: A review. *Water Research* **46,** 2023–2041. ISSN: 00431354 (2012).
12. Lutz, S. R. *et al.* Pesticide fate at catchment scale: conceptual modelling of stream CSIA data. *Hydrology and Earth System Sciences Discussions* **21,** 5243–5261. ISSN: 1812-2116 (2017).
13. Alvarez-Zaldívar, P., Payraudeau, S., Meite, F., Masbou, J. & Imfeld, G. Pesticide degradation and export losses at the catchment scale: Insights from compound-specific isotope analysis (CSIA). *Water Research* **139,** 198–207 (2018).
14. Nolan, B. T. *et al.* Identification of key climatic factors regulating the transport of pesticides in leaching and to tile drains. *Pest Management Science* **64,** 933–944. ISSN: 1526-4998 (2008).
15. Köhne, J. M., Köhne, S. & Simunek, J. A review of model applications for structured soils: b) Pesticide transport. *Journal of Contaminant Hydrology* **104,** 36–60. ISSN: 01697722 (2009).
16. Gassmann, M., Olsson, O., Stamm, C., Weiler, M. & Kümmerer, K. Physico-chemical characteristics affect the spatial distribution of pesticide and transformation product loss to an agricultural brook. *Science of The Total Environment* **532,** 733–743. ISSN: 00489697 (2015).
17. Wu, L. *et al.* Characterizing chemical transformation of organophosphorus compounds by 13 C and 2 H stable isotope analysis. *Science of The Total Environment* **615,** 20–28. ISSN: 00489697 (2018).
18. Elsner, M., Zwank, L., Hunkeler, D. & Schwarzenbach, R. P. A new concept linking observable stable isotope fractionation to transformation pathways of organic pollutants. *Environmental Science and Technology* **39,** 6896–6916. ISSN: 0013936X (2005).

19. Thullner, M., Kampara, M., Richnow, H. H., Harms, H. & Wick, L. Y. Impact of bioavailability restrictions on microbially induced stable isotope fractionation. 1. Theoretical calculation. *Environmental Science and Technology* **42,** 6544–6551. ISSN: 0013936X (2008).

20. Masbou, J., Drouin, G., Payraudeau, S. & Imfeld, G. Carbon and nitrogen stable isotope fractionation during abiotic hydrolysis of pesticides. *Chemosphere* **213,** 368–376. ISSN: 00456535 (2018).

21. Elsner, M. & Imfeld, G. Compound-specific isotope analysis (CSIA) of micropollutants in the environment - current developments and future challenges. *Current Opinion in Biotechnology* **41,** 60–72. ISSN: 18790429 (2016).

22. Ehrl, B. N., Gharasoo, M. & Elsner, M. Isotope Fractionation Pinpoints Membrane Permeability as a Barrier to Atrazine Biodegradation in Gram-negative Polaromonas sp. Nea-C. *Environmental Science and Technology* **52,** 4137–4144. ISSN: 15205851 (2018).

23. Liu, W., Gan, J., Schlenk, D. & Jury, W. A. Enantioselectivity in environmental safety of current chiral insecticides. *Proceedings of the National Academy of Sciences* **102,** 701–706. ISSN: 0027-8424 (2005).

24. Ramezani, M. K. *et al.* Faster degradation of herbicidally-active enantiomer of imidazolinones in soils. *Chemosphere* **79,** 1040–1045. ISSN: 00456535 (2010).

25. Buerge, I. J., Poiger, T., Müller, M. D. & Buser, H. R. Influence of pH on the stereoselective degradation of the fungicides epoxiconazole and cyproconazole in soils. *Environmental Science and Technology* **40,** 5443–5450. ISSN: 0013936X (2006).

26. Gao, B. *et al.* Stereoselective environmental behavior and biological effect of the chiral organophosphorus insecticide isofenphos-methyl. *Science of the Total Environment* **648,** 703–710. ISSN: 18791026 (2019).

27. Badea, S.-L. & Danet, A.-F. Enantioselective stable isotope analysis (ESIA) - A new concept to evaluate the environmental fate of chiral organic contaminants. *The Science of the total environment* **514,** 459–466. ISSN: 1879-1026 (2015).

28. Masbou, J., Meite, F., Guyot, B. & Imfeld, G. Enantiomer-specific stable carbon isotope analysis (ESIA) to evaluate degradation of the chiral fungicide Metalaxyl in soils. *Journal of Hazardous Materials* **353,** 99–107. ISSN: 18733336 (2018).

29. Qiu, S. *et al.* Small13C/12C fractionation contrasts with large enantiomer fractionation in aerobic biodegradation of phenoxy acids. *Environmental Science and Technology* **48,** 5501–5511. ISSN: 15205851 (2014).

30. Jammer, S., Rizkov, D., Gelman, F. & Lev, O. Quantitative structure-activity relationship correlation between molecular structure and the Rayleigh enantiomeric enrichment factor. *Environmental Sciences: Processes and Impacts* **17,** 1370–1376. ISSN: 20507895 (2015).

31. Nzila, A. Update on the cometabolism of organic pollutants by bacteria. *Environmental Pollution* **178,** 474–482. ISSN: 02697491 (2013).

32. Elsayed, O. F., Maillard, E., Vuilleumier, S., Millet, M. & Imfeld, G. Degradation of chloroacetanilide herbicides and bacterial community composition in lab-scale wetlands. *Science of the Total Environment* **520,** 222–231. ISSN: 18791026 (2015).

33. Subirats, J. *et al.* Emerging contaminants and nutrients synergistically affect the spread of class 1 integron-integrase (intI1) and sul1 genes within stable streambed bacterial communities. *Water Research* **138,** 77–85. ISSN: 18792448 (2018).

34. Gulkowska, A., Buerge, I. J., Poiger, T. & Kasteel, R. Time-dependent sorption of two novel fungicides in soils within a regulatory framework. *Pest Management Science* **72,** 2218–2230. ISSN: 15264998 (2016).
35. FOCUS. *FOCUS groundwater scenarios in the EU review of active substances.* tech. rep. 321 (FOCUS Groundwater Scenarios Workgroup, EC, 2000), 1–202.
36. Beven, K. & Germann, P. *Macropores and Water Flow in Soils* 1982.
37. Beven, K. & Germann, P. Macropores and water flow in soils revisited. *Water Resources Research* **49,** 3071–3092. ISSN: 00431397 (2013).
38. Armand, R., Bockstaller, C., Auzet, A. & Van Dijk, P. Runoff generation related to intra-field soil surface characteristics variability. Application to conservation tillage context. *Soil and Tillage Research* **102,** 27–37. ISSN: 0167-1987 (2009).
39. Chahinian, N., Voltz, M., Moussa, R. & Trotoux, G. Assessing the impact of the hydraulic properties of a crusted soil on overland flow modelling at the field scale. *Hydrological Processes* **20,** 1701–1722. ISSN: 0885-6087 (2006).
40. Vaezi, A. R., Ahmadi, M. & Cerdà, A. Contribution of raindrop impact to the change of soil physical properties and water erosion under semi-arid rainfalls. *Science of The Total Environment* **583,** 382–392. ISSN: 0048-9697 (2017).
41. Neitsch, S. L., Arnold, J. G., Kiniry, J. R. & Williams, J. R. Soil & Water Assessment Tool - Theoretical Documentation Version 2009. ISSN: 2151-0040 (2009).
42. Green, H. & Ampt, G. . Studies on Soil Phyics. *The Journal of Agricultural Science* **4,** 1–24. ISSN: 0021-8596 (1911).
43. Brown, C. D. & van Beinum, W. Pesticide transport via sub-surface drains in Europe. *Environmental Pollution* **157,** 3314–3324. ISSN: 02697491 (2009).
44. Zemolin, C., Avila, L. A., Cassol, G., Massey, J. & Camargo, E. Environmental fate of S-metolachlor - A review. *Planta Daninha, Viçosa-MG* **32,** 655–664 (2014).
45. Borah, D. K. & Bera, M. Watershed-Scale Hydrologic and Nonpoint-Source Pollution Models: Review of Mathematical Bases. *Transactions of the ASAE* **46,** 1553–1566. ISSN: 2151-0059 (2003).
46. Merritt, W. S., Letcher, R. A. & Jakeman, A. J. A review of erosion and sediment transport models. *Environmental Modelling and Software* **18,** 761–799. ISSN: 13648152 (2003).
47. Quilbé, R., Rousseau, A. N., Lafrance, P., Leclerc, J. & Amrani, M. Selecting a pesticide fate model at the watershed scale using a multi-criteria analysis. *Water Quality Research Journal of Canada* **41,** 283–295. ISSN: 12013080 (2006).
48. Payraudeau, S. & Gregoire, C. Modelling pesticides transfer to surface water at the catchment scale: A multi-criteria analysis. *Agronomy for Sustainable Development* **32,** 479–500. ISSN: 17740746 (2012).
49. Pandey, A., Himanshu, S. K., Mishra, S. K. & Singh, V. P. Physically based soil erosion and sediment yield models revisited. *Catena* **147,** 595–620. ISSN: 03418162 (2016).
50. König, S. *et al.* Functional resistance to recurrent spatially heterogeneous disturbances is facilitated by increased activity of surviving bacteria in a virtual ecosystem. *Frontiers in Microbiology* **9,** 1–14. ISSN: 1664302X (2018).
51. Rivard, L. *Environmental Fate of Metolachlor* tech. rep. (Environmental Monitoring Branch, Sacramento, California, 2003). `http://www.cdpr.ca.gov/docs/emon/pubs/fatememo/metolachlor.pdf`.

52. Trépos, R., Masson, V., Cordier, M. O., Gascuel-Odoux, C. & Salmon-Monviola, J. Mining simulation data by rule induction to determine critical source areas of stream water pollution by herbicides. *Computers and Electronics in Agriculture* **86,** 75–88. ISSN: 01681699 (2012).

53. Lindahl, A. M. L., Söderström, M. & Jarvis, N. Influence of input uncertainty on prediction of within-field pesticide leaching risks. *Journal of Contaminant Hydrology* **98,** 106–114. ISSN: 01697722 (2008).

54. Mander, Ü., Tournebize, J., Tonderski, K., Verhoeven, J. T. & Mitsch, W. J. Planning and establishment principles for constructed wetlands and riparian buffer zones in agricultural catchments. *Ecological Engineering* **103,** 296–300. ISSN: 09258574 (2017).

55. De Roo, A. P. J., Wesseling, C. G. & Ritsema, C. J. LISEM: A single-event physically based hydrological and soil erosion model for drainage basins. I: Theory, Input and Output. *Hydrological Processes* **10,** 1107–1117. ISSN: 0885-6087 (Nov. 1996).

56. Tiktak, A., Hendriks, R. F. A., Boesten, J. J. T. I. & van der Linden, A. M. A. A spatially distributed model of pesticide movement in Dutch macroporous soils. *Journal of Hydrology* **470-471,** 316–327. ISSN: 00221694 (2012).

57. Boesten, J. J. T. I. & van der Linden, A. M. A. Modeling the Influence of Sorption and Transformation on Pesticide Leaching and Persistence. *Journal of Environment Quality* **20,** 425. ISSN: 0047-2425 (1991).

58. Leistra, M., van der Linden, A. M. A., Boesten, J. J. T. I., Tiktak, A. & van den Berg, F. *PEARL model for pesticide behaviour and emissions in soil-plant systems; Description of the processes in FOCUS PEARL v 1.1.1.* tech. rep. (2001).

Chapter 7

Implications and perspectives

7.1 Pesticide-CSIA at catchment scale: potential, limits and implications

This Ph.D. thesis work presented a pesticide CSIA proof of concept for unsteady hydrological contexts based on carbon isotope data, opening the door to develop more complex field-scale studies. Pesticide CSIA however, provides not only an opportunity to evidence *in situ* degradation, but also to determine under which conditions, by which mechanism and to what extent specific degradation pathways occur. A better account of degradation pathways, and the environments under which these are most likely to occur, should contribute to identify potential environmental compartments where persistence parameters derived from laboratory test guidelines may no longer be valid. For example, although test guidelines require identification of pesticide half-lives (first order) or 50% disappearance time (if not first-order) under aerobic and anaerobic conditions in soils [1], these parameters may vary depending on specific site conditions and affiliated biodegrading microorganisms [2].

Information of the degradation conditions (e.g. metabolic vs. co-metabolic, biotic vs. abiotic) may allow for better information transfer between laboratory and field environments. Such information may in turn help to characterize potential degradation bottlenecks associated to specific environmental compartments by, for example, combination of CSIA data with hydrological tracer experiments allowing to track degradation while chasing hydrological pulses [3, 4]. Reference CSIA information for SM degradation under anaerobic conditions, for example, could be useful in this case to support interpretation of isotope fractionation associated to the environmental background status of the studied catchment. Indeed, a key limitation of this study, was the ability to characterize the low-flow components of catchment discharge in terms of isotope signatures, precluding estimation of long-term degradation potential of the catchment that would be useful for evaluation of continuous in-stream pesticide exposure and chronic toxicity studies [5, 6]. Future studies may thus benefit from a combination of water sampling strategies. Namely, while this study placed emphasis on flow-proportional water sampling, characterization of low flow components may require the development of extraction protocols to conduct grab samples with significantly larger volumes (e.g. >10 L, [7]). Such data may then be useful to characterise the potential delayed leaching of older yet undegraded pesticide bound residues sorbed onto the soil matrix [8]. Furthermore, due to the minimal resources typically required for passive samplers [9], their integration into the stream monitoring tool mix may prove beneficial for the characterization of mean concentrations over extended periods and beyond the agricultural growing season. However, pesticide CSIA implementation at typical concentrations capable for these

instruments (e.g., 20-70 ng L^{-1}, [10]) will require the development of extraction methods demonstrating the lack of fractionation effects associated to the sampler's sorbing phase unit (e.g., [11]).

Principal limitations for field applications of pesticide CSIA, are still however the need for developing more efficient pesticide extraction, enrichment and clean-up protocols, which should allow for feasible environmental sampling at concentrations found below the ppb range. For this study in particular, the small contribution of nitrogen, hydrogen, and chlorine to the molar mass of a chloroacetanilide molecule and the amount required of each element for analysis (about 30 ng on column for nitrogen and hydrogen and 10 ng for chlorine) concentrations with a respective order of magnitude of 38, 25 and 5 times the minimum environmental concentration observed for soils (2.4 μg g^{-1} dry. wt.) and waters (1 μg L^{-1}) would have been required for multi-element CSIA of SM. Aside from background matrix co-enrichment problems, seeking to obtain this information at the chosen sampling resolution would have required the extraction from about 56, 40 and 8 L of water (per sub-event sample) and 192, 122 and 25 g of soil (per weekly transect composite sample) for nitrogen, hydrogen, and chlorine analysis, respectively. While continuous automatic sampler units of these capacities are not generally available in the market, extraction methods associated with these soil masses at the chosen frequency seem beyond current laboratory scale facilities. In combination with improvements in instrument sensitivity, reduction of environmental sample masses required for extraction should be expected to generate more common place applications of multi-element CSIA for pesticides, and micro-pollutants in general, providing more detailed insight into the conditions that drive bottlenecks of pesticide degradation. With advances in multi-element CSIA, the further inclusion of main transformation product CSIA should further improve characterization of rapidly degraded metabolites [12], but also advance understanding of environmental conditions associated to chronic contamination for more persistent molecules [13].

From a regulatory or environmental protection framework, an initial and basic requirement is the need for information on transformation product isotope signature to be made available to the scientific community. Present developments for multi-element CSIA, for example, are already under way for a number of pesticides [14, 15], paving the way towards a richer knowledge base to support interpretation during field studies using LC-IRMS methods. However, from a precautionary principle and an environmental responsibility perspective, the burden associated to improved understanding of the conditions controlling pesticide persistence in the environment should be bared by the pesticide producer. Increased costs associated to, for example, the preparation of safety dossiers, would then be a first step towards better integration of environmental externalities currently accounted for by civil society in general. Indeed, OECD guidelines for aerobic and anaerobic degradation tests already require mass-balance accounts based on heavy-isotope marking [1]. However, due to cost and technical constraints, this information may only be of relevance to the specific experimental conditions, limiting its applicability to realistic environmental contexts. Furthermore, as pesticide producers are already required to report primary degradation products, a desirable next step in responsible regulation would be the requirement of isotope fractionation data associated to both parent compounds and principal metabolites, especially if the latter can be characterized as "relevant for groundwater resources" or "ecotoxicologically relevant" [16].

The development of more accurate environmental risks assessments requires additional consideration of the enantiomeric distribution of chiral compounds, as different enantiomers may have also different fate and toxicological impacts [17]. In this respect, benchmark degradation tests able to characterize enzymes of microbial communities as well as rate limiting steps

during degradation (e.g., cell-uptake, enzyme activity), should facilitate the development of monitoring strategies. For example, in a survey of phenoxy acid herbicide degradation under aerobic environments Qiu et al. [18], found that carbon isotope fractionation was masked by active transport through cell membranes, while enantiomer fractionation was pronounced, indicating that monitoring of enantiomer ratios of phenoxy acid herbicides can be a stronger indicator than CSIA to evidence field degradation in top soils. Therefore, without appropriate information at the time of pesticide registration regarding the mechanistic processes that regulate compound transformation in the environment, efforts to characterize pesticide fate and their toxicological impact will continue to challenge monitoring effort and regulation.

7.2 Improving modelling constraints and uncertainty using CSIA data

As an effort to explain how pesticides are being transported to field-drains, streams and groundwater (and despite their sorbing properties) [19], recent years have observed significant development of catchment-scale hydrological models including their account for preferential flow [20–22]. Although one of the objectives of this Ph.D work was to improve the constrain of degradation parameters regulating mobilization potential of pesticide pools during forcing events, a limitation in the ability to represent drainage (and associated mass transfer) components was observed in the adopted conceptual approximations of the continuous model [23, 24]. In terms of rainfall inputs to the subsurface, this may be of no surprise, as the daily time-steps considered by BEACH [24] are hardly appropriate to represent vertical flow and transport through preferential flow processes (e.g., macropores, fingering, etc.) [20]. However, the use of water dating techniques, for example by tracking stable isotopes ^{18}O and ^{2}H in both rainfall and outlet discharge at periods of both high and low-flow may improve accounts of vertical flow components to drainage [25]. Together with delineation of the artificial drainage system through geophysical detection tools [26] improved parametrization of drainage components therefore could have been achieved.

First improvements of drainage contribution were obtained by coupling PiBEACH with LISEM (chapter 5). By a reduction in time-step size, the coupled model allowed to account for high resolution rainfall patterns and increased infiltration and drainage outflow. This resulted in successfully restricting run-off genesis to the late season, where sealing development and time-of-concentration had been observed to increase [27, 28]. However, based on the poor ability of the coupled model to reproduce observed outlet carbon signatures at tail-ends of daily catchment discharge, additional inferences can be made as regards to potential improvements. As mentioned above, conceptualization of the drainage component could be improved by limiting the drainage network extent, helping to achieve a less pronounced discharge curve associated to lower drainage rates (i.e., both lower maximums and higher minimums). Including water isotope signatures in PiBEACH-oL could then be used to confirm distribution between drainage and baseflow rates from older groundwater components.

Better constraint of the artificial drainage network distribution, for example, could then be used to further evaluate degradation formalisms or process hypothesis including the potential for different transformation rates on sorbed fractions [29], rate dependencies associated to increase depths [27, 30, 31] or bioavailability limitations associated to the heterogeneous distribution and activities of degrading bacteria in subsurface transport paths [32]. The development of more complex models however, is often criticized for leading to over-parametrization [33]. This is exacerbated by the fact that the spatial and temporal heterogeneity of system

forcing (e.g., precipitation, temperature), and boundary conditions (e.g., distribution of preferential flow features, soil hydraulic properties, degrading bacterial distribution), cannot be sufficiently characterized with available observations [34–36]. Therefore, transferability from small-scale experiments will require upscaling efforts to obtain effective rate expression at a larger scales [32, 37, 38].

Irrespective of scale, information associated to the relevant microbial strains responsible for degradation of target contaminants under specific conditions and associated to specific enrichments (e.g., [18]) seems nevertheless to be a preliminary step to better constrain degradation formalisms. Specific improvements in numerical constraints could be made through characterization of half-velocity or half-saturation constants typical for chemical or microbial rate laws [39], allowing for departures from the use of conceptual approximations such as DT_{50} values, which are typically considered as independent of changes in environmental conditions.

Within the context of this work, potential improvements in PiBEACH-oL could be the evaluation of the hypothesis of delayed desorption generating discharge pulses of non-degraded signatures associated to aged fractions [7]. To support model conceptual development in this case, a combination of the experimental setup used during the microcosm degradation experiment (chapter 2) and the principles studied during the soil column leaching experiment (chapter 3) could be used to investigate differences in observable degradation rates within phases (i.e., dissolved and reversible-sorbed phases) and under distinct aerobic (non-saturated) and anaerobic (saturated) conditions. The principle would be to mimic wet-drying cycles during rainfall, followed by slow drainage in top soils and slow drainage in sub-surface saturated soils (anaerobic). All soils would be placed in glass tubes (e.g. 25 g dry wt.) at constant temperature and moisture conditions, spiking to reach observable field concentrations (5 to 10 μg g^{-1} dry wt.), and leaving sufficient air space to encourage oxygen diffusion (i.e., only aerobic modalities). To distinguish degradation between phases, aerobic modalities would require two "flush events" (short and long). Added water to saturation levels for all soils in all steps is extracted through centrifuge after vigorous mixing. The first flush for aerobic soils is extracted immediately after flooding. Water would be collected and combined with replicas to reach necessary volumes for CSIA analysis. Measured isotope signatures may be then associated to bacterial degradation of readily mobile and bioavailable fractions under aerobic conditions. The same procedure is applied to anaerobic soils and water content returned to saturation under anoxic conditions. For aerobic soils, a second saturation step would follow with aerated water and left for a period >24 hrs. (possibly under refrigerated conditions to minimize degradation during this period), allowing pesticide concentrations across phases to re-equilibrate before removing extractable water (i.e., late / second flush). After the second drainage in aerobic soils, modalities are returned to stable conditions (initial water content and temperature). This experiment, along with pesticide extractions from the residual soil fraction with methanol, should support conceptual model development at catchment scale by deriving effective degradation rates across phases for different catchment compartments (top soils and saturated sub-surface). Inclusion of modelling should allow to determine pesticide isotopic enrichment associated to each phase (pore water and reversibly-sorbed phase), modality (aerobic and anaerobic) as well as transfer rates to non-reversible soil fractions, allowing then for improved descriptions of transformation under bioavailability limitations [40]. Furthermore, by focusing on interstitial water, matrix background effects associated to soil extractions could be avoided and solid phase extraction (SPE) methods already developed could be further employed.

7.3 Towards comprehensive and larger-scale pesticide fate studies

Comprehensive studies that incorporate CSIA also present an opportunity to identify how different pesticide sources across multiple hydrological forcing events contribute to river discharge and sediment deposition at regional or river-catchment scale. Although characterization of degradation in source soils at headwater catchment scale is of relevance to support identification of source signatures, chapter 2 and chapter 4 showed that increasing sampling effort may not always provide proportional information gains to characterize catchment subunits or constrain model representations. Namely, chapter 2 showed that headwater stream signature trends, despite their large variability due to changes in flow regimes, followed closely seasonal trends of isotope fractionation in catchment bulk soils. Chapter 4 on the other hand, showed that the use of top-soil detailed plot or transect data did not provide additional information to constrain model parameters beyond that which had been already achieved from bulk soils alone.

These findings provide valuable insights for the design of larger catchment scale studies and with potentially different sampling scopes. If information is required regarding source top-soil pesticide contribution to streams and rivers during periods of relatively fast mobilization (i.e., runoff/erosion), larger catchment scales could make use of simple methodologies to identify areas with high propensity to generate overland-flow, restricting bulk soil sampling to such areas. For example, provided topographic information data is available, the wetness index such as that described in chapter 2 [41] may be useful in identifying areas with high propensity to accumulate water and generate overland-flow. If in addition, agricultural land-use distribution is available, the agronomical model used in PiBEACH (chapter 2) may be used to modify such an index by incorporating dynamic saturated soil permeabilities (e.g., see ref. 42). If the latter approach is followed, PiBEACH may be useful for integration of the above information to generate dynamic spatial maps of high propensity for overland-flow over large catchments.

On the other hand, if top-soil bulk samples are beyond feasible sampling, characterization efforts and model constraints could make use of stream discharge trends to approximate source bulk catchment soil signature evolution. A limited continuous sampling strategy of a catchment with multiple headwaters could employ two refrigerated automatic flow-proportional samplers. The first of these samplers would be dedicated to overall catchment monitoring, setting sampling intervals appropriate to observed in-river discharge. The second of these samplers may be considered as a sentinel observation point, located at the outlet of any given and representative headwater within the catchment, and whose isotope trends may be used as a proxy to interpret (and calibrate, in case of modelling) degradation in source soils throughout other headwaters. If additional resources are available, passive sampler units may be of benefit for calibration of time-weighted-average concentrations at additional points of interest within the catchment [10] as well as to select optimal locations for the primary sampler due to potentially high temporal and spatial variations in micropollutants across the catchment [43].

Although characterization of headwater inputs during fast flow periods, as discussed above, will be of importance, isotope signature information during periods of low flow should also be considered at this scale so as to be able to constraint potential model development with respect to different boundary sources with distinct isotope signatures. As low flow should reflect signatures associated to long-term base-flow contribution from groundwater sources

in the region, such information is of importance to constrain seasonal boundary conditions of the system, before new inputs are introduced. Such efforts could be focused to a short and discrete sampling window well before seasonal pesticide applications within the catchment begin. Sample volumes during periods of low flow however, should be significant (e.g., >10 L). Doing so at different sections of the river catchment may also facilitate corroboration of background system signatures in groundwaters. This may also facilitate the design of a multi-element CSIA sampling strategy to characterize long-term degradation/persistence of pesticide, while focusing on a carbon-based high resolution strategy during the growing season and associated to periods of high flow.

Additional challenges may be expected for characterization at catchment scales larger than headwaters. Although degradation may be of little importance during transport time-scales relevant for headwaters, degradation during transport at river scale may be of relevance [44]. Dominant degradation pathways during river transport may differ from source soils as distinct abiotic and biotic (e.g., degradation, bioaccumulation) attenuation processes may be involved. In some cases, microbial degradation may be an important contributor to pesticide attenuation, where stream biofilms are of relevance [45, 46]. The effects of micropollutants on biofilms structure and function may in turn cause important alterations in river ecosystem functioning [47]. Understanding the relative contribution of multiple processes contributing to pesticide attenuation, may thus be of importance to achieve the aforementioned assessment. Abiotic processes may be evaluated in static batch experiments (e.g., [15, 48]), while stream biofilm degradation may require more complex experimental set-ups. One example may be to mimic environmental conditions such as with streamside flumes and evaluated under different modalities, as community functions, growth and displacement may be affected by hydrodynamic forces [49], light conditions [50] and nutrient fluctuations [51]. The body of knowledge based on mesocosm experiments evaluating biofilm biodegradation capacity of emerging contaminants in natural streams however, is currently limited [6, 52]. Indeed, although enantioselective fractionation has been associated to microbial degradation in streams for several wastewater-derived contaminants [44], little information is available associated to ESIA assessments of pesticides directly linked to biofilm communities. Addressing this gap may therefore, help understanding the spatial and temporal variability of river attenuation potential of pesticides and micropollutants.

References

1. OECD. *OECD Guideline for the Testing of Chemicals: Aerobic and Anaerobic Transformation in Soil* 2002. doi:10.1787/9789264067394-eng. arXiv: arXiv:1011.1669v3. http://biotecnologiebt.com/guide/OECD%7B%5C_%7D227.pdf.

2. Thullner, M., Fischer, A., Richnow, H.-H. & Wick, L. Y. Influence of mass transfer on stable isotope fractionation. *Applied Microbiology and Biotechnology* **97,** 441–452. ISSN: 0175-7598 (2013).

3. Hillebrand, O., Nödler, K., Sauter, M. & Licha, T. Multitracer experiment to evaluate the attenuation of selected organic micropollutants in a karst aquifer. *Science of the Total Environment* **506-507,** 338–343. ISSN: 18791026 (2015).

4. Schürner, H. K. *et al.* Compound-Specific Stable Isotope Fractionation of Pesticides and Pharmaceuticals in a Mesoscale Aquifer Model. *Environmental Science and Technology* **50,** 5729–5739. ISSN: 15205851 (2016).

5. Babcsányi, I., Imfeld, G., Granet, M. & Chabaux, F. Copper stable isotopes to trace copper behavior in wetland systems. *Environmental Science and Technology* **48,** 5520–5529. ISSN: 15205851 (2014).
6. Rožman, M., Acuña, V. & Petrović, M. Effects of chronic pollution and water flow intermittency on stream biofilms biodegradation capacity. *Environmental Pollution* **233,** 1131–1137. ISSN: 18736424 (2018).
7. Torrento, C. *et al.* Fate of four herbicides in an irrigated field cropped with corn: lysimeter experiments. *11th Applied Isotope Geochemistry Conference Aig-11* **13,** 158–161. ISSN: 18785220 (2015).
8. Torrentó, C. *et al.* Assessing pesticide dynamics in soil and vadose zone using compound-specific isotope analysis (CSIA): A lysimeter study. *EGU General Assembly Conference Abstracts* **19,** 14833 (2017).
9. Toušová, Z. *et al.* Analytical and bioanalytical assessments of organic micropollutants in the Bosna River using a combination of passive sampling, bioassays and multi-residue analysis. *Science of the Total Environment* **650,** 1599–1612. ISSN: 18791026 (2019).
10. Guibal, R. *et al.* Two sampling strategies for an overview of pesticide contamination in an agriculture-extensive headwater stream. *Environmental Science and Pollution Research* **25,** 14280–14293. ISSN: 1614-7499 (2018).
11. Passeport, E. *et al.* Diffusion Sampler for Compound Specific Carbon Isotope Analysis of Dissolved Hydrocarbon Contaminants. *Environmental Science & Technology* **48,** 9582–9590. ISSN: 1520-5851 (2014).
12. Lefrancq, M., Payraudeau, S., Guyot, B., Millet, M. & Imfeld, G. Correction to Degradation and Transport of the Chiral Herbicide S-Metolachlor at the Catchment Scale: Combining Observation Scales and Analytical Approaches. *Environmental Science & Technology* **52,** 5517. ISSN: 0013-936X (May 2018).
13. Wood, R. J., Mitrovic, S. M., Lim, R. P. & Kefford, B. J. Chronic effects of atrazine exposure and recovery in freshwater benthic diatoms from two communities with different pollution histories. *Aquatic Toxicology* **189,** 200–208. ISSN: 18791514 (2017).
14. Schreglmann, K., Hoeche, M., Steinbeiss, S., Reinnicke, S. & Elsner, M. Carbon and nitrogen isotope analysis of atrazine and desethylatrazine at sub-microgram per liter concentrations in groundwater. *Analytical and bioanalytical chemistry* **405,** 2857–2867. ISSN: 16182650 (2013).
15. Masbou, J., Drouin, G., Payraudeau, S. & Imfeld, G. Carbon and nitrogen stable isotope fractionation during abiotic hydrolysis of pesticides. *Chemosphere* **213,** 368–376. ISSN: 00456535 (2018).
16. EC No 1107, E.-R. *European Union, Regulation (EC) No. 1107/2009 of the European Parliament and of the Council of 21 October* 2009.
17. Petrie, B., Barden, R. & Kasprzyk-Hordern, B. A review on emerging contaminants in wastewaters and the environment: Current knowledge, understudied areas and recommendations for future monitoring. *Water Research* **72,** 3–27. ISSN: 18792448 (2015).
18. Qiu, S. *et al.* Small13C/12C fractionation contrasts with large enantiomer fractionation in aerobic biodegradation of phenoxy acids. *Environmental Science and Technology* **48,** 5501–5511. ISSN: 15205851 (2014).
19. Flury, M. Experimental Evidence of Transport of Pesticides through Field Soils—A Review. English. *Journal of Environmental Quality* **25,** 25–45 (1996).

20. Paniconi, C. & Putti, M. Physically based modeling in catchment hydrology at 50: Survey and outlook. *Water Resources Research,* 7090–7129. ISSN: 19447973 (2015).

21. Köhne, J. M., Köhne, S. & Šimůnek, J. A review of model applications for structured soils: a) Water flow and tracer transport. *Journal of Contaminant Hydrology* **104,** 4–35. ISSN: 01697722 (2009).

22. Gerke, H. H., Germann, P. & Nieber, J. Preferential and Unstable Flow: From the Pore to the Catchment Scale. *Vadose Zone Journal* **9,** 207. ISSN: 1539-1663 (2010).

23. Manfreda, S., Fiorentino, M. & Iacobellis, V. DREAM: a distributed model for runoff, evapotranspiration, and antecedent soil moisture simulation. *Advances in Geosciences* **2,** 31–39. ISSN: 1680-7359 (2005).

24. Sheikh, V., Visser, S. & Stroosnijder, L. A simple model to predict soil moisture: Bridging Event and Continuous Hydrological (BEACH) modelling. *Environmental Modelling and Software* **24,** 542–556. ISSN: 13648152 (2009).

25. Singh, N. K., Emanuel, R. E. & McGlynn, B. L. Variability in isotopic composition of base flow in two headwater streams of the southern Appalachians. *Water Resources Research* **52,** 4264–4279 (2016).

26. Budhathoki, M., Gokkaya, K., Tank, J., Christopher, S. & Hanrahan, B. *Detecting Subsurface Agricultural Tile Drainage using GIS and Remote Sensing Technique* in *AGU Fall Meeting Abstracts* **2015** (Dec. 2015), NS43B–1971.

27. Lutz, S. R. *et al.* Pesticide fate at catchment scale: conceptual modelling of stream CSIA data. *Hydrology and Earth System Sciences Discussions* **21,** 5243–5261. ISSN: 1812-2116 (2017).

28. Alvarez-Zaldívar, P., Payraudeau, S., Meite, F., Masbou, J. & Imfeld, G. Pesticide degradation and export losses at the catchment scale: Insights from compound-specific isotope analysis (CSIA). *Water Research* **139,** 198–207 (2018).

29. Ren, X. *et al.* Sorption, transport and biodegradation – An insight into bioavailability of persistent organic pollutants in soil. *Science of the Total Environment* **610-611,** 1154–1163. ISSN: 18791026 (2018).

30. Boesten, J. J. T. I. & van der Linden, A. M. A. Modeling the Influence of Sorption and Transformation on Pesticide Leaching and Persistence. *Journal of Environment Quality* **20,** 425. ISSN: 0047-2425 (1991).

31. Leistra, M., van der Linden, A. M. A., Boesten, J. J. T. I., Tiktak, A. & van den Berg, F. *PEARL model for pesticide behaviour and emissions in soil-plant systems; Description of the processes in FOCUS PEARL v 1.1.1.* tech. rep. (2001).

32. Schmidt, S. I., Kreft, J. U., Mackay, R., Picioreanu, C. & Thullner, M. Elucidating the impact of micro-scale heterogeneous bacterial distribution on biodegradation. *Advances in Water Resources* **116,** 67–76. ISSN: 03091708 (2018).

33. Fatichi, S. *et al.* An overview of current applications , challenges , and future trends in distributed process-based models in hydrology. *Journal of Hydrology* **537,** 45–60. ISSN: 0022-1694 (2016).

34. Yeh, W. W.-G. Review of Parameter Identification Procedures in Groundwater Hydrology: The Inverse Problem. *Water Resources Research* **22,** 95–108. ISSN: 0043-1397 (Oct. 1986).

35. Zehe, E., Elsenbeer, H., Lindenmaier, F., Schulz, K. & Blöschl, G. Patterns of predictability in hydrological threshold systems. *Water Resources Research* **43.** ISSN: 0043-1397. doi:10.1029/2006WR005589. https://doi.org/10.1029/2006WR005589 (July 2007).

36. Hrachowitz, M. *et al.* Transit times-the link between hydrology and water quality at the catchment scale. *Wiley Interdisciplinary Reviews: Water* **3,** 629–657. ISSN: 20491948 (2016).
37. Li, L., Peters, C. A. & Celia, M. A. Upscaling geochemical reaction rates using pore-scale network modeling. *Advances in Water Resources* **29,** 1351–1370. ISSN: 0309-1708 (2006).
38. Heße, F., Radu, F. A., Thullner, M. & Attinger, S. Upscaling of the advection-diffusion-reaction equation with Monod reaction. *Advances in Water Resources* **32,** 1336–1351. ISSN: 0309-1708 (2009).
39. Thullner, M., Regnier, P. & Van Cappellen, P. Modeling Microbially Induced Carbon Degradation in Redox-Stratified Subsurface Environments: Concepts and Open Questions. *Geomicrobiology Journal* **24,** 139–155. ISSN: 0149-0451 (2007).
40. Thullner, M., Kampara, M., Richnow, H. H., Harms, H. & Wick, L. Y. Impact of bioavailability restrictions on microbially induced stable isotope fractionation. 1. Theoretical calculation. *Environmental Science and Technology* **42,** 6544–6551. ISSN: 0013936X (2008).
41. Beven, K. J. & Kirkby, M. J. A physically based, variable contributing area model of basin hydrology. *Hydrological Sciences Bulletin* **24,** 43–69. ISSN: 03036936 (1979).
42. Agnew, L. J. *et al.* Identifying hydrologically sensitive areas: Bridging the gap between science and application. *Journal of Environmental Management* **78,** 63–76. ISSN: 03014797 (2006).
43. Burns, E. E., Carter, L. J., Kolpin, D. W., Thomas-Oates, J. & Boxall, A. B. A. Temporal and spatial variation in pharmaceutical concentrations in an urban river system. eng. *Water research* **137,** 72–85. ISSN: 1879-2448 (Electronic) (June 2018).
44. Fono, L. J., Kolodziej, E. P. & Sedlak, D. L. Attenuation of wastewater-derived contaminants in an effluent-dominated river. *Environmental Science and Technology* **40,** 7257–7262. ISSN: 0013936X (2006).
45. Tien, C.-J., Lin, M.-C., Chiu, W.-H. & Chen, C. S. Biodegradation of carbamate pesticides by natural river biofilms in different seasons and their effects on biofilm community structure. *Environmental Pollution* **179,** 95–104. ISSN: 0269-7491 (2013).
46. Tien, C. J., Huang, H. J. & Chen, C. S. Accessing the Carbofuran Degradation Ability of Cultures From Natural River Biofilms in Different Environments. *Clean - Soil, Air, Water* **45.** ISSN: 18630669. doi:10.1002/clen.201600380 (2017).
47. Proia, L. *et al.* Effects of pesticides and pharmaceuticals on biofilms in a highly impacted river. *Environmental Pollution* **178,** 220–228. ISSN: 02697491 (2013).
48. Gutowski, L., Olsson, O., Leder, C. & Kümmerer, K. A comparative assessment of the transformation products of S-metolachlor and its commercial product Mercantor Gold(®) and their fate in the aquatic environment by employing a combination of experimental and in silico methods. *The Science of the total environment* **506-507,** 369–379. ISSN: 1879-1026 (Feb. 2015).
49. Besemer, K., Singer, G., Hödl, I. & Battin, T. J. Bacterial community composition of stream biofilms in spatially variable-flow environments. *Applied and Environmental Microbiology* **75,** 7189–7195. ISSN: 00992240 (2009).
50. Bengtsson, M. M., Wagner, K., Schwab, C., Urich, T. & Battin, T. J. Light availability impacts structure and function of phototrophic stream biofilms across domains and trophic levels. *Molecular Ecology* **27,** 2913–2925. ISSN: 1365294X (2018).

51. Subirats, J. *et al.* Emerging contaminants and nutrients synergistically affect the spread of class 1 integron-integrase (intI1) and sul1 genes within stable streambed bacterial communities. *Water Research* **138,** 77–85. ISSN: 18792448 (2018).

52. Corcoll, N. *et al.* Effects of flow intermittency and pharmaceutical exposure on the structure and metabolism of stream biofilms. *Science of the Total Environment* **503-504,** 159–170. ISSN: 18791026 (2015).

Appendices

Appendix A

Supporting information to chapter 2

A.1 I. Soil collection

Top soil (1 cm) samples were collected weekly along three transects between March 28th and June 28th. Distance between sampling points (3 - 5 m) was determined based on transect length, with the number of samples for each plot being proportional to the transects' plot length. Sampling protocol followed USDA guideline MN-NUTR3. Soil samples were kept in an ice-box during transport to the laboratory and kept frozen at -20°C until analysis. Soils were homogenized and sieved at 2 mm. Samples heavier than 500 g were quartered before sieving, according to NF X 31100 standard. Water content was determined according to NF ISO 11465 standard. A 30 g soil sample was dried at 105°C until a constant mass was achieved (±10 mg between two successive weightings). Soil Organic Matter determination was based on loss on ignition by placing the dried sample for 16 hours at 375°C. The pH was determined according to the NF ISO 10390 standard by placing 5 mL soil sample with five volumes of chloride calcium solution (0.01 M) in a Falcon tube and shaken for 60 min.

Transects where selected to account for variability of moisture conditions, drainage characteristics and to maximise the number of plots where S-met was applied. Digital Elevation Models (DEM), at 0.5 and 2 m resolution, were extracted with ArcGIS 10.1 (ESRI, Redlands,United States) from airborne Light Detection And Ranging (LIDAR) measurements (8 points / m^2 with a vertical accuracy of 15 cm). Local slopes obtained from the DEM where then used to estimate the soil wetness index (WI) [-] (See main manuscript, Section 2.3).

A.2 II. Water collection

The water collection method has been previously described [1]. Discharge was continuously measured by a Doppler flowmeter (2150 Isco, Lincoln, Nebraska, USA) with volume precision of 3%. Water samples were stored in the dark at $4°C$ during collection and placed on ice during transportation to the laboratory for filtering (0.7 μm glass fibre). Sample volume mixing choice for pesticide and isotope analysis is illustrated in Fig. 62. Sample aliquots were pooled to obtain volumes $\geq$ 990 mL.

A.3 III. Hydrological variability and cluster analysis

A divergence in isotope trends between bulk soils and outlet can be observed after mid-May (see manuscript, Fig. 4). This divergence was associated to a late season application (May 25^{th}), lowering isotope signatures along the valley transect, increasing the variability of fractionation extent in source soils. To explore this variability we hypothesized a significant change in the catchment's hydrological connectivity [1], leading to a shift from drainage- to runoff-driven pesticide export resulting in shorter catchment response times and an increases in outlet $\Delta\delta$ variability.

Discharge samples were selected based on their associated event hydrological characteristics. Using principal component analysis (PCA) and a K-means clustering approach we identified three distinct clusters ($P < 0.1$) of hydrological samples (Fig. A1) associated to April events ($\approx 70\%$) of low flow and long duration (C1) and May-June events of high rainfall and high discharge intensity (C2 & C3). Sampled events where clustered using the *stats* R package [2]. Standardization based on the Hellinger approach [3] was conducted with the *vegan* package [4]. Hydrological and response variables used for PCA are given by Table A1.

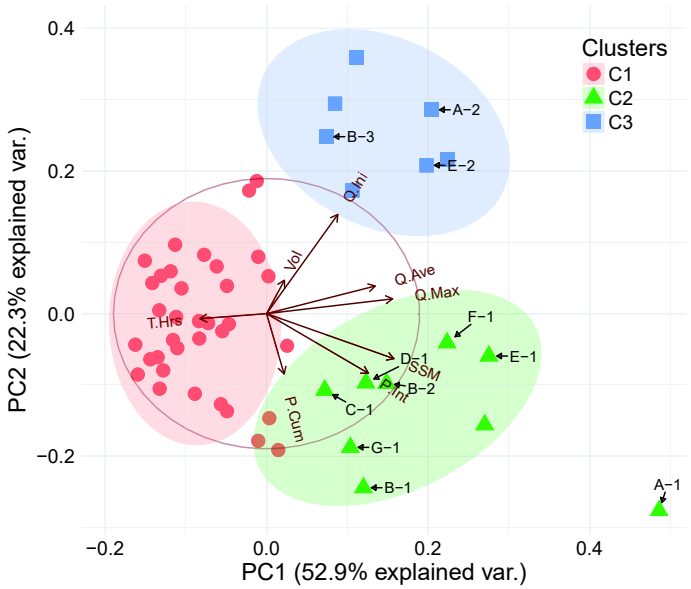

Figure A1: K-means clustering of flow proportional samples based on principal component analysis of hydrological characteristics (n = 51) including sample duration (T.Hrs), discharged volume (Vol), discharge at the start of the sample (Q.Ini), average discharge (Q.Ave), max discharge (Q.Max), suspended solid matter (SSM), average rainfall intensity (P.Int) and cumulative rainfall (P.Cum). Letter labels refer to events, while index numbers refer to the sample order within each event. C1 samples correspond mainly to April events ($\approx 70\%$), while C2 & C3 correspond respectively to the leading and trailing limbs of late season events (May and June). The inner product of vector variables approximates their covariance and the distance between points approximates the Mahalanobis distance. Shaded clouds show the 90% normal probability distribution for each cluster discarding sample A-1 as outlier to C2.

Based on clustering results, a shift towards runoff driven transport may have occurred during May and June. This observation is supported by a reduction in the mean catchment time of concentration (T_C), from April (2.2±1.8 h) to June (0.5±0.2 h). Although subsurface travel times for this catchment may range from 6 to 12 months [5], the computed T_C values are small

Table A1: PCA Clustering Variables

Variable	Definition	Units
P.Cum	Cummulative rainfall after tillage	[mm]
P.Int	Cummulative rainfall per sampled hours	[mm/h]
Q.Ave	Discharged volume per sampled hours	[m^3/h]
Q.Ini	Discharge at the start of the sample	[m^3/h]
Q.Max	Maximum discharge during the sample	[m^3/h]
Vol	Cummulative volume discharged during the sample	[m^3]
SSM	Soils suspended matter exported during the sample	[Kg]
T.Hrs	Duration of the sample	[h]

relative to dry periods. Based on S-met reaction rates ($k = 0.021$ [1/d], Table A3), pesticide travel times during peak discharge would thus yield small Damköhler numbers (Da <¡0.1, $Da = kT_C$ [6]) indicating that isotope signatures at the outlet likely reflect reaction times in top soils.

Contrasting field data to a hillslope model conducted by [7] allowed us to investigate the increase in outlet $\Delta\delta$ variability observed between April and June. The hillslope model considered a set of well-defined hydrological scenarios allowing a comparison of simulation results to multiple sub-event $\delta^{13}C$ observed during this study. The model scenario chosen for comparison was an extreme rainfall simulation event (60 mm/h × 30 min), considering a fresh pesticide source upstream from the outlet [7]. In agreement with the hillslope model [7], discharge peaks arriving at the outlet after major rainfall events during May and June coincided with a rapid drop in $\Delta\delta$ to values characteristic of bulk soils (Fig. A2). However, as the source zone ages, the difference between subsequent signatures of an event also appears to decrease (i.e., Fig. A2, events B *vs.* E and A). The model attributed an early drop in outlet signatures to runoff conditions leading to a rapid increase in outlet discharge [7], conditions that were also likely to occur in the field at the time given a cumulative rainfall (>100 mm since sowing), advanced crust development and T_C measured during this period.

Model and field data comparison therefore suggests that although high-flow conditions may lead to an underestimation of catchment degradation extents, this may be of relevance only during first flushes [8] or shortly after product applications, where runoff is the dominant transport pathway. This underscores the importance of how changes in catchment hydrological response along one growing season may increase the variability of pesticide travel times and fractions exported within an event, thereby influencing scope and choice of monitoring objectives during field studies. Based on these observations, we conclude that the isotope variability increase during May and June was associated to a change in the dominant transport processes and not to an uncertainty increase related to CSIA-based monitoring.

A.4 IV. Pesticide extraction

Water. Solid phase extraction of S-met, MESA and MOXA from water was performed using SolEx C18 cartridges (Dionex®, Sunnyvale, CA, USA) and an AutoTrace 280 SPE system (Dionex®). The water sample recovery rate from spiked samples was 98±11%, with a preconcentration factor of 1000 and determined based on a range of concentrations (0.05, 1, 5, 50 and 150 ug/L), stirred until solvent evaporation (20 min to 1 hr) and evaluated from 1 L Milli-Q water solution in duplicate (n=10). The extraction procedure was described by Elsayed *et al.* 2014. Briefly, extraction cartridges were washed successively with ethanol (5

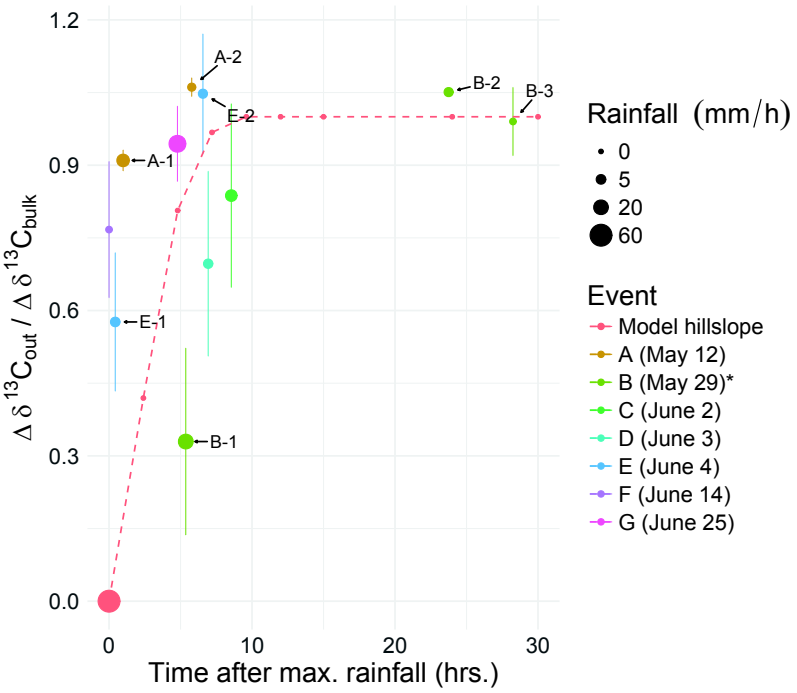

Figure A2: Water $\Delta\delta^{13}C$ normalized to bulk soils (field) and source zone (model by [7]) for run-off generating events (i.e., C2 and C3 samples, Fig A.3) observed at the outlet after max rainfall. Comparison of sub-event samples to model results indicated that runoff was the likely dominant transport pathway during May and June. Error bars for each sample correspond to the normalized SD ($n \geq 3$).*A mid-season application reported on May 25^{th} was associated to a major drop in early signatures of event B.

mL), rinsed with acetonitrile (ACN) (5 mL), and conditioned with dionized water (10 mL). Samples were loaded on the cartridges and dried under nitrogen flux for 10 min. Cartridge elution was performed with 5.0 mL ethyl acetate followed by 5.0 mL ACN. Samples were then concentrated under nitrogen flux to one droplet and 1.0 mL of acetonitrile was added for quantification and isotopic composition analyses.

Soils. Pesticide extraction and purification for soils were adapted from Ivdra *et al.* 2014 and Anastassiades *et al.* 2003. The soil sample recovery rate was 22±2% from spiked soils. Before spiking each soil (about 10 g), pesticide stock solutions in dichloromethane (DCM) were prepared in water to reach soil concentrations of about 0.5, 5, 10, 20, 35 and 50 $\mu g/g$ of S-metolachlor. The pesticide solution was stirred about 1 h until evaporation of the solvent to achieve a homogeneous pesticides contaminated water solution. After spiking, the samples were stirred vigorously for 1 hr for homogenization and incubated one week (7 days) in the dark at 4 °C prior to extraction. Each condition was performed in duplicate (n=10).

Ethyl acetate (2.5 mL) and soil (5 g) were mixed in a Falcon tube, vortex 15 s, sonicating for 5 minutes at 20 $°C$, adding deionized water to reach 80% water content, vortex 1 min and centrifuge for 5 min at 5000 rpm. The organic layer was separated and the solvent extraction procedure was repeated twice without further addition of water. Samples were then concentrated under nitrogen flux to one droplet pesticides re-suspended with acetonitrile (1 mL). Samples were then dried over anhydrous $MgSO_4$ and purified *via* PSA (25 mg) and anhydrous $MgSO_4$ (150 mg), vortex 30 s and centrifuge 1 min at 5000 rpm. Water content was determined according to standard procedure [12].

Table A2: Comparison between EA-IRMS, GC-C-IRMS $\delta^{13}C$ and $\delta^{15}N$ (‰) (mean ± SD) values *vs.* VPDB and Air standards.

Compound	$\delta^{13}C$ (‰) *vs.* VPDB		$\delta^{15}N$ (‰) *vs.* Air	
	EA-IRMS (n=2)	GC-C-IRMS (n=18)	EA-IRMS (n=2)	GC-C-IRMS (n=19)
Rac-metolachlor	-30.6 ± 0.0	-30.7 ± 0.3		
S-metolachlor	-30.9 ± 0.0	-31.3 ± 0.6	0.4 ± 0.1	0.5 ± 0.5

The analytical methods were evaluated for possible isotope artifacts since S-met extraction and pre-concentration procedures may alter the measured $\delta^{13}C$ values. The mean $\delta^{13}C$ shifts ($\Delta\delta^{13}C$) associated with the extraction method from crop soils (20% and 40% soil moisture) and water samples (0.5 to 8 L) confirmed the absence of significant fractionation effects (Tables A2 and A3). However, to include the potential uncertainty limit (UL) associated with the soil extraction method, a minimum isotopic shift ($\Delta\delta^{13}C \approx 2$‰) was considered before degradation (and fractionation) could be concluded. To determine this shift, a propagated error has been calculated by:

$$UL_{grey\ area} = \sqrt{\sigma_a^2 + \sigma_b^2 + \sigma_{au}^2} + \Delta\delta_{ext} \tag{A.1}$$

where standard deviations (σ) accounted for during the soil extraction experiment include 1σ obtained for the initial product signature ($\sigma_a = 0.5$‰), 1σ obtained from samples ($\sigma_b = 0.4$‰), 1σ associated to the maximum analytical uncertainty ($\sigma_{au} = 0.5$‰) and the mean isotope shift ($\Delta\delta_{ext}$).

A.5 V. Quantification

S-met. Quantification of S-met was performed by gas chromatography (Trace 1300, Thermo Fisher Scientific) coupled to a mass spectrometer (ISQ, Thermo Fisher Scientific). Metolachlor-*d11* was automatically added in each sample as an internal standard at a constant concentration by the autosampler (TriPlus RSH^{TM}, Thermo Fisher Scientific). The samples (1.5 μL vol.) and internal standard (1 μL at 300 $\mu g/L$) were injected into a split/splitless injector operated in split mode with a split flow at 6.0 mL/min and held at 280 °C. Separation was performed on a TG-5MS column (30 m x 0.25 mm ID, 0.25 μm film thickness) with helium as carrier gas at a 1.5 mL/min flow rate. The GC oven program was held at 50 °C for 1 min, ramped to 160 °C at 30 °C/min, then to 220 °C at 4 °C/min, and finally to 300 °C at 30 °C/min held for 1 min. The MS transfer line and source were heated at 320 °C. Each sample was measured in triplicate. Equipment detection and quantification limits were 0.01 and 0.001 $\mu g/L$, respectively.

MOXA & MESA. The concentrations of main S-met transformation products (TPs) were measured by liquid chromatrography (LC-MS/MS) (TSQ Quantum Access Max, Thermo Scientific, Waltham, Massachusetts, USA). The mobile phase (0.3 mL/min) consisted of a gradient of acetonitrile (30 to 95%) and water (70 to 5%) in a negative mode which was returned to initial conditions during 6 min. Each time, 20 μL of each sample was injected into an EC 150/3 Nucleodur C18 Pyramid 3 μm column. Equipment detection and quantification limits were 0.05 and 0.5 $\mu g/L$, respectively.

Table A3: Comparison between EA-IRMS, GC-C-IRMS $\Delta\delta^{13}C$ and $\delta^{15}N$ (‰) (mean ± SD) values for soil and water (SPE) extracted standards of racemic (R-) and S-metolachlor (S-met)

Compound	$\Delta\delta^{13}C$ (‰) *vs.* VPDB [a]					
	EA-IRMS *vs.* GC-C-IRMS	GC-C-IRMS extracted *vs.* non-extracted *vs.*				
		From water (1 L)[b]		From soil (5 g)[c]		
		Milli-Q	Run-off water	Crop (20%)	Crop (40%)	Soil Overall
R-met	0.1 ± 0.3	0.0 ± 0.8	0.3 ± 0.4	n.d	n.d	n.d
S-met	0.4 ± 0.6	0.0 ± 0.5	0.6 ± 0.6	0.7 ± 0.4	0.8 ± 0.4	0.8 ± 0.4

Compound	$\Delta\delta^{15}N$ (‰) *vs.* Air [a]					
	EA-IRMS *vs.* GC-C-IRMS	GC-C-IRMS extracted *vs.* non-extracted *vs.*				
		From water (1 L)[b]		From soil (5 g)		
		Milli-Q	Run-off water	Crop (20%)	Crop (40%)	Soil Overall
S-met	0.1 ± 0.6	0.2 ± 0.7	-	-	-	-

a. The error given for the $\Delta\delta^{13}C$ and $\Delta\delta^{15}N$ values was calculated *via* error propagation based on ± 1 SD of the mean δ values from n ≥ 3 measurements for each sample. $\Delta\delta$ values were determined as the difference between the measured δ value of a given compound in the extract and the mean δ value of the corresponding standard obtained by replicate injections in the GC-C-IRMS systems at optimal conditions.

b. Means of measurements (n ≥ 3) of 4 water extraction experiments with different concentrations of S-met (and R-met for carbon measurements). Field run-off water (1L) was spiked with S-met / R-met to reach concentrations of about 1, 5, 50 and 150 $\mu g/L$ (concentrations ranging from 200 $\mu g/L$ to 20 mg/L after SPE extraction).

c. Means of measurements (n ≥ 3) of 5 soil extraction experiments with different concentrations of S-metolachlor and water contents of 20% and 40% for crop soils. Soil racemic extractions were not determined (n.d.). Soils (5 g) were spiked to reach concentrations of 5, 10, 20, 35 and 50 $\mu g/g$. The samples were stirred vigorously for 1 h for homogenization and incubated 7 days in the dark at 4°C prior to extraction. Each experiment was performed in duplicate.

A.6 VI. Isotope analysis

The carbon and nitrogen isotope composition of S-met was analyzed using a GC-C-IRMS system consisting of a TRACE^{TM} Ultra Gas Chromatograph (ThermoFisher Scientific) coupled *via* a GC IsoLink/Conflow IV interface to an isotope ratio mass spectrometer (DeltaV Plus, ThermoFisher Scientific). The carbon and nitrogen isotope ratios are reported in δ notation in parts per thousand [‰] relative to the V-PDB standard for carbon and Air standard for nitrogen, according to:

$$\delta^{13}C_{sample} \text{ or } \delta^{15}N_{sample} = \frac{R_{sample} - R_{standard}}{R_{standard}} \tag{A.2}$$

where R_{sample} and $R_{standard}$ are the ratios $^{13}C/^{12}C$ or $^{15}N/^{14}N$ of sample and standard, respectively.

Given that isotope shifts are provided in $\Delta\delta$ notation, error bars for sample points presented in the manuscript account for error propagation (e.p.) across $\pm 1\sigma$ (standard deviation) of

initial product and $\pm 1\sigma$ from sample signatures such that:

$$e.p. = \sqrt{\sigma_{ini}^2 + \sigma_{smp}^2} \tag{A.3}$$

where σ_{ini} is the standard deviation of the initial product and σ_{smp} the standard deviation of the soil or water sample signature.

The oxidation furnace of the GC/C IV interface was set to a temperature of 1000 °C. A TG-5MS column (60m × 0.25mm ID, 0.25 μm film thickness) was used for chromatographic separation, with helium as the carrier gas at a flow rate of 1.5 mL/min. For carbon, the column was held at 50 °C for 1 min, heated at a rate of 15 ° C/min to 150 °C, then up to 250 °C at 2 °C/min, then heated at 20 ° C/min to 300 °C and held for 3 min. For nitrogen, the column was held at 50 °C for 1 min, heated at a rate of 20 °/min to 150 °C, then up to 270 °C at 10 °C/min, then heated at 30 °C/min to 300 °C and held for 3 min. Samples (3 μL) were injected into a split/splitless injector operated in splitless mode and held at 280°C.

The $\delta^{13}C$ and $\delta^{15}N$ values were calibrated using a three-point calibration against the Vienna Pee Dee Belemnite (V-PDB) and Air standard respectively using international reference materials AIEA600, USGS40, and USGS41 (σ<0.05 ‰). The reproducibility of triplicate measurements was $\leq$ 0.2 ‰(1σ) for $\delta^{13}C$ and $\leq$ 0.5 ‰(1σ) for $\delta^{15}N$. A set of in-house S-met standards with known isotopic composition (determined by EA-IRMS) was measured at least every nine injections to control the measurement quality. Reference $\delta^{13}C$ and $\delta^{15}N$ signatures of standards were obtained at our isotope facility using an elemental analyzer-isotopic ratio mass spectrometer (Flash EA IsoLink^{TM} CN IRMS, Thermo Fisher Scientific, Bremen, Germany). Based on GC-IRMS linearity tests, the minimum peak amplitudes needed for accurate $\delta^{13}C$ and $\delta^{15}N$ measurements were established as about 300 mV and 200 mV, respectively (Fig A4). These signals correspond to 10 ng of carbon and 20 ng of nitrogen injected on column.

Pure product and tractor tank dilutions are shown in Table 23 for Mercantor Gold. Samples from one farmer using Dual Gold, accounting for 1 plot and 3% (0.9 ha) of the applied surface could not be obtained. However, due to the fact that both products originated from the same manufacturer (Syngenta AG), S-metolachlor signatures were assumed to be equivalent for both formulations.

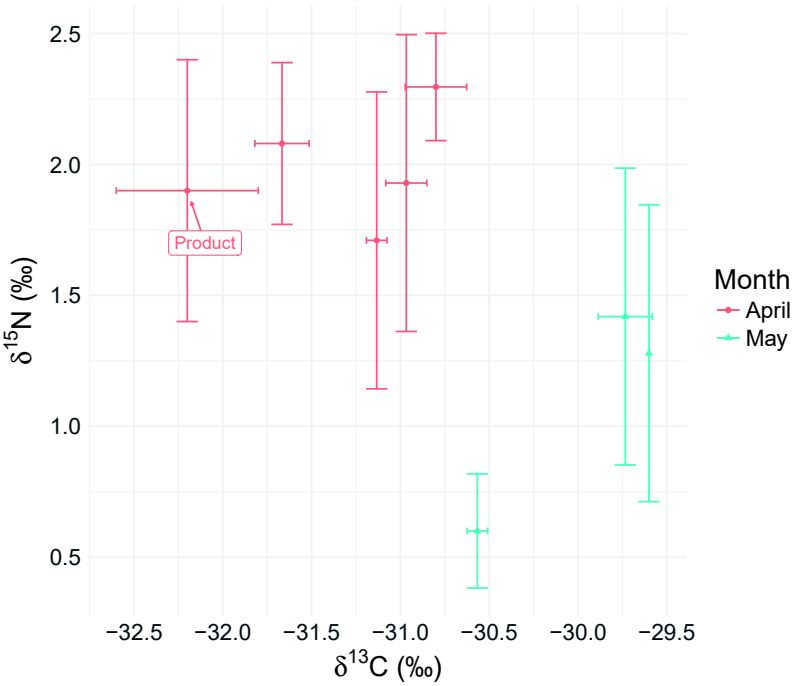

Figure A3: Dual isotope plot for catchment outlet water

A.7 VII. Soil degradation experiments

Soil samples were collected from the referenced catchment on August 6 and 7, 2015. 50 kg of top-soil were sampled systematically along three transects representative of the catchment (See main manuscript, Fig. 1). Soils were thoroughly homogenized and sieved to 2 mm. The physical and chemical properties of the experimental soils are provided in the main manuscript (see Section 2.1.). Soil microcosms consisted of 20 g of air-dried soil spiked to environmental concentrations (5.0 μg/g soil) in 20 mL crimp glass vials, with silicone/natural PTFE caps (Interchim ®, France). All systems' volumetric water content was adjusted to either 20 or 40%, thoroughly mixed by vortex to homogenize systems. To maintain aerobic conditions in the microcosm atmosphere while limiting water loss and avoiding contamination, a 0.2 μm syringe filter (Rotilabo ®, Carl Roth ®, France) was mounted on a syringe tip, which was stuck through the vial cap (Fig. A5).

The pesticide standard solutions in dichloromethane (DCM) were spiked in distilled water and stirred for 6 h, until solvent evaporation. The pesticide aqueous solutions were filter-sterilized with 0.2 μm syringe filters for soil spiking. Soil microcosms spiked with S-met were prepared in triplicate under non-sterilized (biotic) and sterile (abiotic) conditions to evaluate abiotic dissipation. Biotic experiments were set-up by spiking each soil with S-met aqueous solutions at 5 $\mu g/g$ (i.e., within range of environmental S-met concentrations in soils) to reach soil water content of 20% and 40% (soil water content ranges in Alteckendorf). For the abiotic experiments, the soils were autoclaved three times at 24-hour intervals for 15 min. at 125°C. The sterilized soil was spiked with S-met following the same procedure as for the biotic experiments. All microcosms were incubated in dark at 20°C for 200 days. Sampling was carried out based on a sacrificial approach on days 1, 10, 50, 100 and 200. Quantification and CSIA analysis of S-met were carried out using the same extraction and measurement procedures as those used for field soil samples.

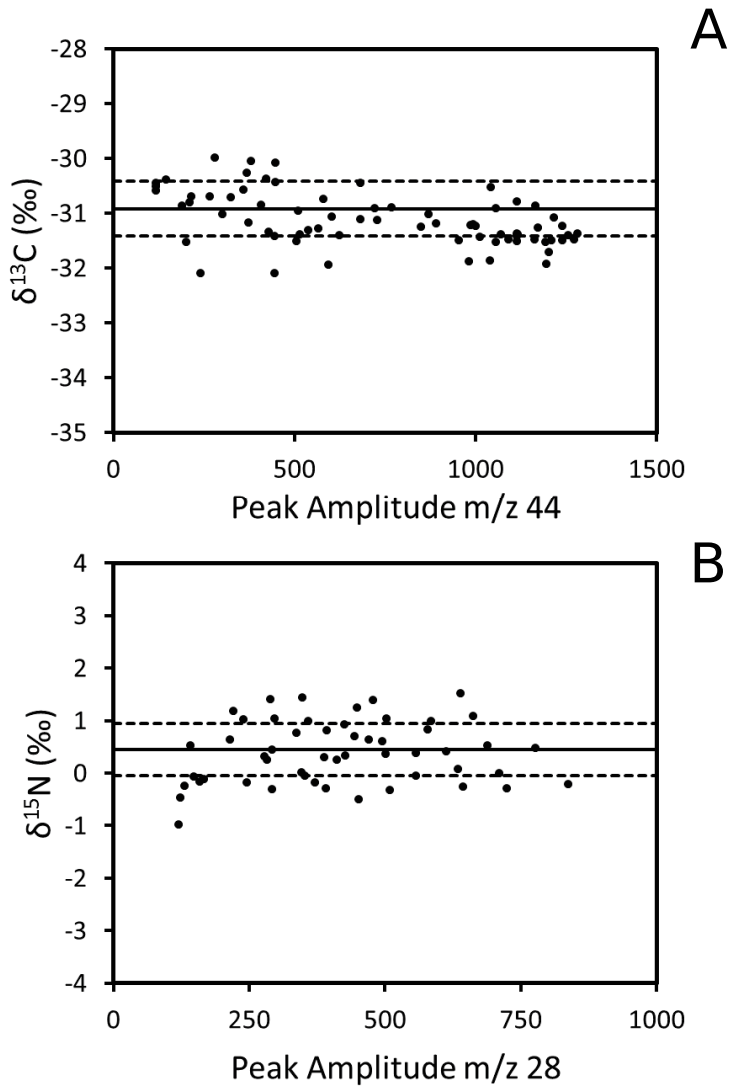

Figure A4: Linearity of $\delta^{13}C$ (A) and $\delta^{15}N$ (B) values obtained for S-met by GC-IRMS as a function of peak amplitude m/z 44 and 28, respectively. Solid and dashed lines indicate the EA-IRMS measurements and typical $\pm$ 0.5‰ associated uncertainties, respectively.

Carbon isotopic fractionation and dissipation kinetics for S-met in laboratory experiments are provided in Table A4 and isotopic fractionation with respect to time is shown on Fig. A6. Derivation of lab and field ε values was performed following the Rayleigh equation [13]:

$$\frac{\delta^{13}C_t + 1}{\delta^{13}C_0 + 1} = f^{\varepsilon} \tag{A.4}$$

where $f = [S-met]_t/[S-met]_0$, is the remaining fraction of S-met at time t.

The apparent kinetic isotope effect (AKIE) was computed as [14]:

$$AKIE \approx \frac{1}{1 + z \cdot \frac{n}{x} \cdot \frac{\epsilon_{bulk}}{1000}} \tag{A.5}$$

Figure A5: Soil microcosm experimental design

where for carbon in S-met, the number of atoms $n = 15$, of which $x = 1$ are located at a reactive position and of which $z = 1$ are in intramolecular competition.

A.8 VIII. Open system Rayleigh calculations

The Rayleigh equation assumes that field sample remaining fraction (f) reflects solely reduction in concentrations due to degradation and should thus be expressed as $f_{degradation}$. Accounting for dilution processes, the remaining fraction that is measured in the field sample becomes then f_{total}, where [15]:

$$f_{total} = f_{degradation} \cdot f_{dilution} \tag{A.6}$$

$$f_{degradation} = f_{total} \cdot F \tag{A.7}$$

where the dilution factor F (i.e. the number of times the source volume has become diluted at the observation location) can be calculated if ϵ_{lab} is known by:

$$F = e^{(\Delta*/\epsilon_{lab} - ln f_{total})} \tag{A.8}$$

$$\Delta* = 1000 \cdot ln\left(\frac{10^{-3}\delta_t^{13}C + 1}{10^{-3}\delta_0^{13}C + 1}\right) \tag{A.9}$$

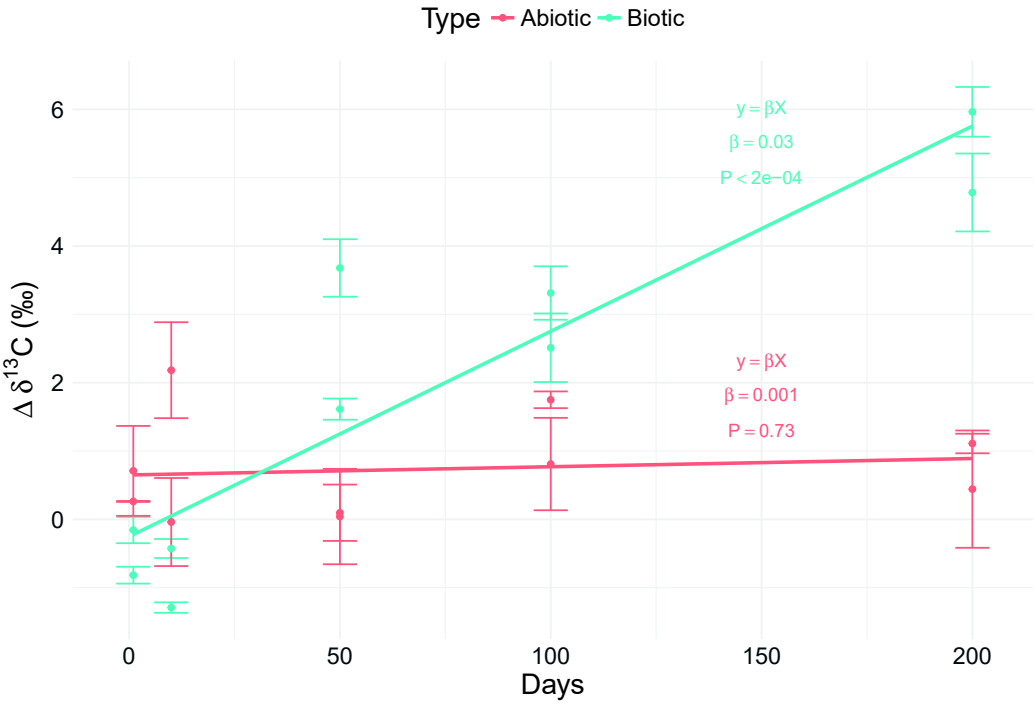

Figure A6: Isotope Fractionation in Soil Degradation Experiments - Biotic *vs.* Abiotic (control) conditions

The relative contribution of dilution (e.g., off-site export, sorption) and degradation to concentration decrease is given by the factor ratio D*/B*. Dilution (D*) and breakdown (B*) factors are given by:

$$D^* = \frac{lnf_{dilution}}{lnf_{total}} \tag{A.10}$$

$$B^* = 1 - D^* \tag{A.11}$$

where $D^* \geq 0$ and $B^* \leq 1$. Note that to meet the relationships D>1 and 0<B<1 initial concentrations need to be accurate. Namely,

- if B*>1, the predicted concentration decrease is larger than observed, and thus ε must be larger.
- if B*<0, initial concentrations must be higher than the surveyed concentration.

Adapted to top soils, in the above cases, application of the open system Rayleigh equation indicates the boundary conditions [e.g. initial concentrations] must be different. Evolution of D*/B* ratios throughout the season for each transect are presented in Tables A5, A6 and A7, with negative values indicated in brackets.

Table A4: Carbon isotopic fractionation and dissipation kinetics for S-met over a 200 day laboratory experiment with Alteckendorf soils

Non-sterile (biotic) soil[a]										
θ [%]	$\Delta\delta^{13}C$ [‰] (SD)[b]	ε_{bulk} [‰] (CI)[c]	R^2 [-]	P [-]	AKIE [-] (CI)[c]	DT_{50} [days] (SE)[d]	DT_{90} [days] (SE)[d]	k [1/day] (SE)[d]	R^2 [-]	P [-]
20	6.8 (0.4)	-1.4 (1.1)	0.85	<0.05	1.021 (0.016)	30 (4)	99 (14)	0.023 (0.004)	0.90	<0.01
40	5.6 (0.6)	-1.8 (0.9)	0.93	<0.01	1.027 (0.01)	41 (4)	135 (11)	0.017 (0.002)	0.97	<0.01
Overall		-1.5 (0.5)	0.87	<0.001	1.023 (0.007)	34 (4)	114 (13)	0.02 (0.002)	0.88	<0.001

a. Biotic and abiotic soil degradation experiments conducted at 20°C at two moisture (θ) conditions of 20 and 40% [wt./wt] for a period of 200 days with dosage of 5.0 $\mu g\ S{-}met\ /g\ soil\ dry\ wt.$ Sacrificial sampling was conducted on days 1, 10, 50, 100 and 200. No significant isotope fraction was observed for autoclaved/abiotic soils ($\Delta\delta^{13}C$<1‰).

b. The error given for the $\Delta\delta^{13}C$ values was calculated *via* error propagation based on ± 1 SD of the mean $\delta^{13}C$ values from n ≥ 3 measurements for each sample.

c. Enrichment 95% confidence intervals (CI) were calculated *via* linear regression analysis.

d. Standard errors were calculated from the regression analysis of the Single First-Order Rate (SFO) model ($DT50 = ln(2)/k$; $DT90 = ln(10)/k$).

e. Abbreviations: k: dissipation rates [1/day]; NA: epsilon values and dissipation kinetics not retrieved due to poor and non-significant (P>0.1) Rayleigh fitting and SFO regressions, respectively, or having less than five sampling dates; CI: confidence intervals (95%); SE: standard error, SD: standard deviation.

Table A5: North degradation (B%), breakdown factors & D*/B* ratios for ε_{lab} : −1.5‰ & ε_{max} : −1.9‰

Date / Median	C_t ($\mu g/L$)	$\delta^{13}C_t$ (‰)	C_t/C_0 (-)	B_{lab} (%)	B_{max} (%)	B^*_{lab} (-)	B^*_{max} (-)	D*/B*$_{lab}$ (-)	D*/B*$_{max}$ (-)
4/5/16	1.9	-31.4	0.4	46.2	38.7	0.6	0.5	0.7	1.1
4/14/16	5.6	-31.2	0.4	53.1	45.0	0.9	0.7	0.2	0.5
4/18/16	7.2	-31.8	0.5	27.5	22.4	0.5	0.4	1.0	1.5
4/26/16	4.2	-31.8	0.3	30.7	25.2	0.3	0.2	2.2	3.0
5/3/16	1.2	-30.7	0.1	66.8	58.1	0.5	0.4	1.2	1.8
5/10/16	1.3	-29.4	0.1	86.1	78.9	0.8	0.7	0.2	0.5
5/24/16	1.2	-29.6	0.1	84.4	76.9	0.8	0.6	0.3	0.7
6/7/16	1.9	-29.8	0.1	82.1	74.3	0.7	0.6	0.4	0.8
6/14/16	1.3	-29.5	0.1	85.9	78.7	0.7	0.6	0.4	0.8
6/28/16	0.4	-29.5	0.0	85.4	78.1	0.5	0.4	1.1	1.7
Early Season				53.1	45.0	0.6	0.5	0.7	1.1
Late Season				85.4	78.1	0.7	0.6	0.4	0.8
Overall				74.4	66.2	0.6	0.5	0.6	1.0

Table A6: Valley degradation (B%), breakdown factors & D*/B* ratios for ε_{lab} : −1.5‰ & ε_{max} : −1.9‰

Date / Median	C_t ($\mu g/L$)	$\delta^{13}C_t$ (‰)	C_t/C_0 (-)	B_{lab} (%)	B_{max} (%)	B^*_{lab} (-)	B^*_{max} (-)	D*/B*$_{lab}$ (-)	D*/B*$_{max}$ (-)
4/5/16	1.7	-30.0	0.3	79.9	71.8	1.4	1.1	(0.26)	(0.06)
4/14/16	3.5	-31.8	0.3	30.7	25.2	0.3	0.2	2.29	3.16
4/18/16	5.1	-31.1	0.4	56.2	47.9	1.0	0.8	0.01	0.28
4/26/16	4.7	-30.6	0.4	68.2	59.6	1.2	1.0	(0.20)	0.01
5/3/16	1.9	-29.8	0.2	81.7	73.8	0.9	0.7	0.06	0.34
5/10/16	2.1	-29.4	0.2	86.9	79.9	1.2	0.9	(0.16)	0.07
5/31/16	2.2	-30.5	0.1	71.0	62.4	0.6	0.4	0.78	1.25
6/7/16	2.6	-29.7	0.1	83.3	75.6	0.9	0.7	0.15	0.45
6/14/16	2.9	-29.9	0.1	80.8	72.8	0.9	0.7	0.17	0.48
6/21/16	3.2	-29.5	0.2	85.1	77.7	1.0	0.8	(0.03)	0.23
6/28/16	2.6	-29.6	0.1	84.0	76.5	0.9	0.7	0.13	0.43
Median Early				56.2	59.6	0.9	0.8	0.06	0.28
Median Late				82.1	75.6	0.9	0.7	0.16	0.45
Median				80.8	73.3	0.9	0.7	0.15	0.45

Table A7: South degradation (B%), breakdown factors & D*/B* ratios for ε_{lab} : −1.5‰ & ε_{max} : −1.9‰

Date / Median	C_t ($\mu g/L$)	$\delta^{13}C_t$ (‰)	C_t/C_0 (-)	B_{lab} (%)	B_{max} (%)	B^*_{lab} (-)	B^*_{max} (-)	D*/B*$_{lab}$ (-)	D*/B*$_{max}$ (-)
4/5/16	7.6	-31.2	0.4	52.0	44.0	0.9	0.7	0.1	0.4
4/14/16	3.7	-31.1	0.2	57.2	48.8	0.5	0.4	1.1	1.6
4/18/16	4.9	-30.9	0.2	61.0	52.4	0.6	0.5	0.6	1.0
4/26/16	2.6	-30.6	0.1	69.0	60.3	0.6	0.4	0.8	1.3
5/3/16	3.2	-30.8	0.1	64.4	55.7	0.5	0.4	0.8	1.3
5/10/16	2.5	-31.1	0.1	57.2	48.8	0.4	0.3	1.6	2.2
5/17/16	1.8	-29.5	0.1	85.8	78.5	0.8	0.6	0.3	0.6
5/31/16	1.2	-28.6	0.1	92.0	86.3	0.9	0.7	0.1	0.4
6/7/16	2.4	-28.9	0.1	90.1	83.9	1.0	0.8	(0.0)	0.2
6/14/16	0.9	-27.6	0.0	96.0	92.2	1.0	0.8	(0.0)	0.3
6/21/16	0.9	-28.2	0.0	94.2	89.4	0.9	0.7	0.1	0.4
Median Early				61.0	52.4	0.6	0.4	0.8	1.3
Median Late				93.1	87.9	0.9	0.7	0.1	0.3
Median				64.4	60.3	0.6	0.6	0.6	0.6

Appendix B

Supporting information to chapter 3

B.1 Soil characteristics

Table B1: Physico-chemical properties of the crop and vineyard soils and concentrations of metalaxyl and S-metolachlor. Analytical uncertainty is 5% for the major elements.

Parameter	Unit	Crop soil	Vineyard soil
Bulk density (ρ_b)	[g cm^{-3}]	0.99	1.05
Clay	[%]	28.3	68.5
Silt	[%]	61.5	23.1
Sand	[%]	10.3	8.4
OM Loss on ignition	[g kg^{-1}]	55.2	16.7
OC Black & Walkley	[g kg^{-1}]	11.8	8.4
$CaCO_3$	[g kg^{-1}]	8.1	271
Fe_2O_3	[g kg^{-1}]	66.6	38.6
MnO	[g kg^{-1}]	1.4	1
Cu	[mg kg^{-1}]	48	171
Zn	[mg kg^{-1}]	77	81
Metalaxyl	[mg kg^{-1}]	0.21	0
S-metolachlor (SM)	[mg kg^{-1}]	0.4	0.41
CEC	[$cmol^{+}$ kg^{-1}]	9.1	15.4
pH	[-]	6.97	8.1

B.2 Methods and standards for analyses

Table B2: Methods and standards for soil analyses

Variables	**Methods in brief**	**Norms and/or procedure**
Soil water content	Drying sample in an oven set at 105 °C	NF ISO 11465
pH	Electrometry in a soil-solvent suspension (1:2.5)	NF EN 12176
Organic matter	Mass loss by ignition at 375 °C during 16 h	NF EN 12875
$CaCO_3$	CO_2 gas with hydrochloric acid	NF ISO 10693
CEC	Cobalt hexamine method	NF X 31-130
Granulometry	Laser granulometer	See Ertlen et al. (2010)
Saturated hydraulic conductivity	Head constant permeameter	See Amoozegar (1989)
Bulk density	Direct measurement of soil cylinder	See Madsen et al. (1986)
Pressure soil-water content curve	Direct measurement of soil cylinder	See Madsen et al. (1986)
Elementary composition	ICP-AES* after lithium tetraborate fusion	See Chabaux et al. (2013)

* Inductively Coupled Plasma Atomic Emission Spectroscopy

Appendix C

Supporting information to chapter 4

C.1 Farmer applications and transect area extents

Three main applications (A1, A2, A3) were confirmed from farmer surveys and observations from weekly transect concentrations [SM] and δ^{13}C (Fig. C1). However, these concentration increases do not correspond with a significant decrease in δ^{13}C that would be expected from a fresh application with a characteristic signature ($\delta^{13}C_0 = -32.2 \pm 0.5‰$).

C.2 Hydrological model

C.2.1 Infiltration and runoff

To calculate infiltration, I (mm) and surface runoff, RO (mm), soil moisture conditions are determined by following the SCS curve number defined by the U.S. Soil Conservation Service [17]. Infiltration is given by,

$$I = R - RO \tag{C.1}$$

where R (mm) is rainfall. The run-off equation is given by [18]:

$$RO = \begin{cases} 0, & R \leq I_a \\ \dfrac{(R - I_a)^2}{R - I_a + S}, & R > I_a \end{cases} \tag{C.2}$$

where I_a (mm) is the initial abstraction capacity of the surface layer, which includes surface storage, interception and infiltration prior to runoff, and typically ranges from 0.05S to 0.2S. The model adopts the latter of these values as it has provided reliable results for previous rainfall-runoff events[19]. S (mm) is the retention parameter after run-off given as a function of the soil profile water content:

$$S = S_{max} \cdot \Big(1 - \frac{SW}{(SW + \exp[w_1 - w_2 \cdot SW])}\Big) \tag{C.3}$$

where w1 (mm) and w2 (-) are shape coefficients, SW (mm) is the soil profile water content of the first two layers, $z0$, $z1$, excluding the amount of water held in the soil profile at wilting point such that:

$$SW = max\Big[\Big\{(\frac{D_{z0}\theta_{z0} + D_{z1}\theta_{z1}}{D_{z0} + D_{z1}} - \theta_{wp}) \cdot (D_{z0} + D_{z1})\Big\}, \Big\{0\Big\}\Big] \tag{C.4}$$

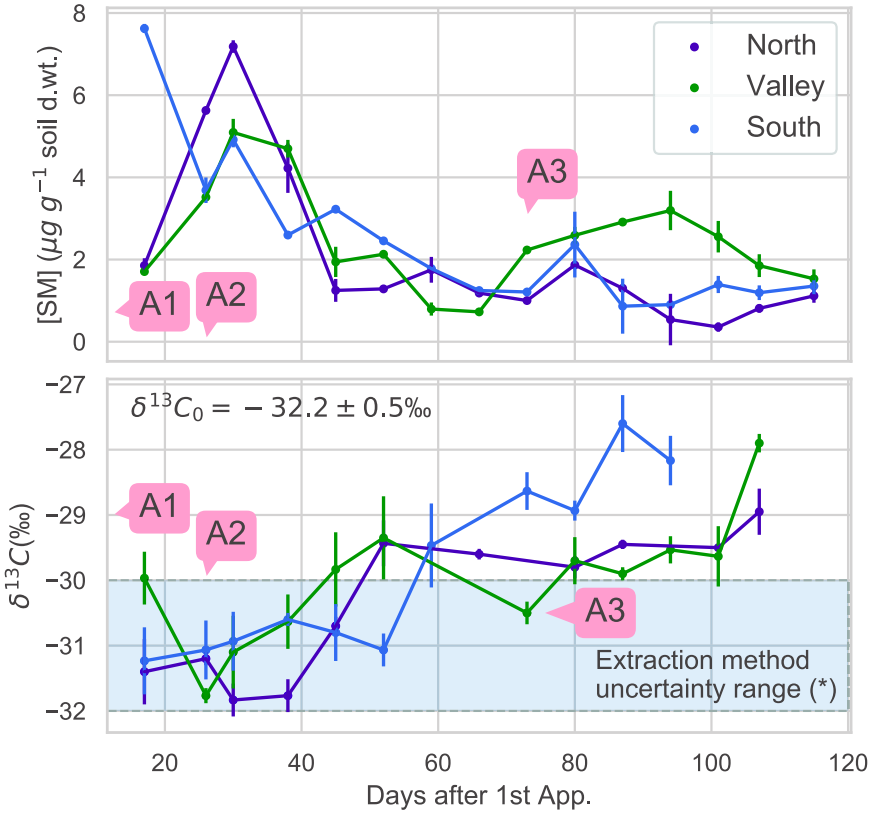

Figure C1: (Top) Measured SM concentrations and (Bottom) δ^{13}C for weekly transects. Confirmed applications A1, A2, and A3 (Table 22). (B) Shaded area indicates uncertainty range of the soil extraction method for SM δ^{13}C and within which no significant change from the application product's signature ($\delta^{13}C_0$) may be concluded, *Ref. 16.

and S_{max} (mm) is the maximum value that the retention parameter can take such that:

$$S_{max} = 254 \cdot \left(\frac{100}{CN_1} - 1\right) \tag{C.5}$$

Calculation of w_1 and w_2 is given by,

$$w_1 = ln\left[\frac{FC}{(1 - \frac{S_3}{S_{max}})} - FC\right] + w_2 \cdot FC \tag{C.6}$$

$$w_2 = \frac{ln\left[\frac{FC}{(1-\frac{S_3}{S_{max}})} - FC\right] - ln\left[\frac{SAT}{(1-\frac{2.54}{S_{max}}} - SAT\right]}{SAT - FC} \tag{C.7}$$

where FC (mm) is the soil profile water content at field capacity, S_3 (mm) is the retention parameter corresponding to field capacity (i.e. CN3) and SAT (mm) is the soil profile water content at saturation. S_3 is given by:

$$S_3 = 254 \cdot \left(\frac{100}{CN_3} - 1\right) \tag{C.8}$$

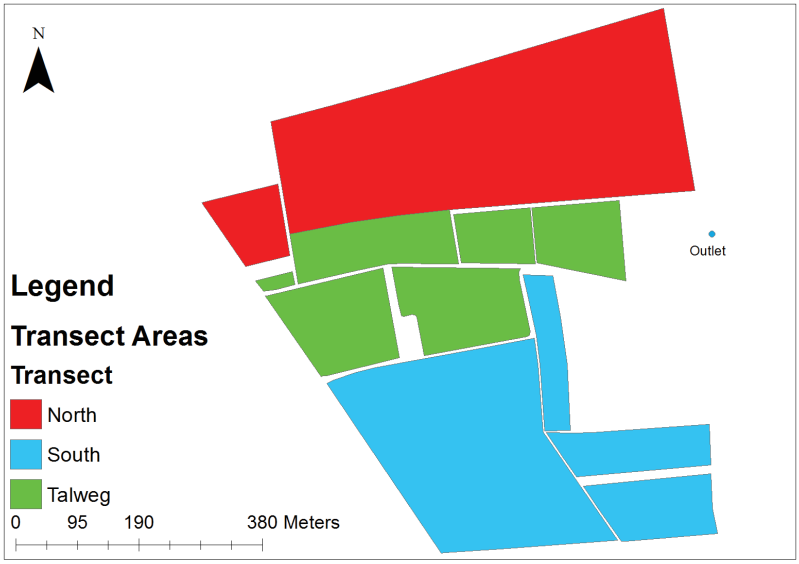

Figure C2: Delimited transect areas used to extrapolate remaining mass from soil concentrations measured for each transect sample weekly.

CN numbers depend on permeability, land use, slope and antecedent moisture conditions. Curve numbers are classified according to three moisture conditions: dry (wilting point - CN_1), average moisture (CN_2) and wet (field capacity - CN_3). Typical CN_2 numbers for various land covers, hydrologic conditions and soil types at a 5% slope are given in Ref. 18. CN_2 values are used to derive CN_3 before slope adjustment,

$$CN_3 = CN_2 \cdot \exp[0.00673 \cdot (100 - CN_2)] \tag{C.9}$$

Before plugging eq. C.9 into eq. C.8, adjustment to local slope of CN_2 is required,

$$CN_{2s} = \frac{CN_3 - CN_2}{3} \cdot [1 - 2 \cdot \exp(-13.86 \cdot slope)] + CN_2 \tag{C.10}$$

where CN_{2s} is the curve number for average moisture conditions adjusted to the local slope. CN_1 values accounting for slope are then calculated as:

$$CN_1 = CN_{2s} - \frac{20 \cdot (100 - CN_{2s}}{\left(100 - CN_{2s} + \exp[2.533 - 0.0636 \cdot (100 - CN_{2s})]\right)} \tag{C.11}$$

Finally, recalculation of eq. C.9, replacing CN_2 with CN_{2s} to adjust for local slope, is done before plugging CN_3 back into eq. C.8.

C.2.2 Percolation

Percolation (P) is assumed to be negligible at moisture levels below field capacity. Above field capacity, percolation is given by [20]:

$$P_z = D_z \tau_z (\theta_{sat,z} - \theta_{fc,z}) \frac{e^{\theta_z - \theta_{fc,z}} - 1}{e^{\theta_{sat,z} - \theta_{fc,z}} - 1}, \quad if\ \theta_z > \theta_{fc,z} \tag{C.12}$$

where D_z (mm) is the soil profile depth of layer z and τ is a dimensionless drainage characteristic given by:

$$\tau = 0.0866 \cdot e^{\gamma_z \cdot log_{10}(K_{sat})}, \quad 0 < \tau \leq 1 \tag{C.13}$$

where γ_z (-) is a calibration coefficient and K_{sat} (mm d^{-1}) is the saturated hydraulic conductivity.

C.2.3 Lateral subsurface flow

Lateral flow (LF_{z_i}) (mm) occurs when the soil moisture content exceeds the field capacity (f_{pot_i}) at each upstream cell (i) and the receiving downstream cell has available pore space capacity (f_{cap_j} ¿ 0). The total flux at each cell is given by,

$$LF_{z_i} = min\Big(f_{pot_i}, f_{cap_j}\Big) \cdot D_z \tag{C.14}$$

$$f_{pot_i} = c_z \cdot (\theta_t - \theta_{fc}) \tag{C.15}$$

$$f_{cap_j} = \frac{\theta_{sat_z} - \theta_{t_z}}{\sum_{i=1}^{I}(i)} \tag{C.16}$$

where c_z (d^{-1}) is a subsurface flow coefficient analogous to Ref. 21, f_{cap_j} (-) the soil water capacity of the downstream cell, $\sum_{i=1}^{I}(i)$ is the sum of upstream contributors and

C.2.4 Evapotranspiration

To account for evapotranspiration processes the FAO56 reference evaporation rate, ET_0 (mm), has been considered and adjusted dynamically according to crop and climate-specific factors. The approach assumes a dual crop coefficient approach appropriate for daily time-step calculations [22] and made up of a basal crop coefficient (K_{cb}) and a soil water evaporation coefficient (K_e). Potential evapotranspiration (ET_p) is then given by

$$ET_p = K_c \cdot ET_0 \tag{C.17}$$

$$K_c = K_{cb} + K_e \tag{C.18}$$

where K_{cb} varies according to crop-specific development stage. In cases where the mean value for daily relative humidity during the mid- or late-season growth stage (RH_{min}%) differs from 45% or where wind speed varies by more than 2 m/s the K_{cb} values for mid- and late-season must be adjusted according to:

$$K_{cb} = K_{cb_{mid/end}} + \Big[0.04(U_2 - 2) - 0.004(RH_{min} - 45)\Big]\Big(\frac{h_{crop}}{3}\Big)^{0.3} \tag{C.19}$$

$$K_e = K_{cmax} - K_{cb} \tag{C.20}$$

where $K_{cb_{mid/end}}$ represent the reference values for sub-humid climate and moderate wind speeds [22]. $U2$ is the wind speed at a height of 2 meters (m/s), RH_{min} is the minimum relative humidity (%) and h_{crop} is crop height. The soil evaporation coefficient, K_e, and K_{cmax} (-) represents an upper limit to evapotranspiration from cropped surfaces (1.05 to 1.30) and given by [22]:

$$K_{cmax} = max\Big[\Big\{K_{cb} + 0.05\Big\}, \Big\{1.2 + [0.04(U_2 - 2) - 0.004(RH_{min} - 45)] \cdot (\frac{h}{3})^{0.3}\Big\}\Big] \tag{C.21}$$

C.2.5 Transpiration

To account for potential transpiration processes, water uptake by roots is considered and regulated by atmospheric demand and soil water content. When there is sufficient water in the soil, potential transpiration (T_p) equals atmospheric demand [22]:

$$T_p = K_{cb} \cdot ET_0 \cdot f_{tr} \tag{C.22}$$

ET_0 is corrected here by including a calibration coefficient f_{tr} (-). Potential transpiration is further subject to root water uptake capacity where the maximum daily uptake $T_{p(z)}$ (mm) at each layer z is given by [23]:

$$T_{p(z)} = 2\Big(1 - \frac{RD_{z/2}}{RD}\Big)\Big(\frac{RD_z}{RD}\Big)T_p \tag{C.23}$$

where RD (mm) and RD_z (mm) are the total and the soil layer's rooting depth, respectively and $RD_{z/2}$ is the soil depth at the middle of the root extension for layer z.

When soil water is insufficient to meet atmospheric demand, actual transpiration is lower than potential transpiration and given by [22]:

$$T_{a(z)} = K_s \cdot T_p \tag{C.24}$$

$$K_s = max\Big[0, min(1, \frac{\theta_t - \theta_{wp}}{\theta_c - \theta_{wp}})\Big] \cdot f_{transp} \tag{C.25}$$

$$\theta_c = \theta_{wp} + (1-p)(\theta_{fc} - \theta_{wp}) \tag{C.26}$$

$$p = p_{tab} + 0.04(5 - ET_p) \tag{C.27}$$

where K_s is a transpiration reduction parameter (0-1), which depends on soil water content, θ_t (m^3/m^3) and the critical soil moisture content θ_c (m^3/m^3) that defines the transition between unstressed and stressed transpiration rate. The the fraction of total depletable soil water is given by p (-) and the depletion factor (-) p_{tab}, for $ET_p \approx 5\ mm/d$ [22][Table no. 22].

C.2.6 Evaporation

Evaporation is considered only on bare surfaces and assumed to be negligible under plant cover and regulated by atmospheric deman along the first ≈ 0.15 m of soil [24]. Considering the difference between actual (E_a, mm/d) and potential evaporation (E_p, mm/d) [22]:

$$E_p = K_e \cdot ET_0 \tag{C.28}$$

$$E_a = K_r \cdot E_p \tag{C.29}$$

where K_r is an evaporation reduction coefficient (-) given by:

$$K_r = \frac{\theta_t - \theta_{dr}}{\theta_{fc} - \theta_{dr}} \tag{C.30}$$

where θ_t is soil moisture (m^3/m^3) and θ_{dr} is the moisture (m^3/m^3) of air-dry soil.

C.2.7 Root growth

Development of the root's depth followed that of [22], which adjusts the crop's maximum root depth relative to the plant's development stage, where the total root depth D_{root} is given by,

$$RD = \begin{cases} 0\ , & J_t < J_{start} \\ RD_{min} + \Big(RD_{max} - RD_{min}\Big) \cdot \dfrac{J_t - J_{sow}}{J_{mid} - J_{start}}, & J_{sow} \leq J_t < J_{max} \\ D_{root,max}\ , & J_t > J_{max} \end{cases} \tag{C.31}$$

where RD_{min} (mm) is the seed depth at sowing time in Julian days J_{sow} (d) and J_{mid} (d) the day at which the plant attains maximum rooting depth, typically at the mid-development stage. Crop development stage duration (L_{stage}) (d) are also provided by [22] for different crops. The Julian days corresponding to each stage are then given by,

$$J_{stage} = \begin{cases} J_{sow} + L_{ini} = J_{dev} \\ J_{dev} + L_{dev} = J_{mid} \\ J_{mid} + L_{mid} = J_{late} \\ J_{late} + L_{end} = J_{end} \end{cases} \tag{C.32}$$

C.3 Agronomic model

C.3.1 Crop cover and height

Crop cover is calculated according to an asymptotic sigmoid function similar to the biomass production function of [25], and which uses the degree-day (DD) approach defined as the difference between daily mean temperature and a crop-dependent base temperature for crop development,

$$COV(t) = \frac{COV_{max}}{1 + \frac{COV_{max} - COV_{ini}}{COV_{ini}} \cdot exp(-COV_{max} \cdot f \cdot \frac{\sum DD}{\sum DD_{COV_{max}}})} \tag{C.33}$$

$$DD_{base} = \begin{cases} T - T_{base}, (T \geq T_{base}) \\ 0, \qquad\quad (T < T_{base}) \end{cases} \tag{C.34}$$

where,
$COV(t)$: crop cover on day t (%);
COV_{max}: crop dependent maximum crop cover (%);
COV_{ini}: initial crop cover (0 ¡ COV_{ini} ¡ 1%, here 0.5%);
f: shape parameter (≈ 0.07);
DD: degree-day (°C);
$\sum$ DD: sum of DD on day t (since sowing);
$\sum DD_{COV_{max}}$: crop dependent sum of DD since sowing necessary to reach the maximum crop cover (COV_{max});
T: daily mean temperature (°C);
T_{base}: crop dependent minimum daily mean temperature necessary for its development (°C).

We only consider temperature as a limiting factor for crop development; water and nutriments deficits are not accounted for. Crop height, $H_v(t)$, is calculated using the same equation with COV_{max} and C_{ini} replaced by analogous crop height parameters (H_{max} and H_{ini}).

C.3.2 Topsoil bulk density

Topsoil bulk density has a strong dynamic character on arable land due to tillage, wheel traffic, root development, biological activity, rainfall impacts, shrinking and swelling, freezing and thawing. In this study we address the effects of tillage and rainfall on dry bulk density using methods inspired by those of the WEPP model [26]. First, a consolidated soil matrix density (BD_m) is calculated using the pedotransfer functions (PTF) of Saxton and Rawls 2006 as a function of soil texture and soil organic matter content. Then tillage and rainfall effects are taken into account as detailed below.

Bulk density on days with tillage

On days with tillage, the topsoil soil bulk density (BD_t) is calculated as,

$$BD_t = BD_{t-1} - F_d BD_{t-1} + \frac{2}{1 + S_{tx}} F_d \frac{3}{4} BD_m \tag{C.35}$$

where:
BD_m: soil matrix density (g cm^{-3}) obtained from the FTP of Saxton and Rawls 2006;
BD_{t-1} and BD_t: bulk density at resp. day $t-1$ and day t (g cm^{-3});
F_d: surface fraction disturbed by tillage (-), determined from lookup tables of the WEPP model [26];
S_{tx}: soil texture related parameter accounting for particle cohesion effects (-), with S_{tx} ¡ 1 for sandy soils and ¿ 1 for clayey soils [28]. Its value is determined from soil texture classes using lookup tables of the RUSLE model [28].

Thus according to equation C.35, tillage reduces the bulk density to 75% of the consolidated soil matrix density for silty soils and tillage affecting the entire surface. This factor is based on bulk density measurements directly after tillage compared to values obtained by the end of the growing season before crop harvest.

Bulk density on days without tillage

On rainy days without tillage, rainfall impact on topsoil bulk density is calculated as a function of the bulk density of the day before, the rainfall on day t, a soil stability factor (S_{stab}), wheel track compaction (wt) and soil cover by either vegetation or crop residues according to,

$$BD_{bs,t} = BD_{bs,t-1} + (BD_m - BD_{bs,t-1})(1 - exp(\frac{-R_t}{S_{stab}})) \tag{C.36}$$

$$BD_{resi,t} = BD_{resi,t-1} + (BD_m - BD_{resi,t-1})(1 - \frac{2 + exp(\frac{R_t}{S_{stab}})}{3}) \tag{C.37}$$

$$BD_{crop,t} = \frac{BD_{resi,t} + BD_{bs,t}}{2} \tag{C.38}$$

$$BD_{wt,t} = 1.15 \cdot BD_m \tag{C.39}$$

where, BD_{bs}, BD_{resi}, BD_{crop}, BD_m (g cm^{-3}) are respectively, topsoil bulk density of bare soil surface parts (bs), parts covered with crop residues (resi), parts covered with living crop (crop), and wheel tracks (wt);
R_t: rainfall on day t (mm);
The soil stability factor S_{stab} (-) is derived from the crusting index of Rémy and Marin-Laflèche (ref. 29) and is defined as:

$$S_{stab} = 1000/I_C \tag{C.40}$$

$$I_C = 5(I_S - 0.2) \tag{C.41}$$

$$I_S = \frac{1.5FS + 0.75CS}{Clay + 10SOM} - Y \tag{C.42}$$

$$Y = \begin{cases} 0.2(pH - 7), (pH > 7) \\ 0, \qquad\qquad (pH \leq 7) \end{cases} \tag{C.43}$$

where:
IS: soil stability index (-);
IC: crusting index (-);
FS: fine silt content (%);
CS: coarse silt content (%);
$Clay$: clay content (%);
SOM: top soil organic matter content (%).

C.3.3 Characteristic water contents and topsoil saturated hydraulic conductivity

The regression PTFs of Saxton and Rawls (ref. 27) were used to calculate the topsoil water contents at saturation (θ_{sat} at 0 kPa moisture tension), wilting point (θ_{wp} at 1500 kPa) and field capacity (θ_{fc} at 33 kPa) by injecting the above modeled bulk densities per surface type (wheel track, bare soil, residue-covered and crop-covered surfaces). Then for each surface type, the saturated hydraulic conductivity is derived from ref. 27,

$$K_{sat} = 1930(\theta_{sat} - \theta_{wp})^{3-\lambda} \tag{C.44}$$

with λ being the slope of the logarithmic tension-moisture curve (-), determined using θ_{fc} and θ_{wp}. The final K_{sat} at the field scale is calculated as the weighted average of K_{sat}, the weight depending on the within-field surface fraction occupied by each of the four surface types.

C.4 Mass transfer model

C.4.1 Mass phase distribution

Mass distribution at time t is given by,

$$M_{tot}(t) = V_{gas}c_{gas} + V_{H_2O}(t)c_{aq}(t) + M_{soil}(t)c_{ads}(t) \tag{C.45}$$

where c_{aq} ($\mu g\ L^{-1}\ H_2O$), c_{ads} (g Kg^{-1} soil), c_{gas} ($\mu g\ L^{-1}$ air) are the dissolved, adsorbed and gaseous SM concentrations, respectively and where $c_{ads} = c_{aq}K_d$ and $c_{gas} = c_{aq}/K_H^{cc}$. V_{gas} and V_{H_2O} are the unsaturated and saturated pore space volume (L), respectively and M_{soil} is the soil mass (Kg).

C.4.2 Volatilisation

Pesticide volatilisation is only considered on the day of application and follows Ref. 30, where a boundary air layer is conceptualised through which pesticide diffuses before escaping into the atmosphere. The thickness (d_a, m) of this layer, was assumed to be equivalent to the topmost soil layer's thickness (10 mm) and regulates the transport resistance (r_a, d/m) such that:

$$r_a(t) = \frac{d_a}{D_a(t)} \tag{C.46}$$

where D_a (m^2/d) is the diffusion coefficient in air for Metolachlor at the observed environmental temperature and adjusted relative to the reference diffusion coefficient ($D_{a,r}$, m^2/d) as:

$$D_a(t) = \Big(\frac{T(t)}{T_r}\Big)^{1.75} D_{a,r} \tag{C.47}$$

where T and T_r are the environmental temperature at time t and at the reference temperature at 293.15°K, respectively.

The total volatilization is given by the flux across the air layer boundary ($J_{v,air}$) and the flux across the topmost soil layer ($J_{v,soil}$) such that:

$$J_{v,air}(t) = -\frac{C_{gas,top}(t) - C_{air}(t)}{r_a} \tag{C.48}$$

$$J_{v,soil}(t) = -\frac{C_{gas,z_0}(t) - C_{gas,top}(t)}{r_s} \tag{C.49}$$

where $C_{gas,top}$ (mg/m^3) is the concentration in gas phase at the soil surface, C_{air} (mg/m^3) the concentration in air, C_{gas,z_0} (mg/m^3) the concentration in gas phase at the center of the uppermost soil layer and r_s (d/m) the diffusion resistance across the topmost soil layer and given by:

$$r_s(t) = \frac{0.5D_z}{D_{rdiff,g}(t)} \tag{C.50}$$

To calculate the relative diffusion ($D_{rdiff,gas}$, m^2/d) the model provides two options. Under option 1 [31],

$$D_{rdiff,gas} = \frac{D_a(t)\Big(\theta_{gas_z}(t)\Big)^a}{\Big(\theta_z(t)\Big)^b} \tag{C.51}$$

where Ref. 32 recommend that $a = 2$ and $b = 2/3$. Under option 2 [33],

$$D_{rdiff,gas} = D_a(t)\Big(a\Big)\Big(\theta_{gas_z}(t)\Big)^b \tag{C.52}$$

where Ref. 34 recommend $a = 2.5$ and $b = 3$ for moderately aggregated plough layers of loamy soils and humic sandy soils [30].

Finally, it is assumed that flux across both layer boundaries is equivalent ($J_{v,soil} = J_{v,air}$) [30]. Considering pesticide concentration in air to be negligble ($C_{air} = 0$), the concentration at the soil surface is:

$$C_{gas,top}(t) = \frac{r_a}{(r_a + r_s)} C_{gas,z_0(t)} \tag{C.53}$$

The gas concentration in the soil layer is related to the dimensionless Henry constant (K_H), where:

$$C_{gas,z_0}(t) = C_{aq,z_0}(t) K_H \tag{C.54}$$

Substituting eq. C.53 into eq. C.48 yields the mass flux lost to the atmosphere ($g/m^2 d$):

$$J_{v,air} = -\frac{C_{gas,z_0}}{(r_a + r_s)} \tag{C.55}$$

C.4.3 Runoff mass

The non-uniform mixing-layer model is adapted from Ahuja and Lehman, 1983 (see Ref. 36, eq. 1 and p. 1217) and given by:

$$\frac{\partial(EDI \cdot \theta \cdot C_{aq})}{\partial t} = -ROe^{(-\beta_{RO} \cdot D_{z0})} C_{aq} \tag{C.56}$$

where the Effective Depth of Interaction (EDI) refers to the mixing layer depth (mm), θ is soil moisture ($m^3\ m^{-3}$), RO is run-off (mm) and C_{aq} is concentration in the mixing layer ($g\ L^{-1}$). The parameter β_{RO} is a calibration constant (assuming, $1 \geq \beta > 0$) and where D_{z0} is the depth (mm) of the top-soil layer.

C.4.4 Leachate mass

Vertical flux can be computed differently across soil layers. Under the first approach, and only for the uppermost layer, the model follows [37]:

$$C_{z_0,aq}(t+1) = C_{z_0,aq}(t) exp\Big(\frac{-P(t)}{\theta_{z_0}(t) \cdot RET_{z_0}(t) \cdot D_{z_0}}\Big) \tag{C.57}$$

where the retardation factor, RET_z (-), is given by:

$$RET_z(t) = 1 + \frac{\rho_{b_z}(t) \cdot K_d}{\theta_z(t)} \tag{C.58}$$

The mass leached (g) is thus given by:

$$M_{z_0,lch}(t) = D_{z_0} \cdot A_i \Big(\theta_{z_0}(t) C_{z_0,aq}(t) - \theta_{z_0}(t+1) C_{z_0,aq}(t+1) \Big) \tag{C.59}$$

where A is the area (m^2) for each cell i. For subsurface layers (i.e., z ¿ 0), mass leached is proportional to the aqueous concentration in percolated water such that,

$$M_{z,lch}(t) = P_z(t) \cdot C_{z,aq}(t) \cdot A_i \tag{C.60}$$

C.4.5 Lateral mass flux

Similarly to vertical mass flux, later mass flux is proportional to lateral water flow and the aqueous concentration at each cell i,

$$M_{z,lf}(t) = LF_{z_i}(t) \cdot C_{z_i,aq}(t) \cdot A_i \tag{C.61}$$

C.5 Degradation model

To account for changes in DT_{50} (days) due to changes in soil moisture, models from Walker 1974 and Schroll *et al.*, 2006 where compared and evaluated against DT_{50} values derived from microcosm degradation experiments conducted at different temperatures (°C) and moistures ($m^3\ m^{-3}$). Observed DT_{50} values were: $DT_{50_{ref}} = 30$ at $\theta = 0.2$, $T = 20$ (used as reference for validation); DT_{50}=41 at $\theta = 0.4$, $T = 20$; DT_{50}=30 at $\theta = 0.4$, $T = 30$). Although both methods mostly underestimated measured DT_{50} (Fig. C3), Walker's approach resulted in smaller error differences and was selected for model implementation.

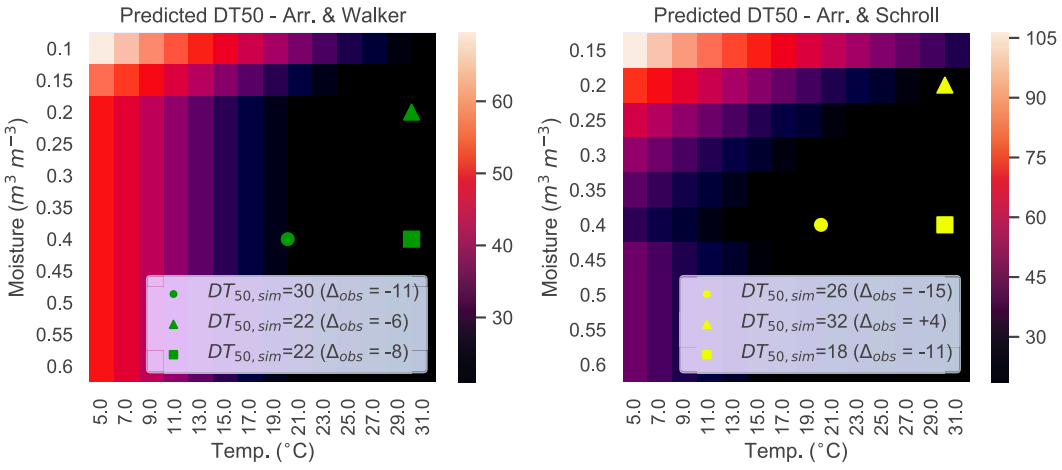

Figure C3: Calculated DT_{50} from Walker 1974 and Schroll *et al.* 2006 and differences to observed (Δ_{obs}) DT_{50} values from SM microcosm degradation experiments. Both approaches follow ref. 40 for adaptation to the Arrhenius equation.

C.6 K_{oc} sensitivity

CSIA information in soils did not permit to reduce uncertainty for K_{oc} values across all sample resolutions. In a virtual experiment evaluating leaching extent based on DT_{50} and K_{oc} correlation scenarios, Lindahl et al., 41 find that when DT_{50} and K_{oc} were negatively

correlated, larger variance in leaching extent was observed in the field, as lower degradation rates complement with higher mobility. In our study, DT_{50} and K_{oc} values were negatively correlated (-0.47, P<0.001), suggesting that spatial variations in organic carbon significantly altered mobility and degradation [42] as previously observed for SM [43, 44]. Namely, although catchment K_{oc} values below 500 L/Kg could be discarded on average (i.e., as shown by WIC models in bulk soils, Fig. C4), improvements in degradation parameter constraints based on temperature and moisture alone were not useful to constrain spatial variability of K_{oc} values (i.e., as shown by transect and plot K_{oc} distributions, Fig. C4). More detailed and explicit representation of organic carbon content evolution in both space and time using available information such as soil type, land-use and agricultural management [45], as it was done in this study for soil hydraulic properties, could further help constraining spatial variability of degradation rates and mobility parameters regulating pesticide leaching.

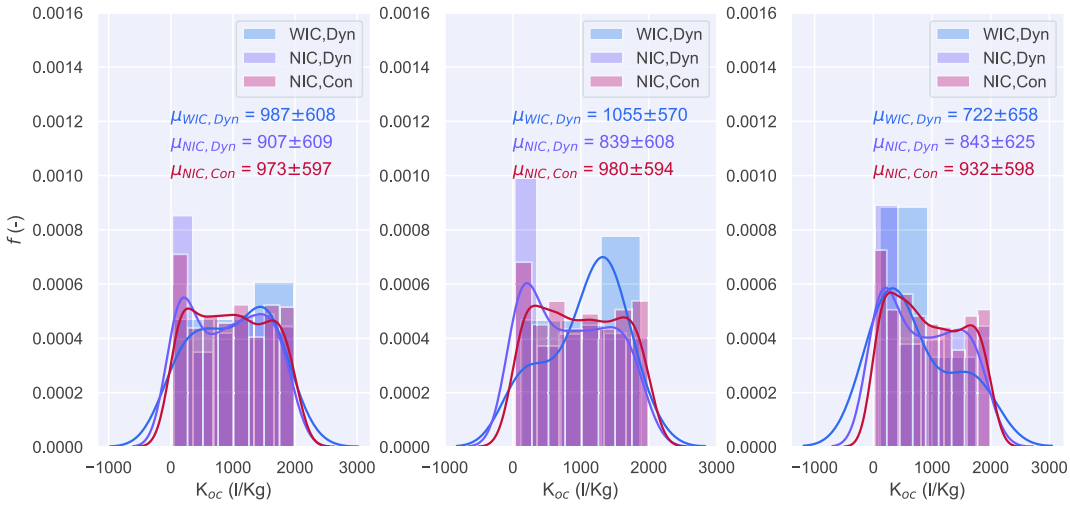

Figure C4: Distribution of K_{oc} for models with no isotope constrains (NIC) vs. models with isotope constraints (WIC) at three analytical resolutions (i.e., bulk, transect and plot soils). NIC models considered KGE_{SM} >0.5, while WIC considered in addition KGE_{δ} >0.5. Statistics for K_{oc} distributions are provided as mean and standard deviations ($\mu \pm$ SD) for models considering dynamic (Dyn) and Constant (Con) DT_{50} values.

References - Appendices

1. Lefrancq, M., Dijk, P. V., Jetten, V., Schwob, M. & Payraudeau, S. Improving runoff prediction using agronomical information in a cropped, loess covered catchment. *Hydrological Processes* **31,** 1408–1423 (2017).
2. R Core Team. *R: A Language and Environment for Statistical Computing* R Foundation for Statistical Computing (Vienna, Austria, 2017). `https://www.r-project.org/`.
3. Legendre, P. & Gallagher, E. Ecologically meaningful transformations for ordination of species data. *Oecologia* **129,** 271–280 (2001).
4. Oksanen, J. *et al. vegan: Community Ecology Package* (2017). `https://cran.r-project.org/package=vegan`.
5. Lutz, S. R. *et al.* Pesticide fate at catchment scale: conceptual modelling of stream CSIA data. *Hydrology and Earth System Sciences Discussions* **21,** 5243–5261. ISSN: 1812-2116 (2017).
6. Abe, Y. & Hunkeler, D. Does the Rayleigh equation apply to evaluate field isotope data in contaminant hydrogeology? *Environmental Science and Technology* **40,** 1588–1596. ISSN: 0013936X (2006).
7. Lutz, S. R., Van Meerveld, H. J., Waterloo, M. J., Broers, H. P. & Van Breukelen, B. M. A model-based assessment of the potential use of compound-Specific stable isotope analysis in river monitoring of diffuse pesticide pollution. *Hydrology and Earth System Sciences* **17,** 4505–4524. ISSN: 10275606 (2013).
8. Bertrand-Krajewski, J. L., Chebbo, G. & Saget, A. Distribution of pollutant mass vs volume in stormwater discharges and the first flush phenomenon. *Water Research* **32,** 2341–2356. ISSN: 00431354 (1998).
9. Elsayed, O. F. *et al.* Using compound-specific isotope analysis to assess the degradation of chloroacetanilide herbicides in lab-scale wetlands. *Chemosphere* **99,** 89–95. ISSN: 00456535 (2014).
10. Ivdra, N., Herrero-Martín, S. & Fischer, A. Validation of user- and environmentally friendly extraction and clean-up methods for compound-specific stable carbon isotope analysis of organochlorine pesticides and their metabolites in soils. *Journal of Chromatography A* **1355,** 36–45. ISSN: 0021-9673 (Aug. 2014).
11. Anastassiades, M., Lehotay, S. J., Štajnbaher, D. & Schenck, F. J. Fast and easy multiresidue method employing acetonitrile extraction/partitioning and "dispersive solid-phase extraction" for the determination of pesticide residues in produce. *Journal of AOAC International* **86,** 412–431. ISSN: 10603271 (2003).
12. Margesin, R. & Schinner, F. *Manual for soil analysis monitoring and assessing soil bioremediation* 370 (Springer, Berlin; New York, 2005).

13. Rayleigh, L. S. Theoretical considerations respecting the separation of gases by diffusion and similar processes. *Philosophical Magazine* **42,** 493–498 (1896).

14. Elsner, M., Zwank, L., Hunkeler, D. & Schwarzenbach, R. P. A new concept linking observable stable isotope fractionation to transformation pathways of organic pollutants. *Environmental Science and Technology* **39,** 6896–6916. ISSN: 0013936X (2005).

15. Van Breukelen, B. M. Quantifying the degradation and dilution contribution to natural attenuation of contaminants by means of an open system Rayleigh equation. *Environ. Sci. Technol.* **41,** 4980–4985 (2007).

16. Alvarez-Zaldívar, P., Payraudeau, S., Meite, F., Masbou, J. & Imfeld, G. Pesticide degradation and export losses at the catchment scale: Insights from compound-specific isotope analysis (CSIA). *Water Research* **139,** 198–207 (2018).

17. Soil Conservation Service. in *National Engineering Handbook, SCS. Soil* (1972).

18. Neitsch, S. L., Arnold, J. G., Kiniry, J. R. & Williams, J. R. Soil & Water Assessment Tool - Theoretical Documentation Version 2009. ISSN: 2151-0040 (2009).

19. Lim, K. J., Engel, B. A., Muthukrishnan, S. & Harbor, J. Effects of initial abstraction and urbanization on estimated runoff using CN technology. *JOURNAL OF THE AMERICAN WATER RESOURCES ASSOCIATION* **42,** 629–643. ISSN: 1093-474X (2006).

20. Raes, D. *BUDGET: a Soil Water and Salt Balance Model. Reference manual. Version 5.0.* tech. rep. (Catholic University of Leuven, Leuven, Belgium, 2002).

21. Manfreda, S., Fiorentino, M. & Iacobellis, V. DREAM: a distributed model for runoff, evapotranspiration, and antecedent soil moisture simulation. *Advances in Geosciences* **2,** 31–39. ISSN: 1680-7359 (2005).

22. Allen, R. G., Pereira, L., Raes, D. & Smith, M. Crop evapotranspiration: Guidelines for computing crop requirements. *Irrigation and Drainage Paper No. 56, FAO,* 300. ISSN: 0254-5284 (1998).

23. Prasad, R. A linear root water uptake model. *Journal of Hydrology* **99,** 297–306. ISSN: 00221694 (1988).

24. Sheikh, V., Visser, S. & Stroosnijder, L. A simple model to predict soil moisture: Bridging Event and Continuous Hydrological (BEACH) modelling. *Environmental Modelling and Software* **24,** 542–556. ISSN: 13648152 (2009).

25. Hunt., R. *Plant Growth Curves – The Functional Approach to Plant Growth.* (ed Arnold, E.) 248. doi:10.1017/s0014479700022857. http://dx.doi.org/10.1017/s0014479700022857 (Cambridge University Press (CUP), London, 1982).

26. Alberts, E. *et al.* in *USDA-Water Erosion Prediction Project, Hillslope Profile and Watershed Model Documentation, NSERL Report #10, July 1995.* (1995).

27. Saxton, K. E. & Rawls, W. J. Soil Water Characteristic Estimates by Texture and Organic Matter for Hydrologic Solutions. *Soil Science Society of America Journal* **70,** 1569–1578. ISSN: 1435-0661 (2006).

28. USDA. *Revised Universal Soil Loss Equation. Version 2. (RUSLE2).* tech. rep. (2003). doi:10.1007/springerreference_77104. http://dx.doi.org/10.1007/springerreference%7B%5C_%7D77104.

29. Rémy, J. & Marin-Laflèche, A. L'analyse de terre : réalisation d'un programme d'interprétation automatique. *Annales Agronomiques* **25,** 607–632 (1974).

30. Leistra, M., van der Linden, A. M. A., Boesten, J. J. T. I., Tiktak, A. & van den Berg, F. *PEARL model for pesticide behaviour and emissions in soil-plant systems; Description of the processes in FOCUS PEARL v 1.1.1.* tech. rep. (2001).

31. Millington, R. & Quirk, J. Transport in porous media. *Transactions 7th Int. Congress Soil Sci.* **1,** 97–106 (1960).

32. Jin, Y. & Jury, W. A. Characterizing the Dependence of Gas Diffusion Coefficient on Soil Properties. *Soil Sci. Soc. Am. J.* **60,** 66–71 (1996).

33. Currie, J. Gaseous diffusion in porous media. 2. Dry granular materials. *British J. Applied Physics* **11,** 318–324 (1960).

34. Bakker, J., Boone, F. & Boekel, P. *Diffusie van gassen in grond en zuurstofdiffusiecoëfficiënten in Nederlandse akkerbouwgronden (Diffusion of gases in soil and oxygen diffusion coefficients in Dutch arable soils). Rapport 20* tech. rep. (ICW, Wageningen, The Netherlands, 1987).

35. Ahuja, L. R. & Lehman, O. R. The Extent and Nature of Rainfall-soil Interaction in the Release of Soluble Chemicals to Runoff. English. *Journal of Environmental Quality* **12,** 34–40 (1983).

36. Shi, X. N., Wu, L. S., Chen, W. P. & Wang, Q. J. Solute Transfer from the Soil Surface to Overland Flow: A Review. *Soil Science Society of America Journal* **75,** 1214–1225. ISSN: 0361-5995 (2011).

37. McGrath, G. S., Hinz, C. & Sivapalan, M. Modeling the effect of rainfall intermittency on the variability of solute persistence at the soil surface. *Water Resources Research* **44,** 1–10 (2008).

38. Walker, A. A Simulation Model for Prediction of Herbicide Persistence1. English. *Journal of Environmental Quality* **3.** doi:10.2134/jeq1974.00472425000300040021x. http://dx.doi.org/10.2134/jeq1974.00472425000300040021x (1974).

39. Schroll, R. *et al.* Quantifying the effect of soil moisture on the aerobic microbial mineralization of selected pesticides in different soils. *Environmental Science and Technology* **40,** 3305–3312. ISSN: 0013936X (2006).

40. Boesten, J. J. T. I. & van der Linden, A. M. A. Modeling the Influence of Sorption and Transformation on Pesticide Leaching and Persistence. *Journal of Environment Quality* **20,** 425. ISSN: 0047-2425 (1991).

41. Lindahl, A. M. L., Söderström, M. & Jarvis, N. Influence of input uncertainty on prediction of within-field pesticide leaching risks. *Journal of Contaminant Hydrology* **98,** 106–114. ISSN: 01697722 (2008).

42. Wu, X., Li, M., Long, Y. & Liu, R. Effects of adsorption on degradation and bioavailability of metolachlor in soil. *Soil Science and Plant Nutrition* **11,** 83–97. ISSN: 07189516 (2011).

43. Rice, P. J., Anderson, T. a. & Coats, J. R. Degradation and persistence of metolachlor in soil: effects of concentration, soil moisture, soil depth, and sterilization. *Environmental toxicology and chemistry / SETAC* **21,** 2640–8. ISSN: 0730-7268 (2002).

44. Long, Y. H., Li, R. Y. & Wu, X. M. Degradation of S -metolachlor in soil as affected by environmental factors. *Journal of Soil Science and Plant Nutrition* **14,** 189–198 (2014).

45. Meersmans, J. *et al.* Spatial analysis of soil organic carbon evolution in Belgian croplands and grasslands, 1960-2006. *Global Change Biology* **17,** 466–479. ISSN: 13541013 (2011).